Electronic Supplementary Material (ESI) for ChemComm.

Synthesis and Reactivity of Ligand-Stabilized Thionyllium (SO^{2+}) Dications

Supporting Information

Ryan J. Andrews,[a] John R. DeBackere,[a] Douglas W. Stephan*[a]

[a] Department of Chemistry, University of Toronto. 80 St. George St. Toronto, ON M5S 3H6.

Table of Contents

1. Chemicals and Materials

All manipulations were performed under an atmosphere of dry and deoxygenated N_2 under standard glovebox or Schlenk techniques unless otherwise stated. All glassware was dried in an oven at 220°C followed by dynamic vacuum over several hours prior to use. After suitable drying procedures, all solvents were stored over 4 Å molecular sieves for a minimum of 24 hours prior to use. 4 Å molecular sieves were activated by heating in a sand bath (>200°C) under dynamic vacuum over 48 hours. Toluene, n-hexane, and n-pentane were purchased from Sigma Aldrich and were dried using a Grubbs-type Innovative Technologies solvent purification system. Dichloromethane (CH_2Cl_2) was purchased from Sigma Aldrich and was dried using a Grubbs-type Innovative Technologies solvent purification system followed by distillation from CaH_2. Acetonitrile (CH_3CN) and acetonitrile-d3 (CD_3CN) were purchased from Sigma Aldrich and were purified by distillation from CaH_2. 2,2'-Bipyridine, 4,4'-ditertbutyl-2,2'-bipyridine, N,N'-dimethylaminopyridine, and 2,2';6',2"-terpyridine were purchased from Sigma Aldrich and were purified by sublimation under vacuum (ca. 100°C) prior to use. 4′-Chloro-2,2′:6′,2″-terpyridine (4-Chloro-Terpyridine) was purchased from HetCat and was used without any further purification. 4′-Phenyl-2,2′:6′,2″-terpyridine (4-Phenyl-Terpyridine) was synthesized according to literature procedures.[1] Trimethylsilyl triflate was purchased from Apollo Scientific and thionyl chloride was purchased from Fischer Scientific and both were distilled prior to use. Other reagents were used as purchased unless otherwise mentioned. Hamilton micro-syringes were used to transfer small amounts of liquids (<50 μL). Plastic syringes and disposable needles were evacuated in the antechamber of the glovebox overnight prior to use.

2. Physical Methods

All NMR spectra were collected at 298K on Bruker Avance III 400, Agilent DD2 400, or Agilent DD2 500 spectrometers in 3- or 5-mm diameter NMR tubes or in a J-Young tube. Chemical shifts (δ) are reported in ppm and absolute values of coupling constants are listed in Hz. ^{1}H NMR spectra are referenced related to residual deuterated-solvent or protio-solvent signals. Departmental facilities were used for mass spectrometry and elemental analysis.

X-Ray data were collected using a graphite monochromator with MoK(α) radiation (λ = 0.71073 Å) and the Bruker APEX3 software package.[2] Single crystals were coated in paratone-N oil and mounted on a MiTeGen cryoloop, and were placed in a cold stream of N_2 prior to collection. Data reduction was performed using the SAINT software package and an absorption correction was applied using SADABS.[3-4] The structures were solved by direct methods using XS and refined by full-matrix least-squares on F2 using XL as implemented in the SHELXTL suite of programs. All non-hydrogen atoms were refined anisotropically. Carbon-bound hydrogen atoms were placed in calculated positions using an appropriate riding model and coupled isotropic temperature factors. The crystal structure of **1[OTf]$_2$** had 4 reflections affected by the beam stop omitted during the refinement. The crystal structure of **3[OTf]$_2$** had one of its triflate anions refined in two alternative orientations due to disorder of the anion fragment, and 2 reflections affected by the beam stop were omitted during the refinement. The crystal structure of 5**[OTf]$_2$** had one of its solvated acetonitrile molecules refined in two alternative orientations due to disorder of the solvent molecule, and 3 reflections affected by the beam stop were omitted during the refinement. The crystal structures of **6[OTf]$_2$, 8[OTf]$_2$,** and **9[OTf]$_2$** had 1, 2, and 3 reflections affected by the beam stop omitted during the refinement, respectively. The crystal structure of [H_2ClTerpy][OTf]$_2$ had 1 reflection affected by the beam stop omitted during the refinement.

3. Synthesis and Characterization

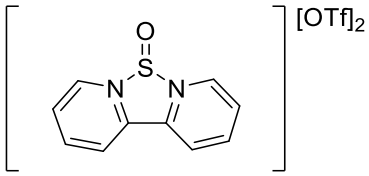

[2,2'-bipyridineSO][Trifluoromethanesulfonate]$_2$ (1[OTf]$_2$): To a stirring solution of thionyl chloride (0.145 mL, 1.86 mmol) and trimethylsilyl trifluoromethanesulfonate (0.70 mL, 3.8 mmol) in 4 mL dichloromethane was added 2,2'-bipyridine (291 mg, 1.86 mmol) in 4 mL dichloromethane over a period of 5 minutes at room temperature. After 1 hour precipitate formation was observed, and the solution was stirred for an additional hour. After cooling at -40^{o}C over night, the solution was filtered through a frit and was washed with cold dichloromethane (2 x 5 mL) and n-pentate (1 x 5 mL). Upon drying under vacuum the product was isolated as a white powder (583 mg, 1.16 mmol, 67% yield). Single colourless crystals suitable for X-Ray diffraction studies were grown from a layered solution of acetonitrile and diethyl ether at -40 ^{o}C.

^{1}H NMR (CD_3CN, 400 MHz, 298K): δ (ppm) 9.80 (dt, $^3J_{H\text{-}H}$ = 6.2 Hz, $^4J_{H\text{-}H}$ = 0.9 Hz, N-C*H*, 2H), 9.10 (dd, $^3J_{H\text{-}H}$ = 6.2 Hz, $^4J_{H\text{-}H}$ = 0.9 Hz, N-C(C)-C(H)-C*H*, 2H), 9.09 (d, $^4J_{H\text{-}H}$ = 3.1 Hz, N-C(C)-C*H*, 2H), 8.54 (td, $^3J_{H\text{-}H}$ = 6.2 Hz, $^4J_{H\text{-}H}$ = 3.1 Hz, N-C(H)-C*H*, 2H).

^{13}C{^{1}H} NMR (CD_3CN, 101 MHz, 298K): δ (ppm) 153.9 (N-C(C)-C(H)-*C*(H)), 144.7 (N-*C*(H)), 143.5 (N-*C*(C)), 133.3 (N-C(H)-*C*(H)), 127.1 (N-C(C)-*C*(H)), 119.0 (q, $^1J_{C\text{-}F}$ = 320 Hz, OTf-*C*F$_3$).

^{19}F NMR (CD_3CN, 377 MHz, 298K): δ (ppm) -79.2 (s, 6F, OTf).

FTIR data (cm^{-1}): 1279 (S-O stretch).

Elemental Analysis (calc'd./expt.): C (28.69/29.75), H (1.61/1.46), N (5.58/6.08).

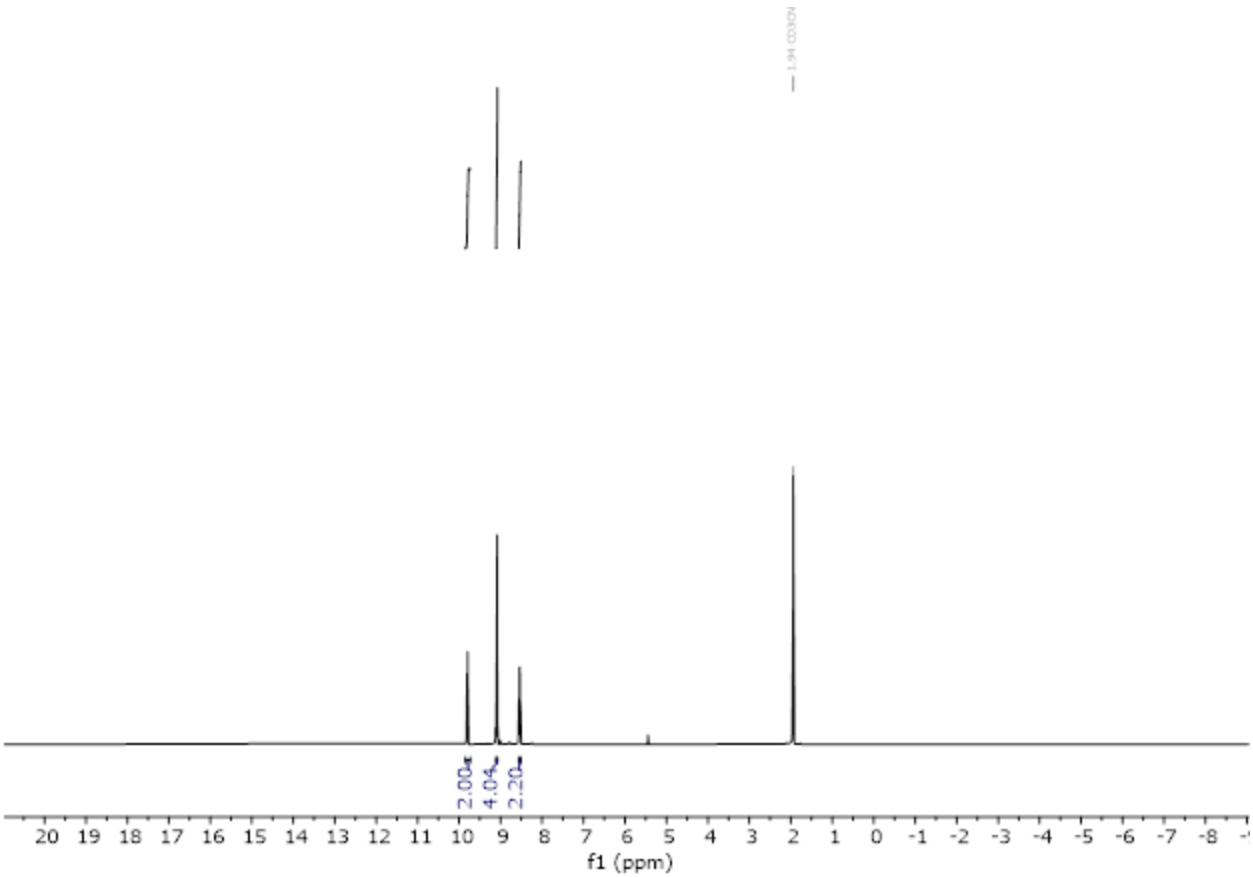

Figure S1. ^{1}H NMR spectrum for **1[OTf]$_2$** (CD_3CN, 500 MHz, 298K). The spectrum is referenced to the residual acetonitrile solvent signal at 1.94 ppm.

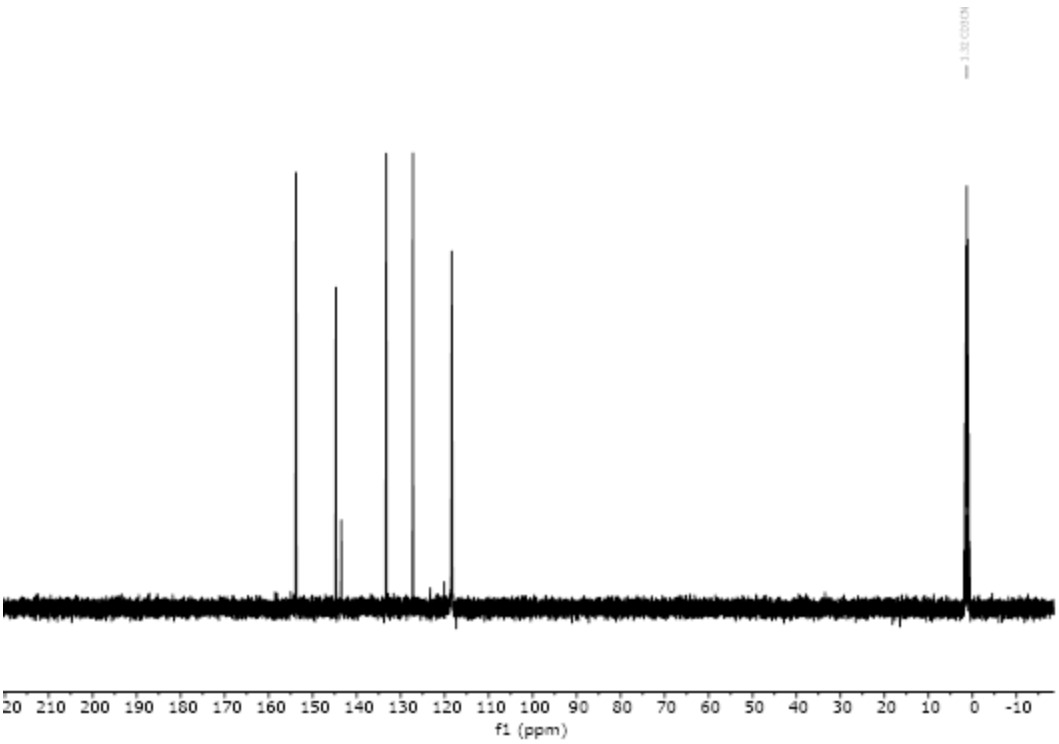

Figure S2. $^{13}C\{^{1}H\}$ NMR spectrum for **1[OTf]$_2$** (CD_3CN, 126 MHz, 298K). The spectrum is referenced to the residual acetonitrile solvent signal at 1.32 ppm.

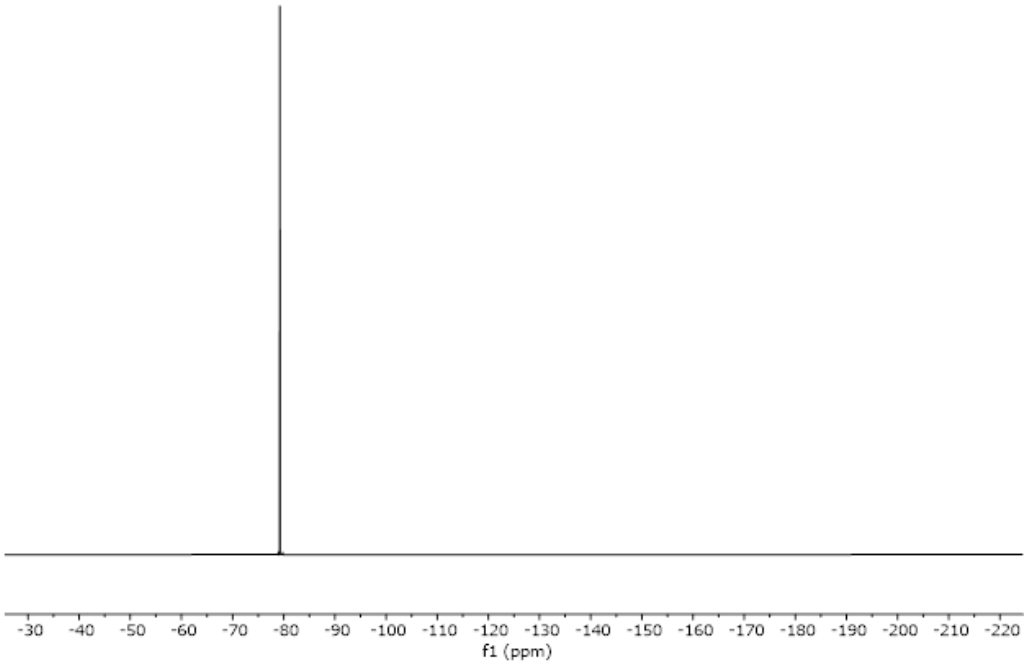

Figure S3. $^{19}F\{^{1}H\}$ NMR spectrum for **1[OTf]$_2$** (CD_3CN, 377 MHz, 298K).

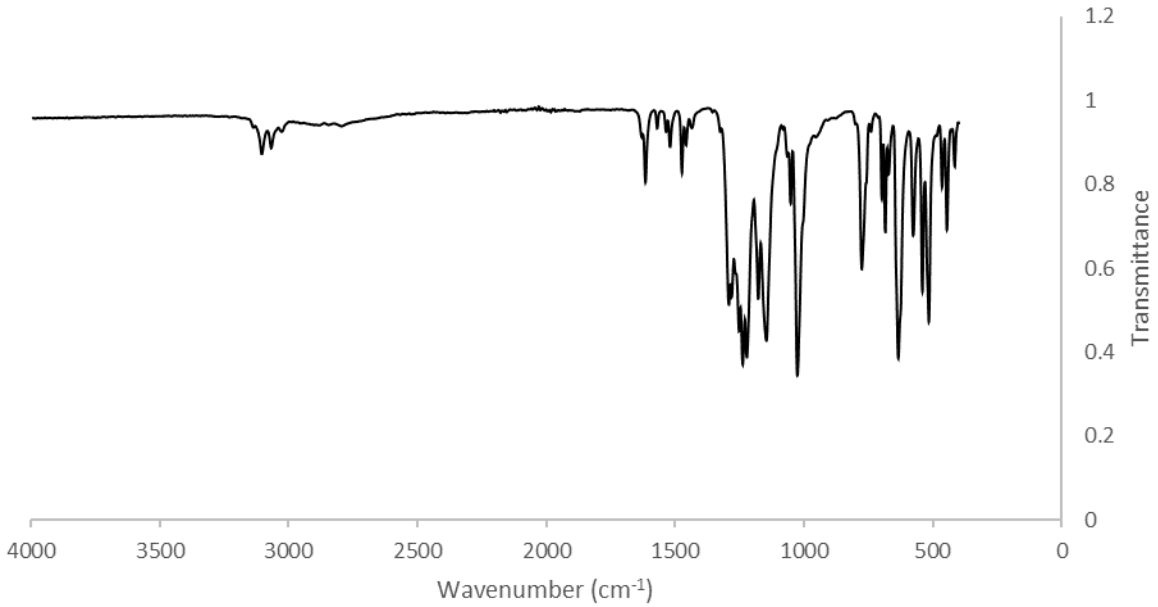

Figure S4. FTIR-ATR spectrum for **1[OTf]$_2$**.

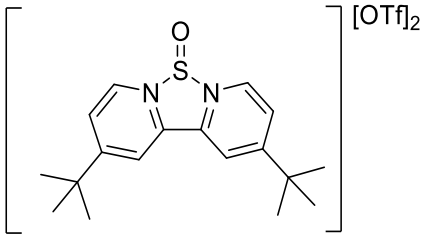

[(4,4'-di-tert-butyl)-2,2'-bipyridineSO][Trifluoromethanesulfonate]$_2$ (2[OTf]$_2$): To a stirring solution of thionyl chloride (0.145 mL, 2.00 mmol) and trimethylsilyl trifluoromethanesulfonate (0.70 mL, 3.86 mmol) in 5 mL dichloromethane was added 4,4'-di-tert-butyl-2,2'-bipyridine (500 mg, 1.86 mmol) in 5 mL dichloromethane over a period of 5 minutes at room temperature. After 1 hour, precipitate formation was observed, and the solution was stirred for an additional hour. After cooling at -40^{o}C over night, the dichloromethane was decanted off and the resulting white powder was washed with cold dichloromethane (3 x 5 mL). Upon drying under vacuum **2** was isolated as a white powder (866 mg, 1.41 mmol, 76 % yield).

^{1}H NMR (CD_3CN, 500 MHz, 298K): δ (ppm) 9.62 (d, $^3J_{H\text{-}H}$ = 6.4 Hz, N-C*H*, 2H), 9.06 (d, $^4J_{H\text{-}H}$ = 1.9 Hz, N-C(C)-C*H*, 2H), 8.48 (dd, $^3J_{H\text{-}H}$ = 6.4 Hz, $^4J_{H\text{-}H}$ = 1.9 Hz, N-C(H)-C*H*, 2H), 1.54 (s, C(CH_3)$_3$).

^{13}C{^{1}H} NMR (CD_3CN, 126 MHz, 298K): δ (ppm) 180.8, 143.4, 143.0, 129.9, 124.9, 121.7 (q, $^1J_{C\text{-}F}$ = 320 Hz, OTf-*C*F$_3$), 39.3, 29.9.

^{19}F NMR (CD_3CN, 377 MHz, 298K): δ (ppm) -79.2 (s, 6F, OTf).

FTIR data (cm^{-1}): 1278 (S-O stretch).

Elemental Analysis (calc'd./expt.): C (39.09/39.80), H (3.94/4.43), N (4.56/4.53) .

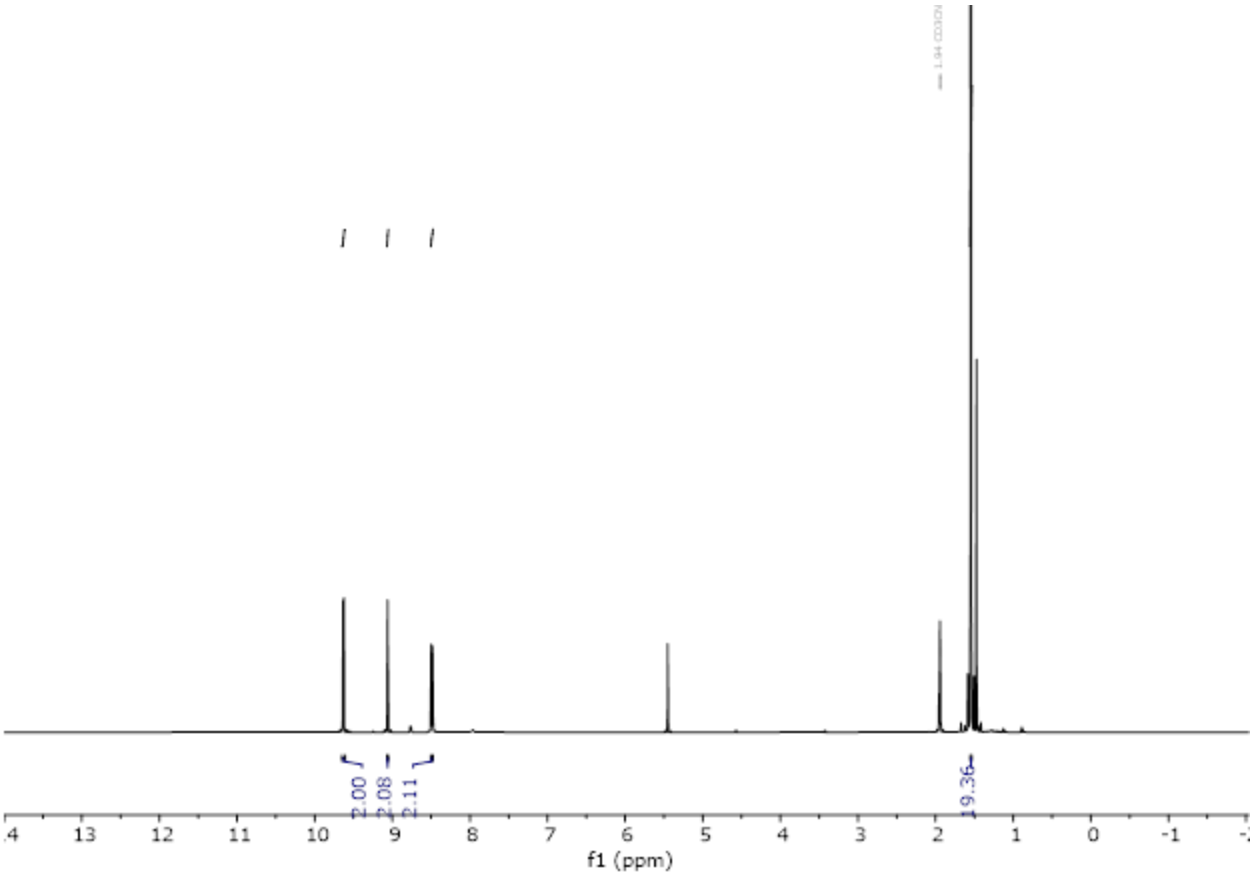

Figure S5. ^{1}H NMR spectrum for **2[OTf]$_2$** (CD_3CN, 500 MHz, 298K). The spectrum is referenced to the residual acetonitrile solvent signal at 1.94 ppm.

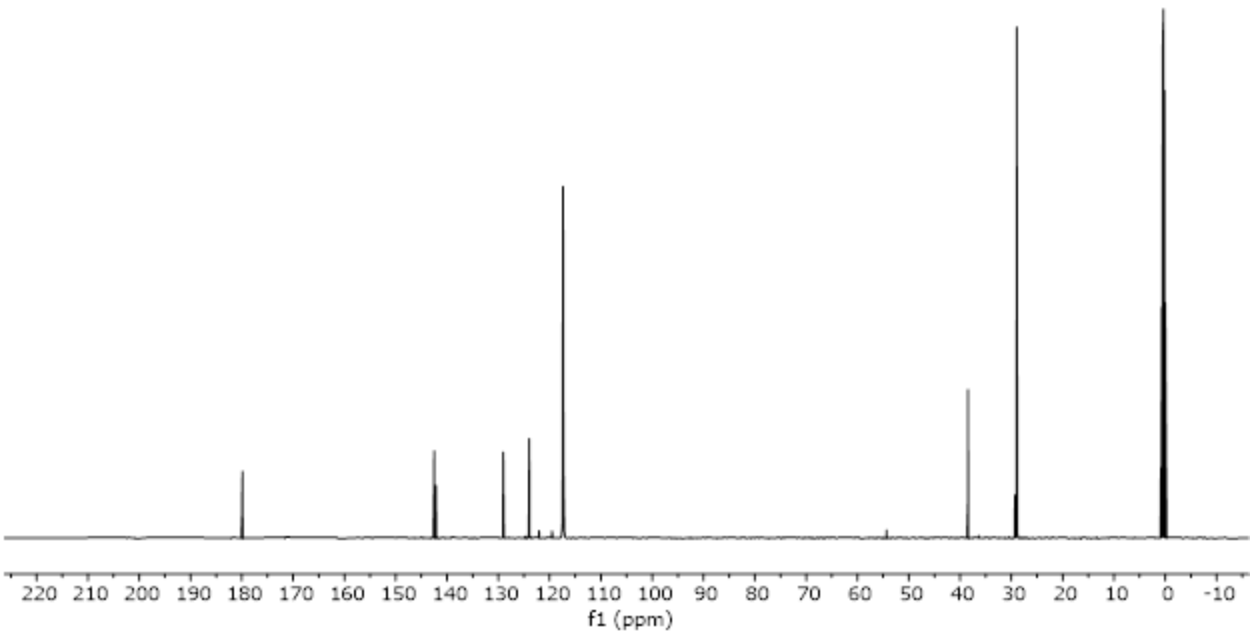

Figure S6. $^{13}C\{^{1}H\}$ NMR spectrum for **2[OTf]$_2$** (CD_3CN, 126 MHz, 298K). The spectrum is referenced to the residual acetonitrile solvent signal at 1.32 ppm.

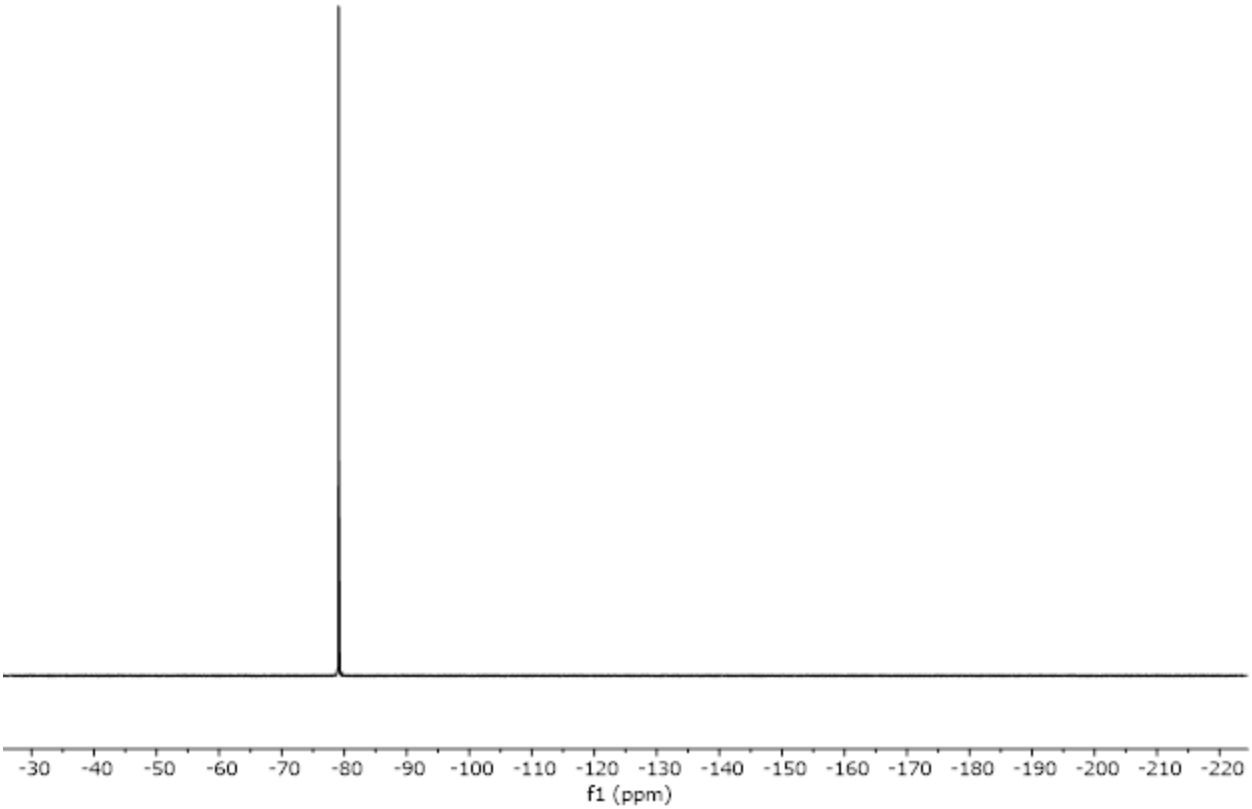

Figure S7. $^{19}F\{^{1}H\}$ NMR spectrum for **2[OTf]$_2$** (CD_3CN, 377 MHz, 298K).

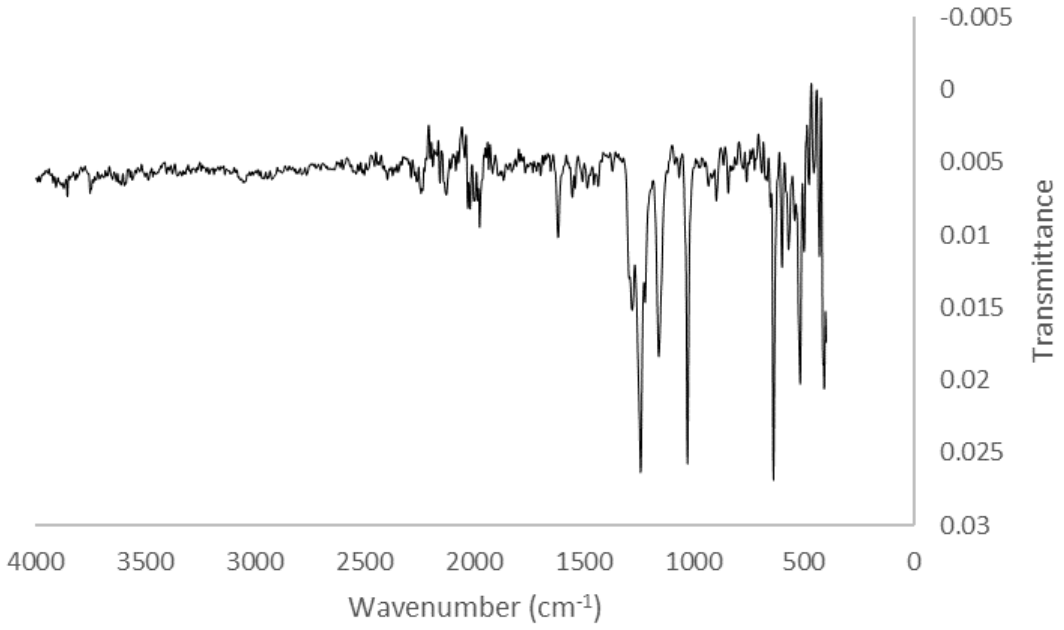

Figure S8. FTIR-ATR spectrum for **2[OTf]$_2$**.

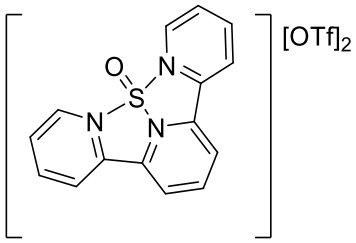

[(2,2′:6′,2″-terpyridine)SO][Trifluoromethanesulfonate]$_2$ (3[OTf]$_2$): To a stirring solution of thionyl chloride (31 μL, 0.427 mmol) and trimethylsilyl trifluoromethanesulfonate (0.27 mL, 0.884 mmol) in 4 mL dichloromethane was added 2,2′:6′,2″-terpyridine (0.100 g, 0.429 mmol) in 4 mL dichloromethane over a period of 5 minutes at room temperature. Immediate precipitate formation was observed, and the resulting solution was stirred for an additional hour. After cooling at -40^{o}C for 1 hour, the dichloromethane was decanted off and the resulting white powder was washed with cold dichloromethane (2 x 5 mL). Upon drying under vacuum, **3[OTf]$_2$** was isolated as a white powder (210 mg, 0.362 mmol, 85 % yield).

^{1}H NMR (CD_3CN, 400 MHz, 298K): δ (ppm) 9.41 (d, $^3J_{H\text{-}H}$ = 5.6 Hz, N-C*H*, 2H), 9.14 (dd, *J* = 9.1 Hz, J = 6.4 Hz, 1H, *p*-C-*H* central ring), 9.08 (m, 2H, *p*-C-*H* outside rings), 8.90 (d, $^3J_{H\text{-}H}$ = 9.1 Hz, 2H, *m*-C-*H* outside rings), 8.73 (td, $^3J_{H\text{-}H}$ = 7.7 Hz, $^4J_{H\text{-}H}$ = 1.3 Hz, 2H, *m*-C-*H* outside rings (N-C(C)-C-*H*)), 8.30 (dd, $^3J_{H\text{-}H}$ = 7.7 Hz, $^3J_{H\text{-}H}$ = 5.6 Hz, $^4J_{H\text{-}H}$ = 1.3 Hz, 2H, *m*-C-*H* outside rings (N-C(H)-C-*H*)).

^{13}C{^{1}H} NMR (CD_3CN, 101 MHz, 298K): δ (ppm) 153.6, 147.4, 147.1, 143.4, 139.5, 132.6, 127.7, 126.2, 121.9 (q, $^1J_{C\text{-}F}$ = 320 Hz, OTf-*C*F_3).

^{19}F NMR (CD_3CN, 377 MHz, 298K): δ (ppm) -79.3 (s, 6F, OTf).

Elemental Analysis (calc'd./expt.): C (35.24/36.22), H (1.91/1.69), N (7.25/7.29).

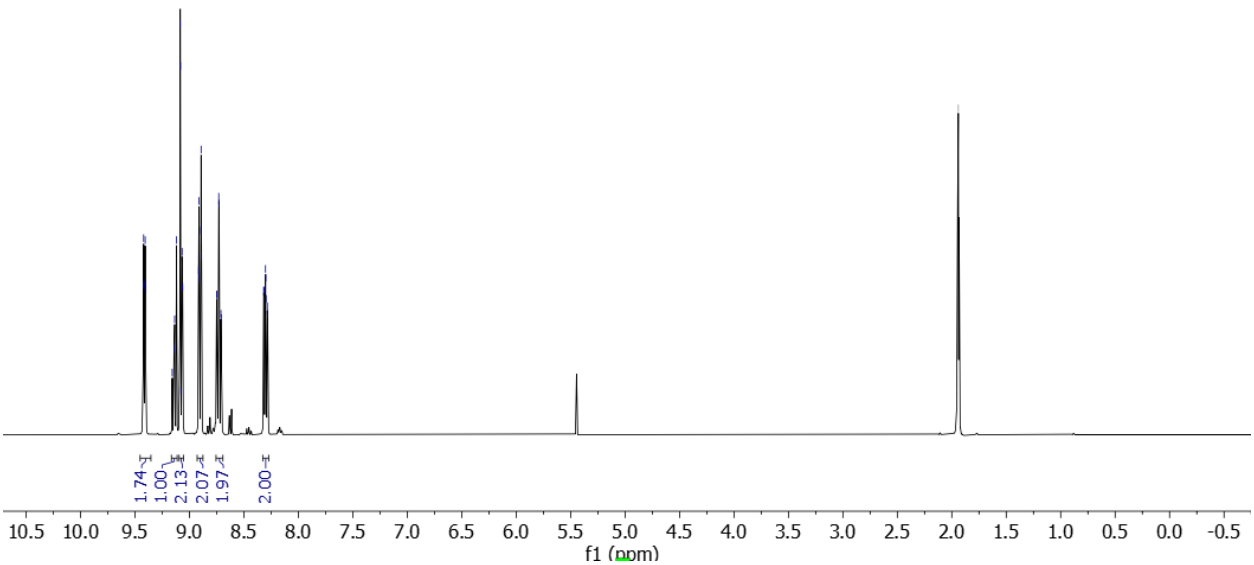

Figure S9. ^{1}H NMR spectrum for **3[OTf]$_2$** (CD_3CN, 500 MHz, 298K). The spectrum is referenced to the residual acetonitrile solvent signal at 1.94 ppm.

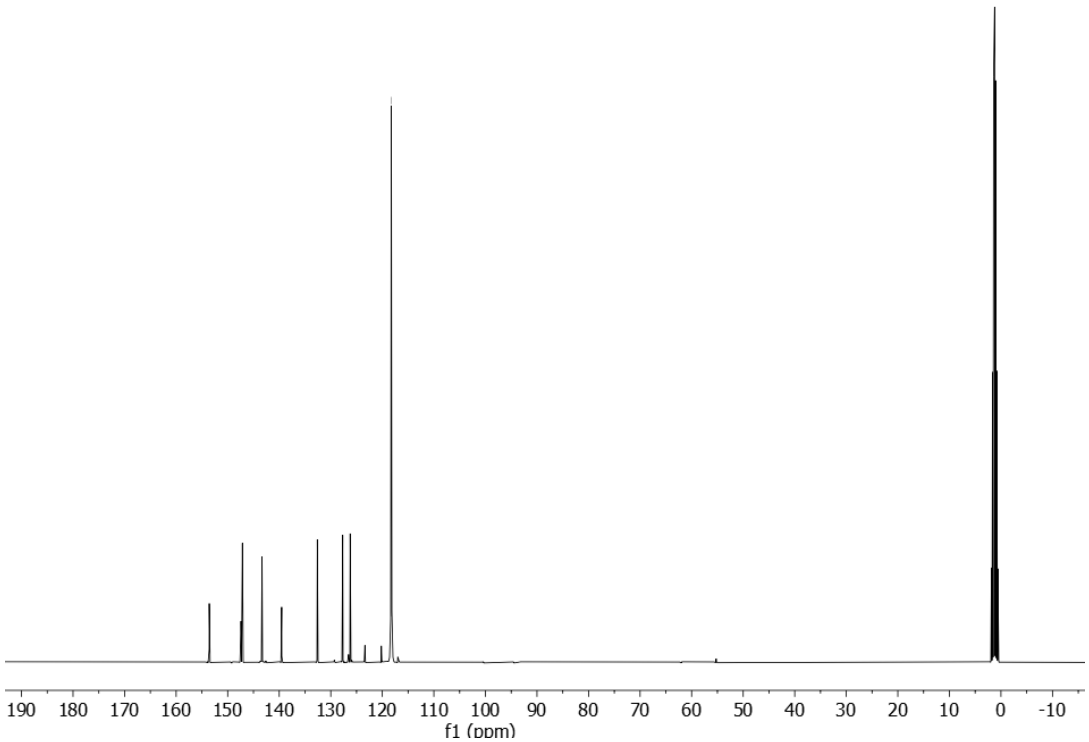

Figure S10. $^{13}C\{^{1}H\}$ NMR spectrum for **3[OTf]$_2$** (CD_3CN, 101 MHz, 298K). The spectrum is referenced to the residual acetonitrile solvent signal at 1.32 ppm.

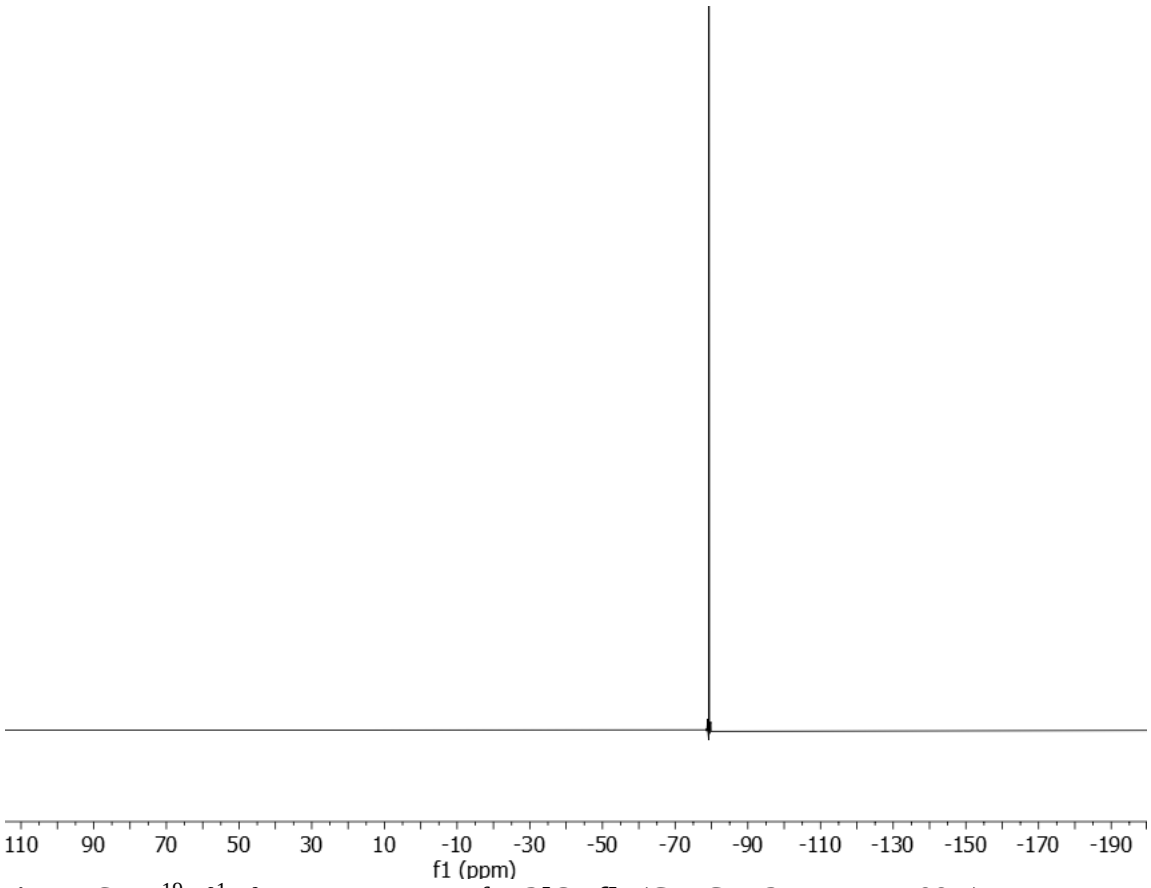

Figure S11. $^{19}F\{^{1}H\}$ NMR spectrum for **3[OTf]$_2$** (CD_3CN, 377 MHz, 298K).

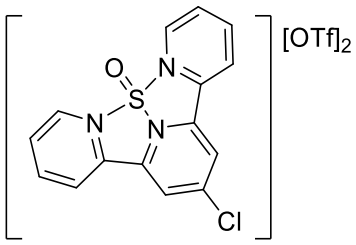

[(4′-Chloro-2,2′:6′,2″-terpyridine)SO][Trifluoromethanesulfonate]$_2$ (4[OTf]$_2$): To a stirring solution of thionyl chloride (54.5 μL, 0.750 mmol) and trimethylsilyl trifluoromethanesulfonate (0.27 mL, 1.49 mmol) in 4 mL dichloromethane was added 4′-Chloro-2,2′:6′,2″-terpyridine (0.200 g, 0.747 mmol) in 4 mL dichloromethane over a period of 5 minutes at room temperature. After 1 hour precipitate formation was observed, and the solution was stirred for an additional hour. After cooling at -40^{o}C over night, the dichloromethane was decanted off and the resulting white powder was washed with cold dichloromethane (1 x 5 mL) and n-pentane (2 x 5 mL). Upon drying under vacuum, **4[OTf]$_2$** was isolated as a white powder (315 mg, 0.512 mmol, 69 % yield).

^{1}H NMR (CD_3CN, 500 MHz, 298K): δ (ppm) 9.42 (ddd, $^3J_{H\text{-}H}$ = 5.5 Hz, $^4J_{H\text{-}H}$ = 1.2 Hz, $^5J_{H\text{-}H}$ = 0.7 Hz, N-C*H*, 2H), 9.15 (s, C(Cl)-C*H*, 2H), 8.87 (dt, $^3J_{H\text{-}H}$ = 8.1 Hz, $^4J_{H\text{-}H}$ = 1.2 Hz, N-C(H)-C(H)-C(H)-C*H*, 2H), 8.73 (td, $^3J_{H\text{-}H}$ = 8.1 Hz, $^4J_{H\text{-}H}$ = 1.2 Hz, N-C(H)-CD(H)-C*H*) 2H), 8.31 (ddd, $^3J_{H\text{-}H}$ = 8.1 Hz, $^3J_{H\text{-}H}$ = 5.5 Hz, $^4J_{H\text{-}H}$ = 1.2 Hz, N-C(H)-C*H*, 2H).

^{13}C{^{1}H} NMR (CD_3CN, 126 MHz, 298K): δ (ppm) 161.7, 148.0, 147.3, 143.7, 138.9, 133.2, 127.9, 126.5, 121.9 (q, $^1J_{C\text{-}F}$ = 320 Hz, OTf-*C*F$_3$).3

^{19}F NMR (CD_3CN, 377 MHz, 298K): δ (ppm) -79.3 (s, 6F, OTf).

FTIR data (cm^{-1}): 1260 (S-O stretch).

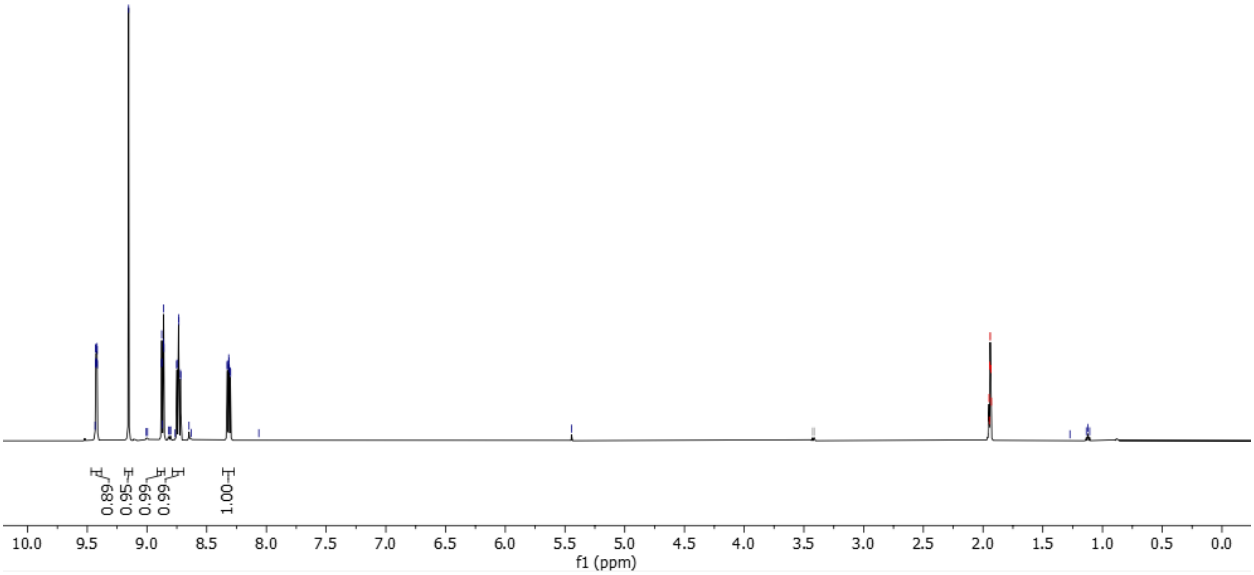

Figure S12. ^{1}H NMR spectrum for **4[OTf]$_2$** (CD_3CN, 500 MHz, 298K). The spectrum is referenced to the residual acetonitrile solvent signal at 1.94 ppm.

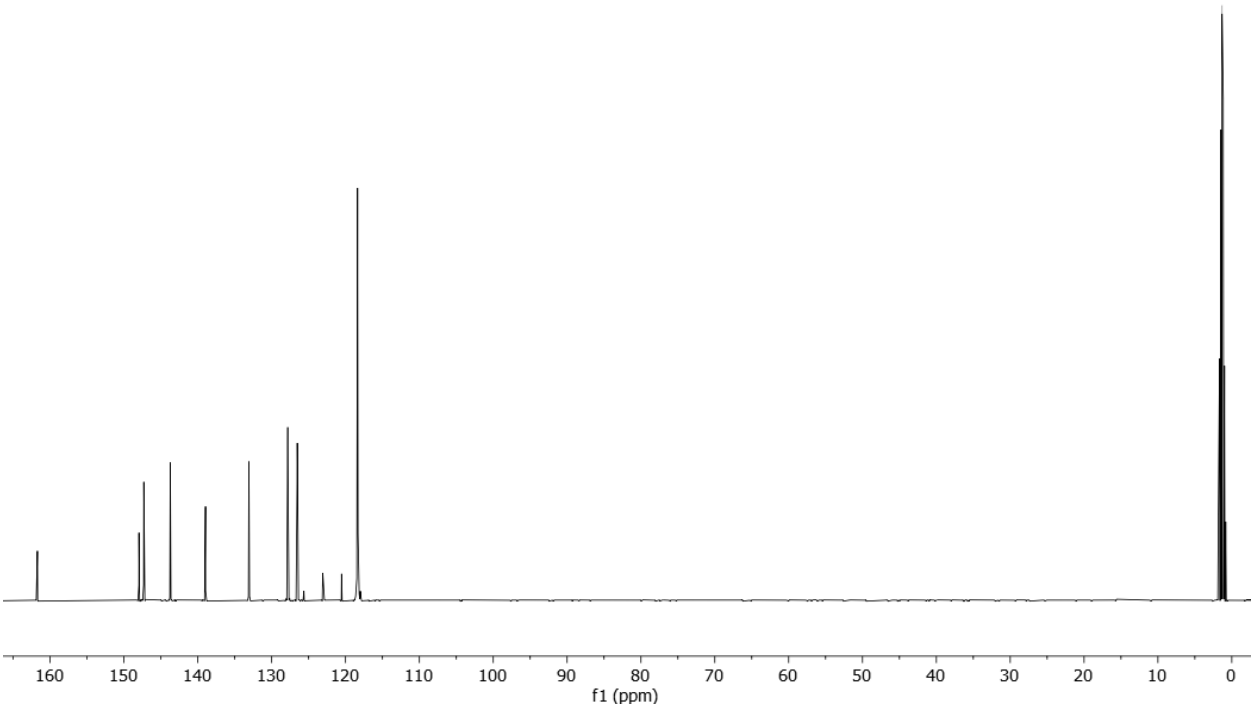

Figure S13. $^{13}C\{^{1}H\}$ NMR spectrum for **4[OTf]$_2$** (CD_3CN, 126 MHz, 298K). The spectrum is referenced to the residual acetonitrile solvent signal at 1.32 ppm.

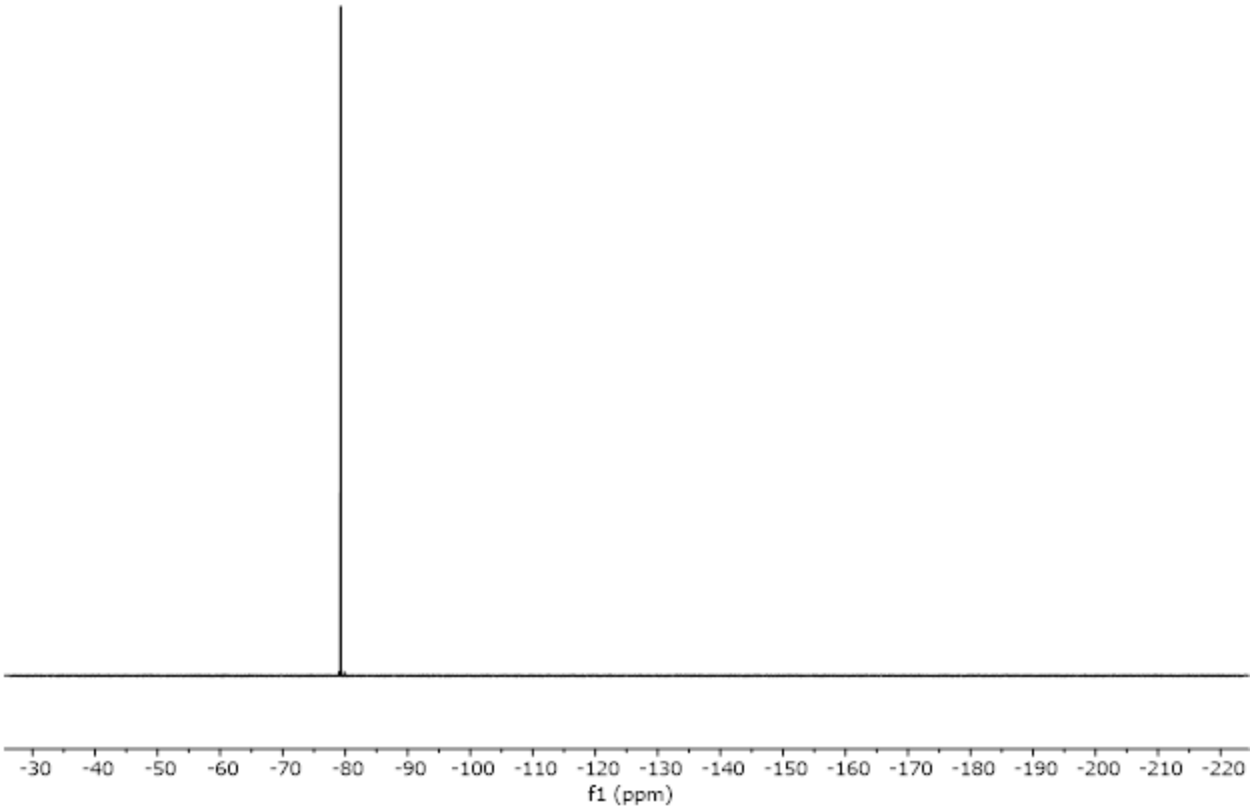

Figure S14. $^{19}F\{^{1}H\}$ NMR spectrum for **4[OTf]$_2$** (CD_3CN, 377 MHz, 298K).

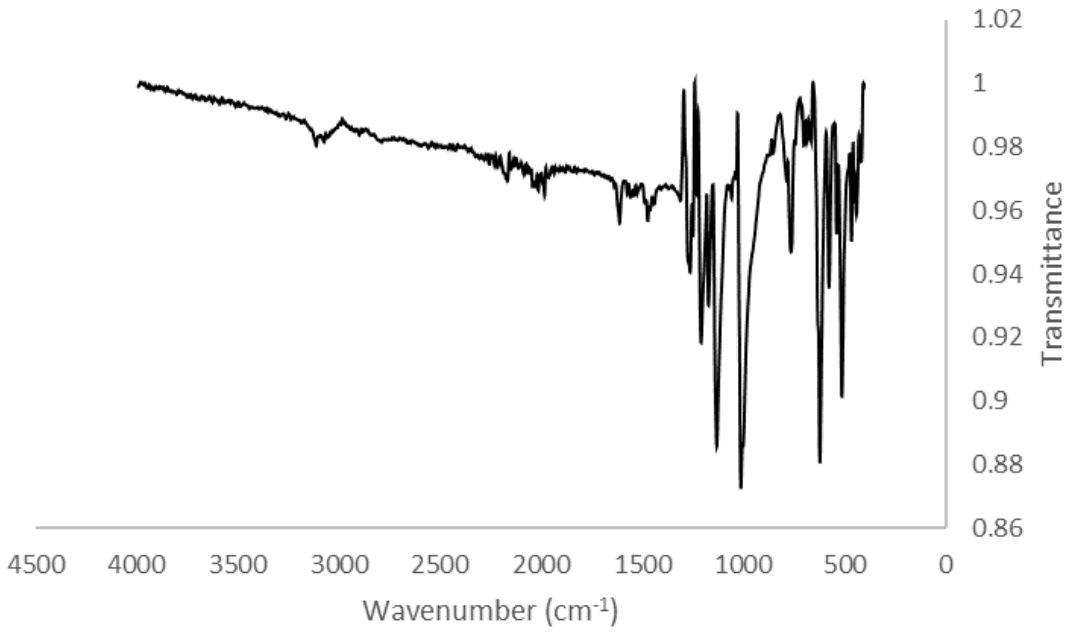

Figure S15. FTIR-ATR spectrum for **4[OTf]**$_2$.

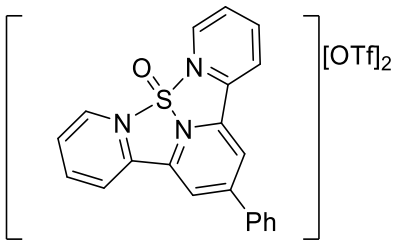

[(4′-Phenyl-2,2′:6′,2″-terpyridine)SO][Trifluoromethanesulfonate]$_2$ (5[OTf]$_2$): To a stirring solution of thionyl chloride (0.221 μL, xmmol) and trimethylsilyl trifluoromethanesulfonate (83 μL, 0.46 mmol) in 4 mL dichloromethane was added 4′-Phenyl-2,2′:6′,2″-terpyridine (67.2 mg, 0.221 mmol) in 4 mL dichloromethane over a period of 5 minutes at room temperature. After 1 hour precipitate formation was observed, and the solution was stirred for an additional hour. After cooling at -40^{o}C over night, the dichloromethane was decanted off and the resulting white powder was washed with cold dichloromethane (2 x 5 mL) and n-pentane (2 x 5 mL). Upon drying under vacuum, **5[OTf]$_2$** was isolated as an off-white powder (120 mg, 0.207 mmol, 94% yield). Suitable crystals for single-crystal X-ray diffraction were grown from a layered solution of acetonitrile and diethyl ether at -40^{o}C.

^{1}H NMR (CD_3CN, 500 MHz, 298K): 9.12 (ddd, $^3J_{H\text{-}H}$ = 5.8 Hz, $^4J_{H\text{-}H}$ = 1.6 Hz, $^5J_{H\text{-}H}$ = 0.7 Hz, N-C*H*, 2H), 8.93 (ddd, $^3J_{H\text{-}H}$ = 8.3 Hz, $^4J_{H\text{-}H}$ = 1.2 Hz, $^5J_{H\text{-}H}$ = 0.7 Hz, N-C(H)-C(H)-C*H*, 2H), 8.83 (s, C(Ph)-C*H*, 2H), 8.80 (td, $^3J_{H\text{-}H}$ = 8.1 Hz, $^4J_{H\text{-}H}$ = 1.6 Hz, N-C(H)-C(H)-C*H*, 2H), 8.21 (ddd, $^3J_{H\text{-}H}$ = 8.1 Hz, $^3J_{H\text{-}H}$ = 5.8 Hz, $^4J_{H\text{-}H}$ = 1.2 Hz, N-C(H)-C*H*, 2H), 8.06-8.04 (m, *o*-PhC*H*, 2H), 7.70-7.63 (m, *m*-PhC*H* and *p*-PhC*H* overlapping signals, 3H).

^{13}C{^{1}H} NMR (CD_3CN, 126 MHz, 298K): δ (ppm) 154.7, 149.1, 148.3, 147.5, 143.6, 136.7, 132.0, 130.6, 129.6, 128.8, 126.4, 124.6, 121.9 (q, $^1J_{C\text{-}F}$ = 320 Hz, OTf-*C*F_3).

^{19}F NMR (CD_3CN, 377 MHz, 298K): δ (ppm) -79.2 (s, 6F, OTf).

FTIR data (cm^{-1}): 1262 (S-O stretch).

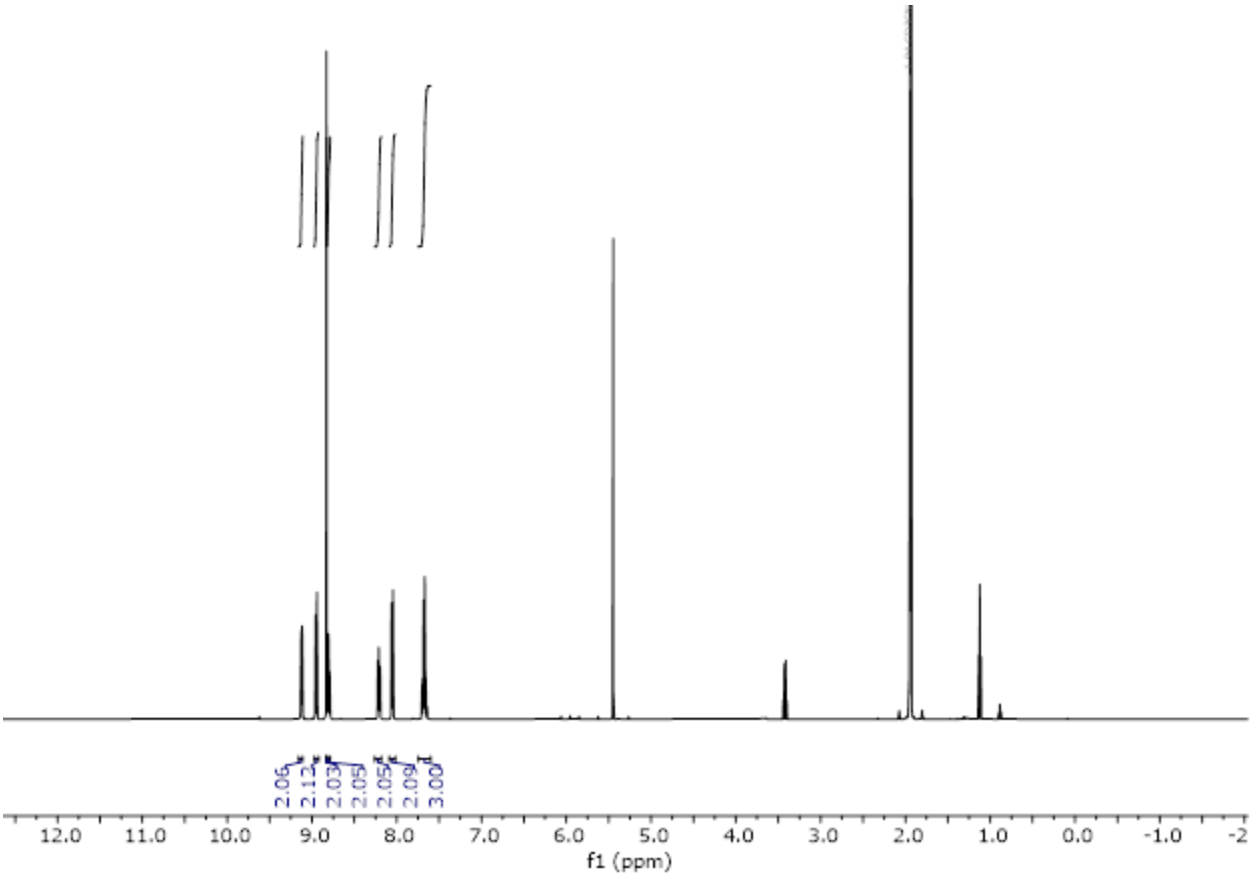

Figure S16. ^{1}H NMR spectrum for **5[OTf]$_2$** (CD_3CN, 500 MHz, 298K). The spectrum is referenced to the residual acetonitrile solvent signal at 1.94 ppm.

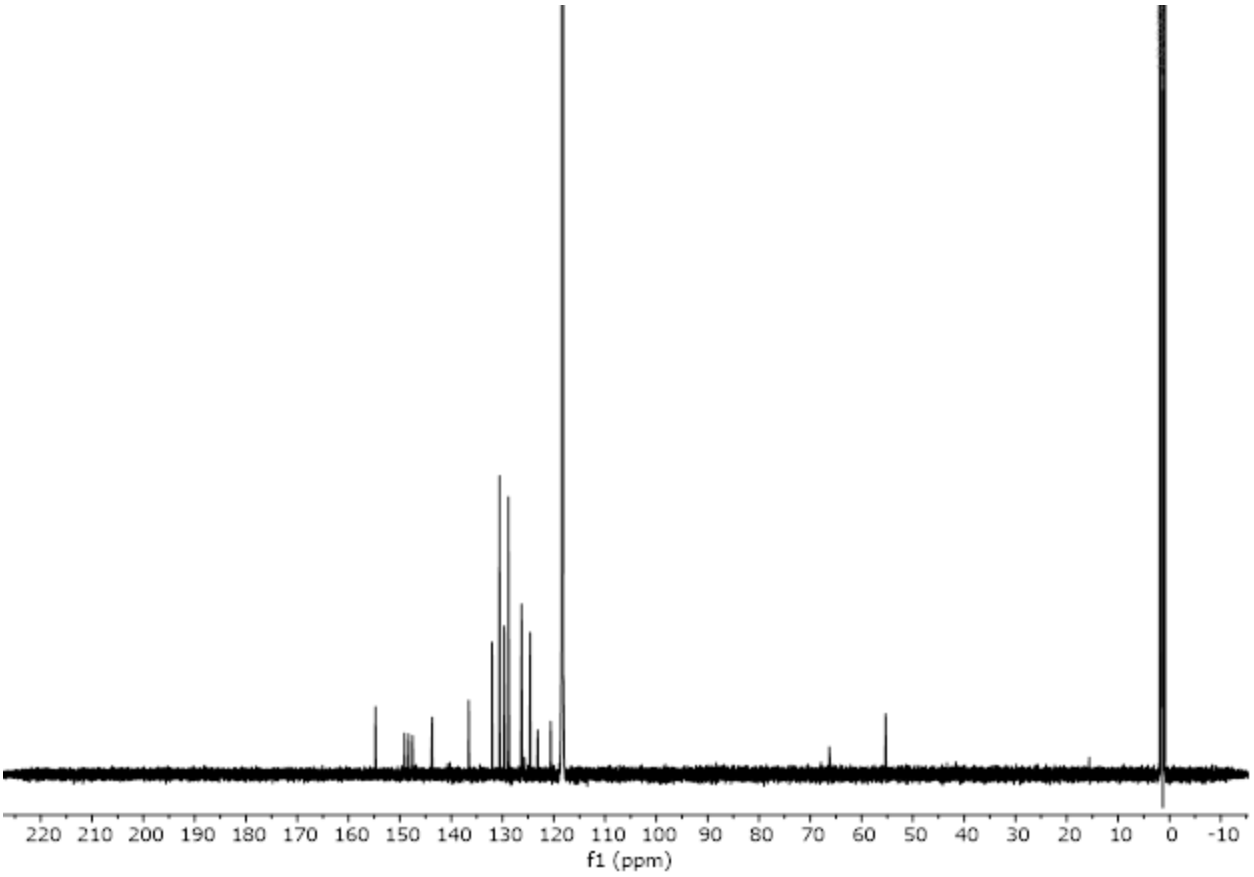

Figure S17. $^{13}C\{^{1}H\}$ NMR spectrum for **5[OTf]$_2$** (CD_3CN, 126 MHz, 298K). The spectrum is referenced to the residual acetonitrile solvent signal at 1.32 ppm.

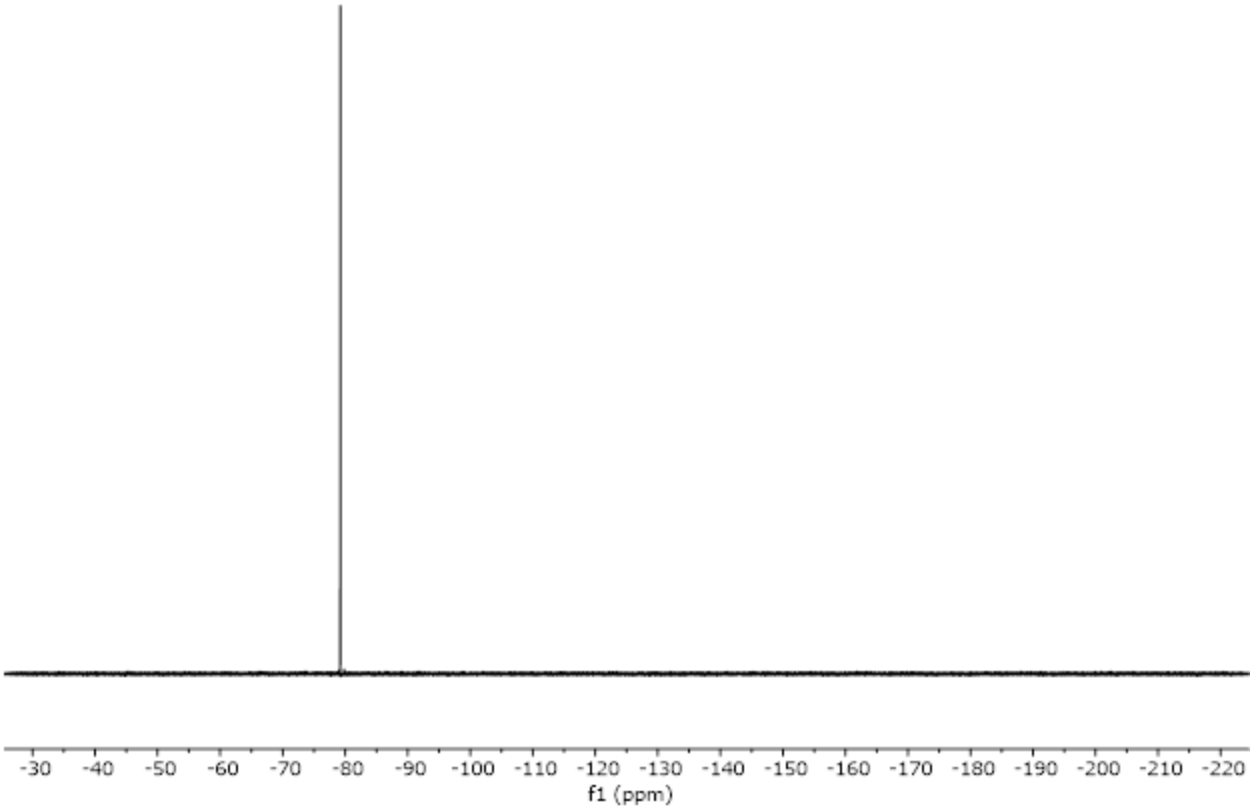

Figure S18. $^{19}F\{^{1}H\}$ NMR spectrum for **5[OTf]$_2$** (CD_3CN, 377 MHz, 298K).

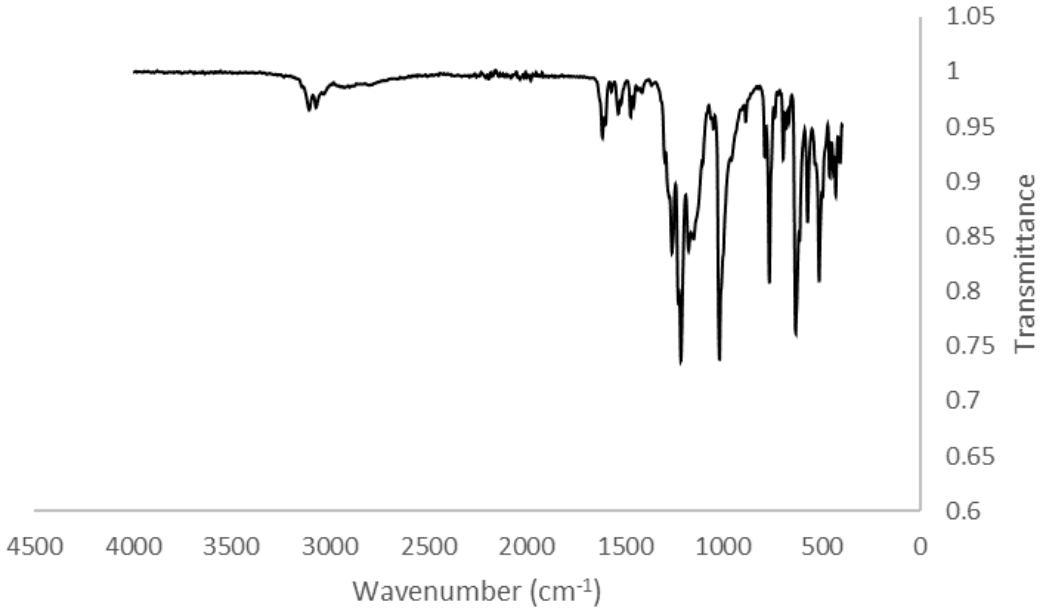

Figure S19. FTIR-ATR spectrum for **5[OTf]$_2$**.

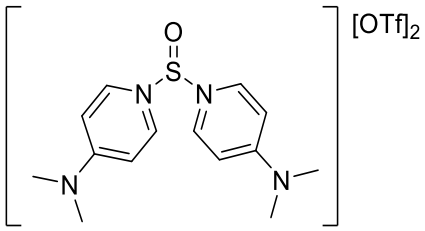

[Bis(4-Dimethylaminopyridine)SO][Trifluoromethanesulfonate]$_2$ (6[OTf]$_2$):

To a stirring solution of thionyl chloride (0.265 mL, 3.65 mmol) and trimethylsilyl trifluoromethanesulfonate (1.33 mL, 7.33 mmol) in 4 mL dichloromethane was added 4-dimethylaminopyridine (0.900 g, 7.37 mmol) in 4 mL dichloromethane over a period of 5 minutes at room temperature. After 1 hour precipitate formation was observed, and the solution was stirred for an additional hour. After cooling at -40^{o}C over night, the dichloromethane was decanted off and the resulting white powder was washed with cold dichloromethane (2 x 5 mL) and n-pentane (2 x 5 mL). Upon drying under vacuum, **6[OTf]$_2$** was isolated as an off-white powder (1.96 g, 3.32 mmol, 91% yield). Suitable crystals for single-crystal X-ray diffraction were grown from a layered solution of acetonitrile and diethyl ether at -40^{o}C.

^{1}H NMR (CD_3CN, 500 MHz, 298K): 8.38 (d, $^3J_{H\text{-}H}$ = 8.1 Hz, C(N(CH_3)$_2$)-C*H*, 4H), 7.02 (d, $^3J_{H\text{-}H}$ = 8.1 Hz, N-C*H*, 4H), 3.28 (s, N(C*H*$_3$)$_2$, 12H).

^{13}C{^{1}H} NMR (CD_3CN, 126 MHz, 298K): δ (ppm) 159.3, 134.7, 121.9 (q, $^1J_{C\text{-}F}$ = 320 Hz, OTf-*C*F$_3$), 109.8, 41.8.

^{19}F NMR (CD_3CN, 377 MHz, 298K): δ (ppm) -78.4 (s, 6F, OTf).

FTIR data (cm^{-1}): 1269 (S-O stretch).

Elemental Analysis (calc'd./expt.): C (32.54/32.57), H (3.41/3.37), N (9.49/9.63).

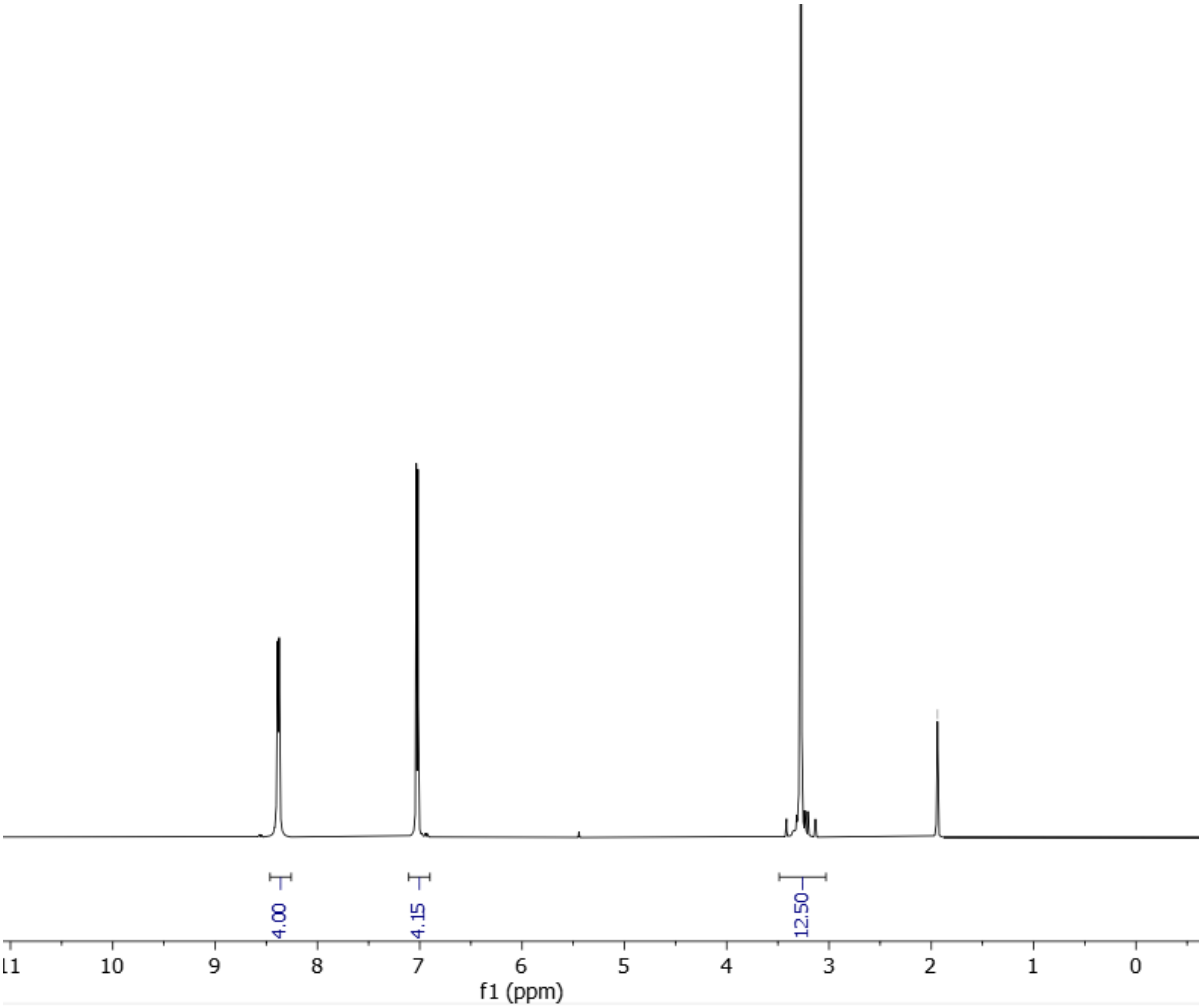

Figure S20. ^{1}H NMR spectrum for **6[OTf]$_2$** (CD_3CN, 500 MHz, 298K). The spectrum is referenced to the residual acetonitrile solvent signal at 1.94 ppm.

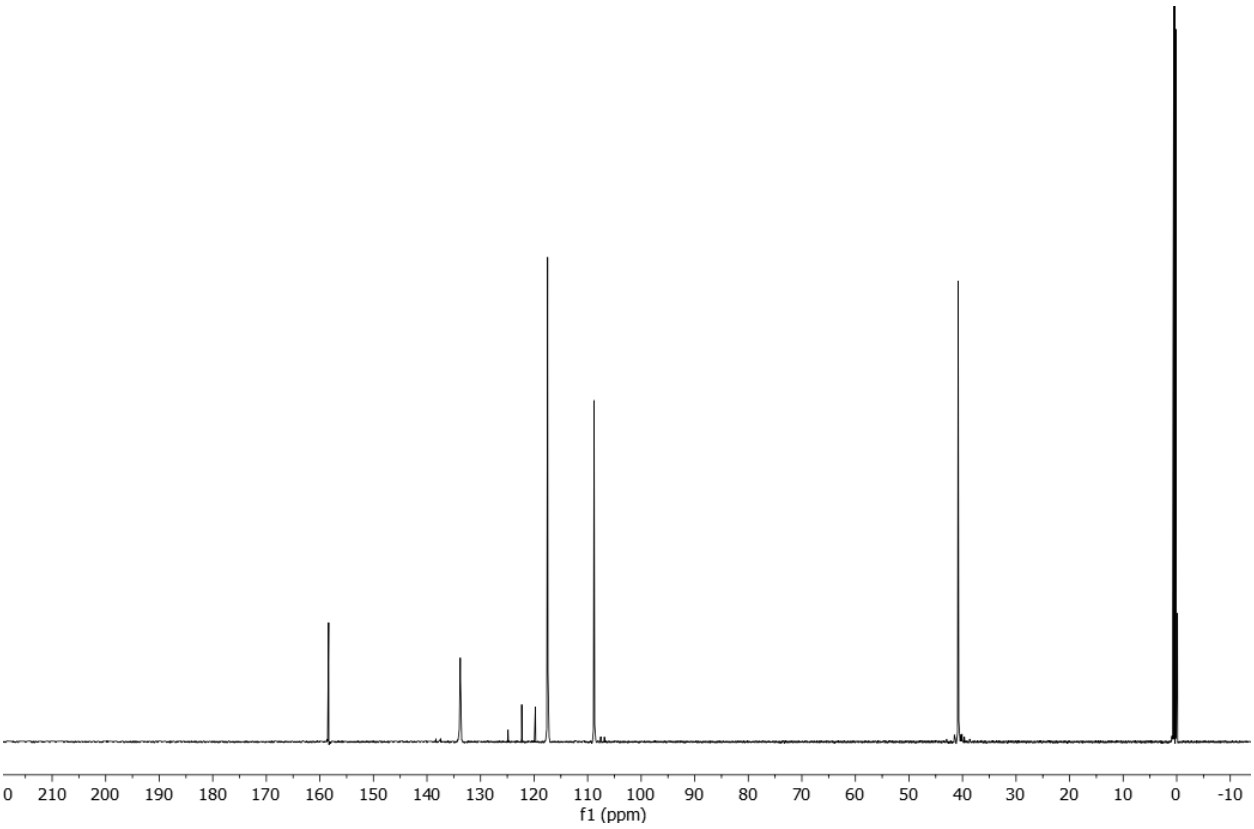

Figure S21. $^{13}C\{^{1}H\}$ NMR spectrum for **6[OTf]$_2$** (CD_3CN, 126 MHz, 298K). The spectrum is referenced to the residual acetonitrile solvent signal at 1.32 ppm.

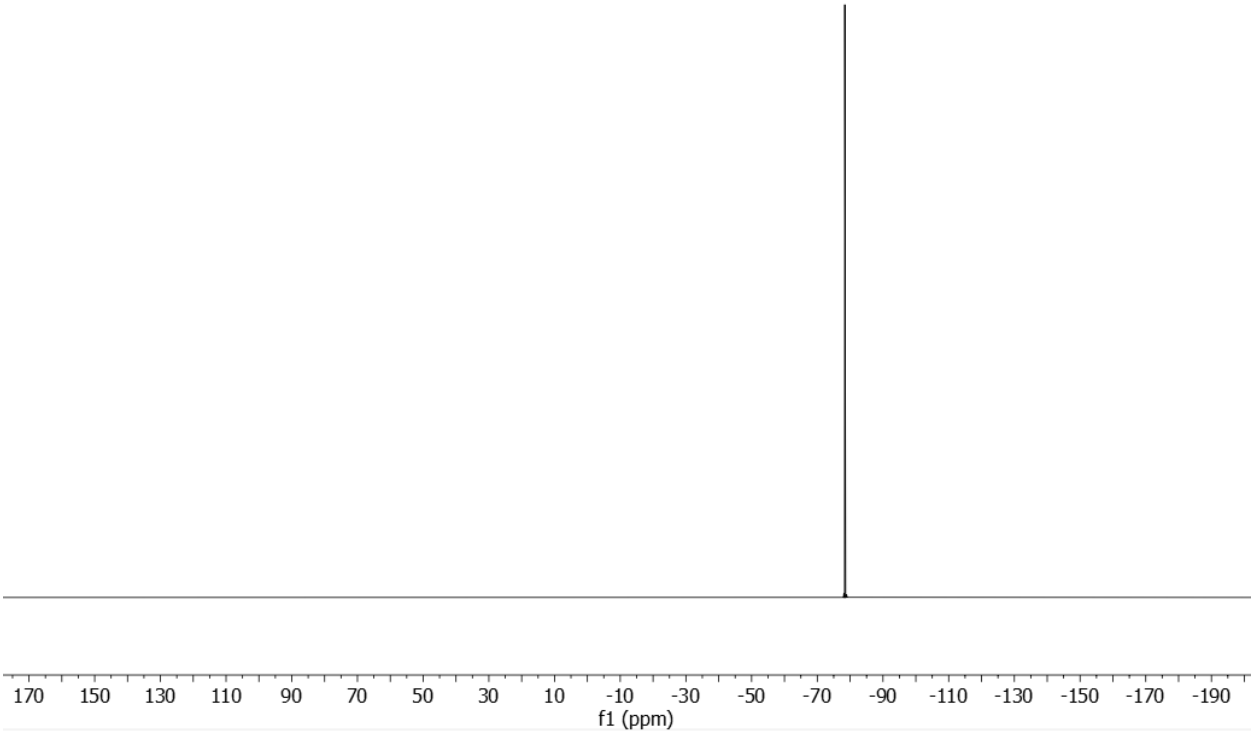

Figure S22. $^{19}F\{^{1}H\}$ NMR spectrum for **6[OTf]$_2$** (CD_3CN, 377 MHz, 298K).

4. Other Experimental Procedures

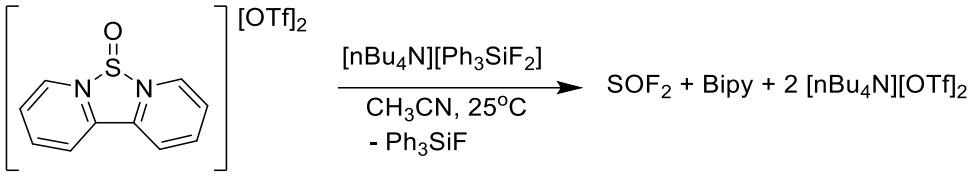

Reaction of 1[OTf]$_2$ with [*n*Bu$_4$N][Ph$_3$SiF$_2$]:

To a stirring solution of **1[OTf]$_2$** (20 mg, 0.040 mmol) ina acetonitrile (0.5 mL) was added [*n*Bu$_4$N][Ph$_3$SiF$_2$] (42.9 mg, 0.080 mmol) in acetonitrile (0.5 mL). The clear and colourless reaction was stirred for 1 hour and the reaction progress was monitored using ^{1}H and ^{19}F NMR spectroscopy. NMR spectroscopic data indicate the quantitative formation of Ph$_3$SiF (-170 ppm by ^{19}F NMR), 2,2'-bipyridine (8.64 ppm, 8.40 ppm, 7.89 ppm, and 7.38 ppm by ^{1}H NMR data), and SOF$_2$ (72 ppm by ^{19}F NMR data).

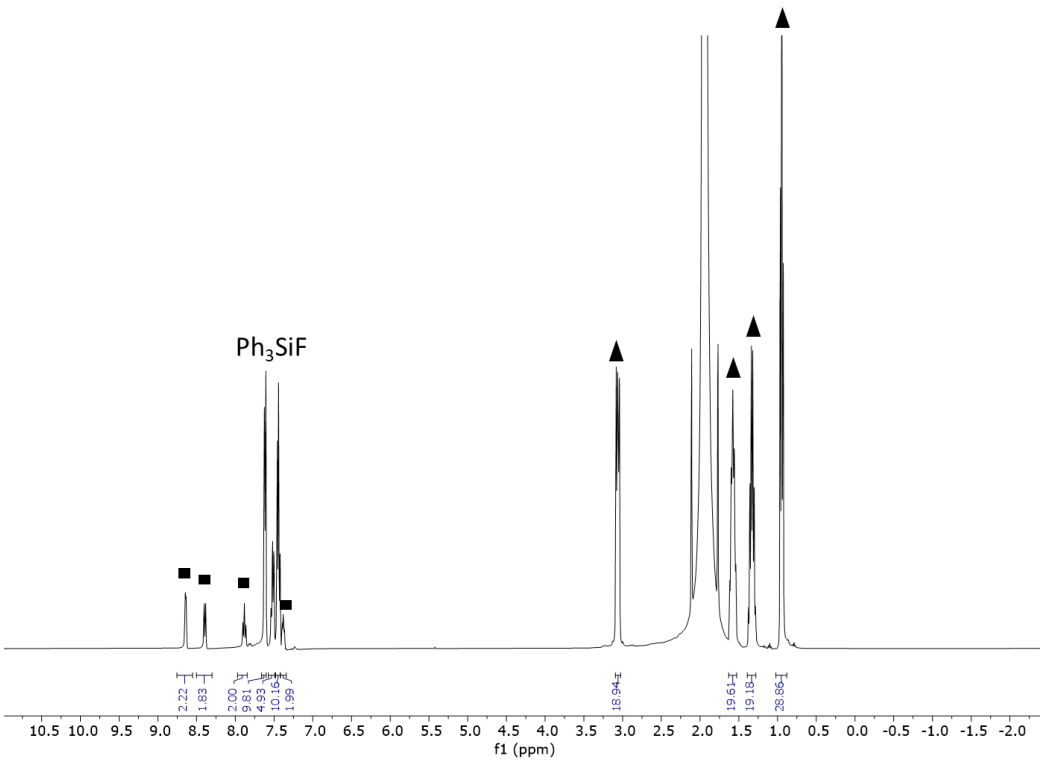

Figure S23. ^{1}H NMR spectrum of the reaction between **1[OTf]$_2$** and [*n*Bu$_4$N][Ph$_3$SiF$_2$] (CH$_3$CN, 400 MHz, 298K). The spectrum is referenced to the CH$_3$CN signal at 1.94 ppm. Squares: Bipy, triangles: [*n*Bu$_4$N][OTf].

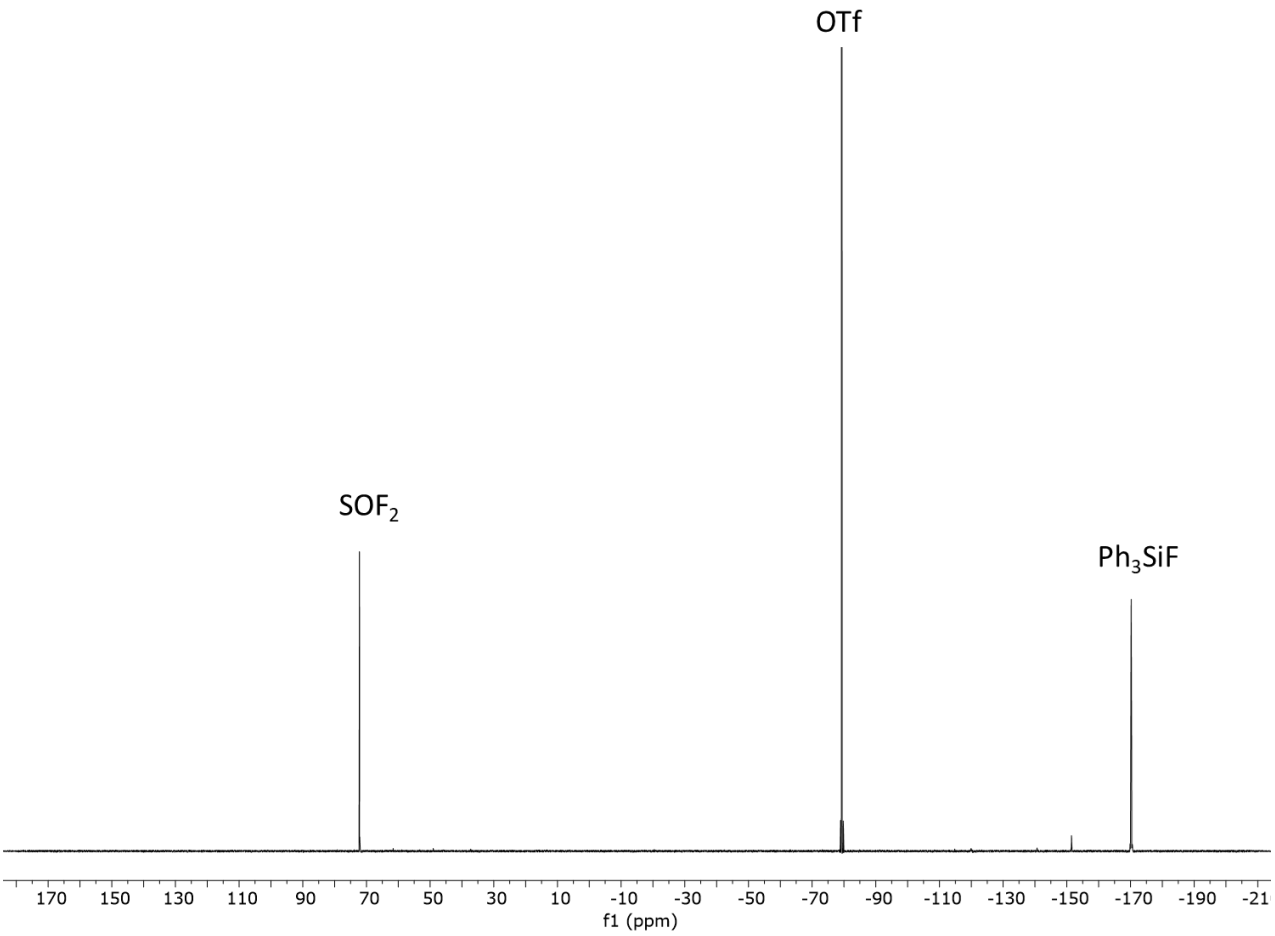

Figure S24. $^{19}F\{^{1}H\}$ NMR spectrum of the reaction between **1[OTf]$_2$** and [*n*Bu$_4$N][Ph$_3$SiF$_2$] (CH$_3$CN, 377 MHz, 298K).

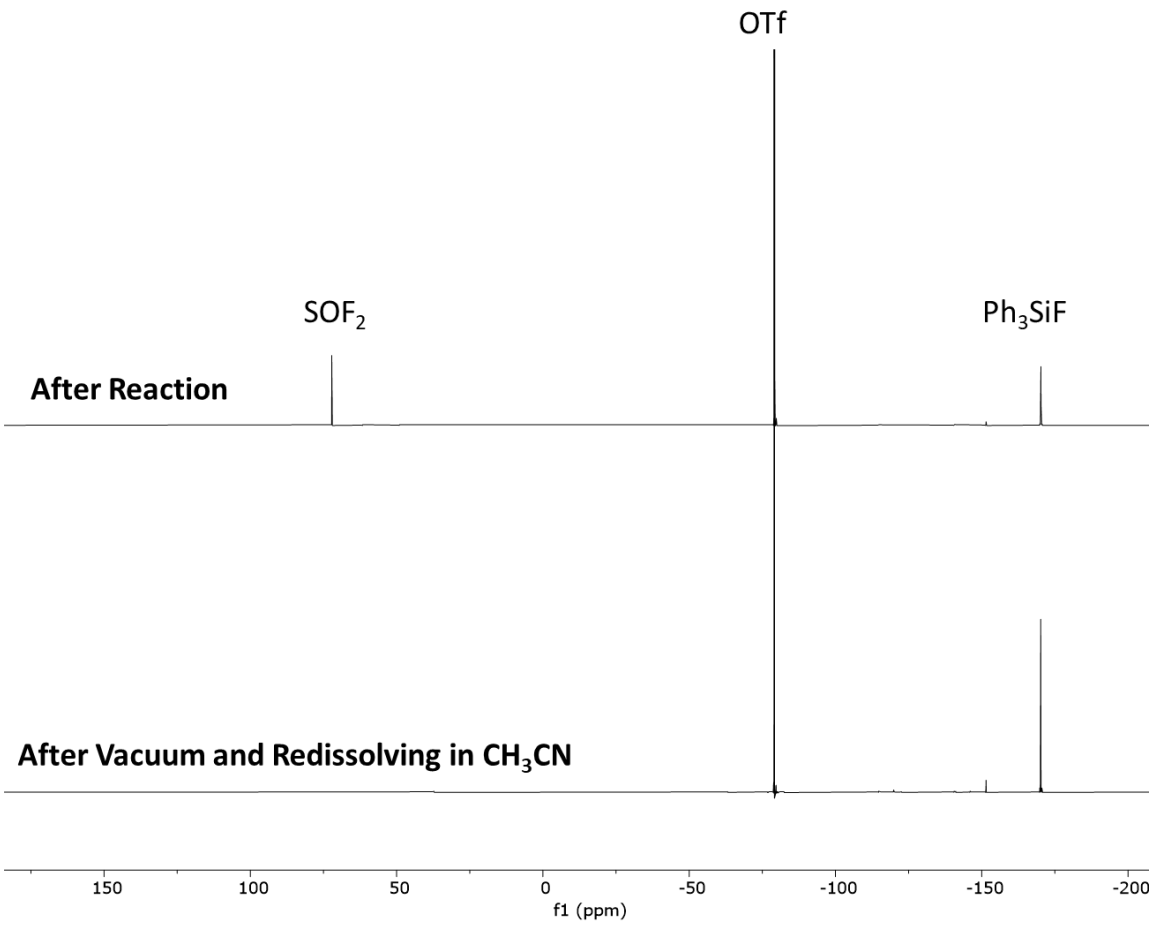

Figure S25. Stacked $^{19}F\{^{1}H\}$ NMR spectra of the reaction between **1[OTf]$_2$** and [*n*Bu$_4$N][Ph$_3$SiF$_2$] (CH$_3$CN, 377 MHz, 298K) before and after applying vacuum to the completed reaction mixture.

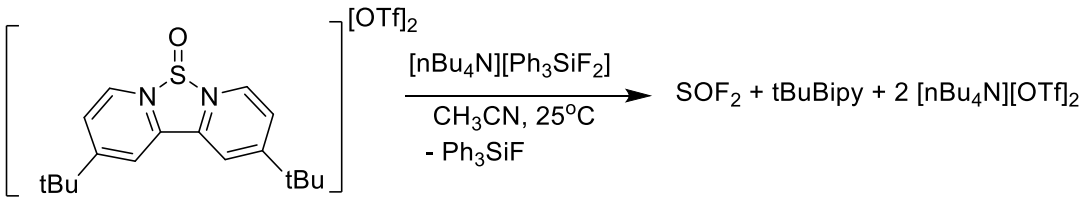

Reaction of 2[OTf]$_2$ with [*n*Bu$_4$N][Ph$_3$SiF$_2$]:

To a stirring solution of **2[OTf]$_2$** (20 mg, 0.033 mmol) in acetonitrile (0.5 mL) was added [*n*Bu$_4$N][Ph$_3$SiF$_2$] (17.6 mg, 0.033 mmol) in acetonitrile (0.5 mL). The clear and colourless reaction was stirred for 1 hour and the reaction progress was monitored using ^{1}H and ^{19}F NMR spectroscopy. NMR spectroscopic data indicate the quantitative formation of Ph$_3$SiF (-169.4 ppm

from the ^{19}F NMR data), [*n*Bu$_4$N][OTf] (3.05 ppm, 1.59 ppm, 1.34 ppm, 0.95 ppm from the ^{1}H NMR data and -78.4 ppm from the ^{19}F NMR data), and SOF_2 (72.7 ppm from the ^{19}F NMR data). Removal of the solvent *in vacuo* and then redissolving of the residue led to a disappearance of the ^{19}F NMR signal for SOF_2 (72.7 ppm). One set of broadened 4,4′-di-*tert*-butyl-2,2′-dipyridine signals (9.07 ppm, 8.72 ppm, 7.97 ppm, 1.44 ppm from the ^{1}H NMR data) shifted downfield from free *t*BuBipy suggests an equilibrium process between the formed free *t*BuBipy and the remaining **2[OTf]$_2$**.

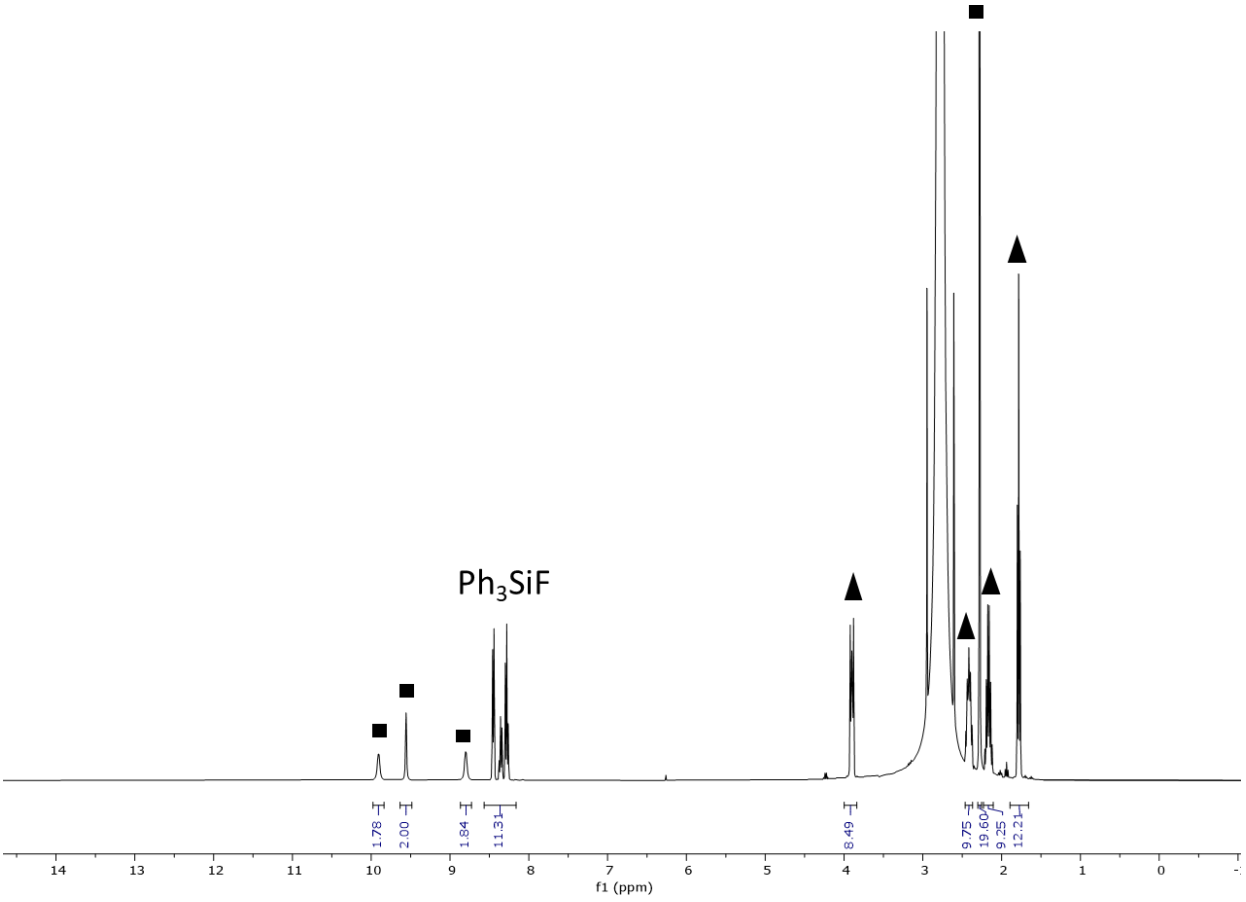

Figure S26. ^{1}H NMR spectrum of the reaction between **2[OTf]$_2$** and [*n*Bu$_4$N][Ph$_3$SiF$_2$] (CH_3CN, 400 MHz, 298K). The spectrum is referenced to the CH_3CN signal at 1.94 ppm. Squares: *t*BuBipy fragment, triangles: [*n*Bu$_4$N][OTf].

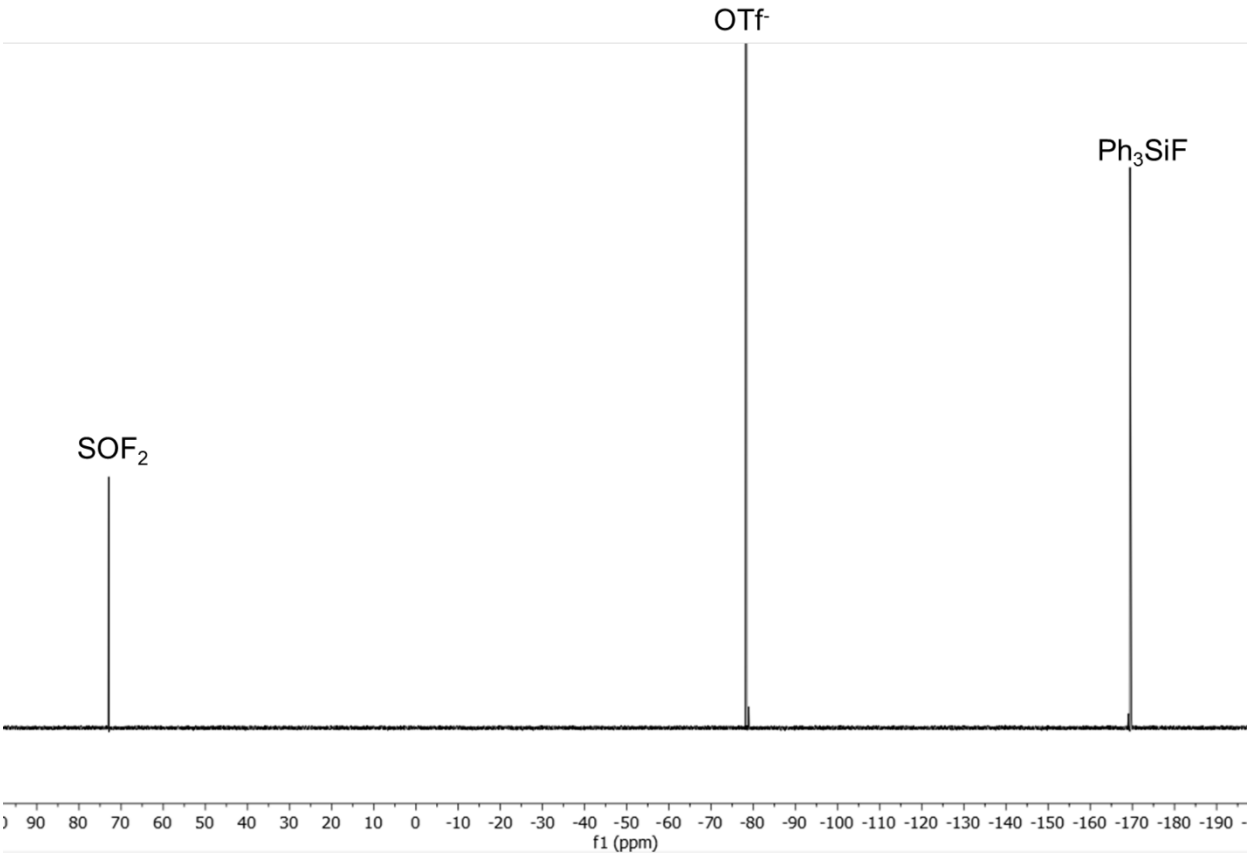

Figure S27. $^{19}F\{^{1}H\}$ NMR spectrum of the reaction between **2[OTf]$_2$** and [*n*Bu$_4$N][Ph$_3$SiF$_2$] (CH$_3$CN, 377 MHz, 298K).

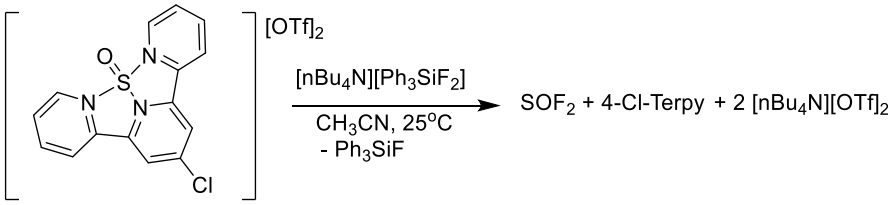

Reaction of 4[OTf]$_2$ with [*n*Bu$_4$N][Ph$_3$SiF$_2$]:

To a stirring solution of **4[OTf]$_2$** (20 mg, 0.033 mmol) in acetonitrile (0.5 mL) was added [*n*Bu$_4$N][Ph$_3$SiF$_2$] (17.6 mg, 0.033 mmol) in acetonitrile (0.5 mL). The clear and colourless reaction was stirred for 1 hour and the reaction progress was monitored using ^{1}H and ^{19}F NMR spectroscopy. NMR spectroscopic data indicate the quantitative formation of Ph$_3$SiF (-169.3 ppm from the ^{19}F NMR data), 4-Cl-Terpyridine (see ^{1}H NMR spectrum), [*n*Bu$_4$N][OTf] (3.05 ppm,

1.59 ppm, 1.34 ppm, 0.95 ppm from the ^{1}H NMR data and -78.4 ppm from the ^{19}F NMR data), SOF_2 (72.9 ppm from the ^{19}F NMR data), and a remaining 0.5 equivalent of **4[OTf]$_2$**.

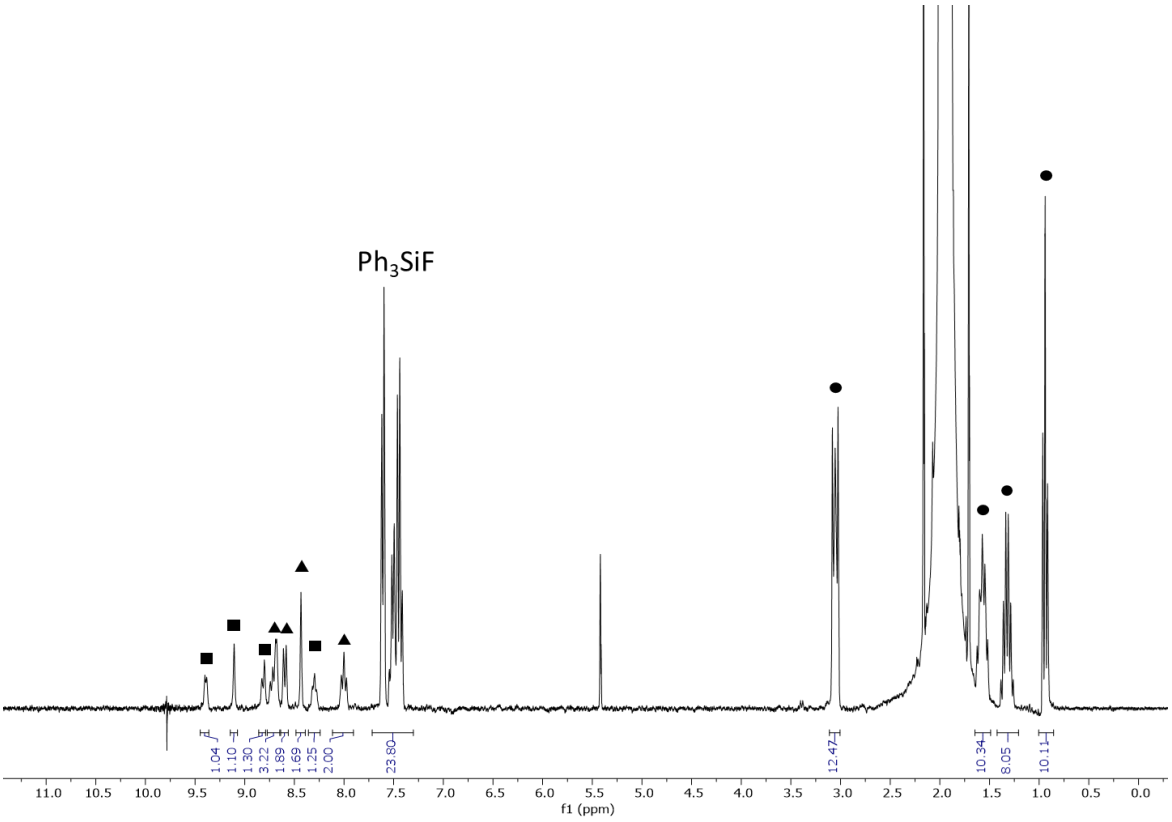

Figure S28. ^{1}H NMR spectrum of the reaction between **4[OTf]$_2$** and [*n*Bu$_4$N][Ph$_3$SiF$_2$] (CH_3CN, 400 MHz, 298K). The spectrum is referenced to the CH_3CN signal at 1.94 ppm. Squares: **4[OTf]$_2$**, Triangles: Free 4-Cl-Terpy, circles: [*n*Bu$_4$N][OTf]

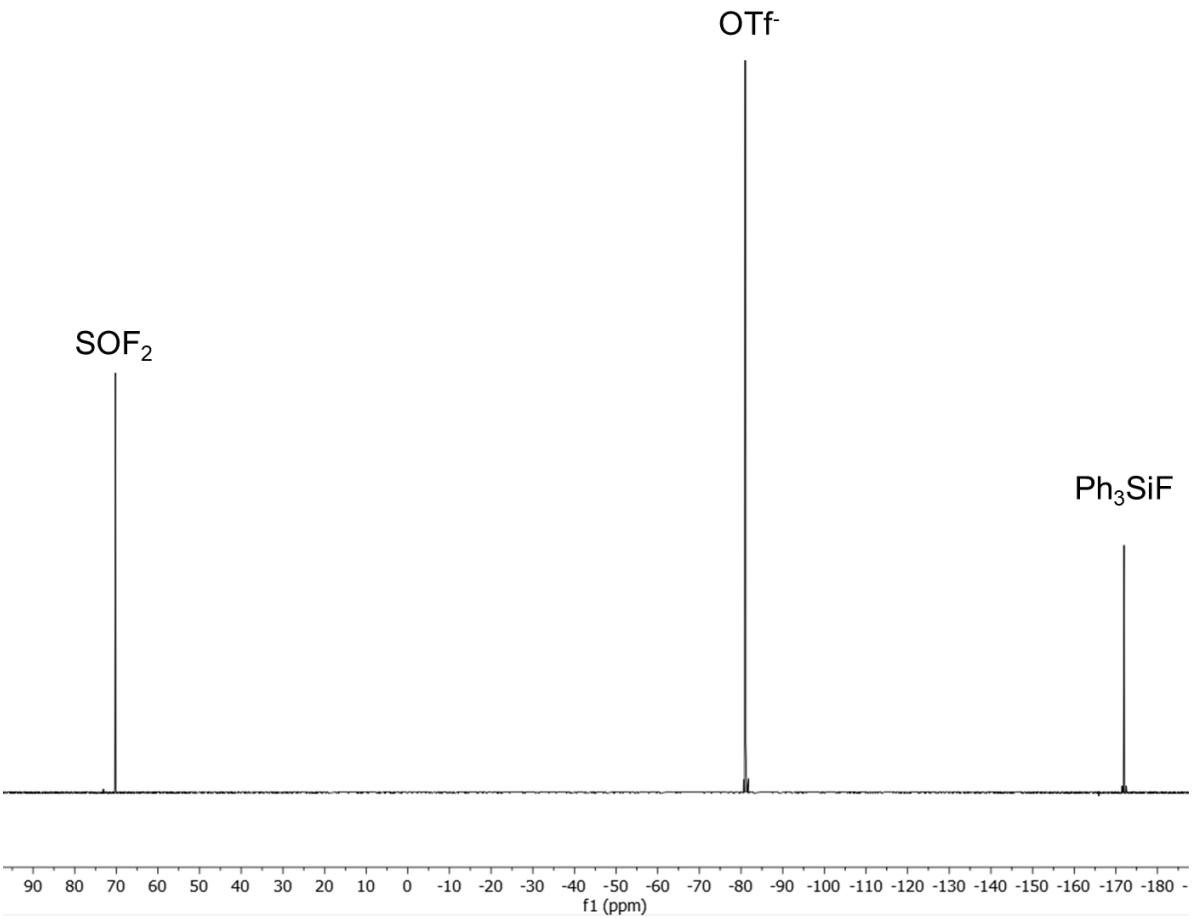

Figure S29. $^{19}F\{^{1}H\}$ NMR spectrum of the reaction between **4[OTf]$_2$** and [*n*Bu$_4$N][Ph$_3$SiF$_2$] (CH$_3$CN, 377 MHz, 298K).

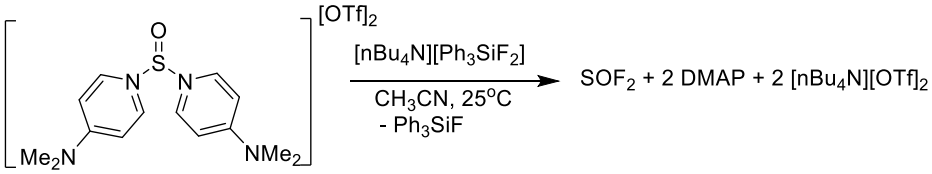

Reaction of 6[OTf]$_2$ with 1 eq. [*n*Bu$_4$N][Ph$_3$SiF$_2$]:

To a stirring solution of **6[OTf]$_2$** (15 mg, 0.025 mmol) in acetonitrile (0.5 mL) was added [*n*Bu$_4$N][Ph$_3$SiF$_2$] (13.7 mg, 0.025 mmol) in acetonitrile (0.5 mL). The clear and colourless reaction was stirred for 1 hour and the reaction progress was monitored using ^{1}H and ^{19}F NMR spectroscopy. NMR spectroscopic data indicate the quantitative formation of Ph$_3$SiF (-169.2 ppm

from the ^{19}F NMR data), [*n*Bu$_4$N][OTf] (3.05 ppm, 1.59 ppm, 1.34 ppm, 0.95 ppm from the ^{1}H NMR data and -78.4 ppm from the ^{19}F NMR data), and SOF_2 (72.7 ppm from the ^{19}F NMR data). Only one set of broadened DMAP signals is observed (8.21 ppm, 6.74 ppm, 3.09 ppm from the ^{1}H NMR data), shifted slightly downfield from free DMAP, indicating an equilibrium process between free DMAP and **6[OTf]$_2$**. A minor byproduct is observed (45.7 ppm in the ^{19}F NMR spectrum), suggesting the potential intermediate formed from the addition of one fluoride to **6[OTf]$_2$**.

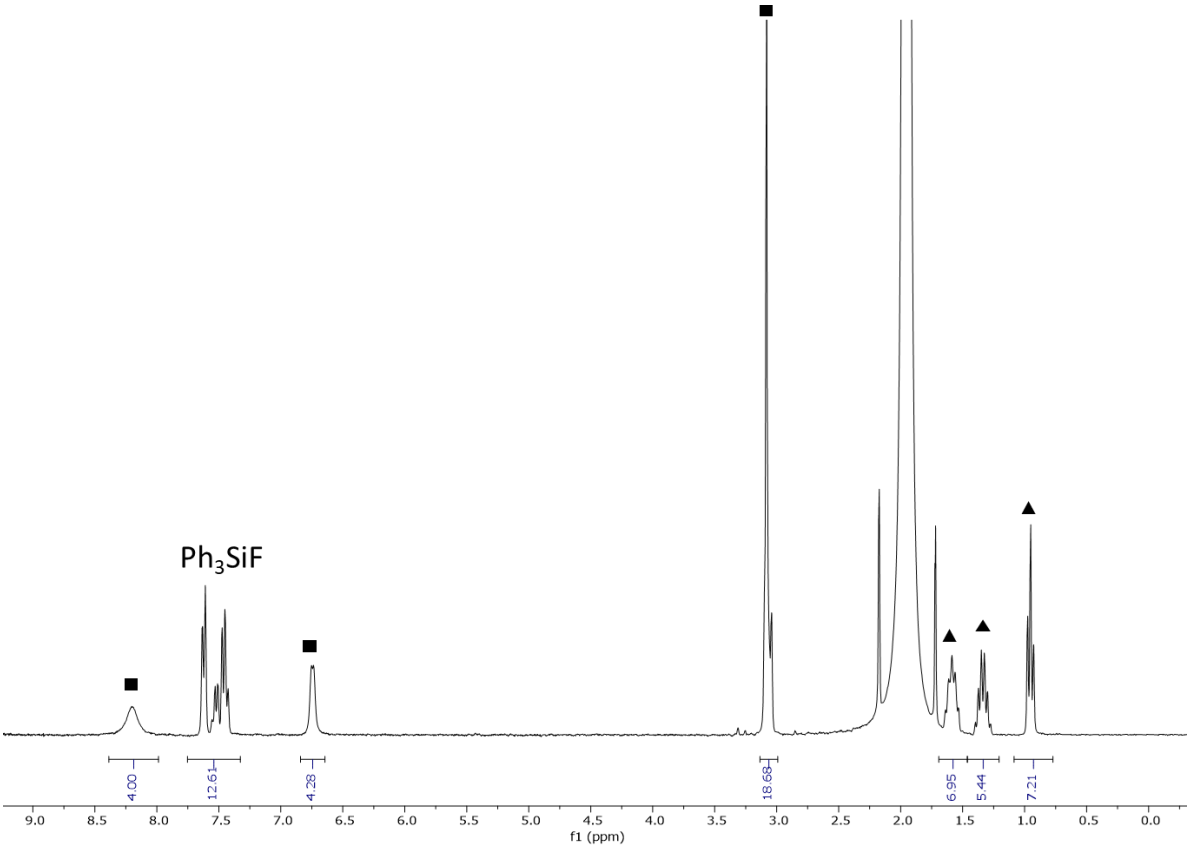

Figure S30. ^{1}H NMR spectrum of the reaction between **6[OTf]$_2$** and [*n*Bu$_4$N][Ph_3SiF_2] (CH_3CN, 400 MHz, 298K). The spectrum is referenced to the CH_3CN signal at 1.94 ppm. Squares: DMAP fragment, triangles: [*n*Bu$_4$N][OTf]

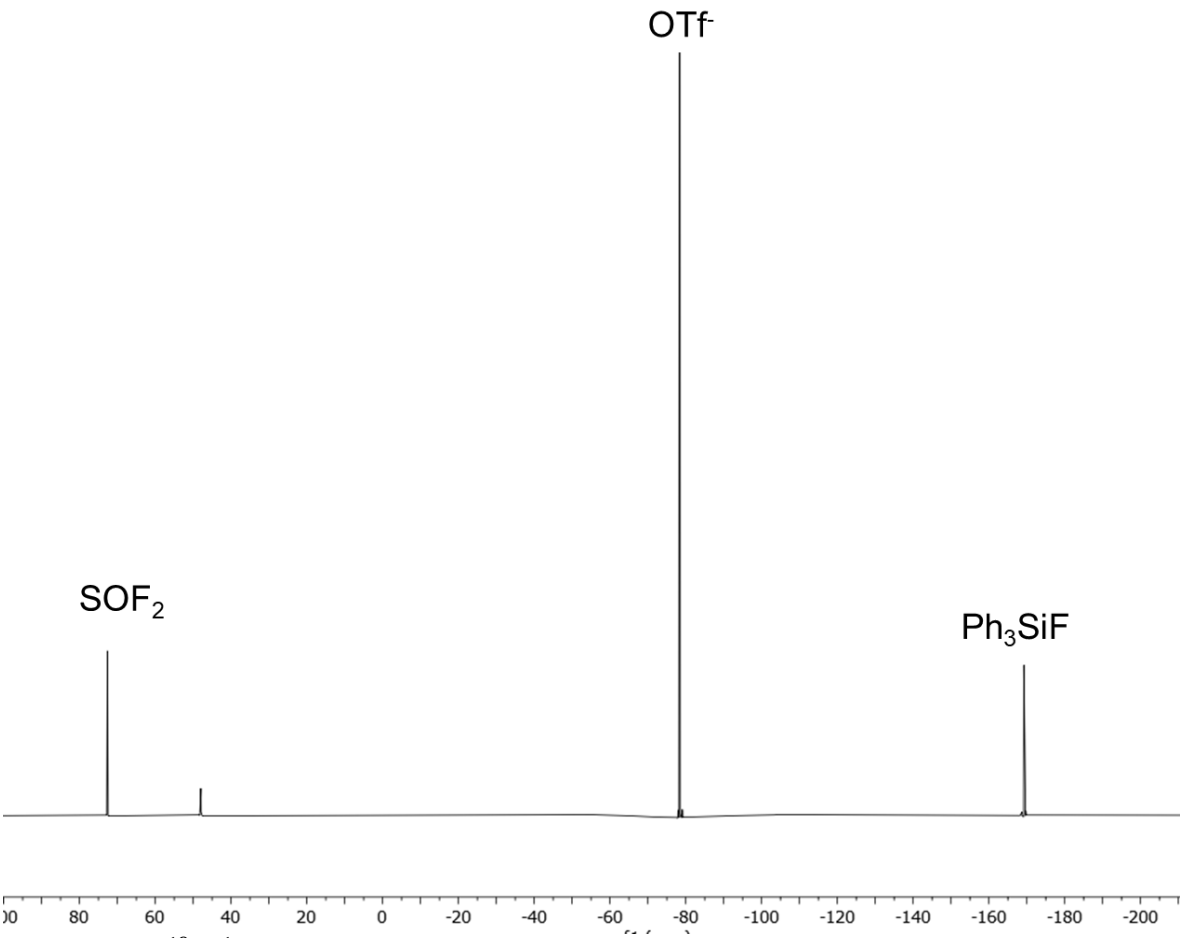

Figure S31. $^{19}F\{^{1}H\}$ NMR spectrum of the reaction between **6[OTf]$_2$** and [*n*Bu$_4$N][Ph$_3$SiF$_2$] (CH$_3$CN, 377 MHz, 298K).

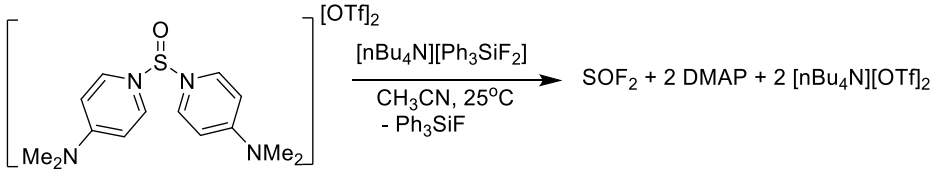

Reaction of 6[OTf]$_2$ with 2 eq. [*n*Bu$_4$N][Ph$_3$SiF$_2$]:

To a stirring solution of **6[OTf]$_2$** (15 mg, 0.025 mmol) in acetonitrile (0.5 mL) was added [*n*Bu$_4$N][Ph$_3$SiF$_2$] (27.5 mg, 0.051 mmol) in acetonitrile (0.5 mL). The clear and colourless reaction was stirred for 1 hour and the reaction progress was monitored using ^{1}H and ^{19}F NMR spectroscopy. NMR spectroscopic data indicate the quantitative formation of Ph$_3$SiF (-169 ppm from the ^{19}F NMR data), N,N'-dimethylaminopyridine (8.09 ppm, 6.54 ppm, 2.94 ppm from the

^{1}H NMR data), [*n*Bu$_4$N][OTf] (3.05 ppm, 1.59 ppm, 1.34 ppm, 0.95 ppm from the ^{1}H NMR data and -78.4 ppm from the ^{19}F NMR data), and SOF_2 (72.6 ppm from the ^{19}F NMR data).

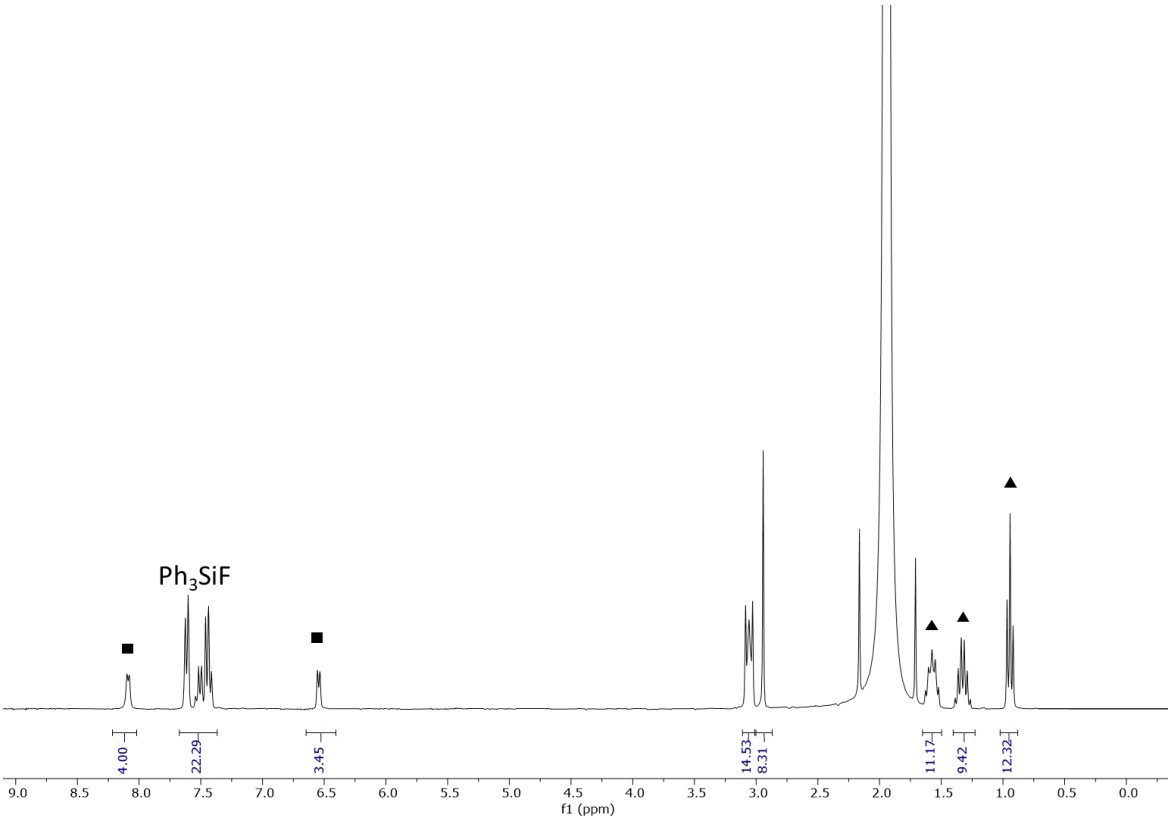

Figure S32. ^{1}H NMR spectrum of the reaction between **6[OTf]$_2$** and 2 equivalents of [*n*Bu$_4$N][Ph_3SiF_2] (CH_3CN, 400 MHz, 298K). The spectrum is referenced to the CH_3CN signal at 1.94 ppm. Squares: DMAP, triangles: [*n*Bu$_4$N][OTf].

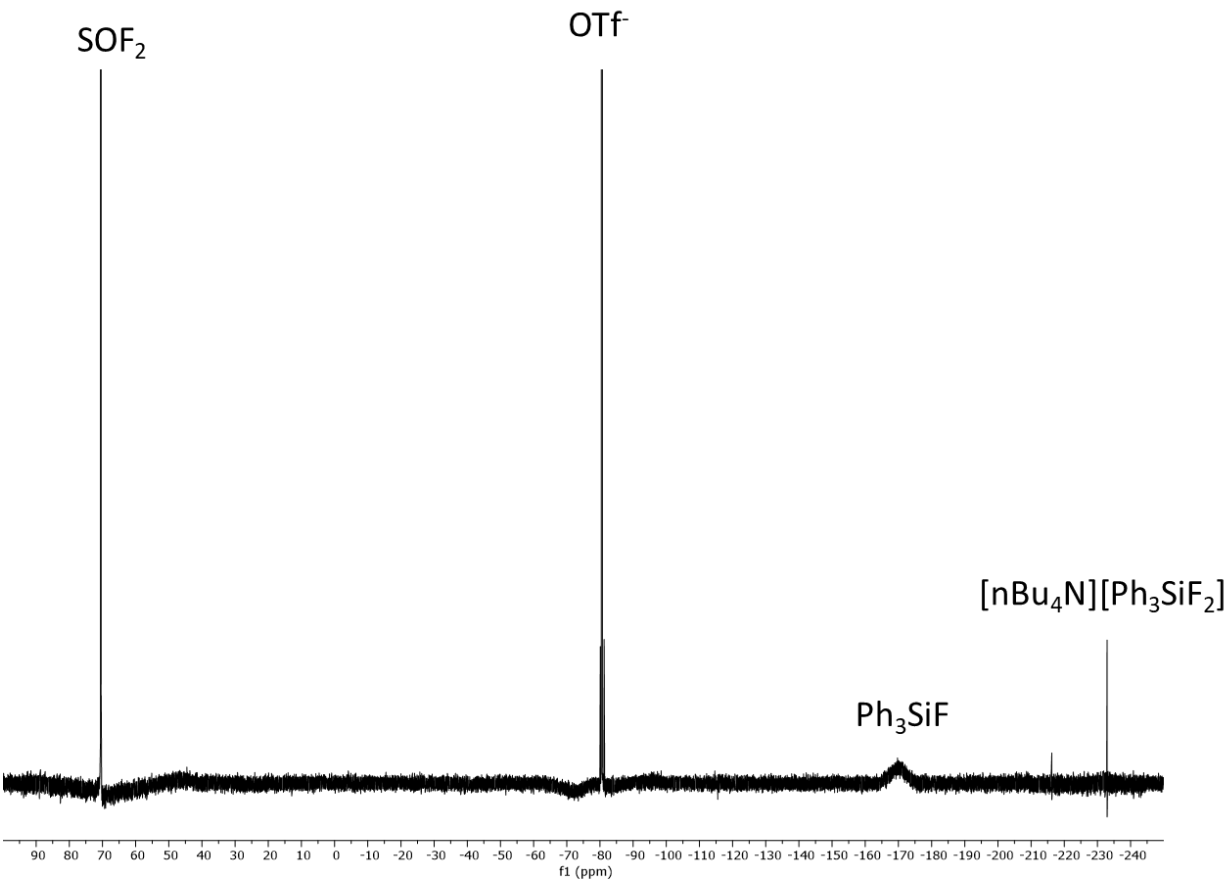

Figure S33. $^{19}F\{^{1}H\}$ NMR spectrum of the reaction between **6[OTf]$_2$** and 2 equivalents of [nBu$_4$N][Ph$_3$SiF$_2$] (CH$_3$CN, 377 MHz, 298K).

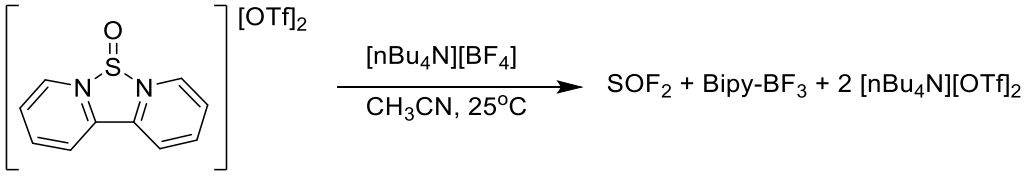

Reaction of 1[OTf]$_2$ with 1 eq. [*n*Bu$_4$N][BF$_4$]:

To a stirring solution of **1[OTf]$_2$** (10 mg, 0.020 mmol) in acetonitrile (0.5 mL) was added [*n*Bu$_4$N][BF$_4$] (6.6 mg, 0.020 mmol) in acetonitrile (0.5 mL). The colourless reaction was stirred for 16 hours and the reaction progress was monitored using ^{1}H and ^{19}F NMR spectroscopy. Consumption of the BF$_4$ fragment was observed and the following were observed by the NMR data: SOF$_2$ (72 ppm from the ^{19}F NMR data), ligand-stabilized BF$_3$ fragments (-154.5 ppm from

the ^{19}F NMR data, 5.1 ppm and -0.8 ppm from ^{11}B NMR data), [nBu_nN][OTf] (3.05 ppm, 1.59 ppm, 1.34 ppm, 0.95 ppm from the ^{1}H NMR data and -78.4 ppm from the ^{19}F NMR data). New ^{1}H NMR resonances are downfield of free 2,2'-bipyridine, suggesting coordination to the BF_3 generated in the reaction

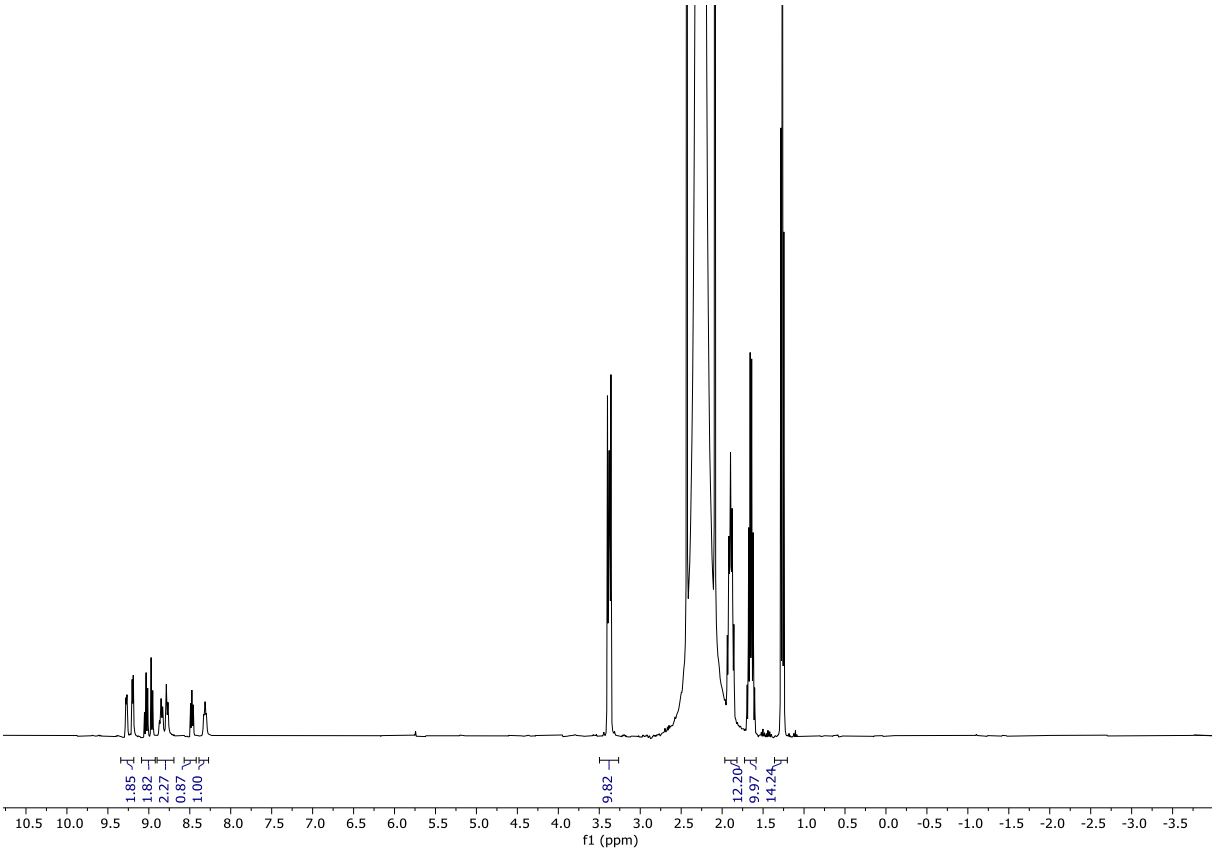

Figure S34. ^{1}H NMR spectrum for the reaction between **1[OTf]$_2$** and 1 eq. [*n*Bu_4N][BF_4] (CH_3CN, 400 MHz, 298K). The spectrum is referenced to the CH_3CN signal at 1.94 ppm.

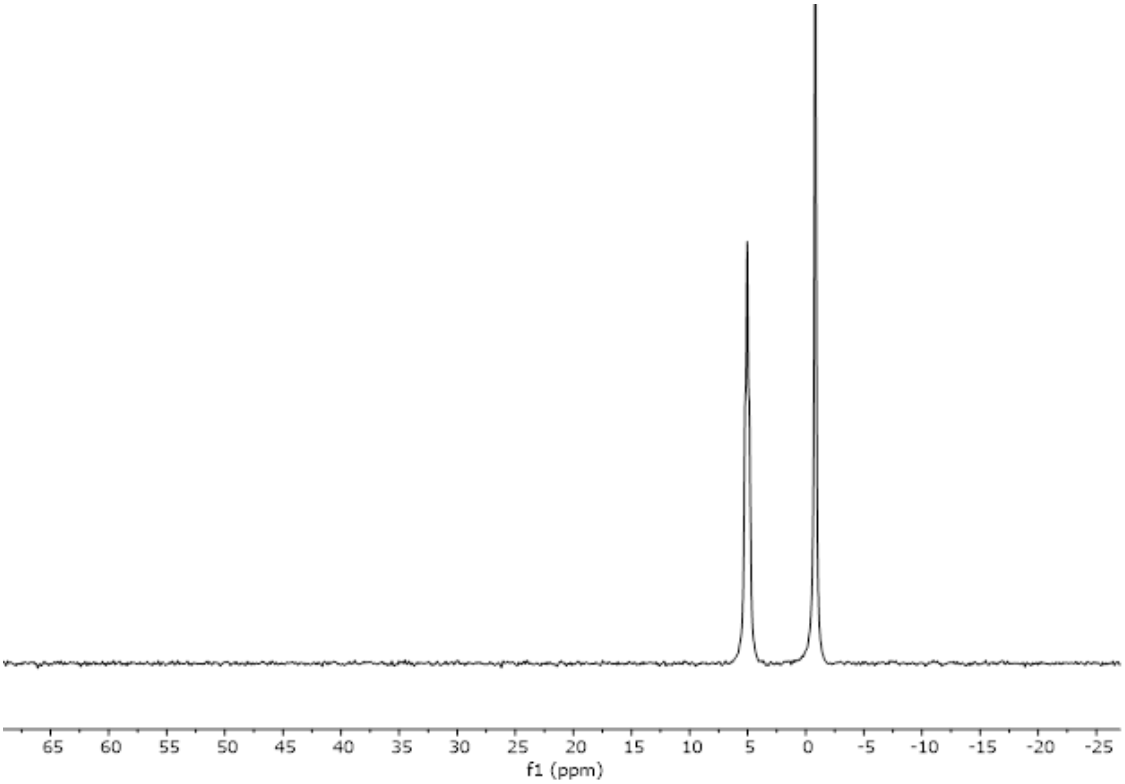

Figure S35. $^{11}B\{^{1}H\}$ NMR spectrum of the reaction between **1[OTf]$_2$** and 1 eq. [*n*Bu$_4$N][BF$_4$] (CH_3CN, 128 MHz, 298K).

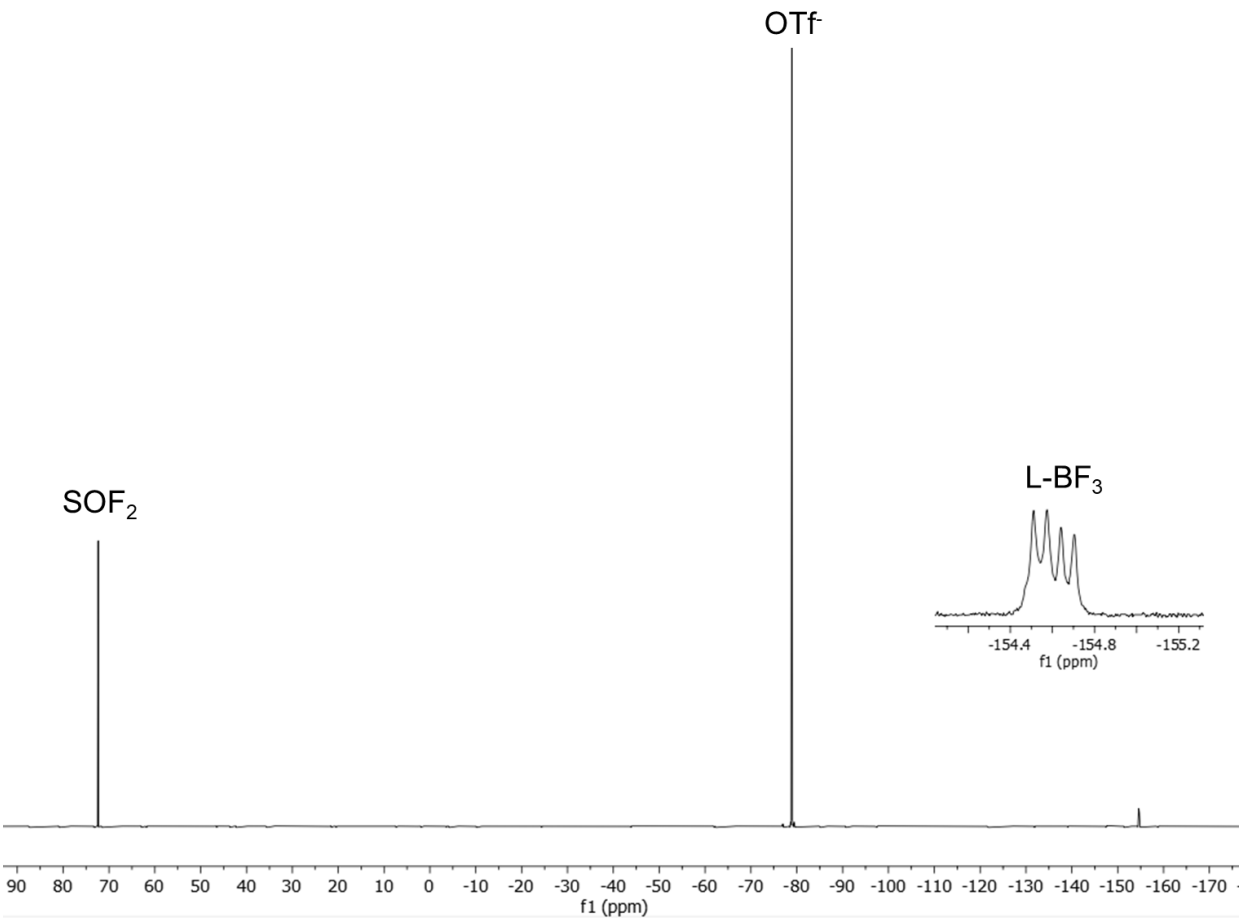

Figure S36. $^{19}F\{^{1}H\}$ NMR spectrum of the reaction between **1[OTf]$_2$** and 1 eq. [*n*Bu$_4$N][BF$_4$] (CH$_3$CN, 377 MHz, 298K).

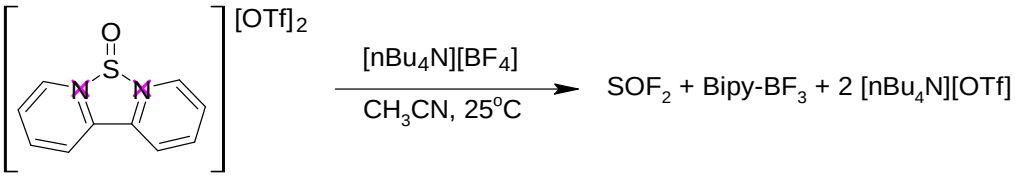

Reaction of 1[OTf]$_2$ with 2 eq. [*n*Bu$_4$N][BF$_4$]:

To a stirring solution of **1[OTf]$_2$** (10 mg, 0.020 mmol) in acetonitrile (0.5 mL) was added [*n*Bu$_4$N][BF$_4$] (13.2 mg, 0.040 mmol) in acetonitrile (0.5 mL). The colourless reaction was stirred for 16 hours and the reaction progress was monitored using ^{1}H and ^{19}F NMR spectroscopy. Consumption of the BF$_4$ fragment was observed and the following were observed by the NMR

data: SOF_2 (72.6 ppm from the ^{19}F NMR data), ligand-stabilized BF_3 fragments (-150 ppm and -154.3 ppm from the ^{19}F NMR data, 5.5 ppm and -0.7 ppm from the ^{11}B NMR data), [nBu_4N][OTf] (3.05 ppm, 1.59 ppm, 1.34 ppm, 0.95 ppm from the ^{1}H NMR data and -78.4 ppm from the ^{19}F NMR data). New ^{1}H NMR resonances are downfield of free 2,2'-bipyridine, suggesting coordination to the BF_3 generated in the reaction.

\

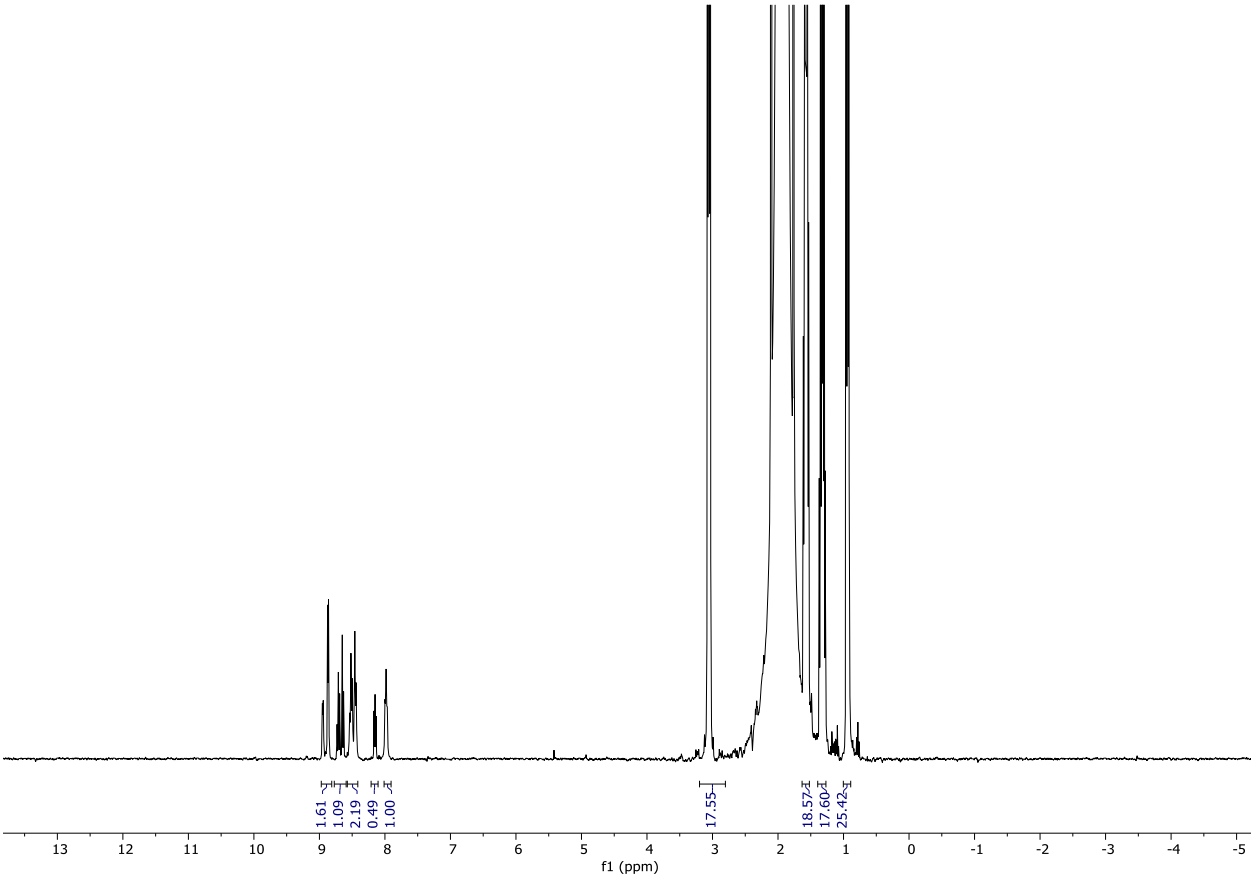

Figure S37. ^{1}H NMR for the reaction between **1[OTf]$_2$** and two equivalents of [*n*Bu_4N][BF_4] (CH_3CN, 400 MHz, 298K).

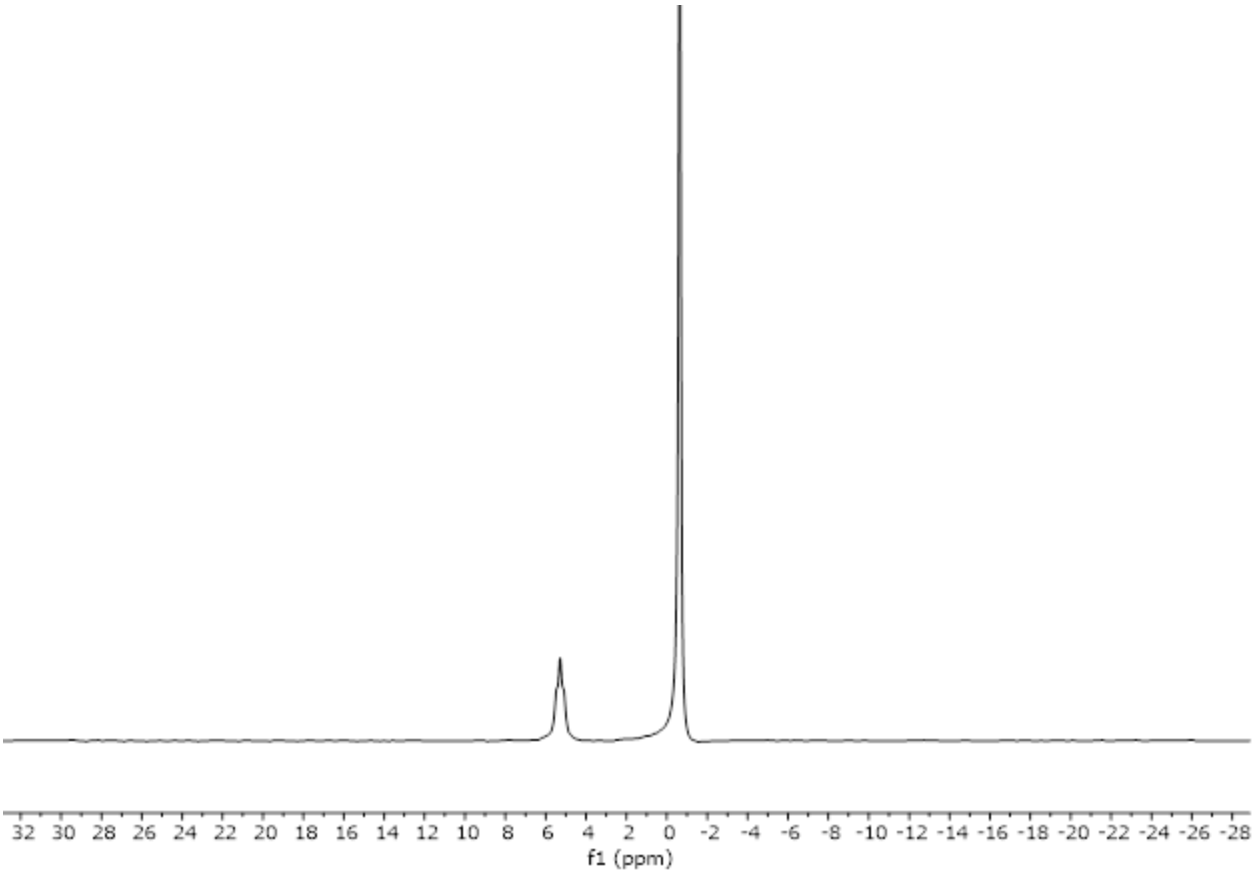

Figure S38. $^{11}B\{^{1}H\}$ NMR spectrum of the reaction between **1[OTf]$_2$** and two equivalents of [*n*Bu$_4$N][BF$_4$] (CH$_3$CN, 128 MHz, 298K).

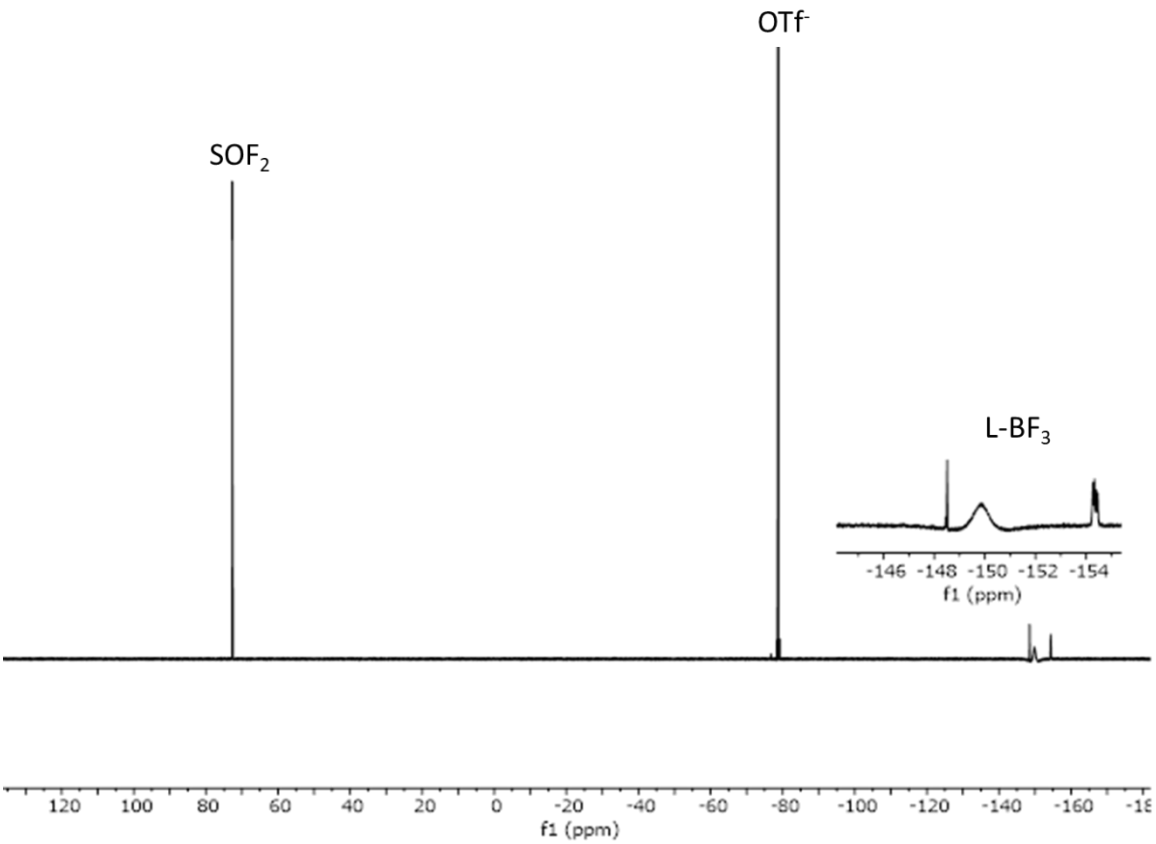

Figure S39. $^{19}F\{^{1}H\}$ NMR spectrum of the reaction between **1[OTf]$_2$** and two equivalents of [*n*Bu$_4$N][BF$_4$] (CH$_3$CN, 128 MHz, 298K).

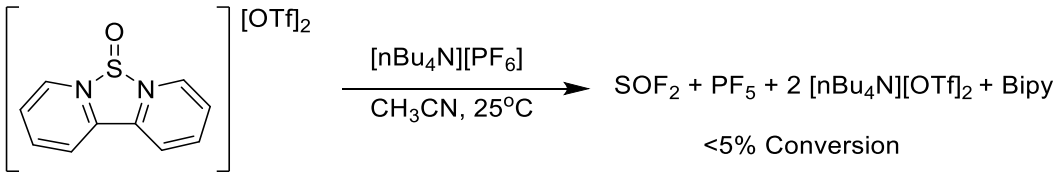

Reaction of 1[OTf]$_2$ with 1 eq. [*n*Bu$_4$N][PF$_6$]:

To a stirring solution of **1[OTf]$_2$** (10 mg, 0.020 mmol) in acetonitrile (0.5 mL) was added [*n*Bu$_4$N][PF$_6$] (7.7 mg, 0.020 mmol) in acetonitrile (0.5 mL). The colourless reaction was stirred for 16 hours and the reaction progress was monitored using ^{1}H and ^{19}F NMR spectroscopy. <5% conversion was observed from the NMR Spectroscopic data, and the following compounds were observed: [*n*Bu$_4$N][PF$_6$] (-72.4 ppm from ^{19}F NMR data, -144.3 ppm from the ^{31}P NMR data), and

SOF_2 (72.9 ppm from the ^{19}F NMR data). The expected PF_5 that would be formed from the generation of SOF_2 is not observed; however, its reported chemical shift overlaps with the observed residual PF_6^- signal in the ^{19}F NMR spectrum.[5] Free **1[OTf]$_2$** is observed as the major remaining product in the ^1H NMR spectrum.

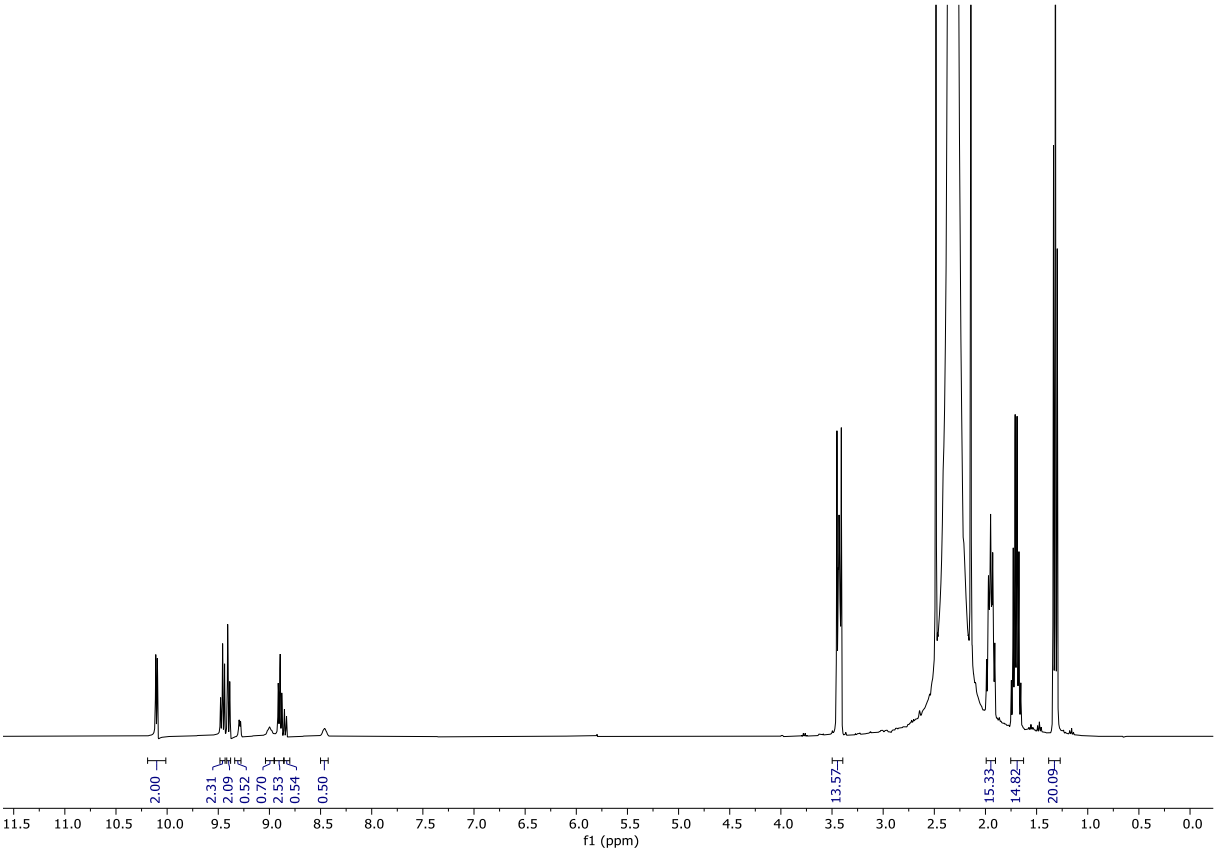

Figure S40. ^1H NMR spectrum for the reaction between **1[OTf]$_2$** and 1 equivalent of [*n*Bu$_4$N][PF_6] (CH_3CN, 400 MHz, 298K).

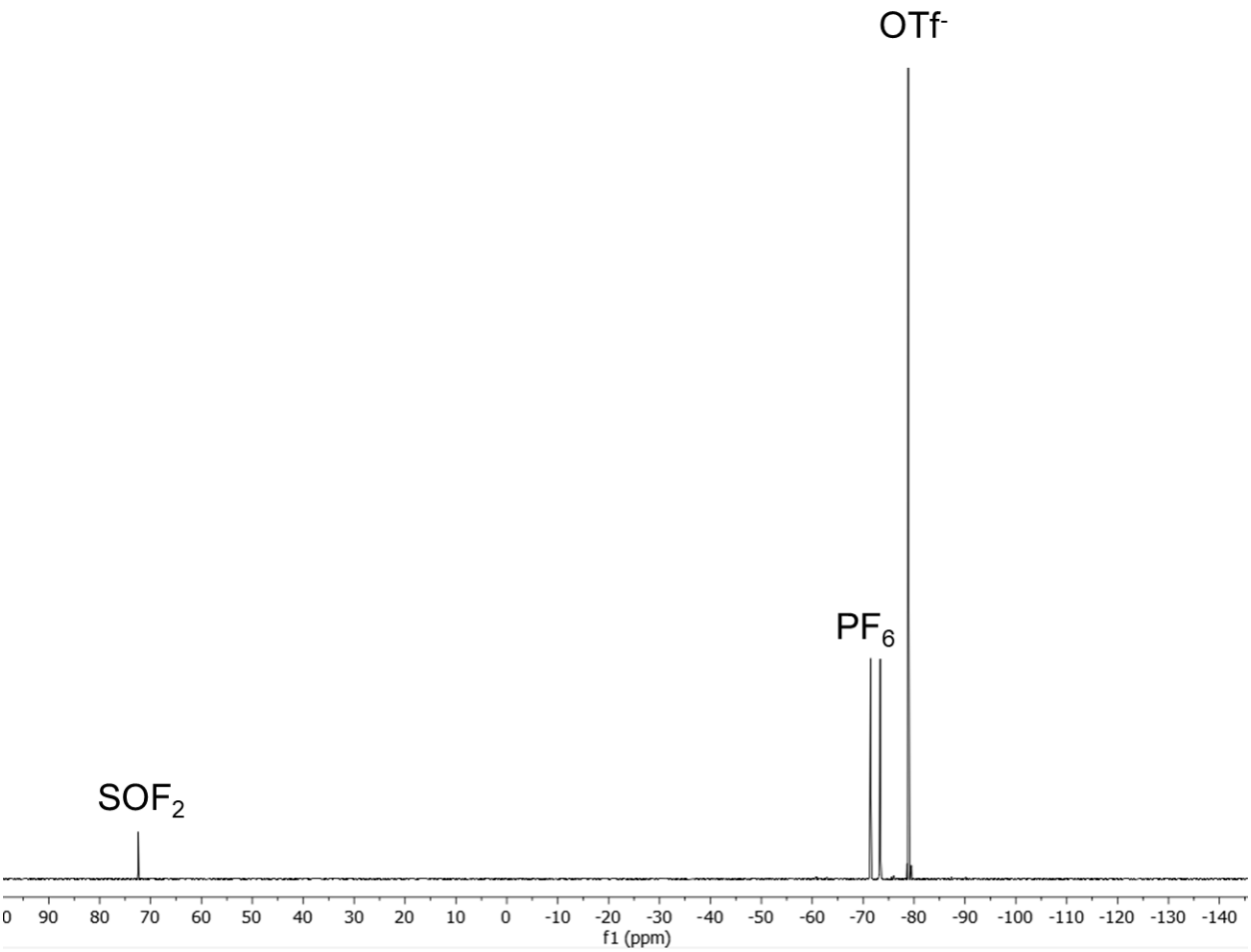

Figure S41. $^{19}F\{^{1}H\}$ for the reaction between **1[OTf]$_2$** and 1 equivalent of [*n*Bu$_4$N][PF$_6$] (CH$_3$CN, 377 MHz, 298K).

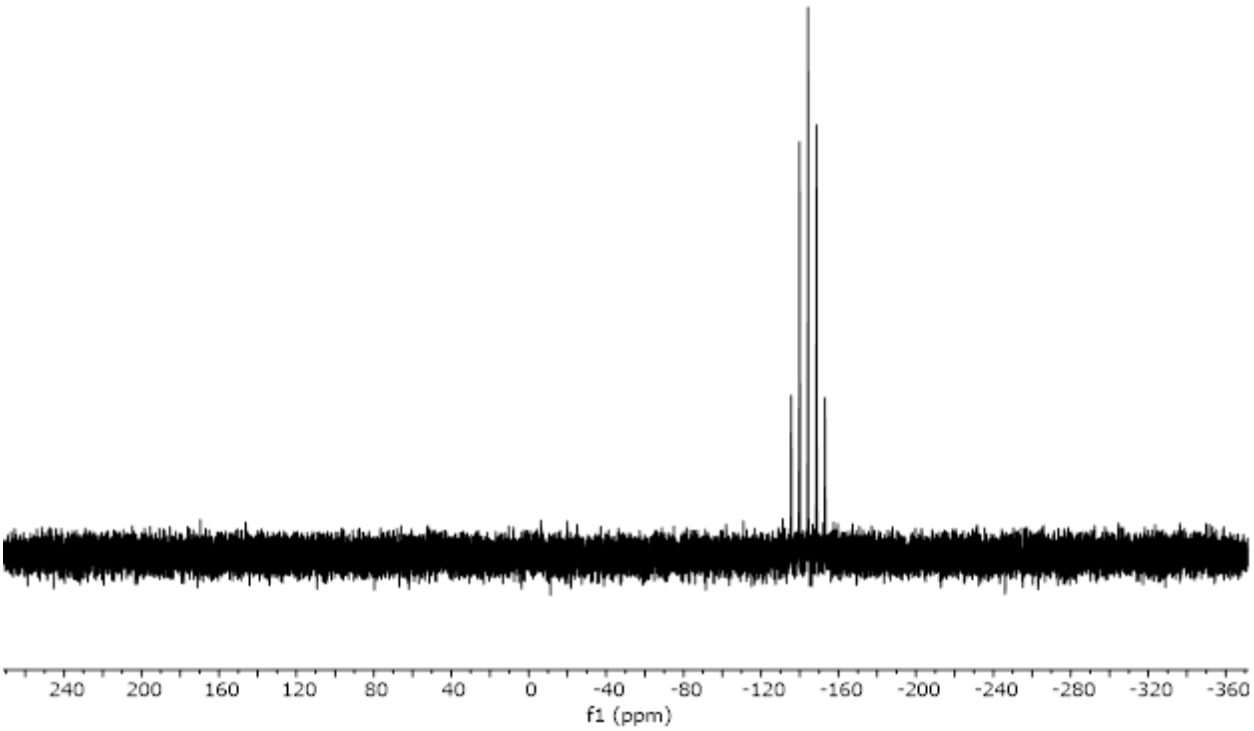

Figure S42. $^{31}P\{^{1}H\}$ NMR spectrum for the reaction between **1[OTf]$_2$** and 1 equivalent [*n*Bu$_4$N][PF$_6$] (CH$_3$CN, 162 MHz, 298K).

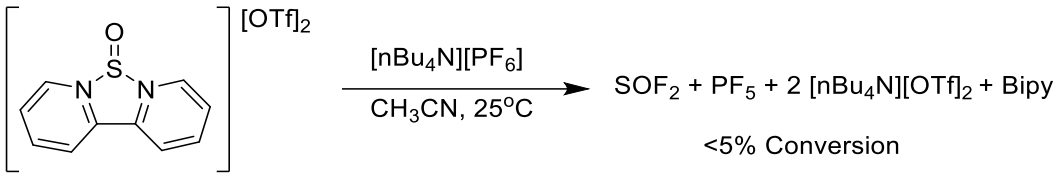

Reaction of 1[OTf]$_2$ with 2 eq. [*n*Bu$_4$N][PF$_6$]:

To a stirring solution of **1[OTf]$_2$** (10 mg, 0.020 mmol) in acetonitrile (0.5 mL) was added [*n*Bu$_4$N][PF$_6$] (15.4 mg, 0.040 mmol) in acetonitrile (0.5 mL). The colourless reaction was stirred for 16 hours and the reaction progress was monitored using ^{1}H and ^{19}F NMR spectroscopy. <5% conversion was observed from the NMR Spectroscopic data, and the following compounds were

observed: [*n*Bu$_4$N][PF$_6$] (-72.2 ppm from ^{19}F NMR data, -144.1 ppm from the ^{31}P NMR data), SOF_2 (72.7 ppm from the ^{19}F NMR data). The expected PF_5 that would be formed from the generation of SOF_2 is not observed; however, its reported chemical shift overlaps with the observed residual PF_6^- signal in the ^{19}F NMR spectrum.[5] Free **1[OTf]$_2$** is observed as the major remaining product in the ^{1}H NMR spectrum.

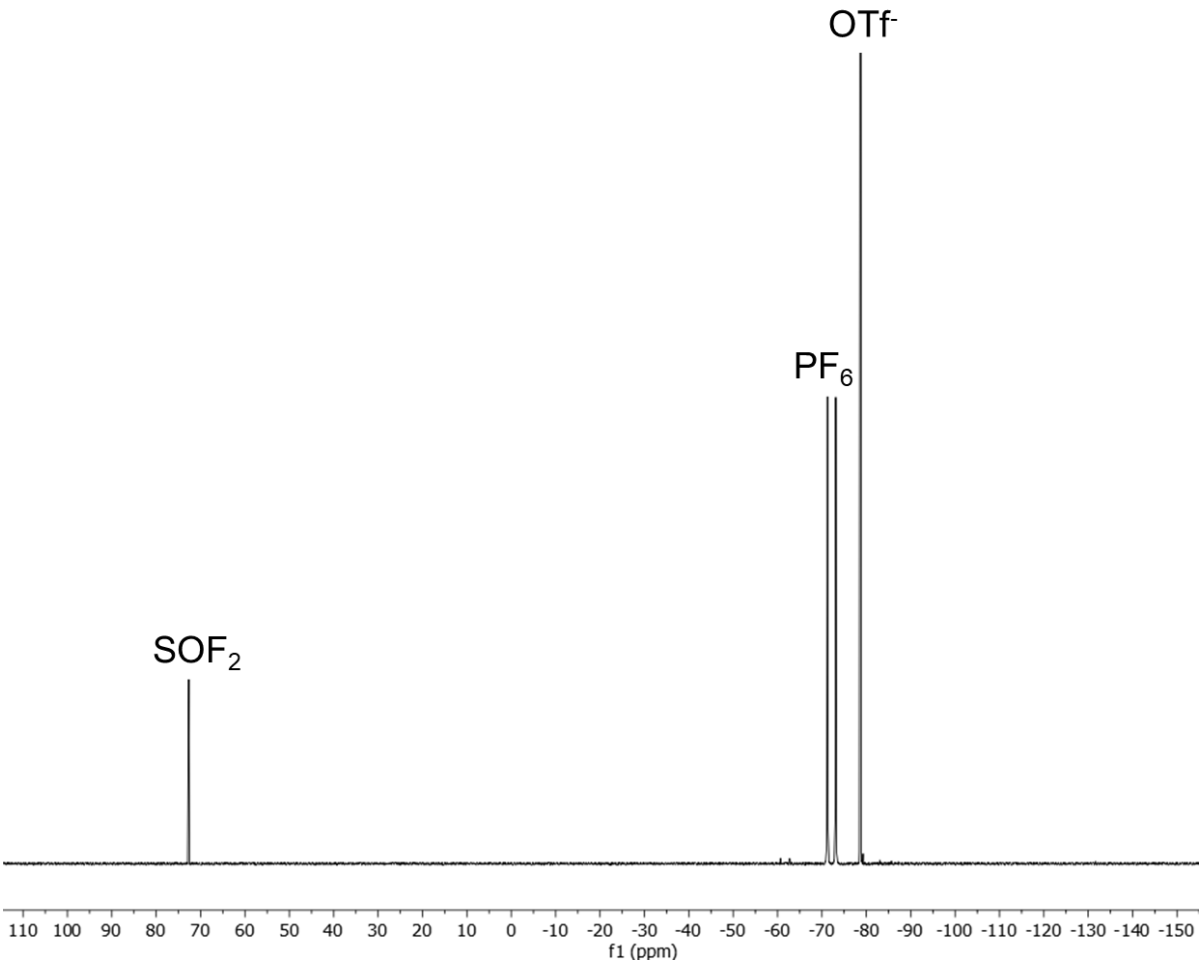

Figure S43. ^{19}F{^{1}H} NMR spectrum for the reaction between **1[OTf]$_2$** and [*n*Bu$_4$N][PF$_6$] (CH_3CN, 377 MHz, 298K).

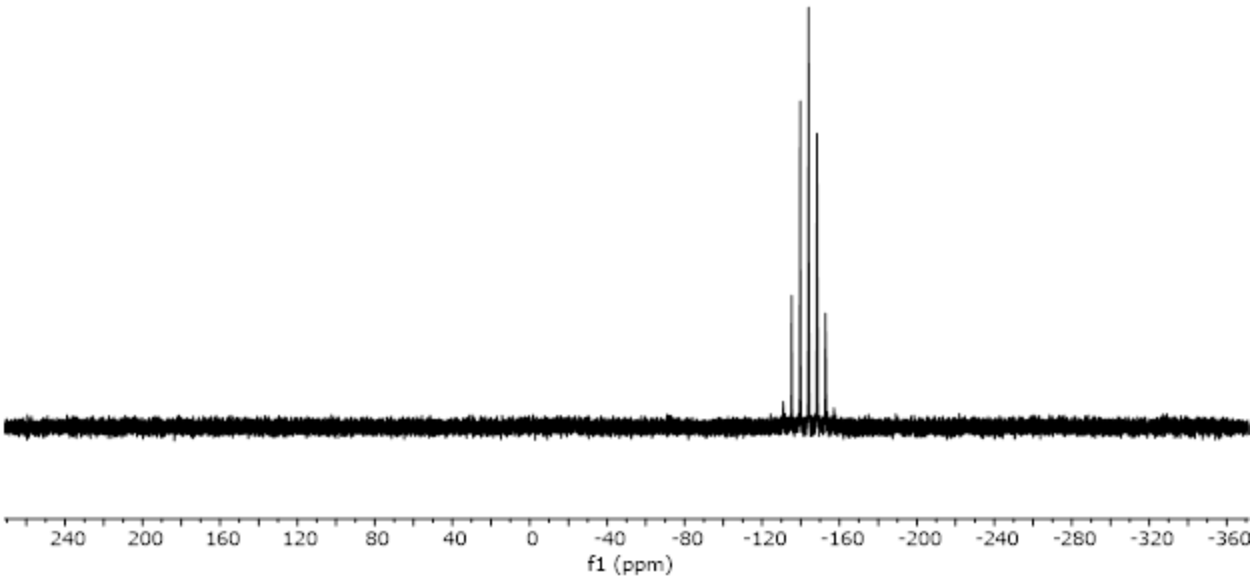

Figure S44. $^{31}P\{^{1}H\}$ NMR spectrum for the reaction of **1[OTf]$_2$** and [*n*Bu$_4$N][PF$_6$] (CH_3CN, 162 MHz, 298K).

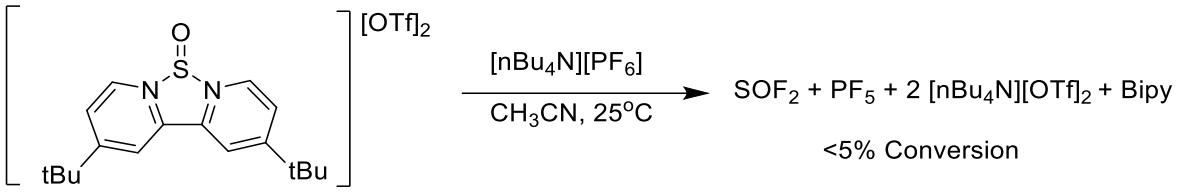

Reaction of 2[OTf]$_2$ with 2 eq. [*n*Bu$_4$N][PF$_6$]:

To a stirring solution of **2[OTf]$_2$** (10 mg, 0.016 mmol) in acetonitrile (0.5 mL) was added [*n*Bu$_4$N][PF$_6$] (12.6 mg, 0.033 mmol) in acetonitrile (0.5 mL). The colourless reaction was stirred for 16 hours and the reaction progress was monitored using ^{1}H and ^{19}F NMR spectroscopy. <1% conversion was observed from the ^{19}F NMR data, and only [*n*Bu$_4$N][PF$_6$] (-72.8 ppm from the ^{19}F NMR data) was observed in the ^{19}F NMR data. No SOF$_2$ was spectroscopically observed (72.7 ppm).

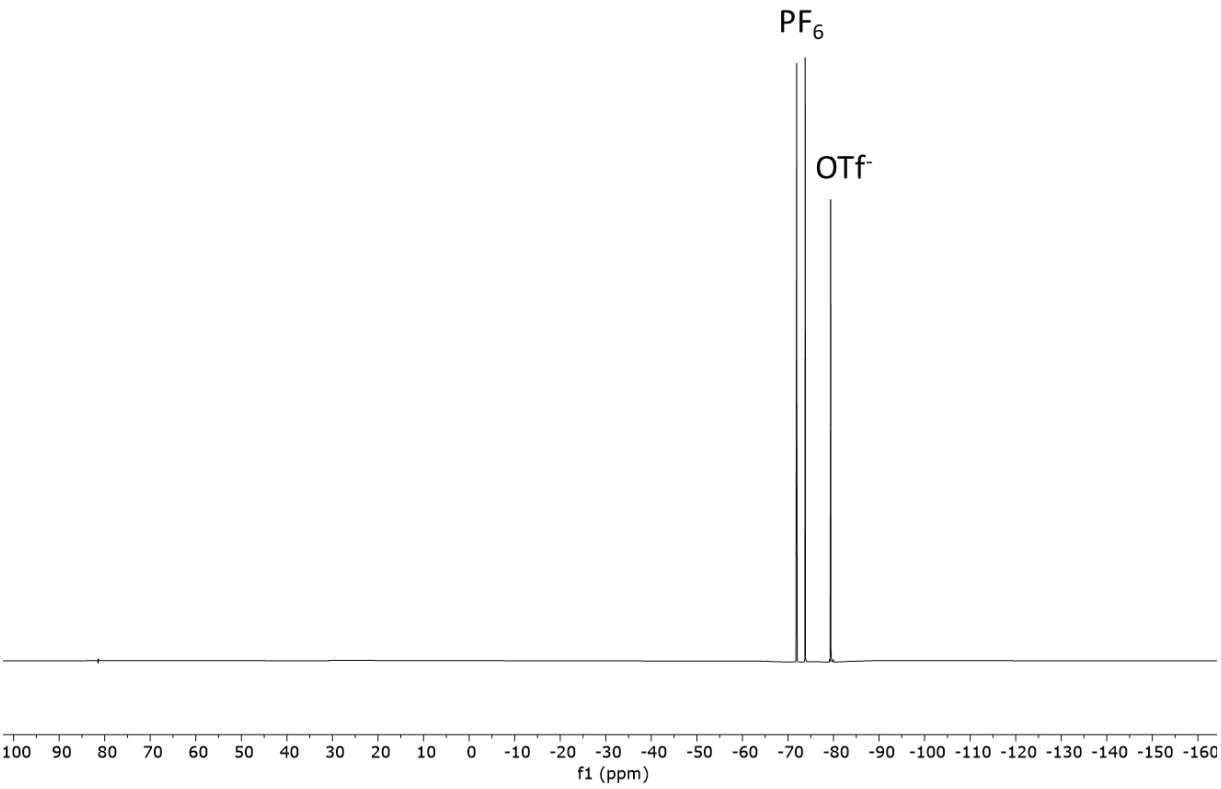

Figure S45. ^{19}F{^{1}H} NMR spectrum for the reaction between **2[OTf]$_2$** and [*n*Bu$_4$N][PF$_6$] (CH$_3$CN, 377 MHz, 298K).

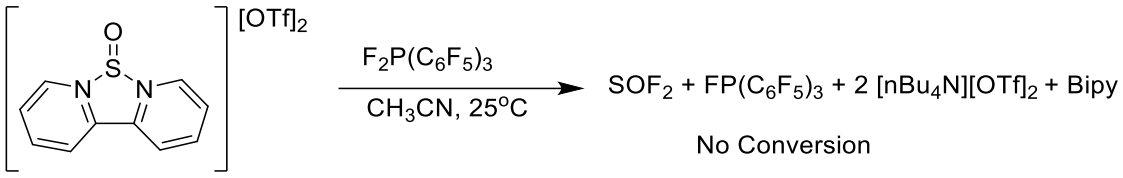

Reaction of 1[OTf]$_2$ with $F_2P(C_6F_5)_3$:

To a stirring solution of **1[OTf]$_2$** (10 mg, 0.020 mmol) in acetonitrile (0.5 mL) was added $F_2P(C_6F_5)_3$ (11.3 mg, 0.020 mmol) in acetonitrile (0.5 mL). The colourless reaction was stirred for 16 hours and the reaction progress was monitored using ^{1}H and ^{19}F NMR spectroscopy. The spectroscopic data shows no conversion of **1[OTf]$_2$** and $F_2P(C_6F_5)$.

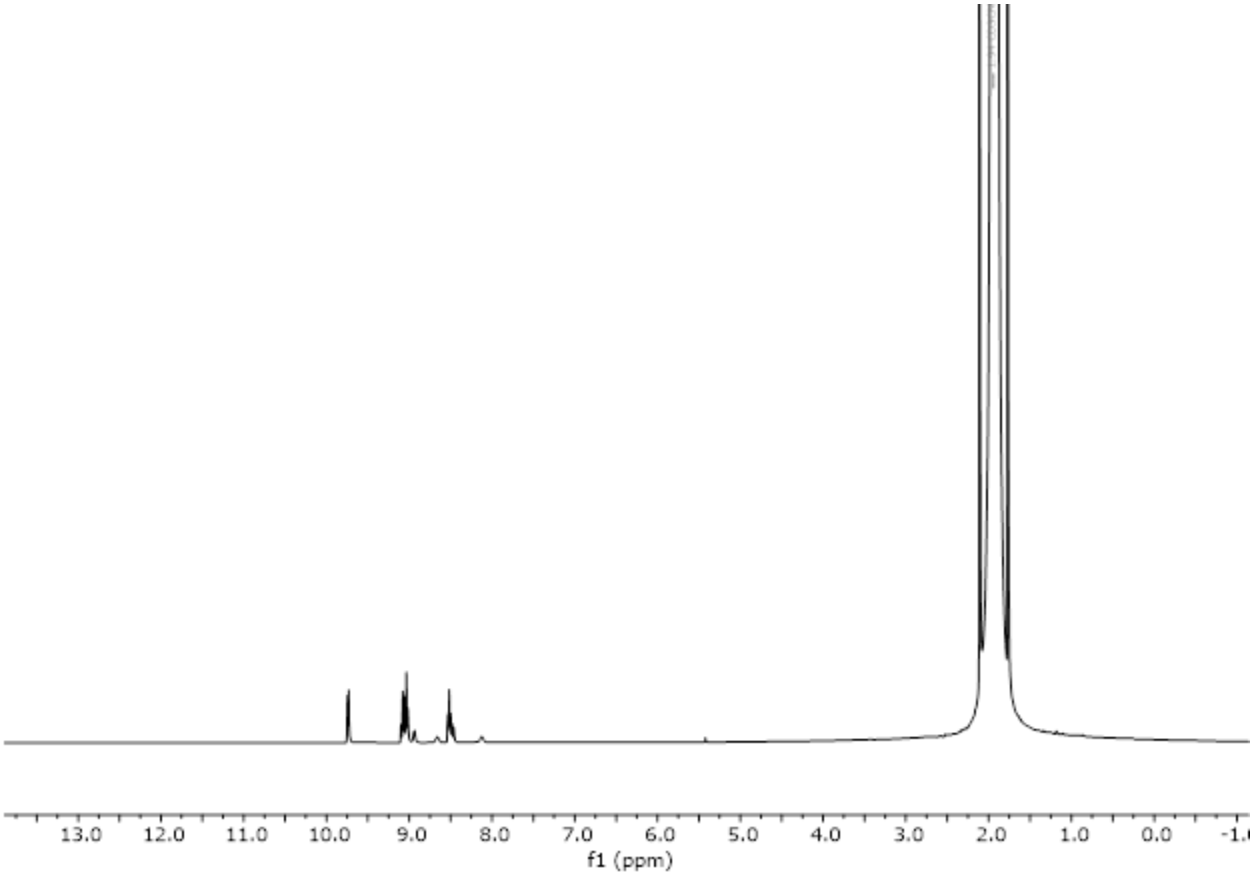

Figure S46. ^{1}H NMR spectrum for the reaction between **1[OTf]$_2$** and $F_2P(C_6F_5)_3$ (CH_3CN, 400 MHz, 298K).

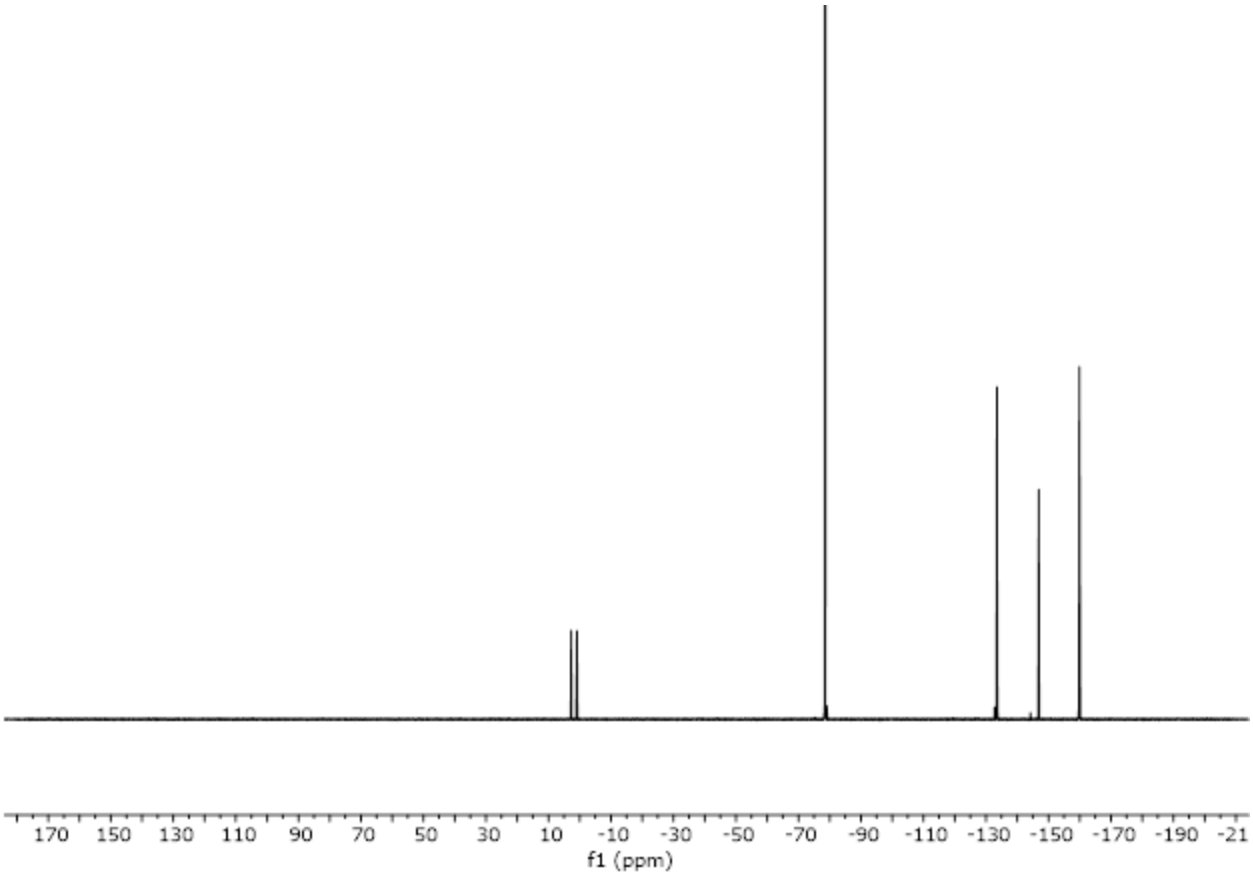

Figure S47. $^{19}F\{^{1}H\}$ NMR spectrum for the reaction between **1[OTf]$_2$** and $F_2P(C_6F_5)_3$ (CH_3CN, 377 MHz, 298K).

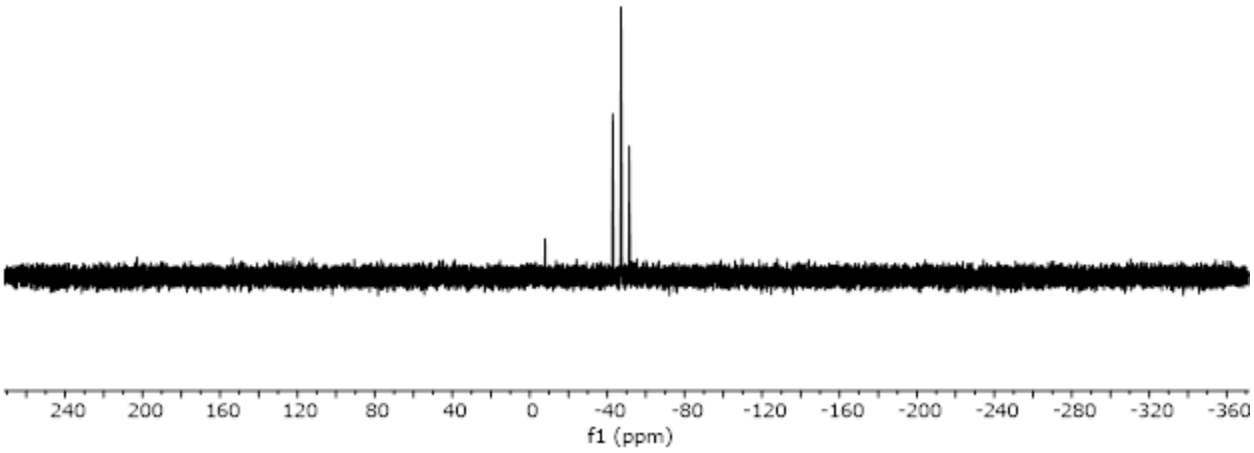

Figure S48. $^{31}P\{^{1}H\}$ NMR spectrum for the reaction between **1[OTf]$_2$** and $F_2P(C_6F_5)_3$ (CH_3CN, 162 MHz, 298K).

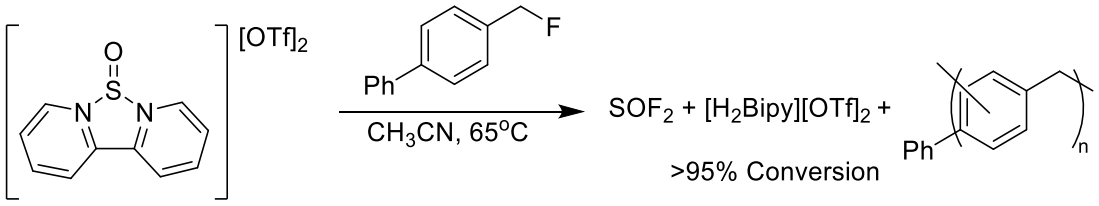

Reaction of 1[OTf]$_2$ with 4-Ph-PhCH$_2$F:

To a stirring solution of **1[OTf]$_2$** (15 mg, 0.030 mmol) in acetonitrile (0.5 mL) was added 4-Ph-PhCH$_2$F (5.5 mg, 0.030 mmol) in acetonitrile (0.5 mL). The reaction was stirred for 8 hours to which the solution darkened and a precipitate formed. The reaction was monitored by ^{1}H NMR and ^{19}F NMR spectroscopy which indicated the complete formation of SOF_2 (72.9 ppm) in the ^{19}F NMR spectra) and [H_2Bipy][OTf]$_2$, alongside the consumption of 4-phenylbenzyl fluoride (205.8 ppm in the ^{19}F NMR spectra). The formed precipitate is suggested to be a polymeric alkane formed through Friedel-Crafts alkylation as has been previously observed with benzyl fluorides with strong Lewis acids.[6-7]

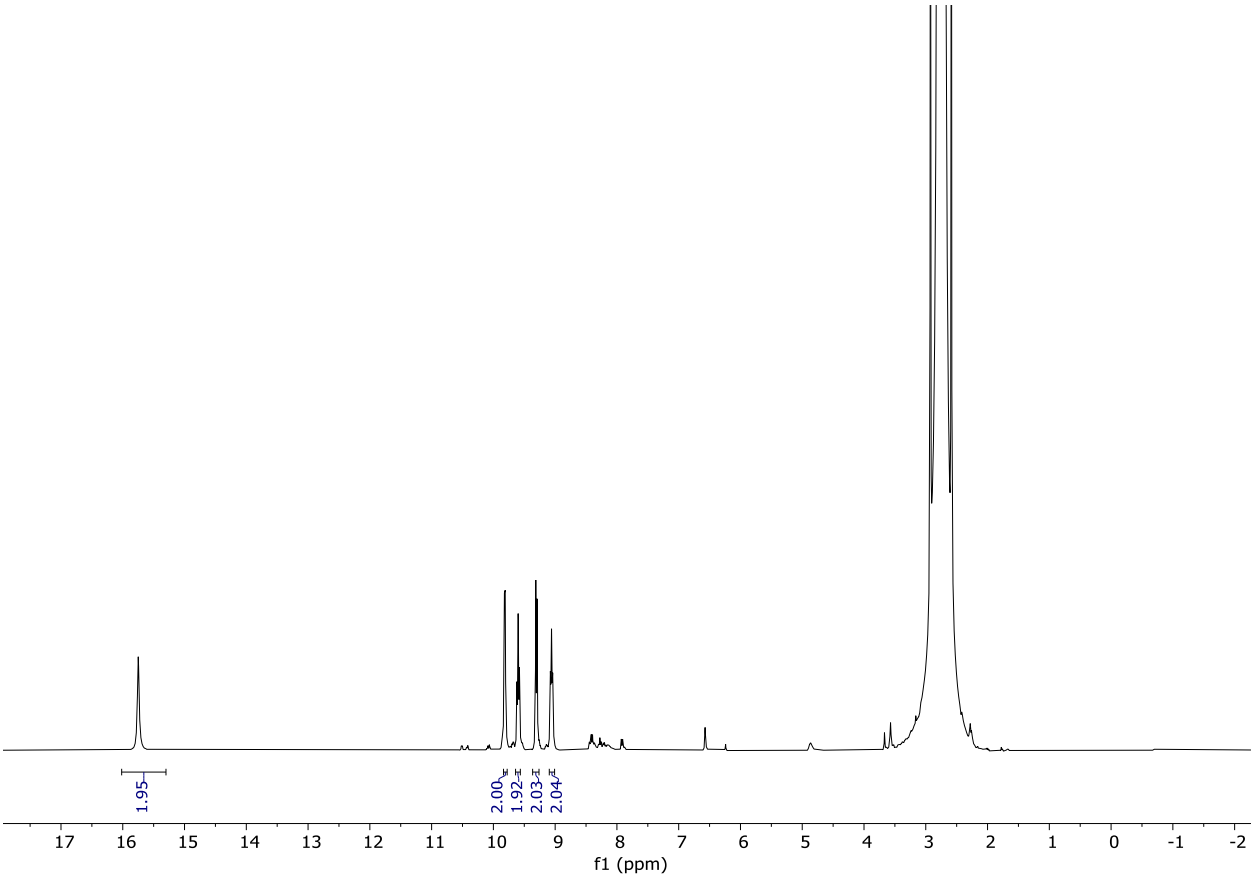

Figure S49. ^{1}H NMR spectrum for the completed reaction between **1[OTf]$_2$** and 4-Phenyl-benzylfluoride (CH_3CN, 400 MHz, 298K).

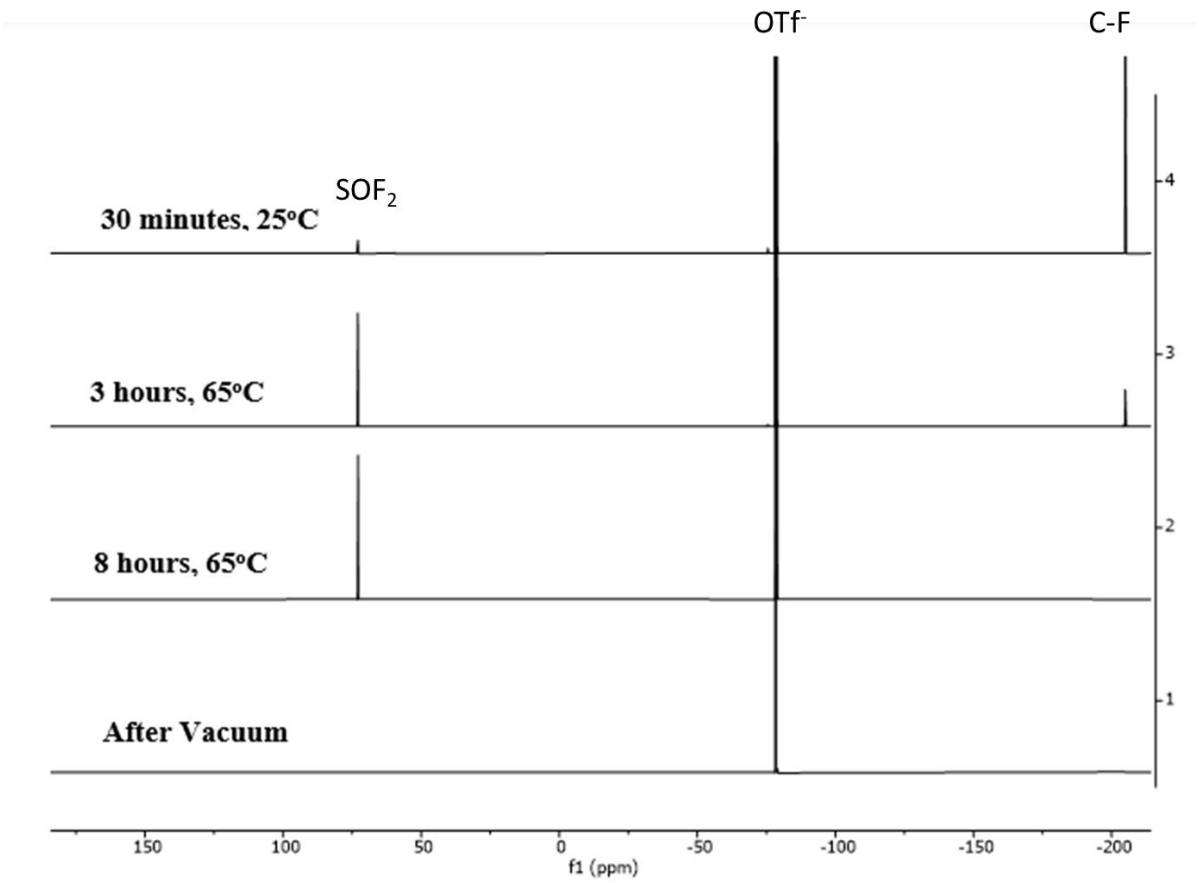

Figure S50. Stacked $^{19}F\{^{1}H\}$ NMR spectra for the reaction between **1[OTf]$_2$** and 4-phenyl-benzylfluoride (CH_3CN, 377 MHz, 298K).

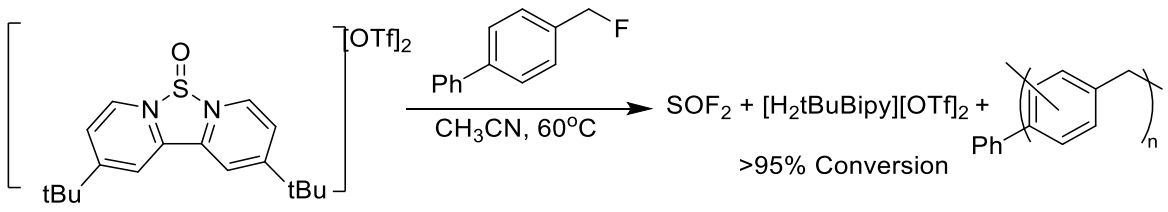

Reaction of 2[OTf]$_2$ with 4-Ph-PhCH$_2$F:

To a stirring solution of **1[OTf]$_2$** (15 mg, 0.024 mmol) in acetonitrile (0.5 mL) was added 4-Ph-PhCH$_2$F (4.5 mg, 0.024 mmol) in acetonitrile (0.5 mL). The reaction was stirred for 16 hours at 60°C to which the solution darkened and a precipitate formed. The reaction was monitored by ^{1}H NMR and ^{19}F NMR spectroscopy which indicated the formation of SOF_2 (72.9 ppm in the ^{19}F

NMR spectrum) and [H_2*t*BuBipy][OTf]$_2$. Other byproducts observed in the ^{1}H NMR spectrum are expected to be short-chained oligomers formed from the Lewis acid mediated polymerization. The formed precipitate is suggested to be a polymeric alkane formed through Friedel-Crafts alkylation as has been previously observed with benzyl fluorides with strong Lewis acids.[6-7]

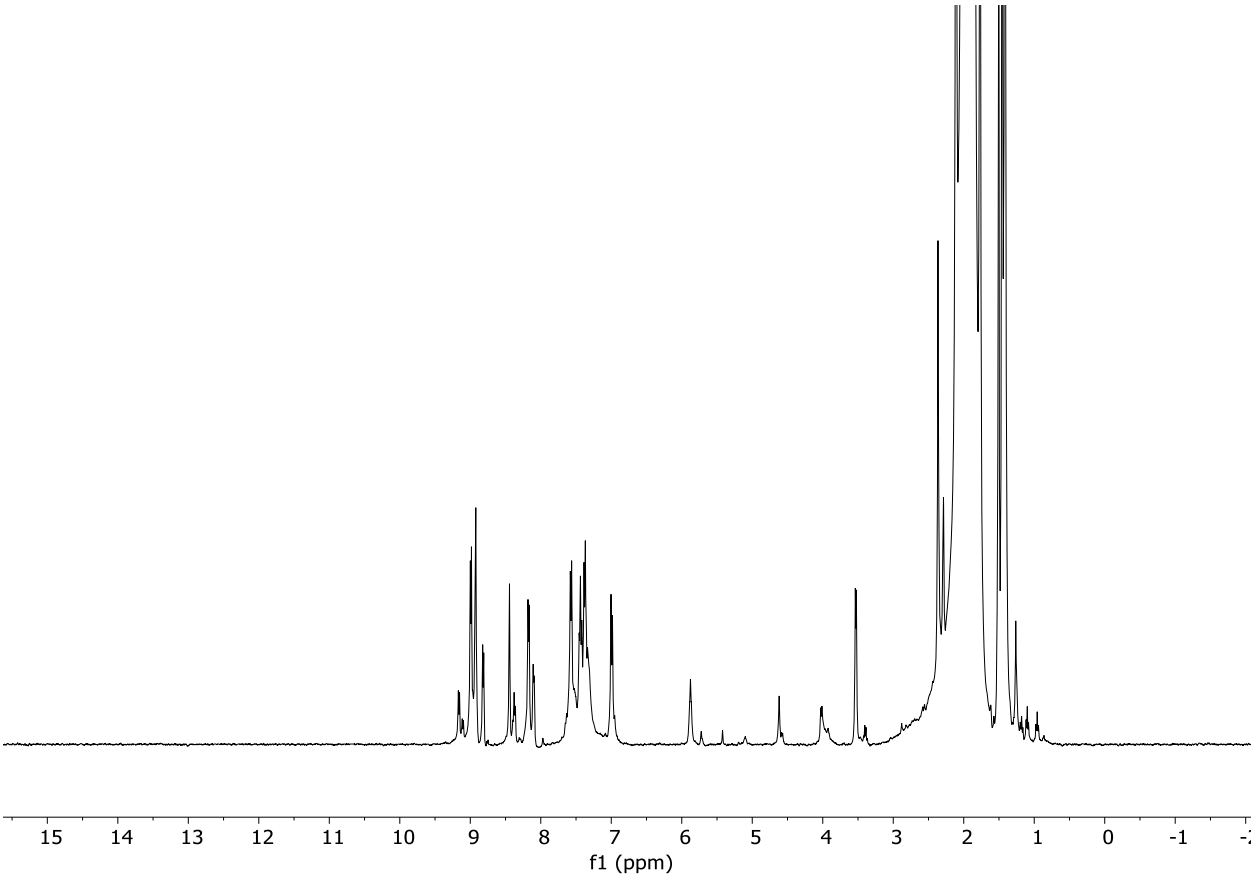

Figure S51. ^{1}H NMR spectrum for the reaction between **2[OTf]$_2$** and 4-phenyl-benzylfluoride (CH_3CN, 400 MHz, 298K).

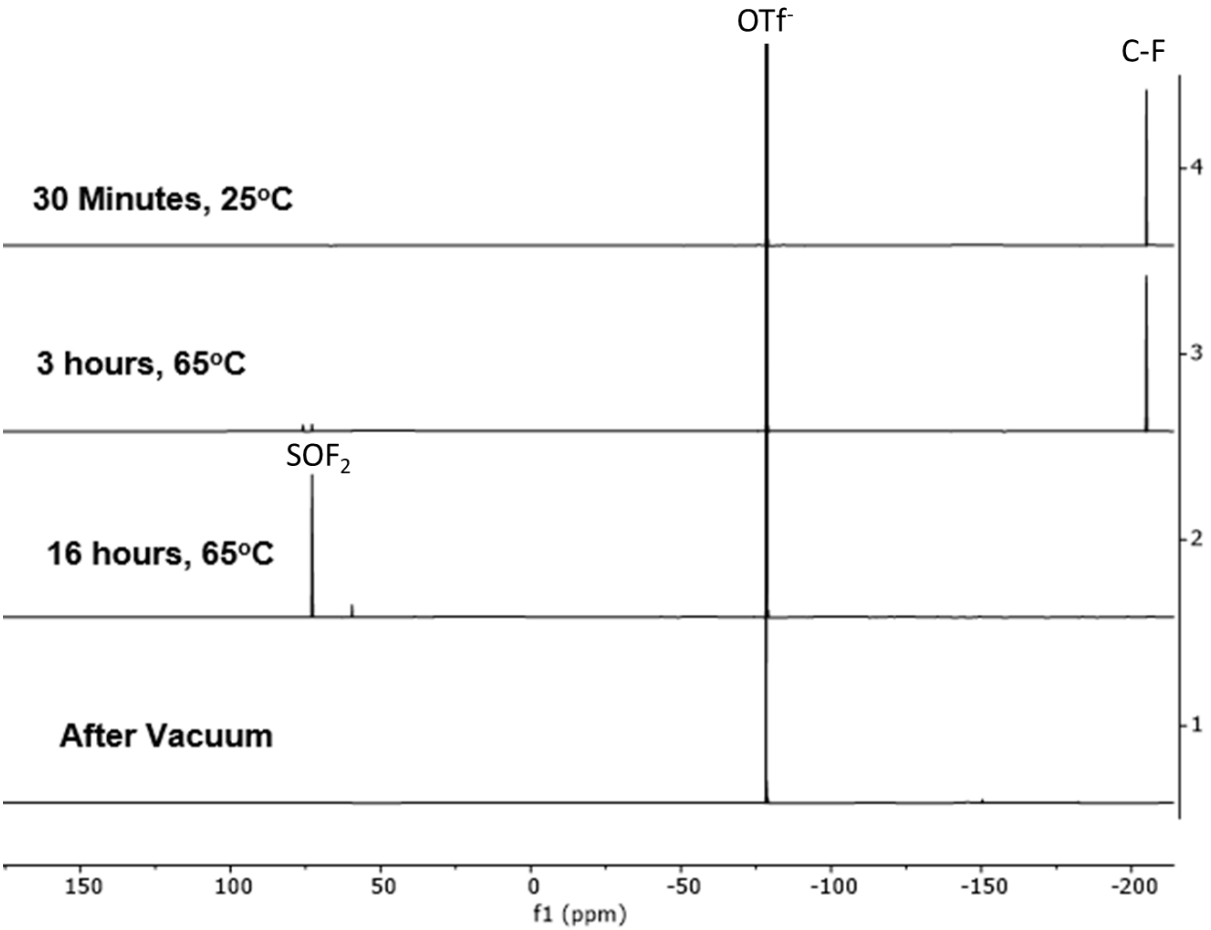

Figure S52. Stacked $^{19}F\{^{1}H\}$ NMR spectra for the reaction between **2[OTf]$_2$** and 4-phenyl-benzylfluoride (CH_3CN, 377 MHz, 298K).

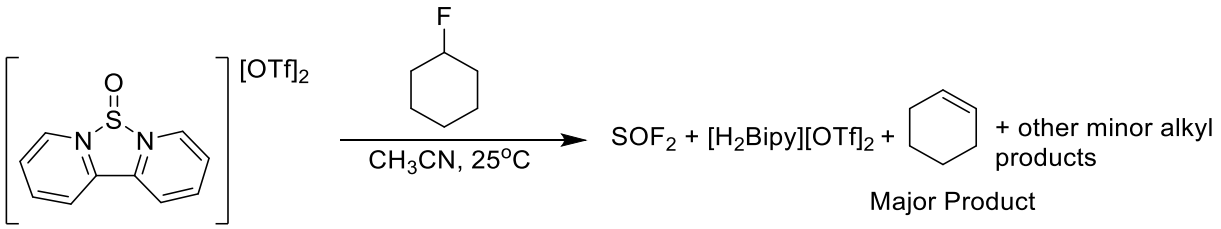

Reaction of 1[OTf]$_2$ with fluorocyclohexane:

To a stirring solution of **1[OTf]$_2$** (15 mg, 0.030 mmol) in acetonitrile (0.5 mL) was added flourocyclohexane (6.5μL, 6.0 mg, 0.059 mmol) in acetonitrile (0.5 mL). The reaction was stirred for 24 hours at 65^{o}C providing a colourless product. The reaction was monitored by ^{1}H NMR and ^{19}F NMR spectroscopy indicating the consumption of fluorocyclohexane. Spectroscopically, the formation of cyclohexene (C=C-*H* signal at 5.64 ppm in the ^{1}H NMR spectrum; 52% yield) presumably through an overall dehydrofluorination reaction where the sulfur centre abstracts fluoride, overall forming SOF_2 (72.9 ppm in the ^{19}F NMR spectrum), and releasing bipyridine that deprotonates at the β-carbon ([H_2Bipy][OTf]$_2$ was observed in the ^{1}H NMR spectrum). Some other alkane products were observed as minor products, likely as a result of isomeration of formed carbocation intermediates.

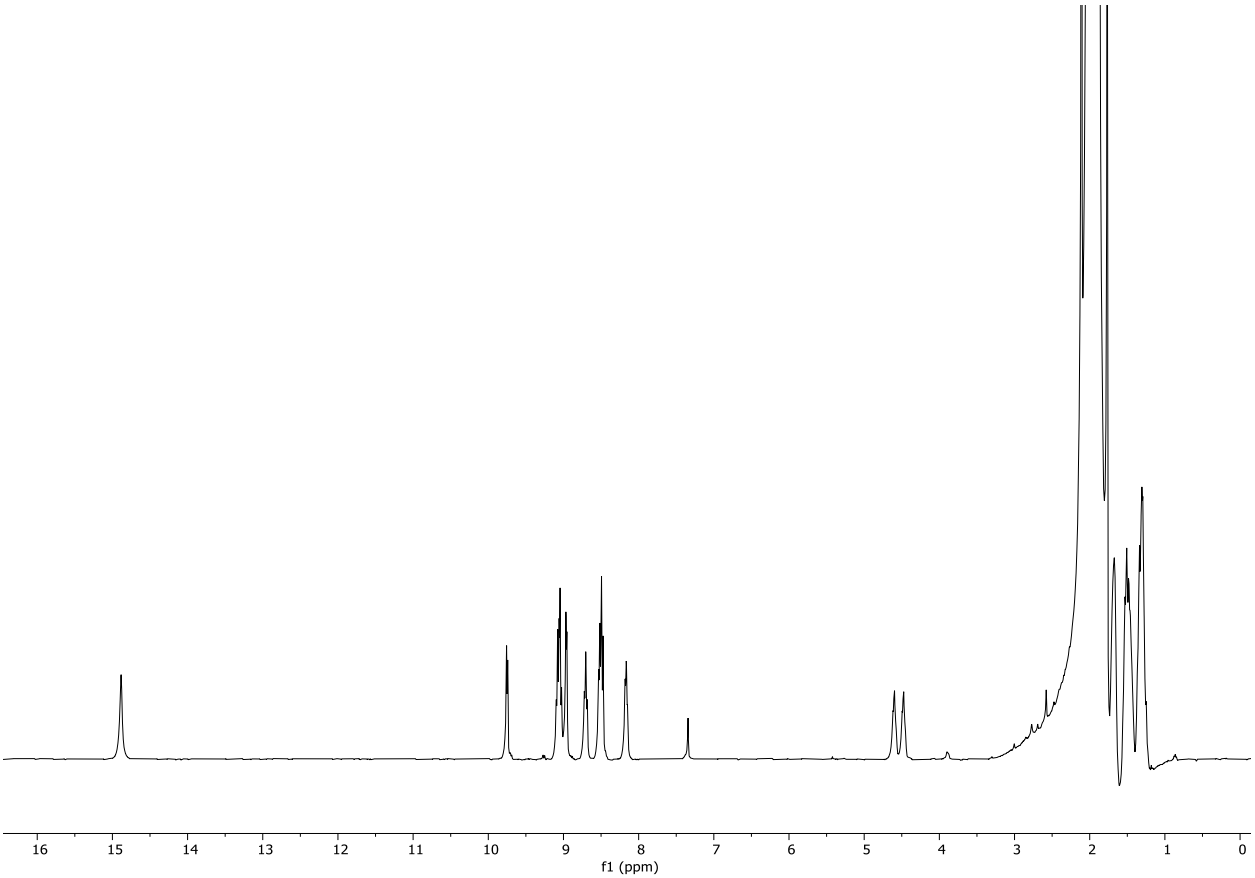

Figure S53. ^{1}H NMR spectrum for the reaction between **1[OTf]$_2$** and fluorocyclohexane after 1 hour at 65°C (CH_3CN, 400 MHz, 298K). The spectra are referenced to the CH_3CN signal at 1.94 ppm.

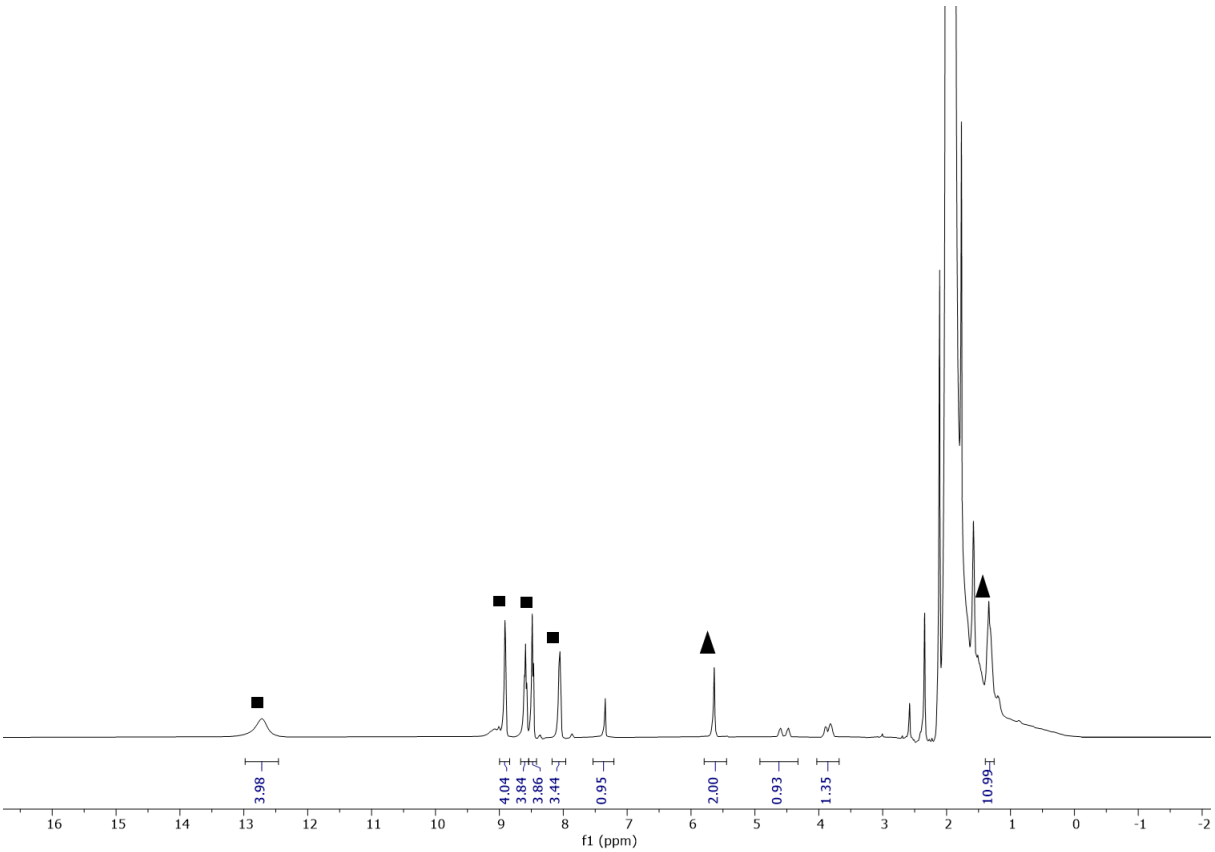

Figure S54. ^{1}H NMR spectrum for the reaction between **1[OTf]$_2$** and fluorocyclohexane after 24 hours at 65°C (CH_3CN, 400 MHz, 298K). The spectra are referenced to the CH_3CN signal at 1.94 ppm. Square: $[H_2Bipy][OTf]_2$, Triangle: Cyclohexene.

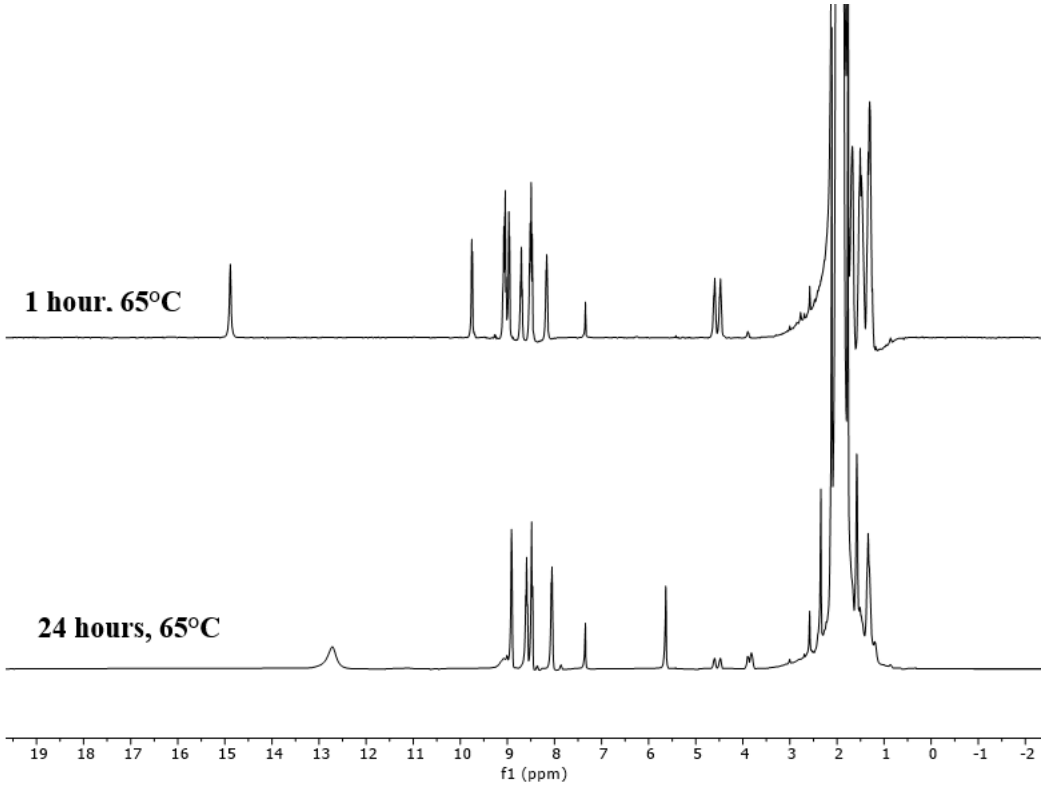

Figure S55. Stacked ^{1}H NMR spectra for the reaction between **1[OTf]$_2$** and fluorocyclohexane (CH_3CN, 400 MHz, 298K). The spectra are referenced to the CH_3CN signal at 1.94 ppm.

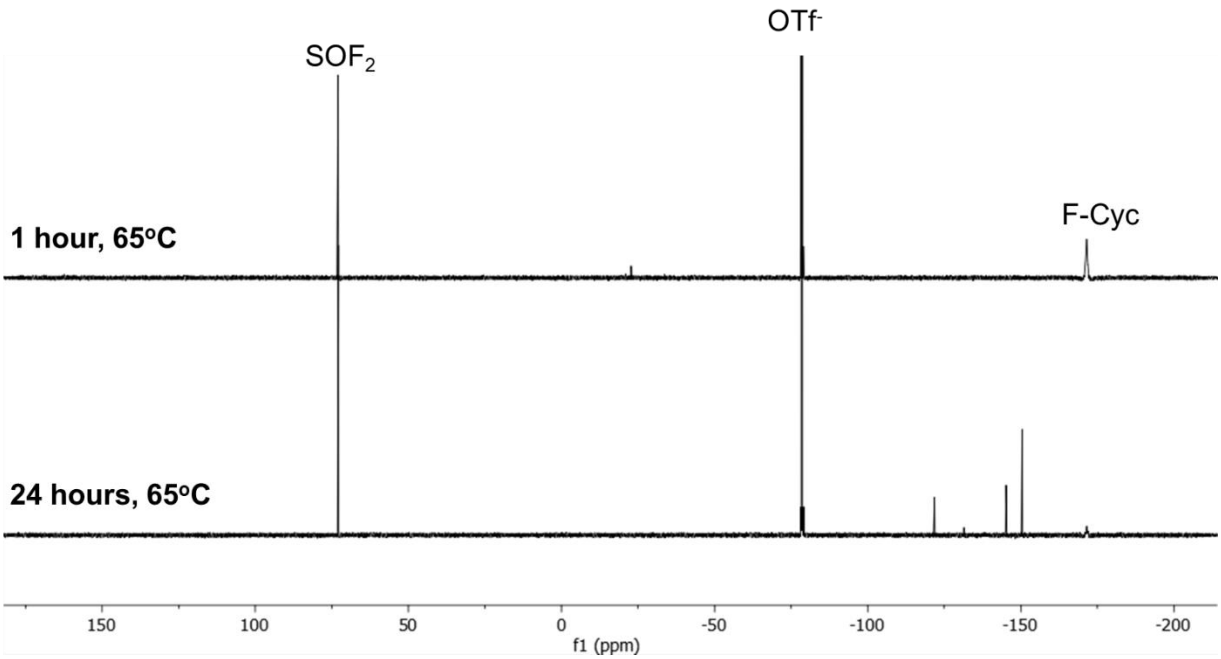

Figure S56. Stacked $^{19}F\{^{1}H\}$ NMR spectra for the reaction between **1[OTf]$_2$** and fluorocyclohexane (CH_3CN, 377 MHz, 298K).

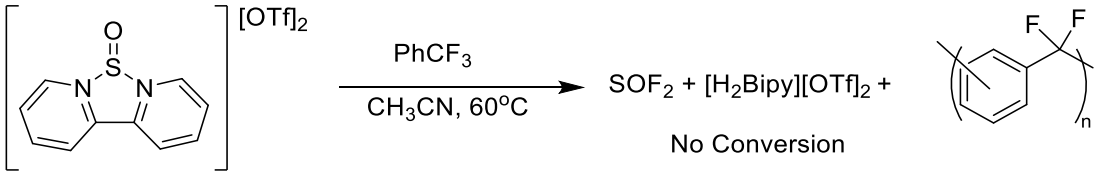

Reaction of 1[OTf]$_2$ with $PhCF_3$:

To a stirring solution of **1[OTf]$_2$** (15 mg, 0.030 mmol) in acetonitrile (0.5 mL) was added $PhCF_3$ (3.7 μL, 4.4 mg, 0.030 mmol) in acetonitrile (0.5 mL). The colourless reaction was stirred for 16 hours at 60°C and was monitored by ^{19}F NMR spectroscopy which indicated no new product formation and no consumption of $PhCF_3$.

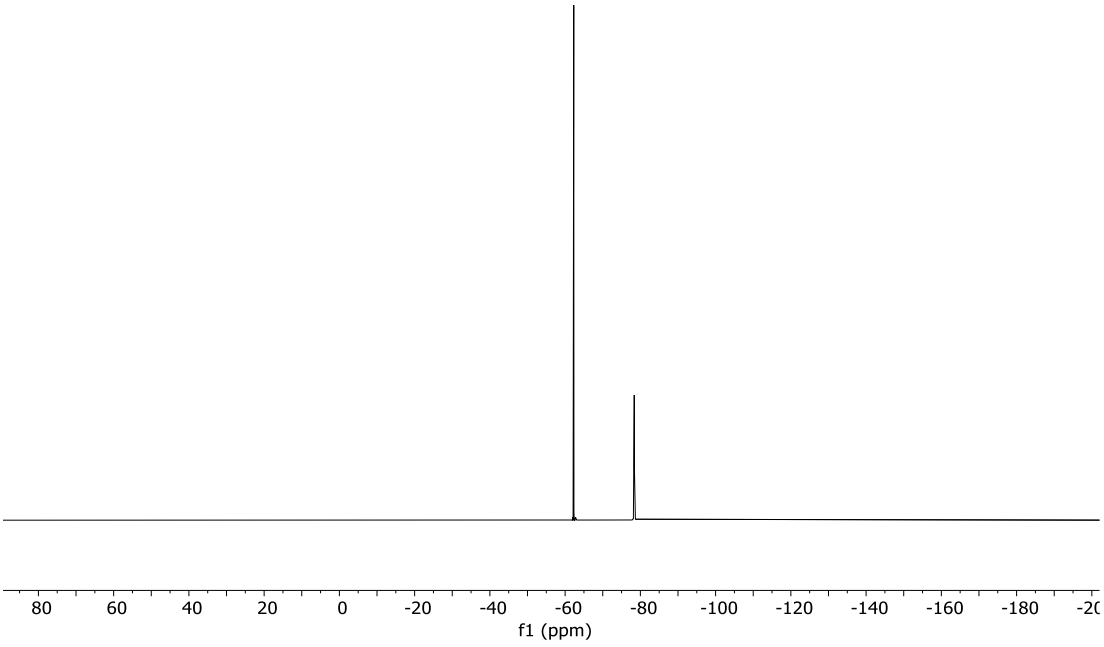

Figure S57. $^{19}F\{^{1}H\}$ NMR spectrum for the reaction between **1[OTf]$_2$** and $PhCF_3$ (CH_3CN, 377 MHz, 298K).

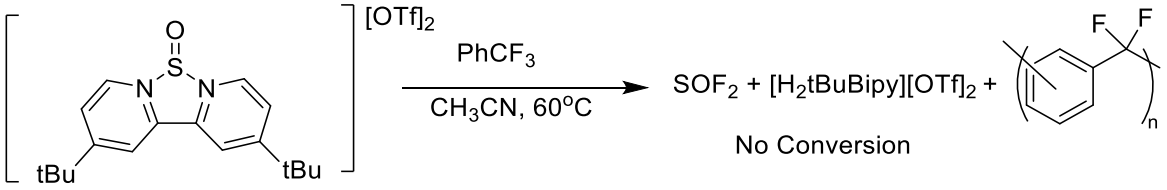

Reaction of 2[OTf]$_2$ with $PhCF_3$:

To a stirring solution of **2[OTf]$_2$** (15 mg, 0.024 mmol) in acetonitrile (0.5 mL) was added $PhCF_3$ (2.3μL, 2.8 mg, 0.024 mmol) in acetonitrile (0.5 mL). The colourless reaction was stirred for 16 hours at 60°C and was monitored by ^{19}F NMR spectroscopy which indicated no new product formation and no consumption of $PhCF_3$.

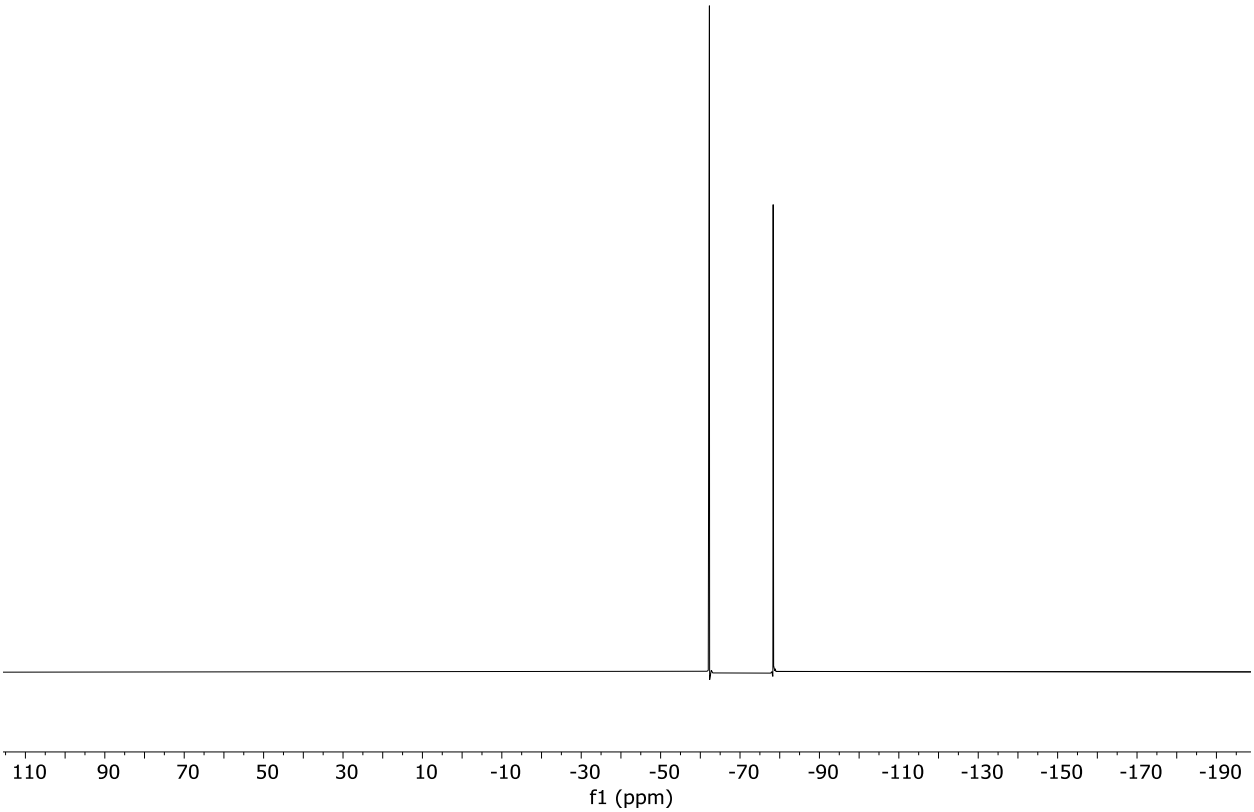

Figure S58. $^{19}F\{^{1}H\}$ NMR spectrum for the reaction between **2[OTf]$_2$** and $PhCF_3$ (CH_3CN, 377 MHz, 298K).

Reaction of 1[OTf]$_2$ with Ph-F:

To a stirring solution of **1[OTf]$_2$** (15 mg, 0.030 mmol) in acetonitrile (0.5 mL) was added fluorobenzene (2.8μL, 2.9 mg, 0.030 mmol) in acetonitrile (0.5 mL). The colourless reaction was stirred for 16 hours at 65^{o}C and was monitored by ^{1}H NMR and ^{19}F NMR spectroscopy which indicated no new product formation and no consumption of Ph-F.

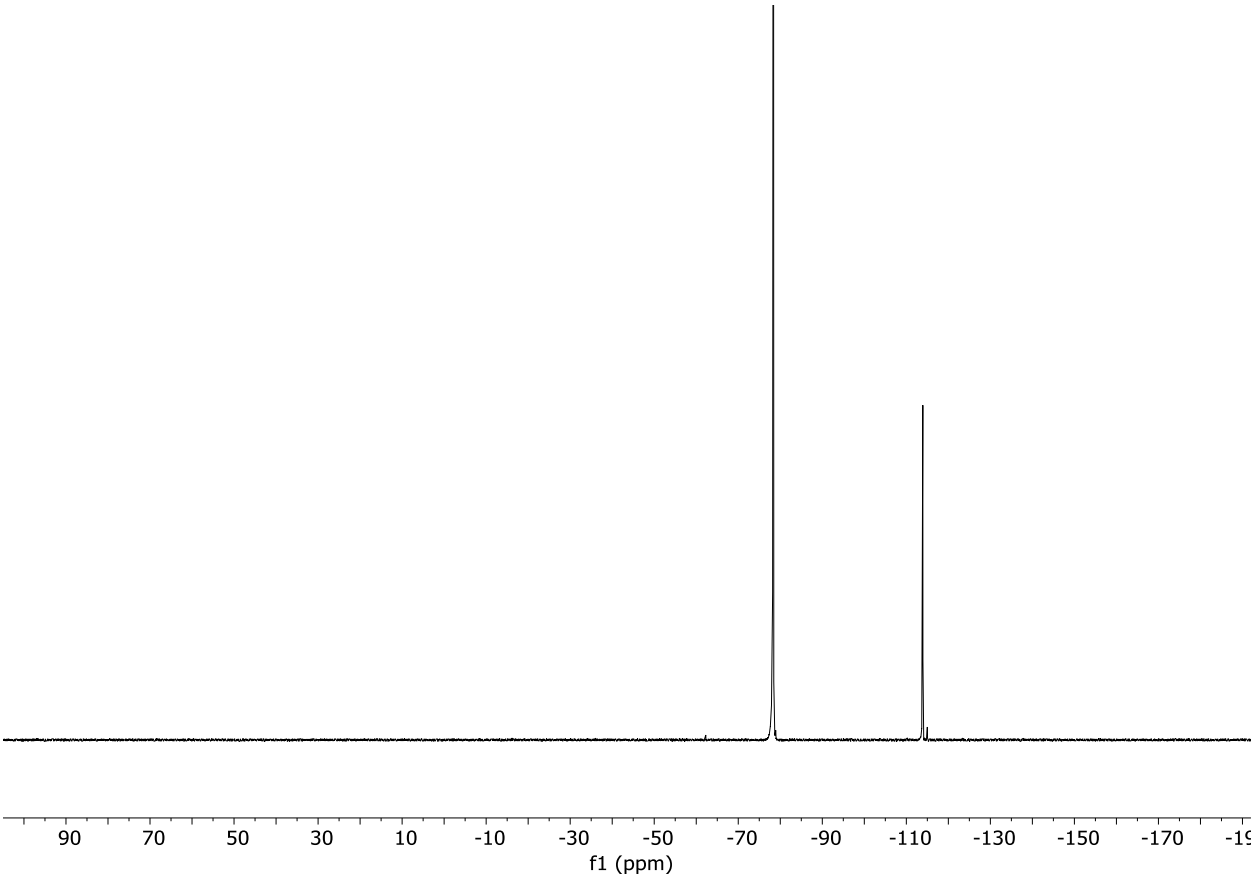

Figure S59. $^{19}F\{^{1}H\}$ NMR spectrum for the reaction between **1[OTf]$_2$** and PhF (CH_3CN, 377 MHz, 298K).

Reaction of 2[OTf]$_2$ with Ph-F:

To a stirring solution of **2[OTf]$_2$** (15 mg, 0.024 mmol) in acetonitrile (0.5 mL) was added fluorobenzene (2.3μL, 2.3 mg, 0.024 mmol) in acetonitrile (0.5 mL). The colourless reaction was stirred for 16 hours at 65ºC and was monitored by ^{1}H NMR and ^{19}F NMR spectroscopy which indicated no new product formation and no consumption of Ph-F.

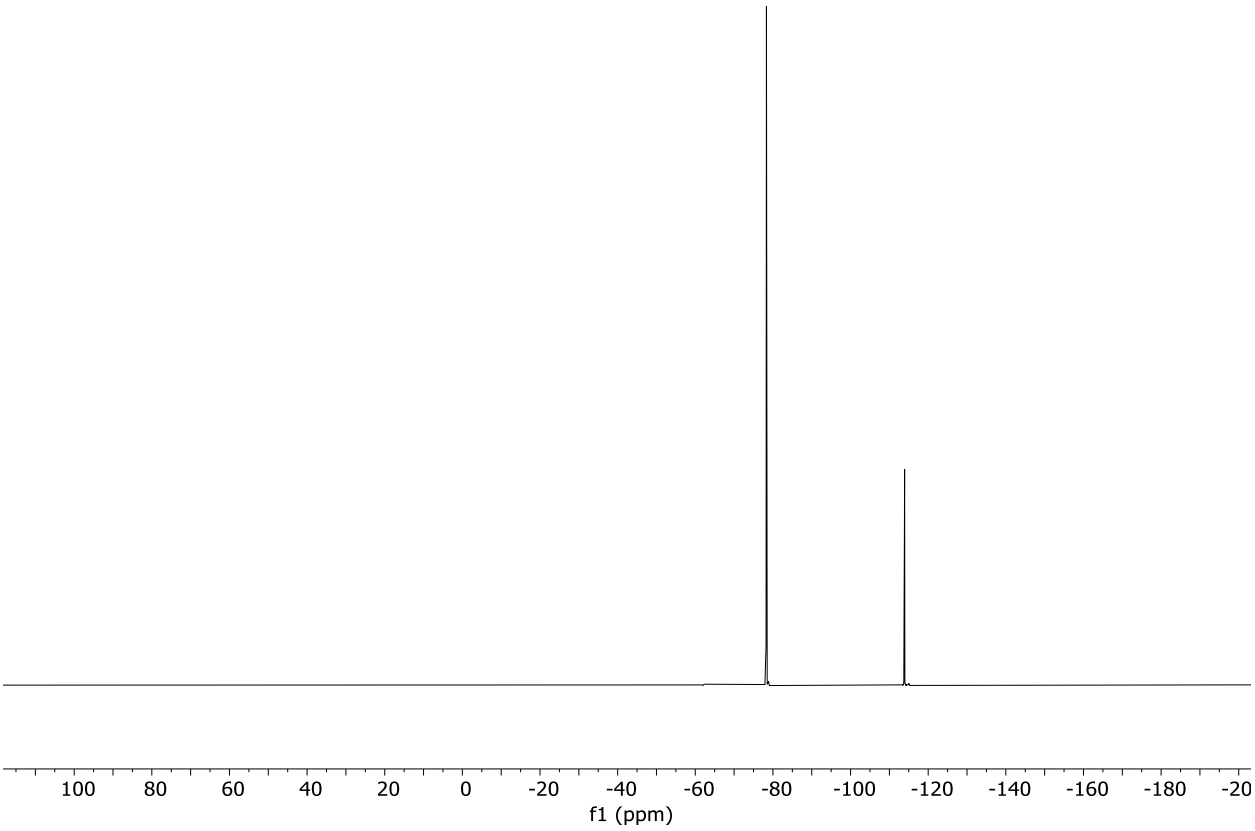

Figure S60. $^{19}F\{^{1}H\}$ NMR spectrum for the reaction between **2[OTf]$_2$** and PhF (CH_3CN, 377 MHz, 298K).

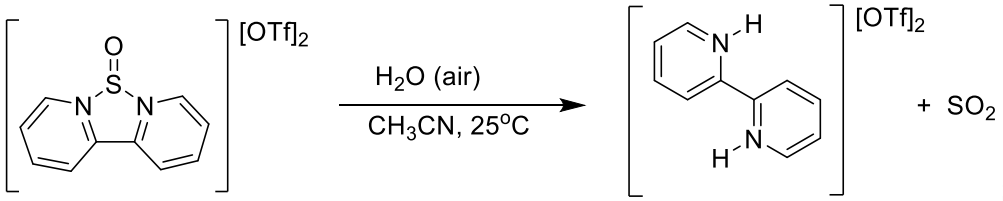

Slow Hydrolysis of 1[OTf]$_2$:

A solution of **1[OTf]$_2$** (15 mg, 0.030 mmol) in acetonitrile (0.5 mL) in a sealed NMR tube opened to air and had compressed air bubbled in to it. The tube was let sit over 8 days whereupon the solution was monitored by ^{1}H NMR spectroscopy. After 5 days significant decomposition of **1[OTf]$_2$** was observed. Complete hydrolysis of **1[OTf]$_2$** was observed after 8 days. It is noteworthy that the N-H resonance shifts upfield and significantly broadens as **1[OTf]$_2$** reaches complete

decomposition, with the NMR data indicating the formation of $[H_2Bipy][OTf]_2$. The broadening of the N-H signal would be consistent with exchange between the N-H protons with O-H protons from sulfur oxyacids formed from the reaction between SO_2 and any excess water.

^{1}H NMR (CH_3CN, 400 MHz, 298K): δ (ppm) 10.29 (br s, N-*H*, 2H), 9.00 (d, $^3J_{H\text{-}H}$ = 5.6 Hz, *o*-C-*H*, 2H), 8.78 (d, $^3J_{H\text{-}H}$ = 8.1 Hz, *m*-C-*H* (N-C(C)-C-*H*), 2H), 8.48 (t, $^3J_{H\text{-}H}$ = 8.1 Hz, *m*-C-*H* (N-C(H)-C-*H*), 2H), 8.24 (t, $^3J_{H\text{-}H}$ = 6.7 Hz, *p*-C-*H*).

^{19}F{^{1}H} NMR (CH_3CN, 400 MHz, 298K): δ (ppm) 78.5 (s).

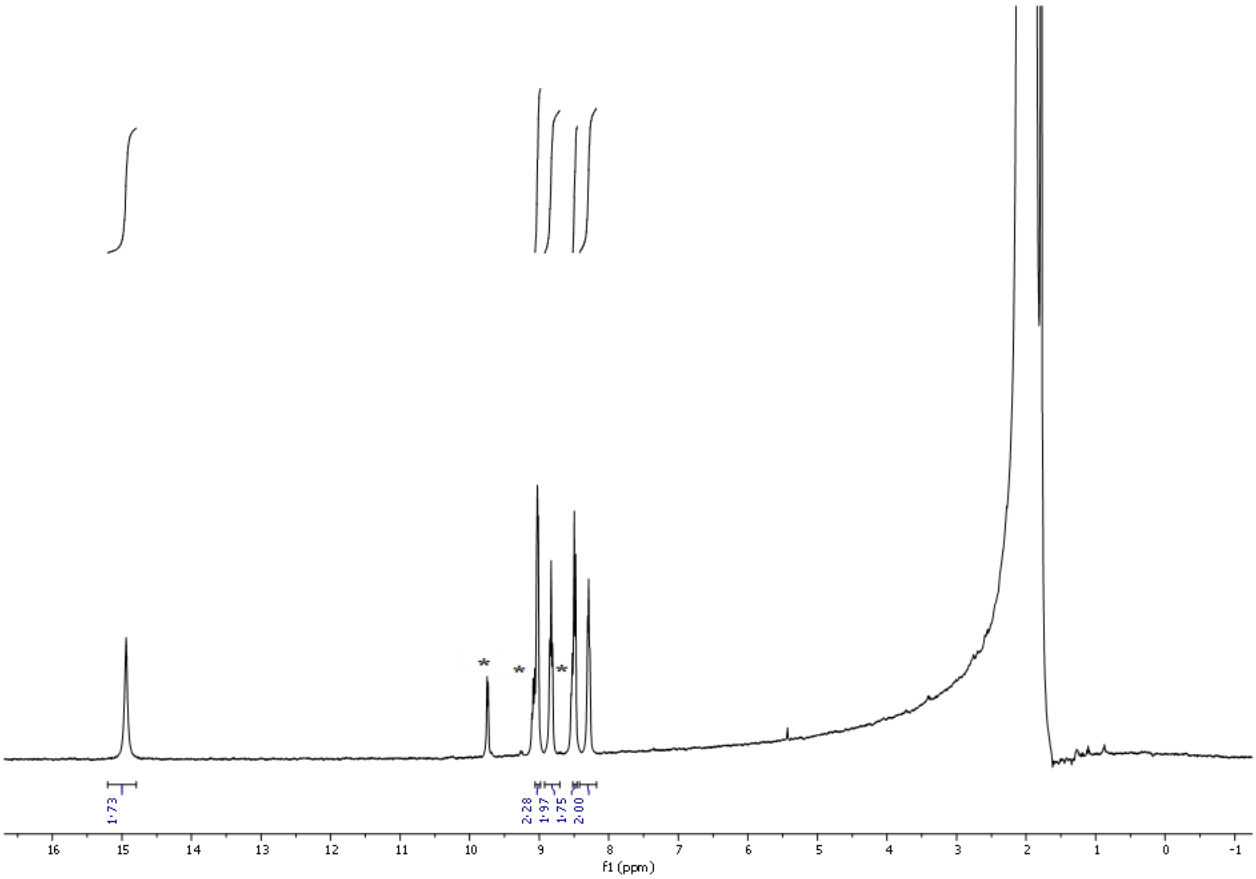

Figure S61. ^{1}H NMR spectrum from the decomposition of **1[OTf]$_2$** after being exposed to air over 5 days (CH_3CN, 400 MHz, 298K). The spectrum is referenced the CH_3CN signal at 1.94 ppm. * = residual **1[OTf]$_2$**.

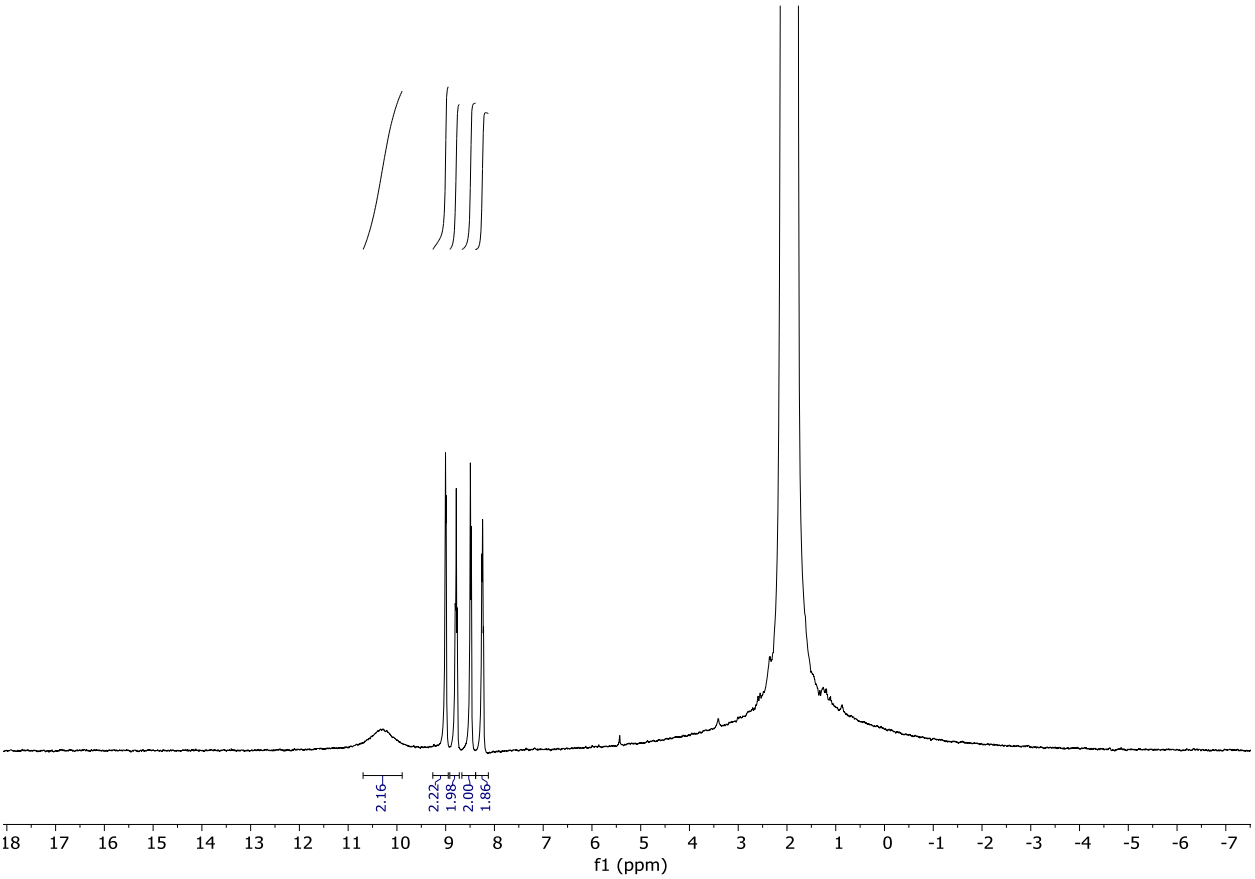

Figure S62. ^{1}H NMR spectrum from the decomposition of **1[OTf]$_2$** after being exposed to air over 8 days (CH_3CN, 400 MHz, 298K). The spectrum is referenced the CH_3CN signal at 1.94 ppm.

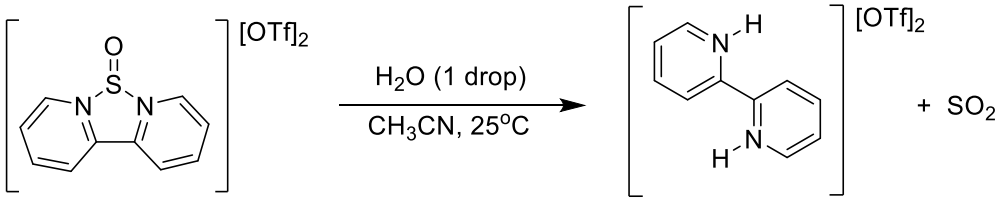

Hydrolysis of 1[OTf]$_2$:

To a solution of **1[OTf]$_2$** (15 mg, 0.030 mmol) in acetonitrile (0.5 mL) in a sealed NMR tube was added 1 drop of deionized water, and the tube was shaken over 1 minute. The tube was monitored by ^{1}H NMR spectroscopy to reveal $[H_2Bipy][OTf]_2$ as the only spectroscopically observable

product. The broadening of the N-H signal would be consistent with exchange between the N-H protons with O-H protons from sulfur oxyacids formed from the reaction between SO_2 and any excess water.

^{1}H NMR (CH_3CN, 400 MHz, 298K): δ (ppm) 8.81 (m, *o*-C-*H*, 2H), 8.47 (d, $^3J_{H\text{-}H}$ = 8.3 Hz, *m*-C-*H* (N-C(C)-C-*H*), 2H), 8.39 (t, $^3J_{H\text{-}H}$ = 8.3 Hz, *m*-C-*H* (N-C(H)-C-*H*), 2H), 7.86 (t, $^3J_{H\text{-}H}$ = 6.5 Hz, *p*-C-*H*), N-H signals are not observed due to extensive broadening.

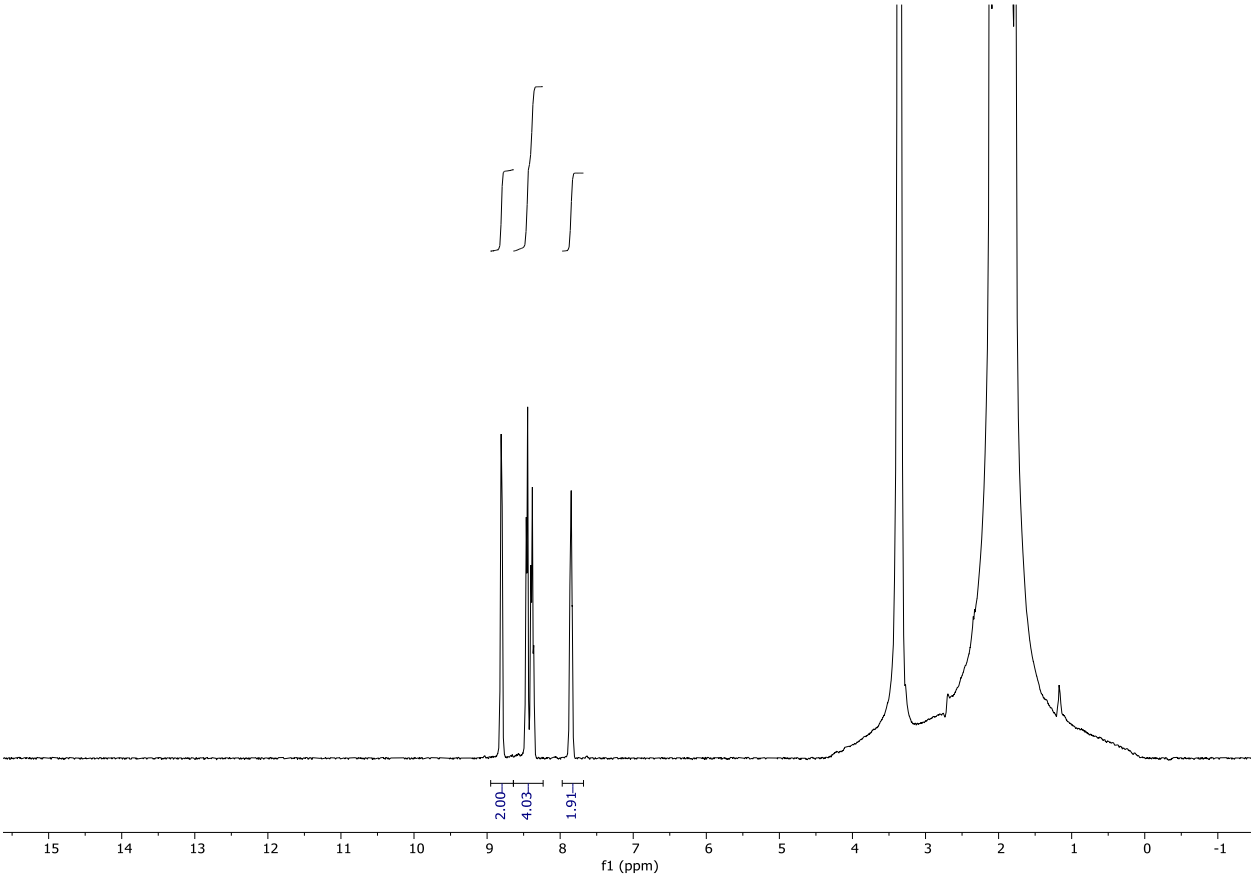

Figure S63. ^{1}H NMR spectrum from the decomposition of **1[OTf]$_2$** after being exposed to 1 drop of H_2O (CH_3CN, 298K, 400 MHZ). The spectrum is referenced the CH_3CN signal at 1.94 ppm.

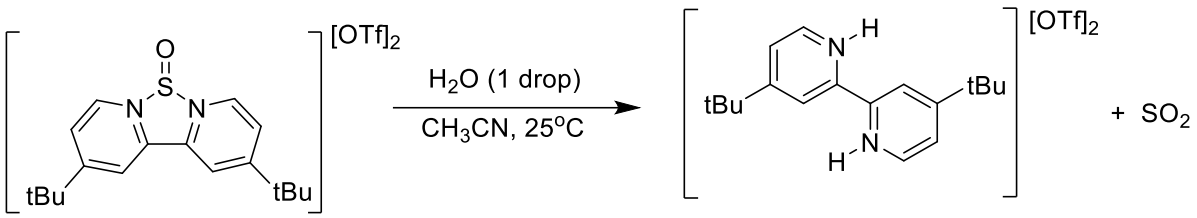

Hydrolysis of 2[OTf]$_2$:

To a solution of **2[OTf]$_2$** (15 mg, 0.024 mmol) in acetonitrile (0.5 mL) in a sealed NMR tube was added compressed air. The tube was monitored by ^{1}H NMR spectroscopy to reveal decomposition to [H$_2$*t*BuBipy][OTf]$_2$ as the only spectroscopically observable product after 6 days. The observed broadening of the N-H signal upon complete decomposition would be consistent with exchange between the N-H protons with the O-H protons from sulfur oxyacids formed from the reaction between SO_2 and any excess water.

^{1}H NMR (CH_3CN, 400 MHz, 298K): δ (ppm) 14.58 (br s, N-*H*, 2H), 8.89 (d, $^3J_{H\text{-}H}$ = 6.3 Hz, *o*-C-*H*, 2H), 8.43 (d, $^4J_{H\text{-}H}$ = 2.0 Hz, *m*-C-*H* (N-C(C)-C-*H*), 2H), 8.24 (dd, $^3J_{H\text{-}H}$ = 6.3 Hz, $^4J_{H\text{-}H}$ = 2.0 Hz, *m*-C-*H* (N-C(H)-C-*H*), 2H), 1.46 (s, C-(C*H*$_3$)$_3$, 18H), N-H signals are not observed after full decomposition due to extensive broadening.

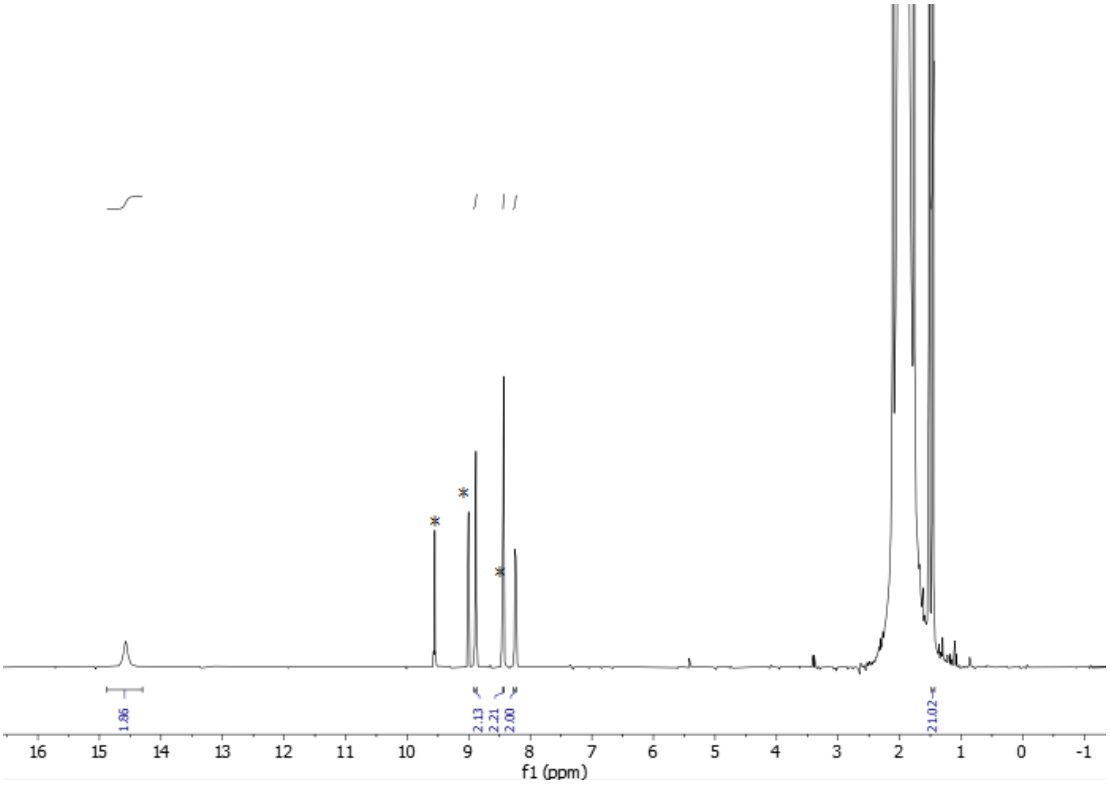

Figure S64. ^{1}H NMR spectra for the decomposition of **2[OTf]$_2$** in air after 24 hours (CH_3CN, 298K, 400 MHZ). The spectra are referenced to the CH_3CN signal at 1.94 ppm. * = residual **2[OTf]$_2$**.

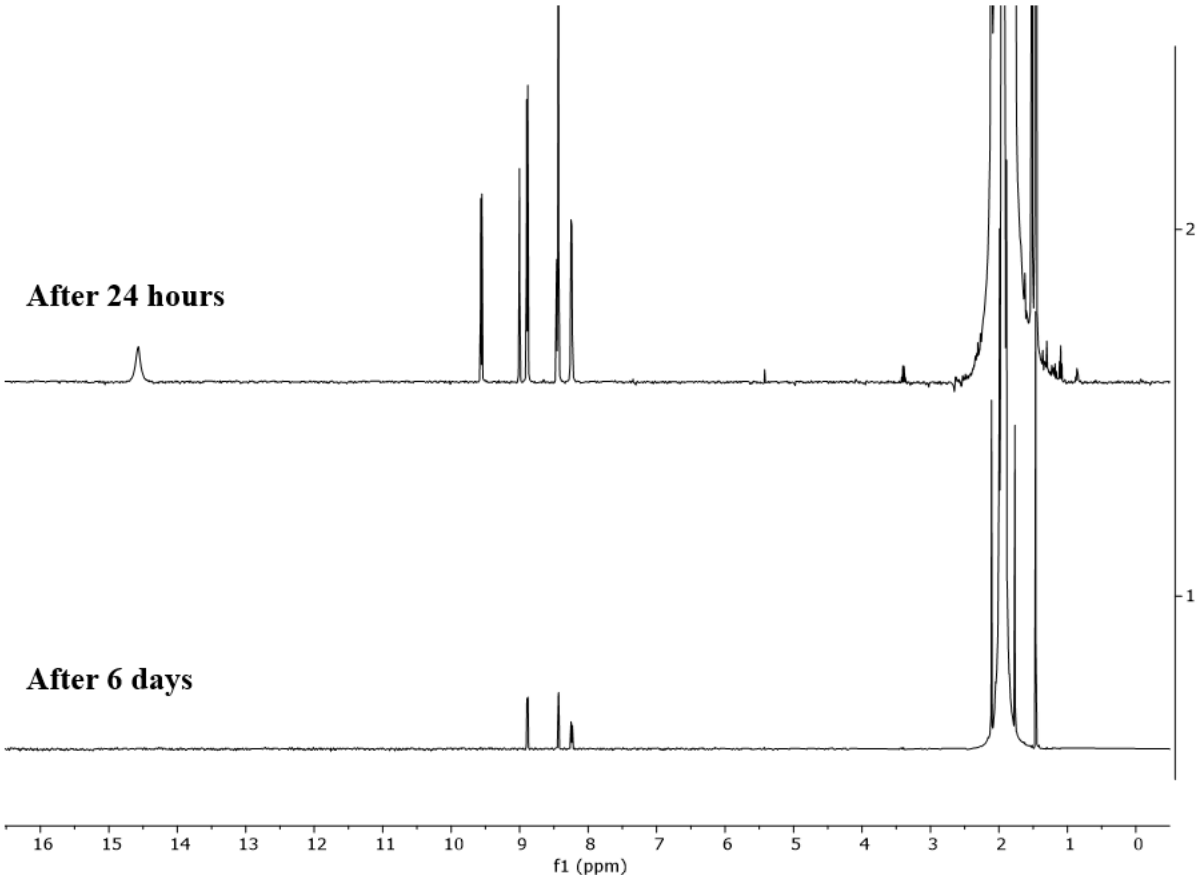

Figure S65. Stacked ^{1}H NMR spectra for the decomposition of **2[OTf]$_2$** in air (CH_3CN, 298K, 400 MHZ). The spectra are referenced to the CH_3CN signal at 1.94 ppm.

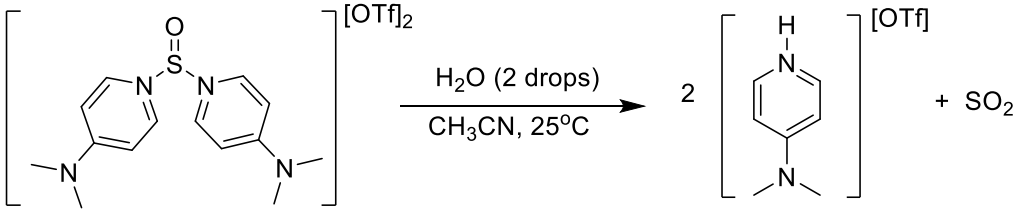

Hydrolysis of 6[OTf]$_2$:

To a solution of **6[OTf]$_2$** (50 mg) in acetonitrile (0.5 mL) in a sealed NMR tube was added 2 drops of deionized water, and the tube was shaken over 1 minute. The tube was monitored by ^{1}H NMR spectroscopy to reveal [HDMAP][OTf] as the only spectroscopically observable product. The broadening of the N-H signal would be consistent with exchange between the N-H protons with

O-H protons from sulfur oxyacids formed from the reaction between SO_2 and any excess water. Crystals of [HDMAP][OTf[were grown from mixtures of CH_3CN/Et_2O at -40°C.

^{1}H NMR (CH_3CN, 400 MHz, 298K): δ (ppm) 12.16 (br s, N-H, 1H), 7.95 (d, $^3J_{H\text{-}H}$ = 7.7 Hz, *o*-C-*H*, 2H), 6.82 (d, $^3J_{H\text{-}H}$ = 7.7 Hz, *m*-C-*H*, 2H), 3.13 (s, N-(CH_3)$_2$).

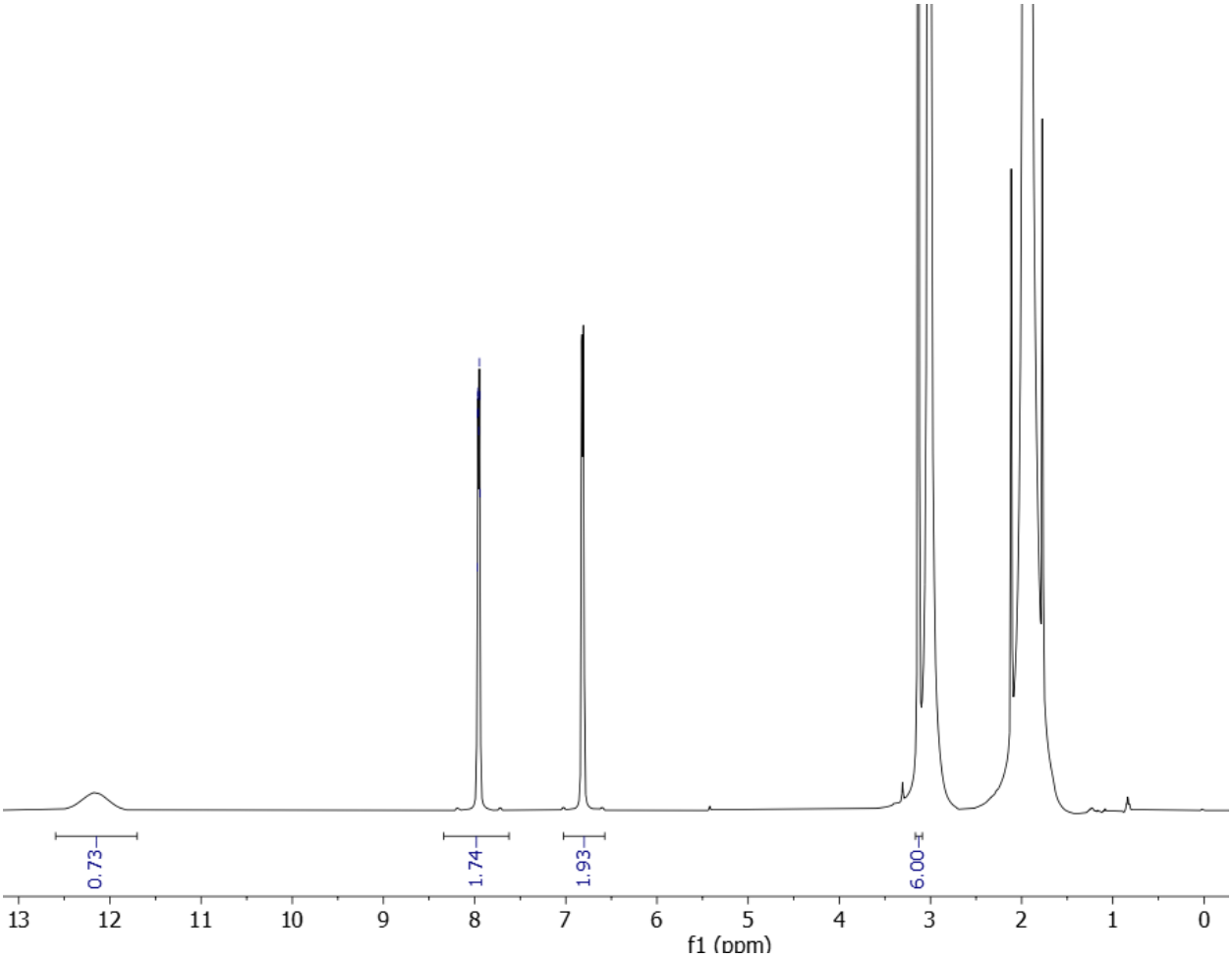

Figure S66. ^{1}H NMR spectrum from the decomposition of **6[OTf]$_2$** after being exposed to 2 drops of H_2O (CH_3CN, 298K, 400 MHZ). The spectrum is referenced the CH_3CN signal at 1.94 ppm

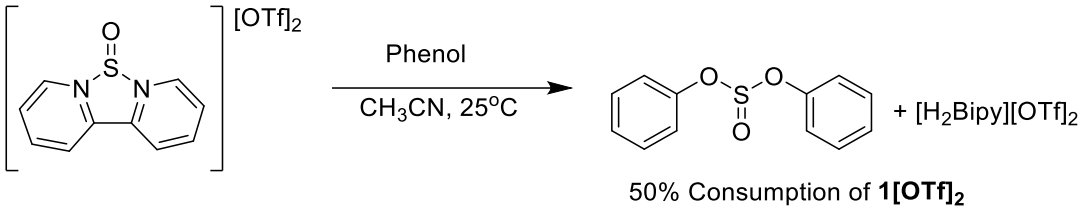

Reaction of 1[OTf]$_2$ with 1 equivalent of PhOH:

To a solution of **1[OTf]$_2$** (20 mg, 0.040 mmol) in acetonitrile (0.5 mL) was added phenol (3.7 mg, 0.039 mmol) in acetonitrile (0.5 mL). The resulting clear and colourless solution was monitored by ^{1}H NMR spectroscopy. After 1 hour, 50% formation of $(PhO)_2SO$ and $[H_2Bipy][OTf]_2$ (quantitative) was observed, along with (50%) remaining **1[OTf]$_2$**.

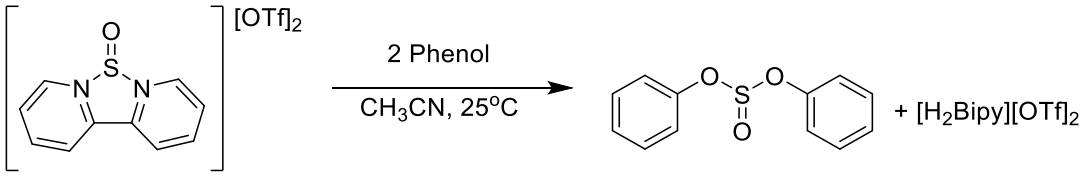

Reaction of 1[OTf]$_2$ with 2 equivalents of PhOH:

To a solution of **1[OTf]$_2$** (40 mg, 0.080 mmol) in acetonitrile (0.5 mL) was added phenol (15 mg, 0.16 mmol) in acetonitrile (0.5 mL). The resulting clear and colourless solution was monitored by ^{1}H NMR spectroscopy. After 1 hour, complete consumption of phenol and **1[OTf]$_2$** were observed. Removal of the volatiles *in vacuo*, left a white residue that was extracted with diethyl ether (3 mL). The extracts were then dried *in vacuo* to isolate $(PhO)_2SO$ (17 mg, 0.072 mmol, 90% yield).

^{1}H NMR (CD_3CN, 500 MHz, 298K): δ (ppm) 7.41 (tm, $^3J_{H\text{-}H}$ = 7.5 Hz, *m*-C-*H*, 4H), 7.29 (t, $^3J_{H\text{-}H}$ = 7.5 Hz, *p*-C-*H*, 2H), 7.21 (dm, $^3J_{H\text{-}H}$ = 7.5 Hz, *o*-C-*H*, 4H).

^{13}C{^{1}H} NMR (CD_3CN, 500 MHz, 298K): δ (ppm) 148.7 (*ipso-C*), 130.0 (*meta-C*), 126.6 (*para-C*), 122.4 (*ortho-C).*

HRMS (DART+, CH_3CN): m/z found 252.06914 ($[(PhO)_2SO + NH_4]^+$ ($C_{12}H_{14}S_1N_1O_3^+$) calc'd 252.06889).

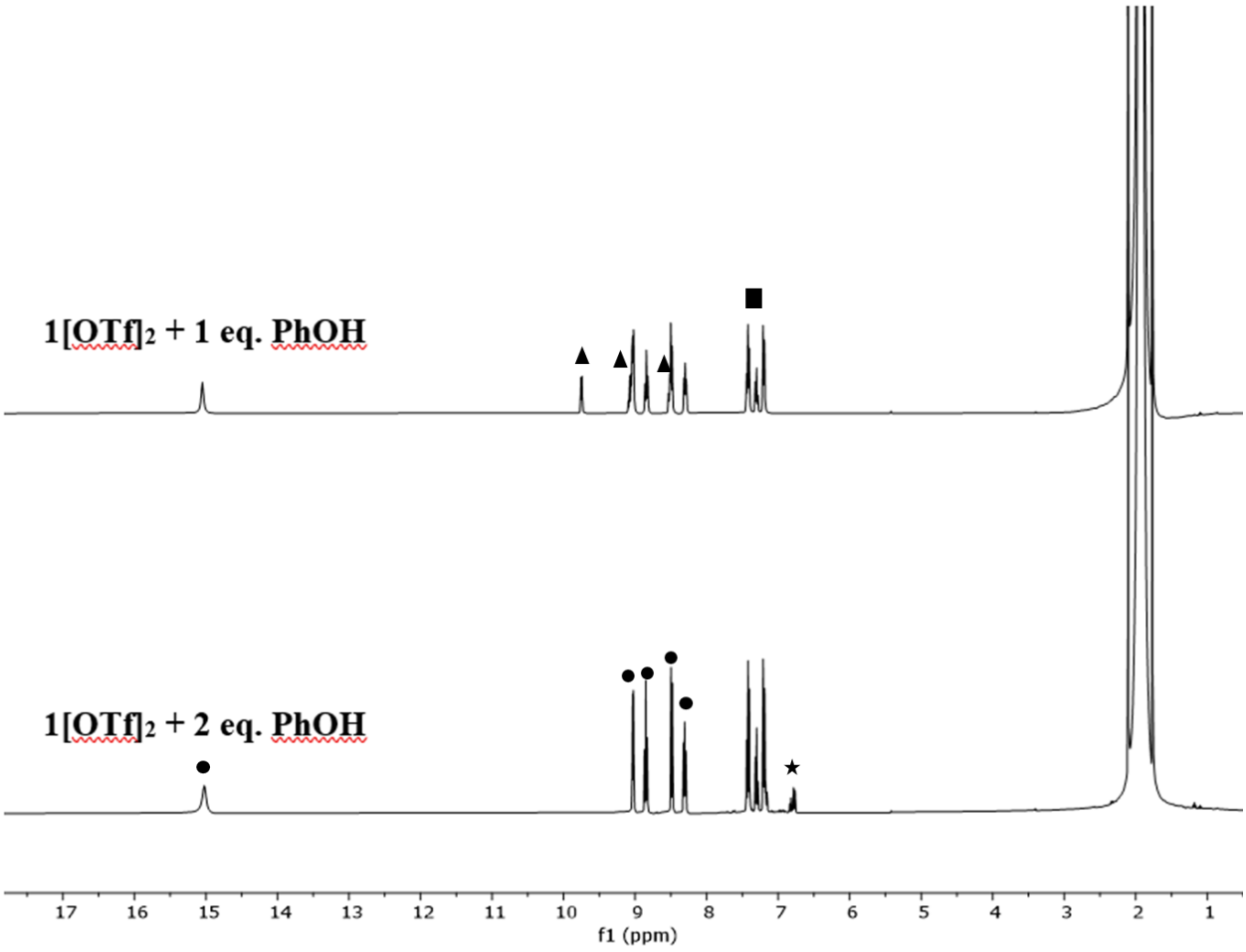

Figure S67. Stacked ^1H NMR spectra for the reaction between **1[OTf]$_2$** and phenol (CH_3CN, 298K, 400 MHZ). The spectra are referenced to the CH_3CN signal at 1.94 ppm. Circle: $[H_2Bipy][OTf]_2$, Square: $(PhO)_2SO$, Triangle: Residual **1[OTf]$_2$**, Star: Residual PhOH.

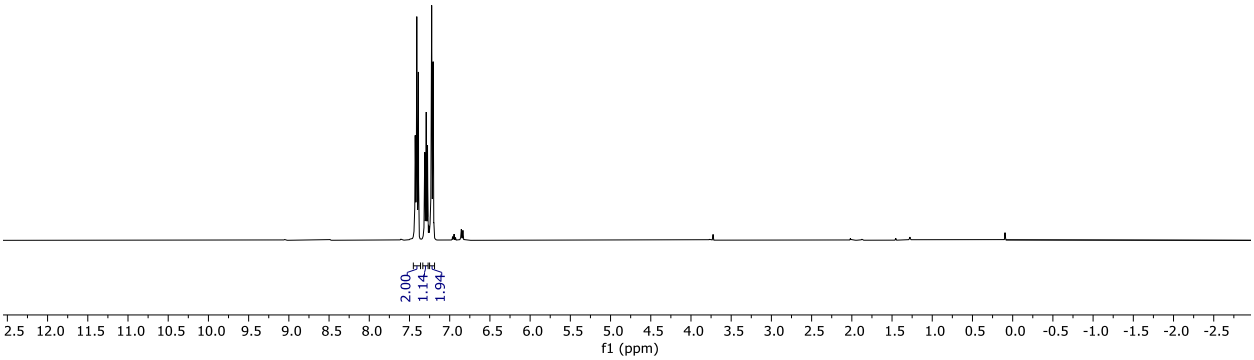

Figure S68. ^{1}H NMR spectrum the isolated $(PhO)_2SO$ formed from the reaction between **1[OTf]$_2$** and phenol ($CDCl_3$, 500 MHz, 298K) for. The spectrum is referenced the residual chloroform signal at 7.26 ppm.

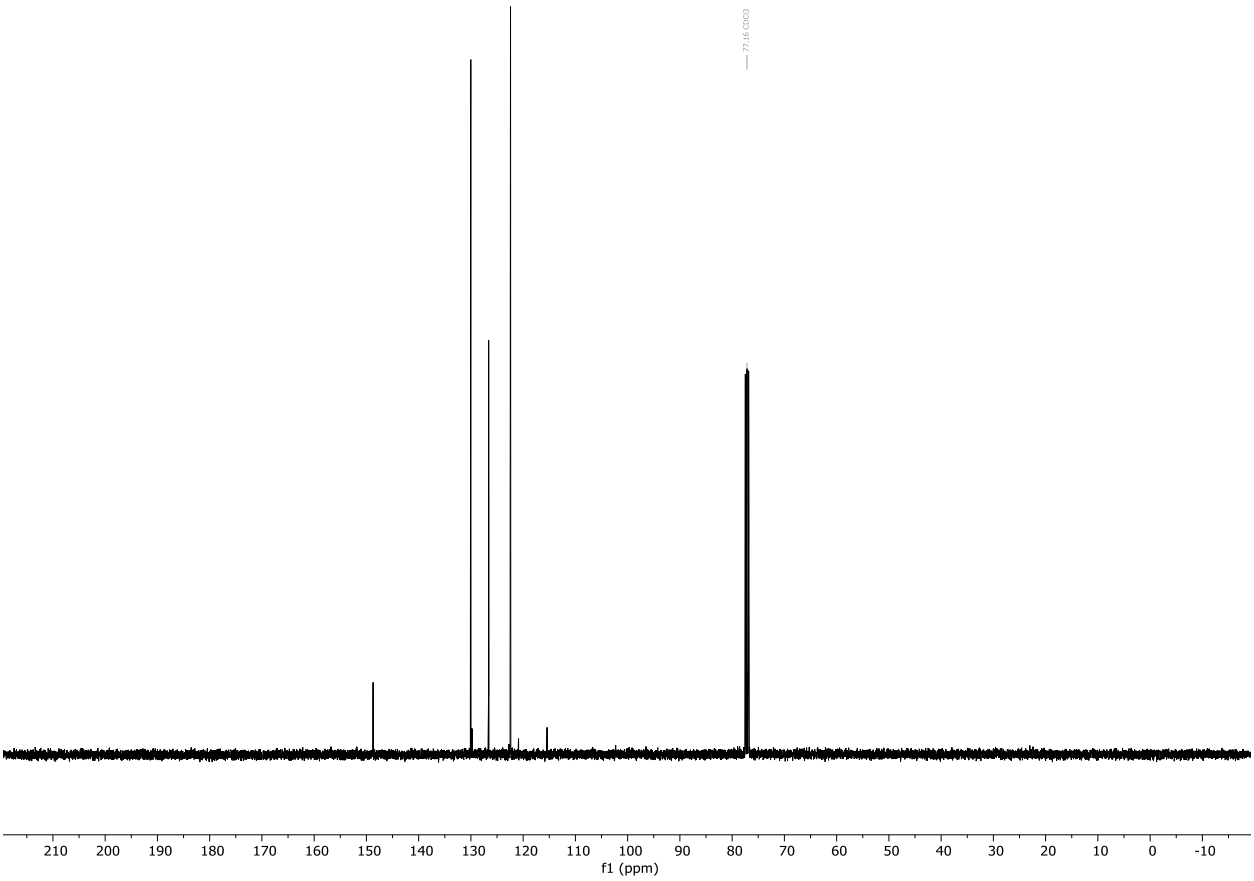

Figure S69. $^{13}C\{^{1}H\}$ NMR spectrum for the isolated $(PhO)_2SO$ formed from the reaction between **1[OTf]$_2$** and phenol ($CDCl_3$, 298K, 126 MHz). The spectrum is referenced the residual chloroform signal at 77.16 ppm.

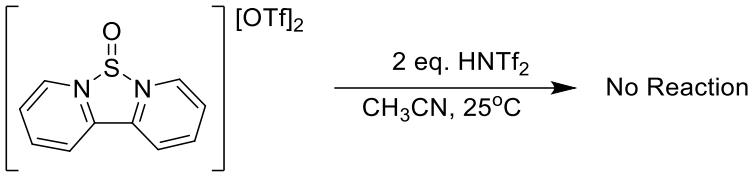

Reaction of 1[OTf]$_2$ with HNTf$_2$:

To a solution of **1[OTf]$_2$** (15 mg, 0.030 mmol) in acetonitrile (0.5 mL) was added HNTf$_2$ (16.8 mg, 0.060 mmol) in acetonitrile (0.5 mL). The resulting clear and colourless solution was monitored by ^{1}H NMR spectroscopy. After 12 hours, <5% conversion of **1**[**OTf]$_2$** was observed from the ^{1}H NMR spectroscopic data. A new unidentified product was observed after 48 hours.

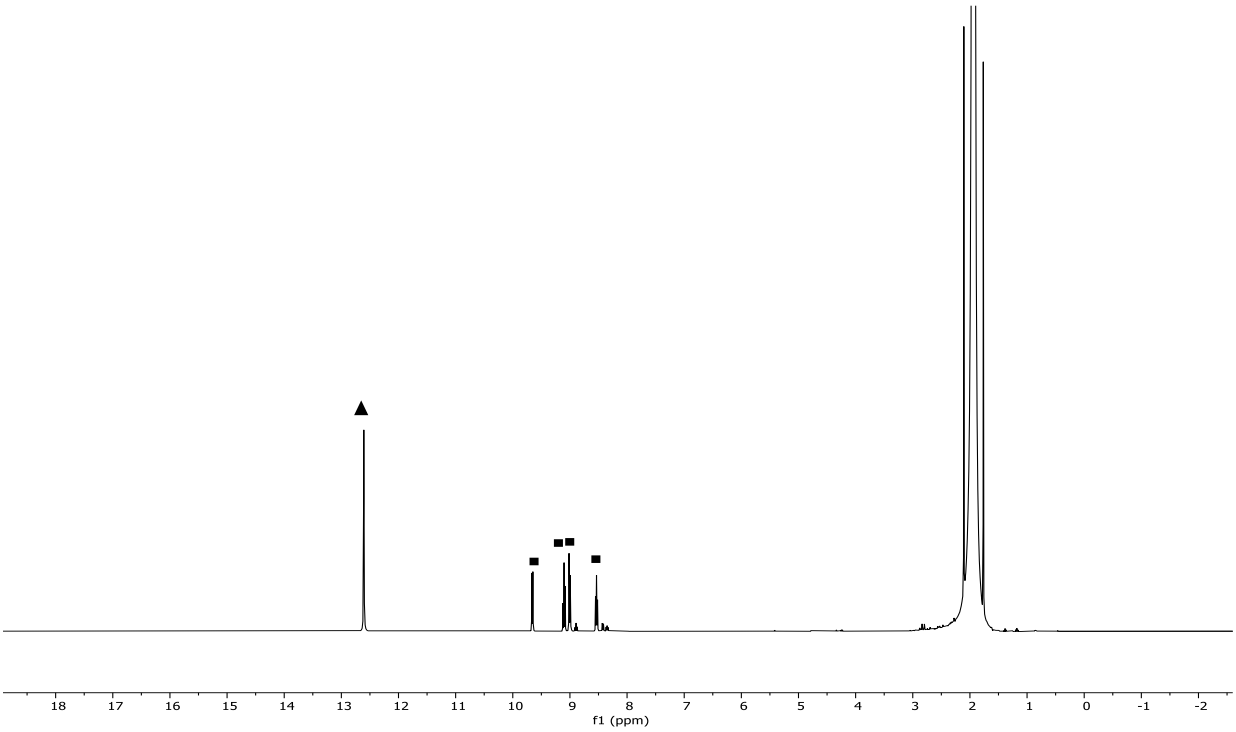

Figure S70. ^{1}H NMR spectrum for the reaction between **1[OTf]$_2$** and HNTf$_2$ after 12 hours (CH$_3$CN, 400 MHz, 298K). The spectrum is referenced to the CH$_3$CN signal at 1.94 ppm. Triangle: HNTf$_2$, Square: **1[OTf]$_2$**.

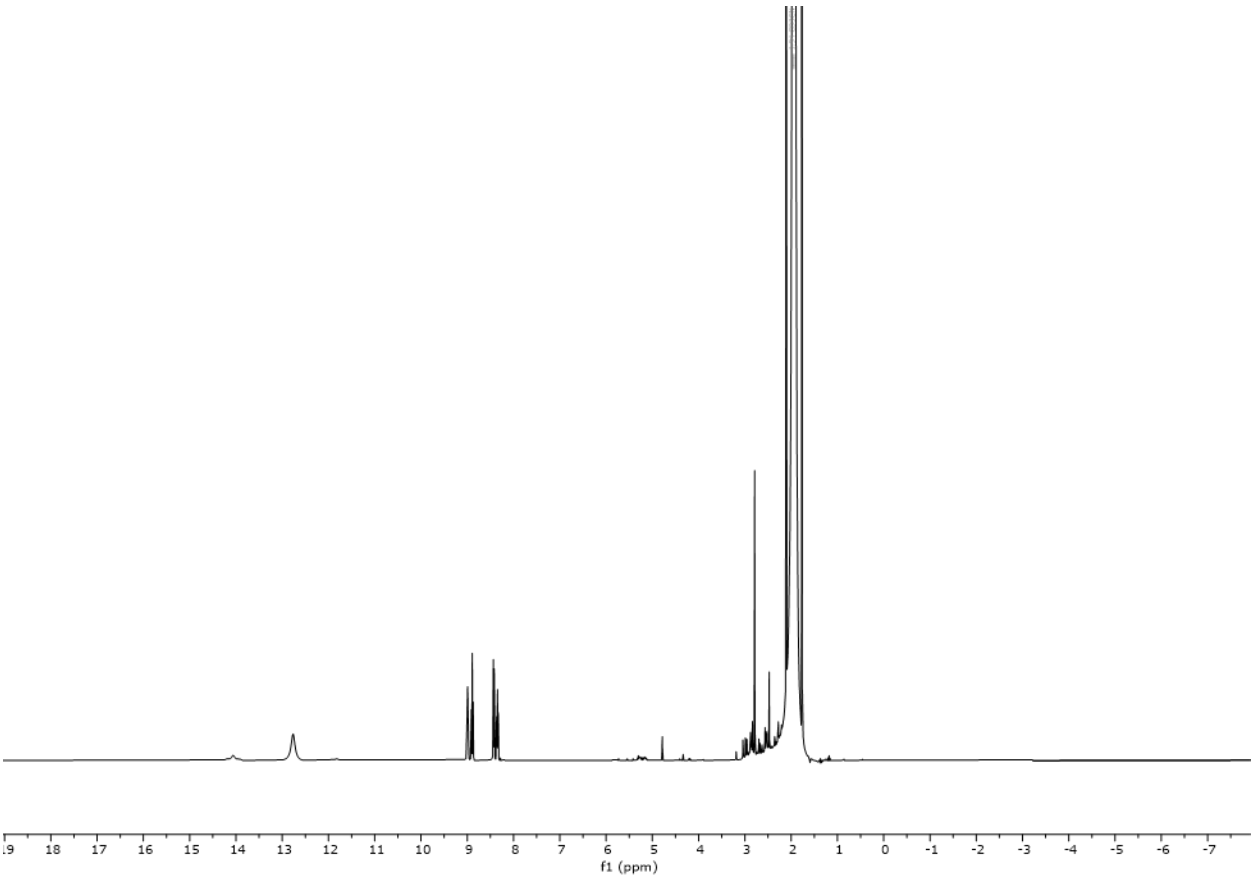

Figure S71. ^{1}H NMR spectrum for the reaction between **1[OTf]$_2$** and $HNTf_2$ after 48 hours (CH_3CN, 400 MHz, 298K). The spectrum is referenced to the CH_3CN signal at 1.94 ppm.

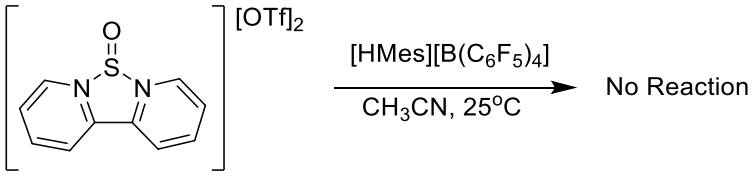

Reaction of 1[OTf]$_2$ with [HMes][B(C_6F_5)$_4$]:

To a solution of **1[OTf]$_2$** (10 mg, 0.020 mmol) in acetonitrile (0.5 mL) was added [HMes][B(C_6F_5)$_4$] (15.8 mg, 0.020 mmol) in acetonitrile (0.5 mL). The resulting clear and light

yellow solution was monitored by ^{1}H NMR spectroscopy. After 24 hours, <5% conversion of **1**[**OTf**]$_2$ was observed from the ^{1}H NMR data.

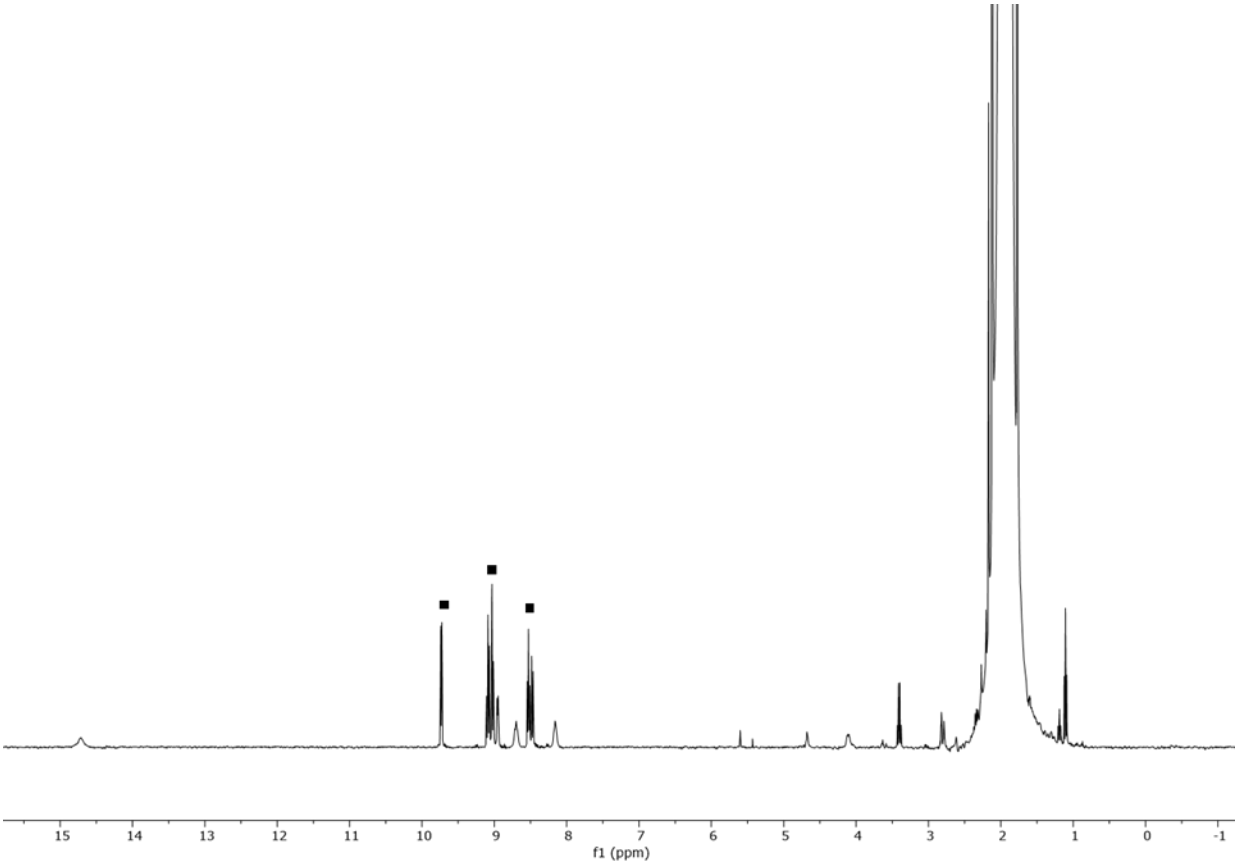

Figure S72. ^{1}H NMR spectrum for the reaction between **1[OTf]**$_2$ and [HMes][B(C_6F_5)$_4$] after 12 hours (CH_3CN, 400 MHz, 298K). The spectrum is referenced to the CH_3CN signal at 1.94 ppm. Square: **1[OTf]**$_2$.

Reaction of 1[OTf]$_2$ with 1 equivalent of Et_3PO:

To a stirring solution of **1[OTf]**$_2$ (20 mg, 0.040 mmol) in acetonitrile (0.5 mL) was added Et_3PO (5.5 mg, 0.041 mmol) in acetonitrile (0.5 mL). The orange-red reaction was stirred for 1 hour and the reaction progress was monitored using ^{1}H and ^{31}P NMR spectroscopy. ^{31}P NMR spectroscopy reveals one new product at 127 ppm in the ^{31}P NMR spectrum. The ^{1}H NMR spectrum shows the formation of new bipyridine products.

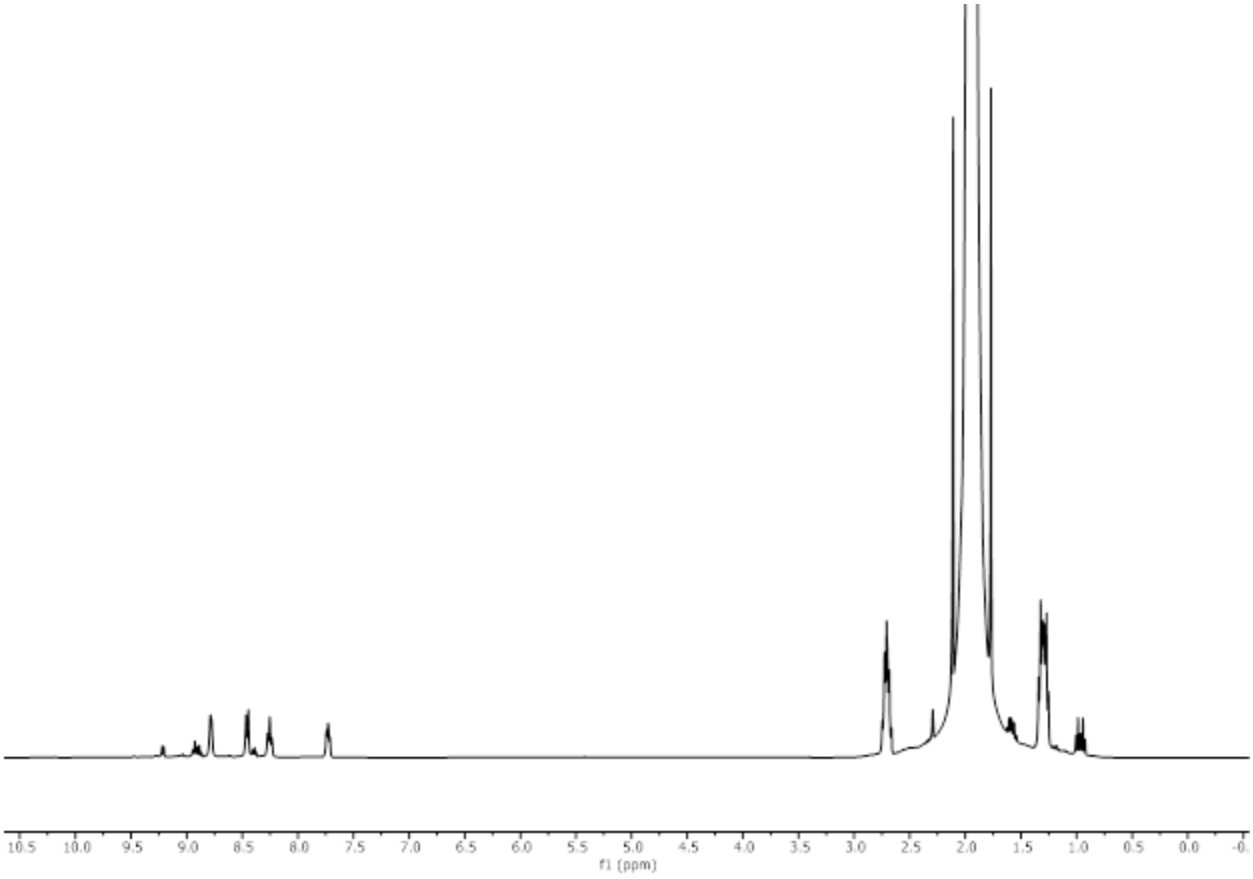

Figure S73. ^{1}H NMR spectrum for the reaction between **1[OTf]$_2$** and Et_3PO after 1 hour (CH_3CN, 400 MHz, 298K). The spectrum is referenced to the CH_3CN signal at 1.94 ppm.

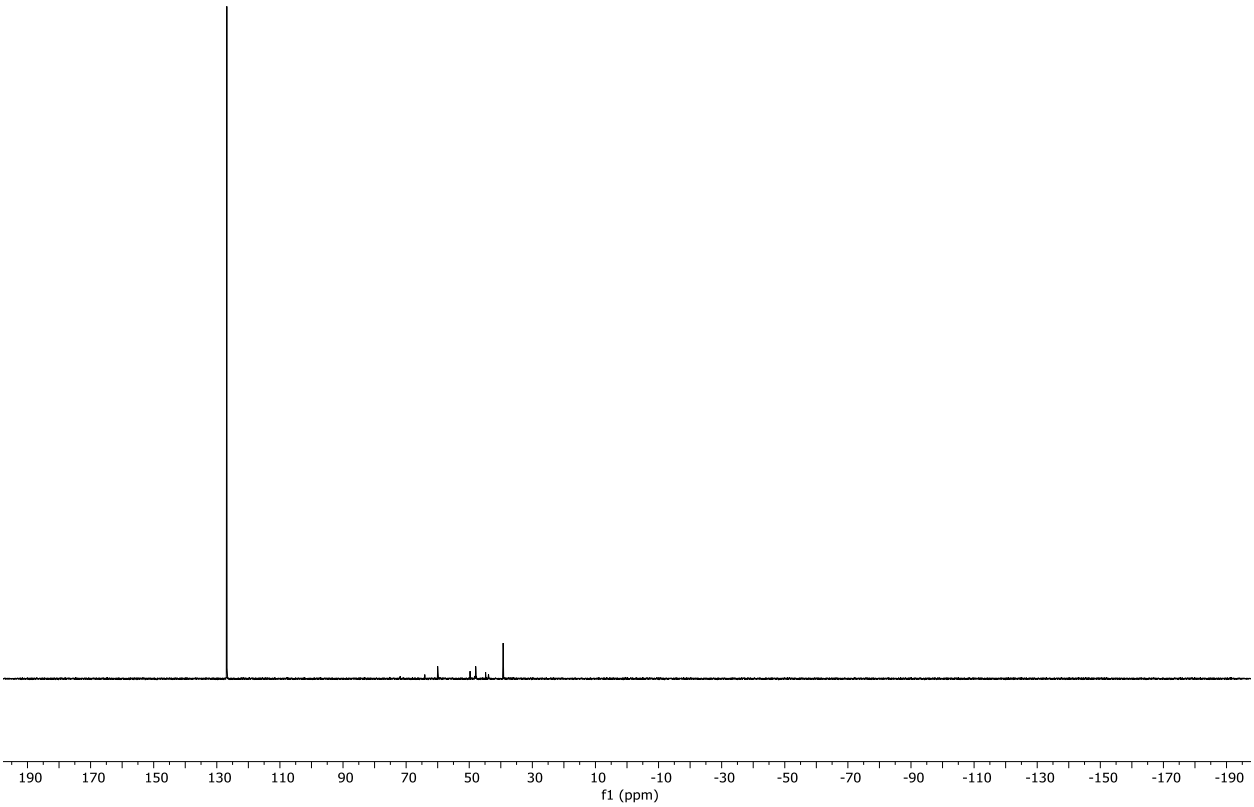

Figure S74. $^{31}P\{^{1}H\}$ NMR spectrum for the reaction between **1[OTf]$_2$** and Et_3PO (CH_3CN, 162 MHz, 298K).

Reaction of 1[OTf]$_2$ with 2 equivalent of Et_3PO:

To a stirring solution of **1[OTf]$_2$** (20 mg, 0.040 mmol) in acetonitrile (0.5 mL) was added Et_3PO (10.9 mg, 0.081 mmol) in acetonitrile (0.5 mL). The colourless reaction was stirred for 1 hour and the reaction progress was monitored using ^{1}H and ^{31}P NMR spectroscopy. ^{31}P NMR spectroscopy reveals one new product at 104 ppm in the ^{31}P NMR spectrum. The ^{1}H NMR spectrum shows the formation of 2,2'-bipyridine as the only bipyridine product formed in appreciable amounts. By analogy to the Ph_3PO reaction, the phosphorus product is proposed to be $[Et_3POPEt_3][OTf]_2$.

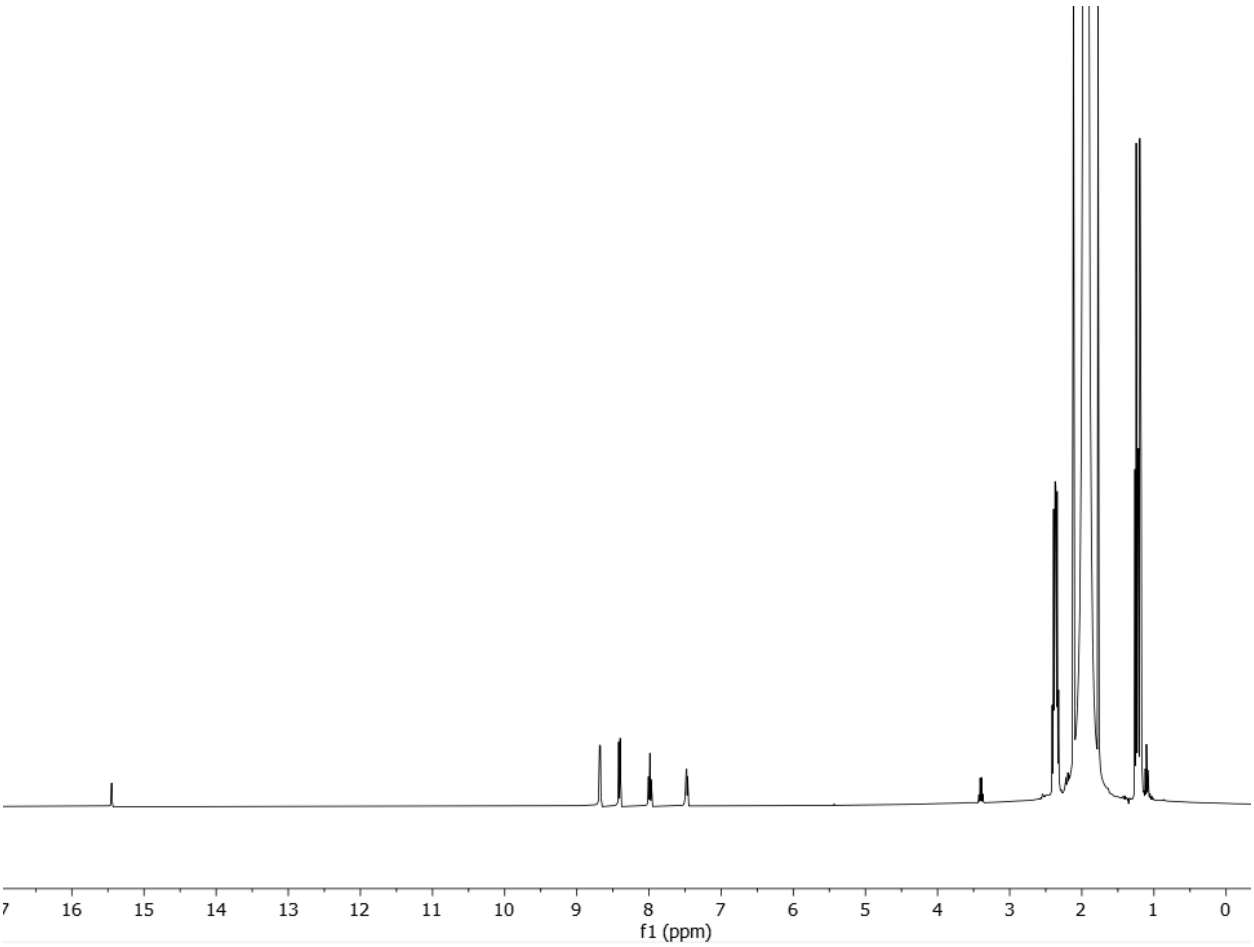

Figure S75. ^{1}H NMR spectrum for the reaction between **1[OTf]$_2$** and 2 equivalents of Et_3PO after 1 hour (CH_3CN, 400 MHz, 298K). The spectrum is referenced to the CH_3CN signal at 1.94 ppm.

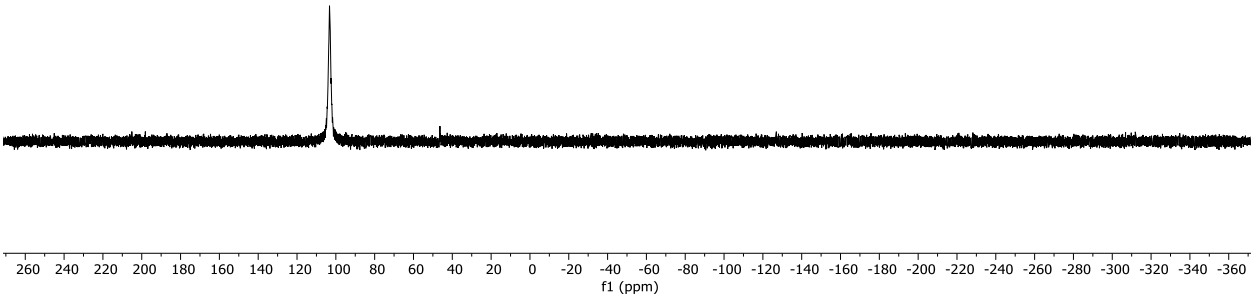

Figure S76. $^{31}P\{^{1}H\}$ NMR spectrum for the reaction between **1[OTf]$_2$** and 2 equivalents Et_3PO (CH_3CN, 162 MHz, 298K).

Reaction of 2[OTf]$_2$ with 1 equivalent of Et_3PO:

To a stirring solution of **2[OTf]$_2$** (7.3 mg, 0.012 mmol) in acetonitrile (0.5 mL) was added Et_3PO (1.6 mg, 0.012 mmol) in acetonitrile (0.5 mL). The orange-red reaction was stirred for 1 hour and the reaction progress was monitored using ^{1}H and ^{31}P NMR spectroscopy. ^{31}P NMR spectroscopy reveals one new product at 127 ppm in the ^{31}P NMR spectrum. The ^{1}H NMR spectrum shows the formation of a new 4,4'-ditertbutyl-2,2'-bipyridine product.

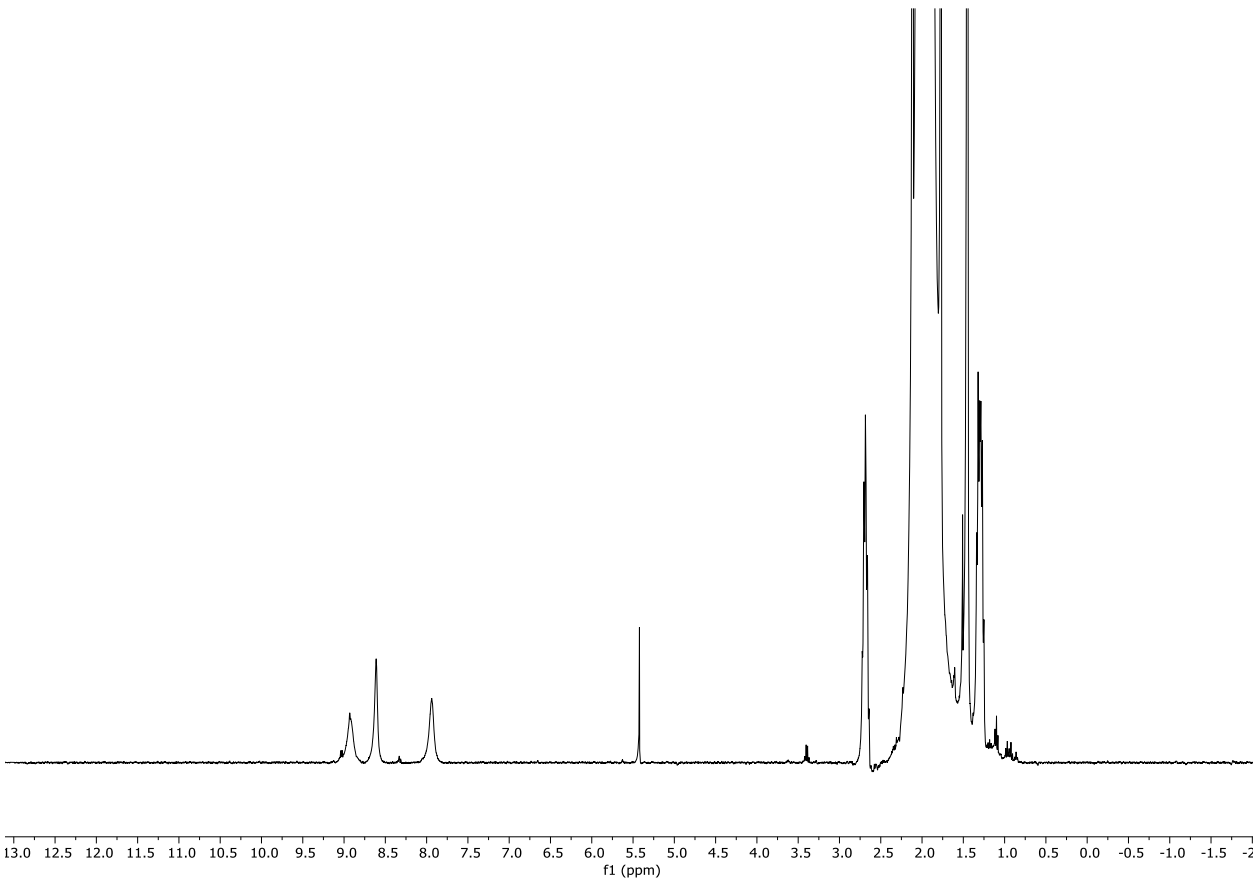

Figure S77. ^{1}H NMR spectrum for the reaction between **2[OTf]$_2$** and of Et_3PO after 1 hour (CH_3CN, 400 MHz, 298K). The spectrum is referenced to the CH_3CN signal at 1.94 ppm.

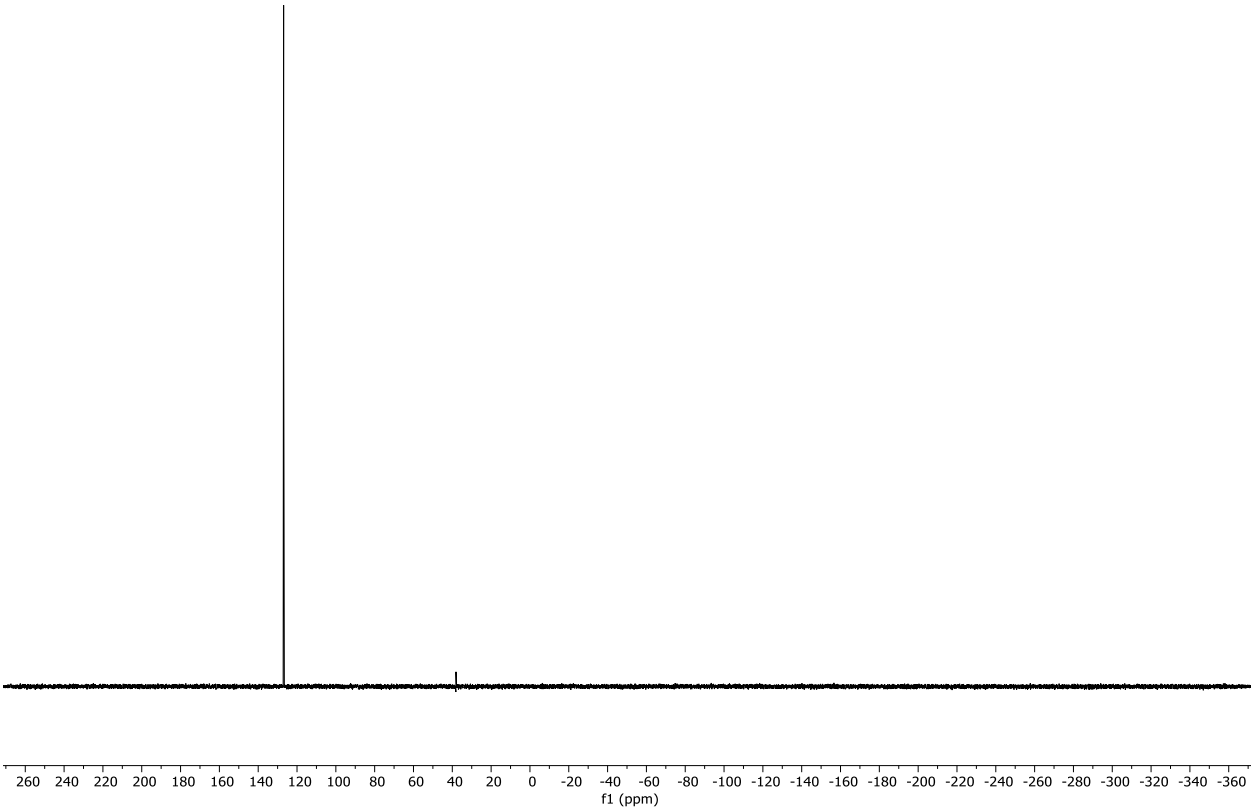

Figure S78. $^{31}P\{^{1}H\}$ NMR spectrum for the reaction between **2[OTf]$_2$** and Et_3PO (CH_3CN, 162 MHz, 298K).

Reaction of 4[OTf]$_2$ with 1 equivalent of Et_3PO:

To a stirring solution of **4[OTf]$_2$** (7.3 mg, 0.012 mmol) in acetonitrile (0.5 mL) was added Et_3PO (1.6 mg, 0.012 mmol) in acetonitrile (0.5 mL). The orange-red reaction was stirred for 1 hour and the reaction progress was monitored using ^{1}H and ^{31}P NMR spectroscopy. ^{31}P NMR spectroscopy reveals one new product at 127 ppm in the ^{31}P NMR spectrum. The ^{1}H NMR spectrum shows the formation of a new 4-Cl-Terpyridine product.

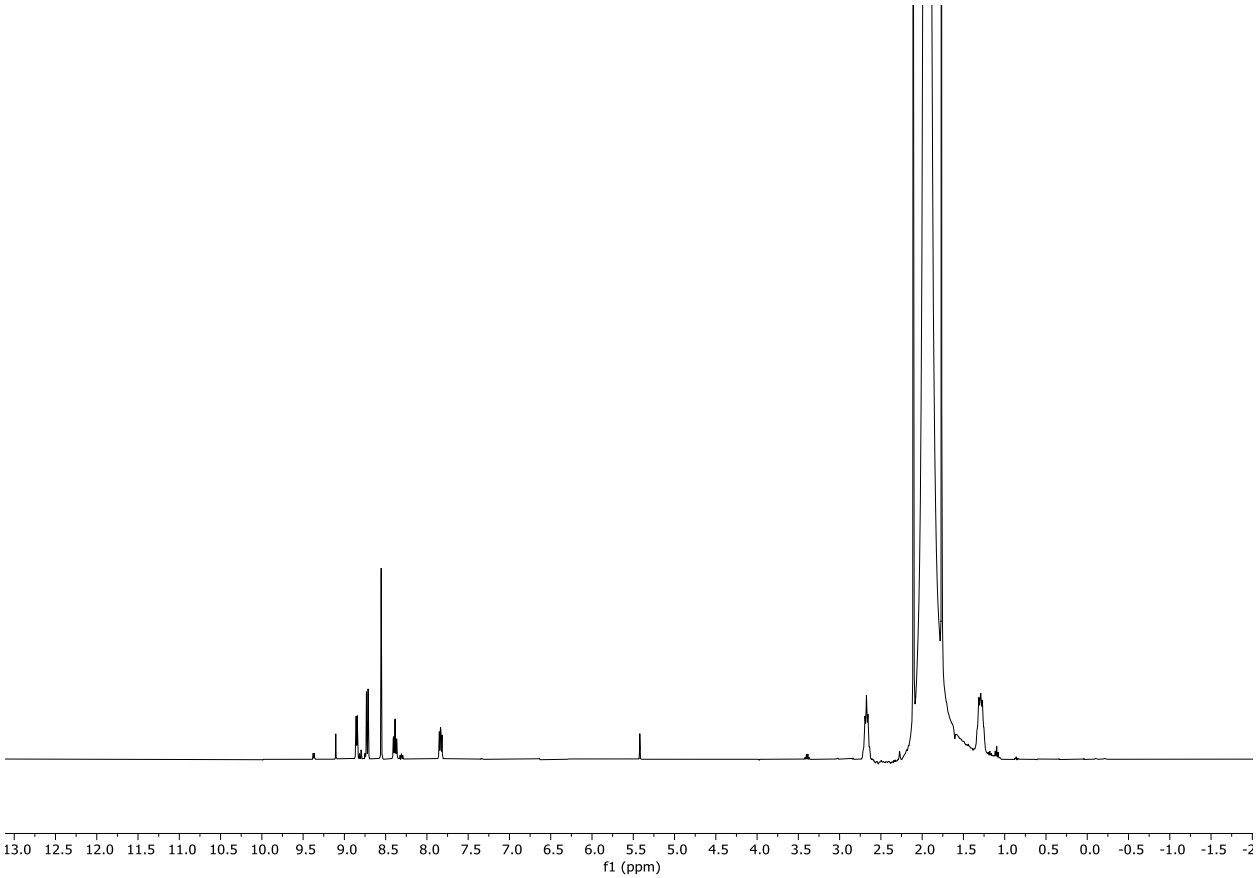

Figure S79. ^{1}H NMR spectrum for the reaction between **4[OTf]$_2$** and of Et_3PO after 1 hour (CH_3CN, 400 MHz, 298K). The spectrum is referenced to the CH_3CN signal at 1.94 ppm.

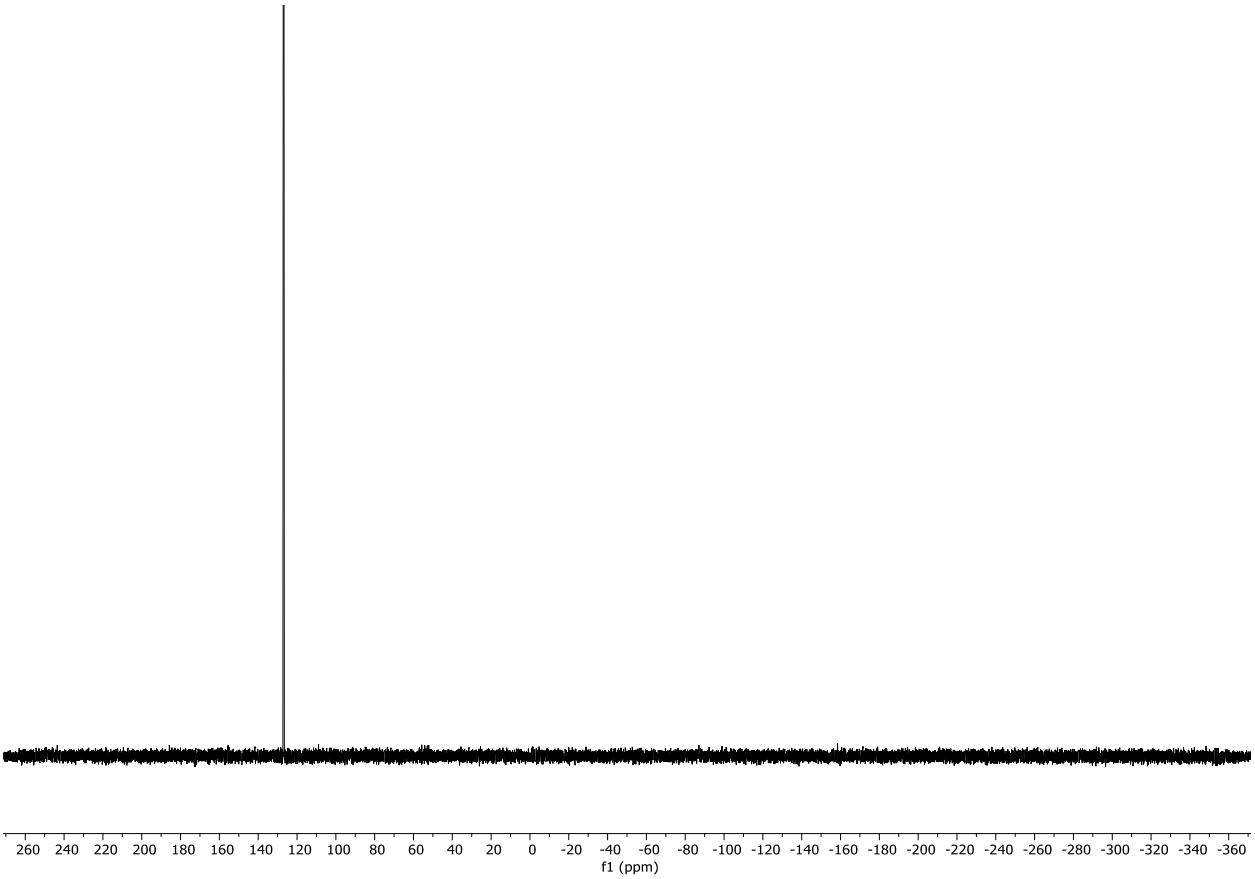

Figure S80. $^{31}P\{^{1}H\}$ NMR spectrum for the reaction between **4[OTf]$_2$** and Et_3PO (CH_3CN, 162 MHz, 298K).

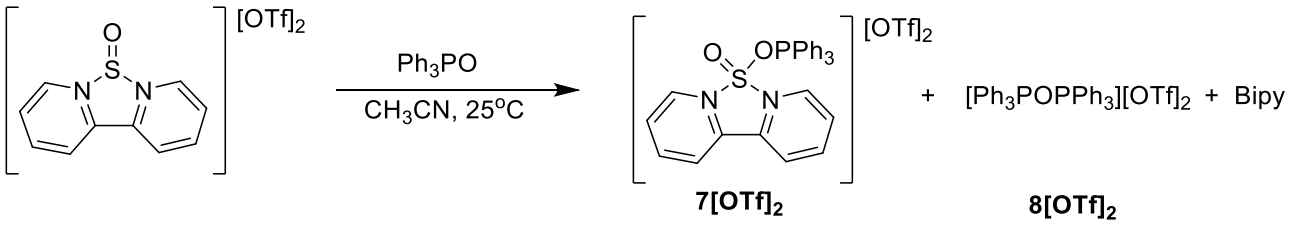

Reaction of 1[OTf]$_2$ with 1 equivalent of Ph_3PO:

To a stirring solution of **1[OTf]$_2$** (20 mg, 0.040 mmol) in acetonitrile (0.5 mL) was added Ph_3PO (11 mg, 0.040 mmol) in acetonitrile (0.5 mL). The yellow-orange reaction was stirred for 1 hour and the reaction progress was monitored using ^{1}H and ^{31}P NMR spectroscopy. Slow evaporation of the reaction mixture at -40°C led to the formation of yellow crystal of **7[OTf]$_2$** (11 ppm in the ^{31}P NMR spectrum), whereas a layered solution of the reaction mixture in CH_3CN/Et_2O led to the

formation of colourless crystals of **8[OTf]$_2$** (75 ppm in the ^{31}P NMR spectrum). ^{1}H NMR and ^{31}P NMR data confirm the formation of **9[OTf]$_2$** and **8[OTf]$_2$**. Multiple new sets of bipyridine signals are identified in the ^{1}H NMR spectrum, including a broadened set of signals attributed to an equilibrium interaction between **1[OTf]$_2$** and free 2,2'-bipyridine. The addition of Ph_3PO to **1[OTf]$_2$** at -40°C or using highly dilute solutions led to no changes in the observed product distributions.[8-9]

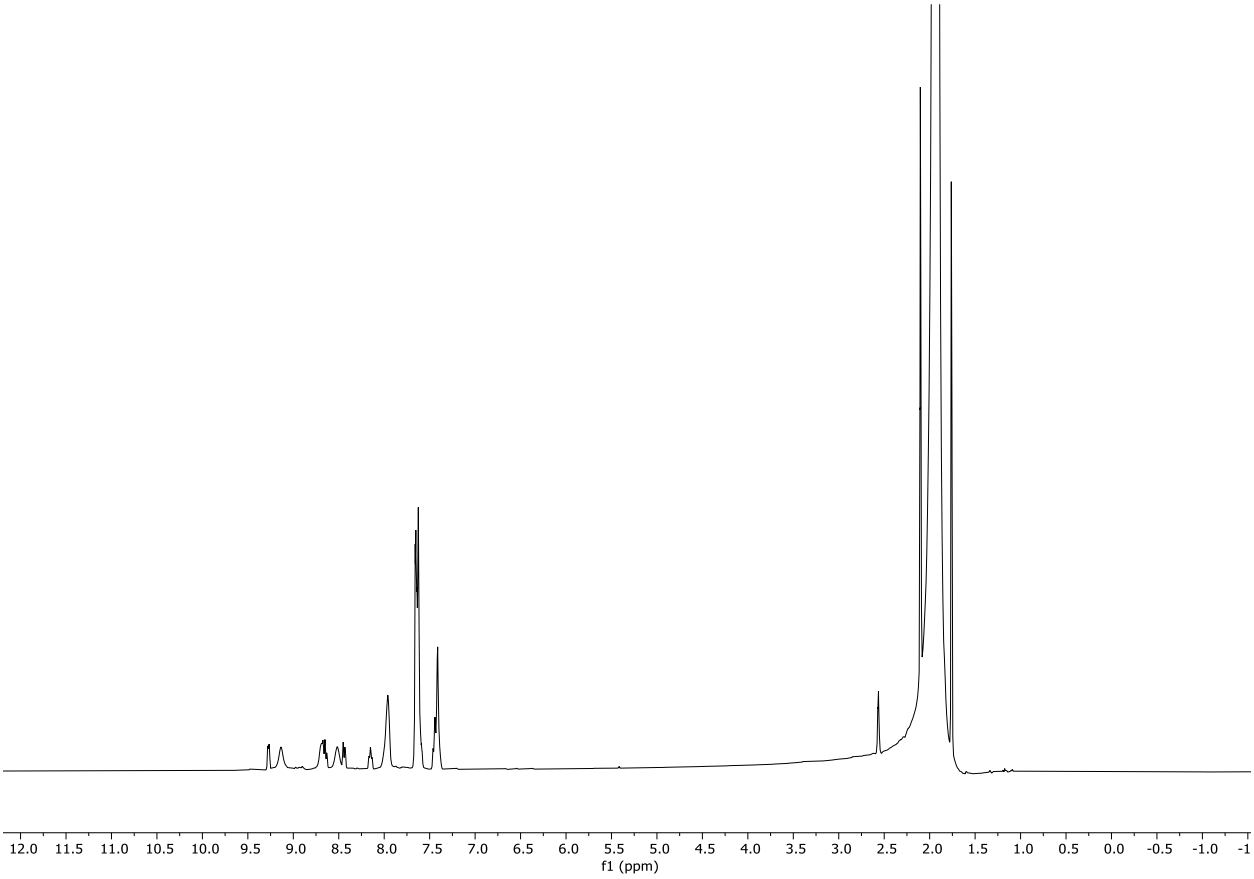

Figure S81. ^{1}H NMR spectrum for the reaction between **1[OTf]$_2$** and Ph_3PO (CH_3CN, 400 MHz, 298K).

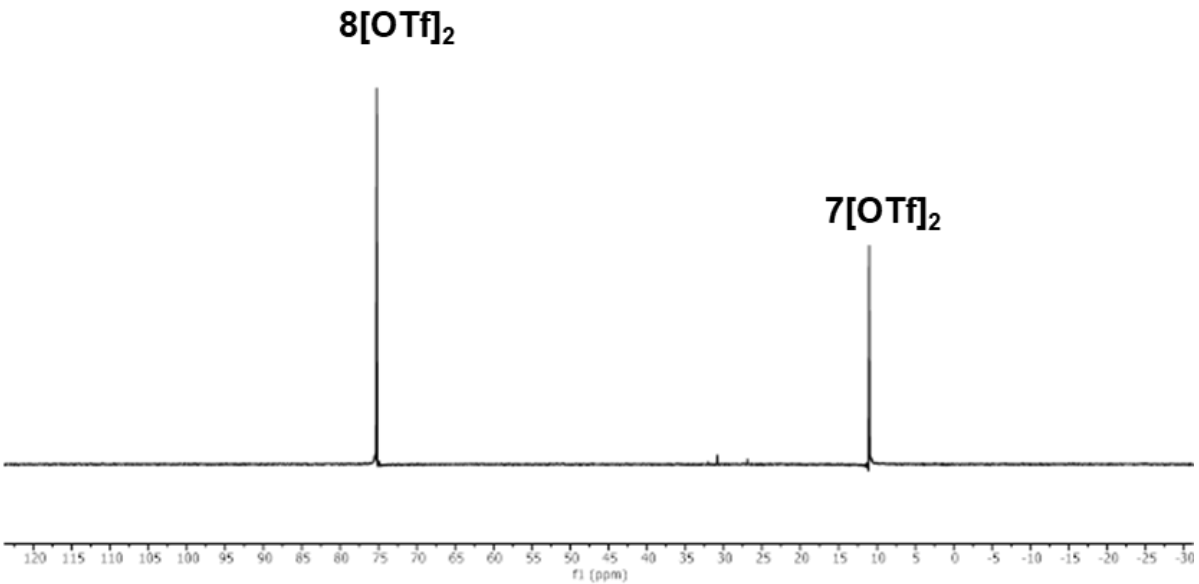

Figure S82. $^{31}P\{^{1}H\}$ NMR spectrum for the reaction between **1[OTf]2** and Ph_3PO (CH_3CN, 162 MHz, 298K).

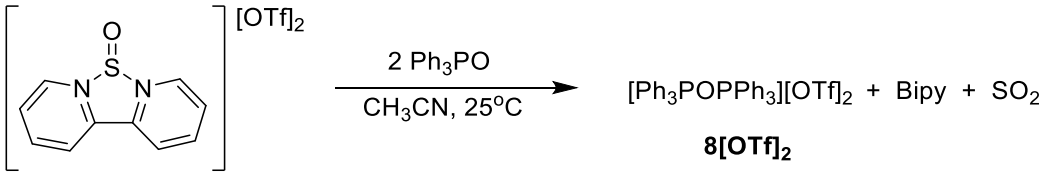

Reaction of 1[OTf]2 with 2 equivalents of Ph_3PO:

To a stirring solution of **1[OTf]2** (50 mg, 0.10 mmol) in acetonitrile (0.5 mL) was added Ph_3PO (55 mg, 0.20 mmol) in acetonitrile (0.5 mL). The colourless reaction was stirred for 1 hour and the reaction progress was monitored using ^{1}H and ^{31}P NMR spectroscopy. The spectroscopic data confirms quantitative formation of **8[OTf]2** (72 ppm in the ^{31}P NMR spectrum) and bipyridine. Balancing the equation suggests this reaction is driven by the release of SO_2. Removal of the

volatiles *in vacuo*, washing the white residues, and further drying leads to the isolation of **8[OTf]$_2$** as a white powder (76 mg, 0.091 mmol, 91% yield).[8-9]

^{1}H NMR (CD_3CN, 500 MHz, 298K): δ (ppm) 7.93 (t, $^3J_{H\text{-}H}$ = 7.2 Hz, *p*-C-*H*, 6H), 7.75-7.65 (m, overlapping signals of *m*-C-*H*, and *o*-C-*H*, 24H).

$^{13}C\{^1H\}$ NMR (CD_3CN, 500 MHz, 298K): δ (ppm) 137.8 (s, *p*-*C*), 134.8 (d, $^3J_{C\text{-}P}$ = 11.5 Hz, *m*-*C*), 131.3 (d, $^2J_{C\text{-}P}$ = 114.6 Hz, *o*-*C*), 121.7 (q, $^1J_{C\text{-}F}$ = 322.1 Hz, OTf *C*-F).

$^{19}F\{^1H\}$ NMR (CD_3CN, 377 MHz, 298K): δ (ppm) -79.2 (s, OTf).

$^{31}P\{^1H\}$ NMR (CD_3CN, 162 MHz, 298K): δ (ppm) 71.7 (s).

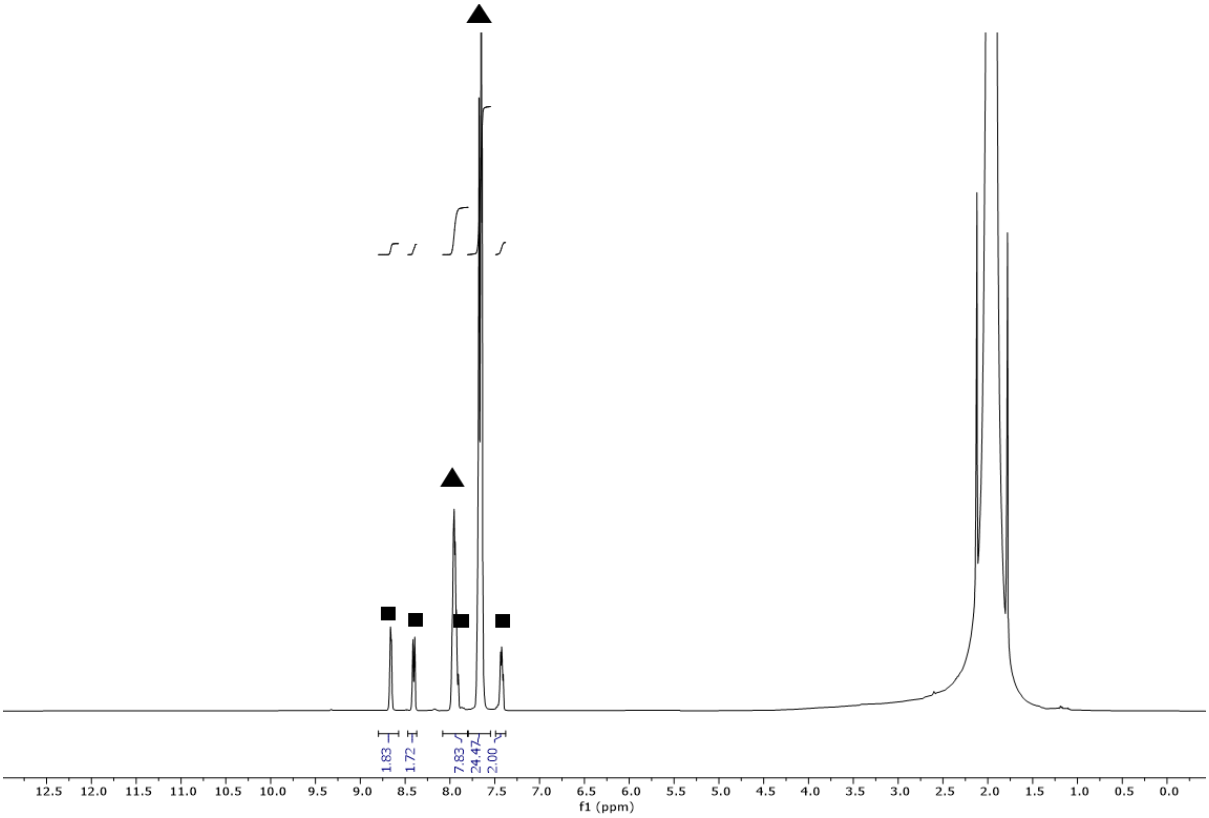

Figure S83. ^{1}H NMR spectrum for the reaction between **1[OTf]$_2$** and 2 equivalents of Ph_3PO (CH_3CN, 400 MHz, 298K). The NMR spectrum is referenced to the CH_3CN signal at 1.94 ppm. Triangle: **8[OTf]$_2$**, Square: 2,2'-bipyridine.

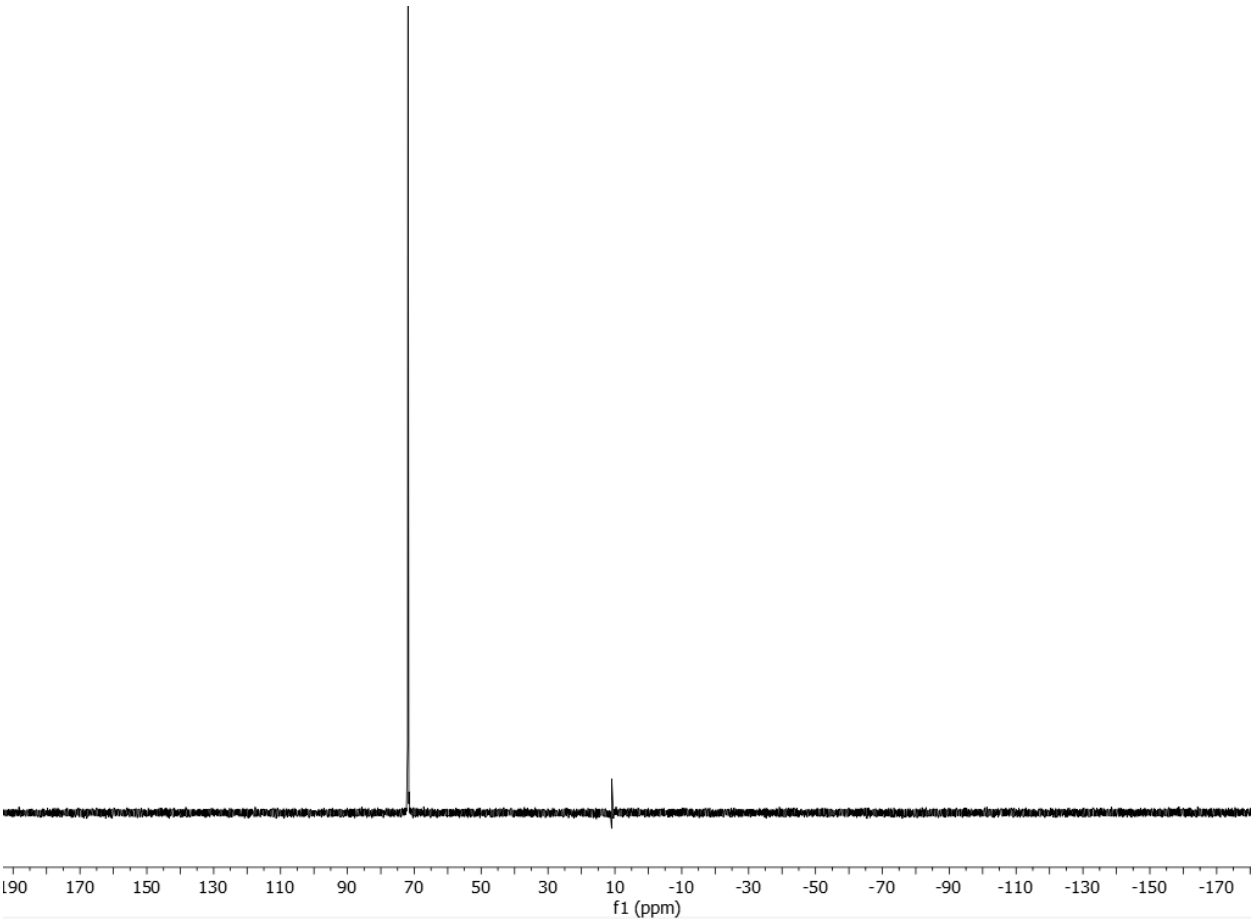

Figure S84. $^{31}P\{^{1}H\}$ NMR spectrum for the reaction between **1[OTf]$_2$** and 2 equivalents of Ph_3PO (CH_3CN, 162 MHz, 298K).

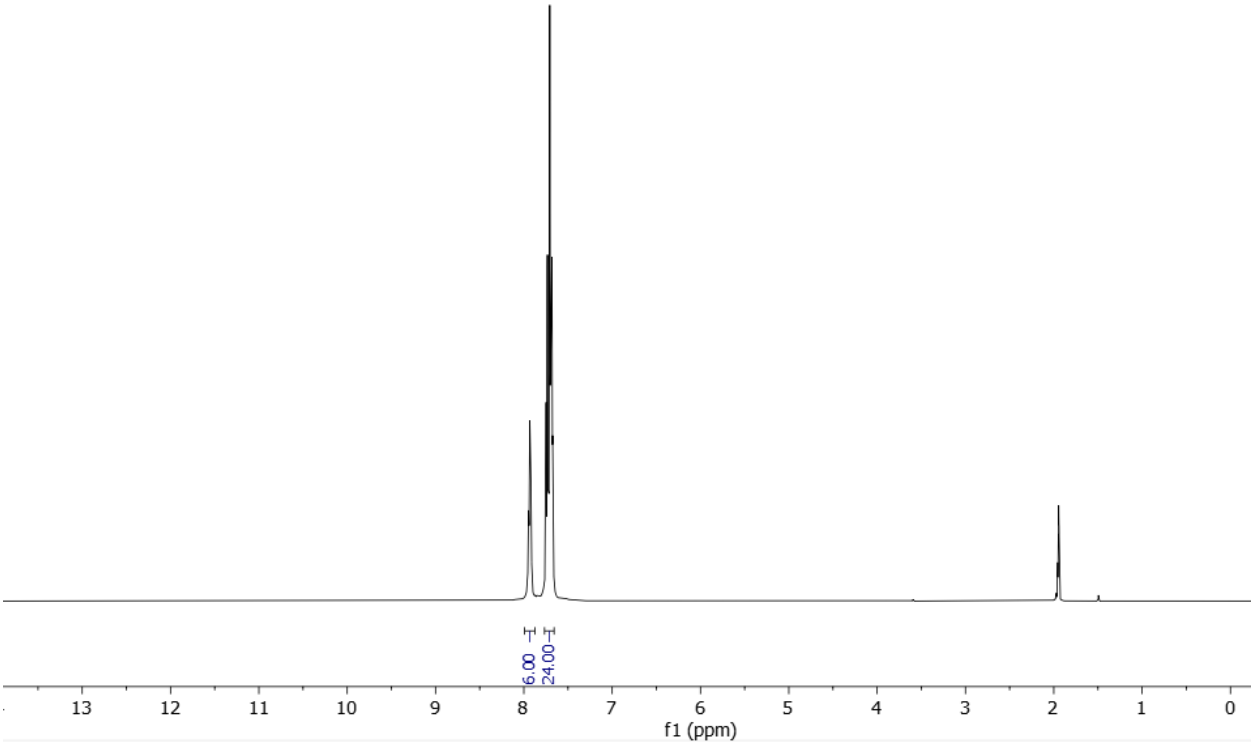

Figure S85. ^{1}H NMR spectrum for the isolated $[Ph_3POPPh_3][OTf]_2$ isolated from the reaction between **1[OTf]$_2$** and 2 equivalents of Ph_3PO (CD_3CN, 500 MHz, 298K). The NMR spectrum is referenced to the residual acetonitrile signal at 1.94 ppm.

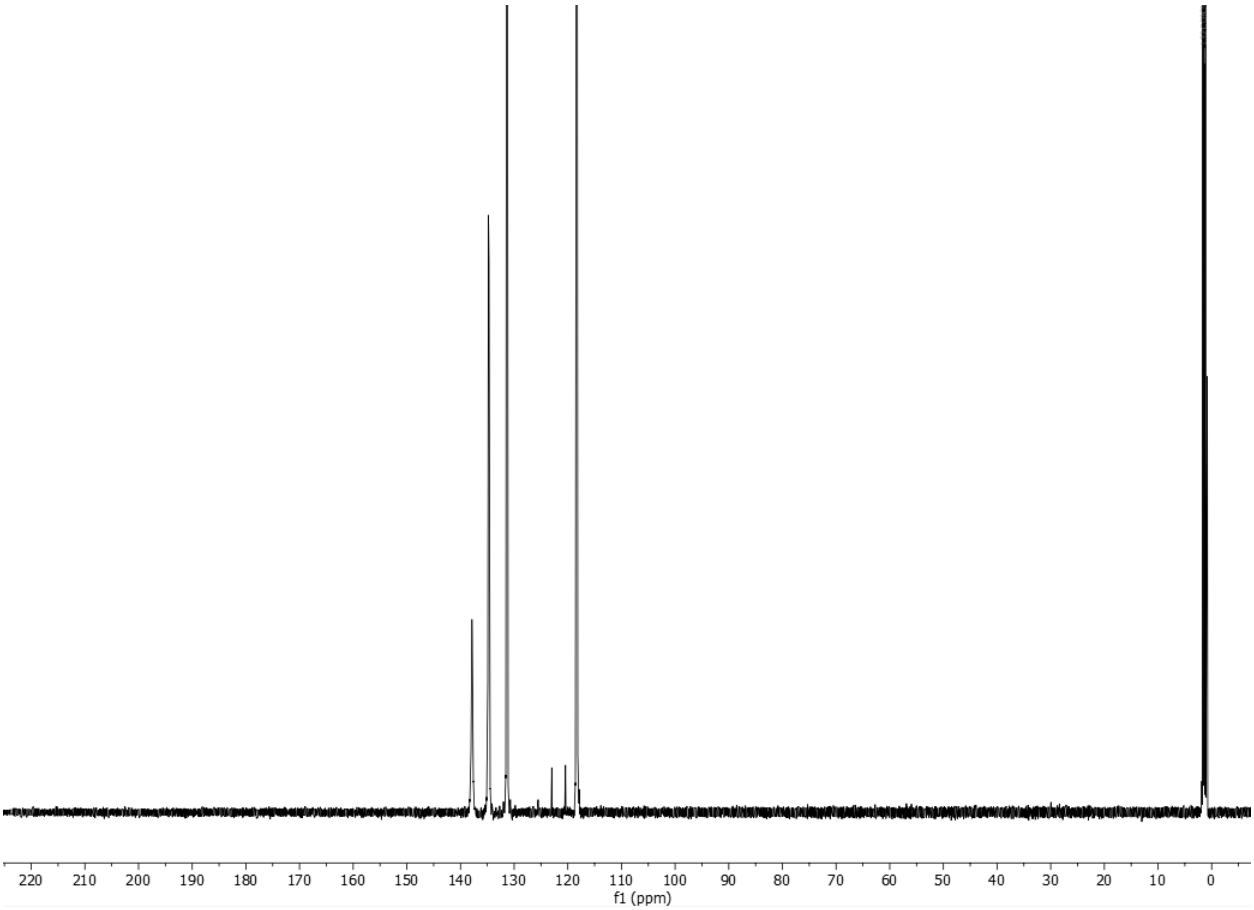

Figure S86. $^{13}C\{^{1}H\}$ NMR spectrum for the isolated $[Ph_3POPPh_3][OTf]_2$ isolated from the reaction between **1[OTf]$_2$** and 2 equivalents of Ph_3PO (CD_3CN, 126 MHz, 298K). The NMR spectrum is referenced to the residual acetonitrile signal at 1.32 ppm.

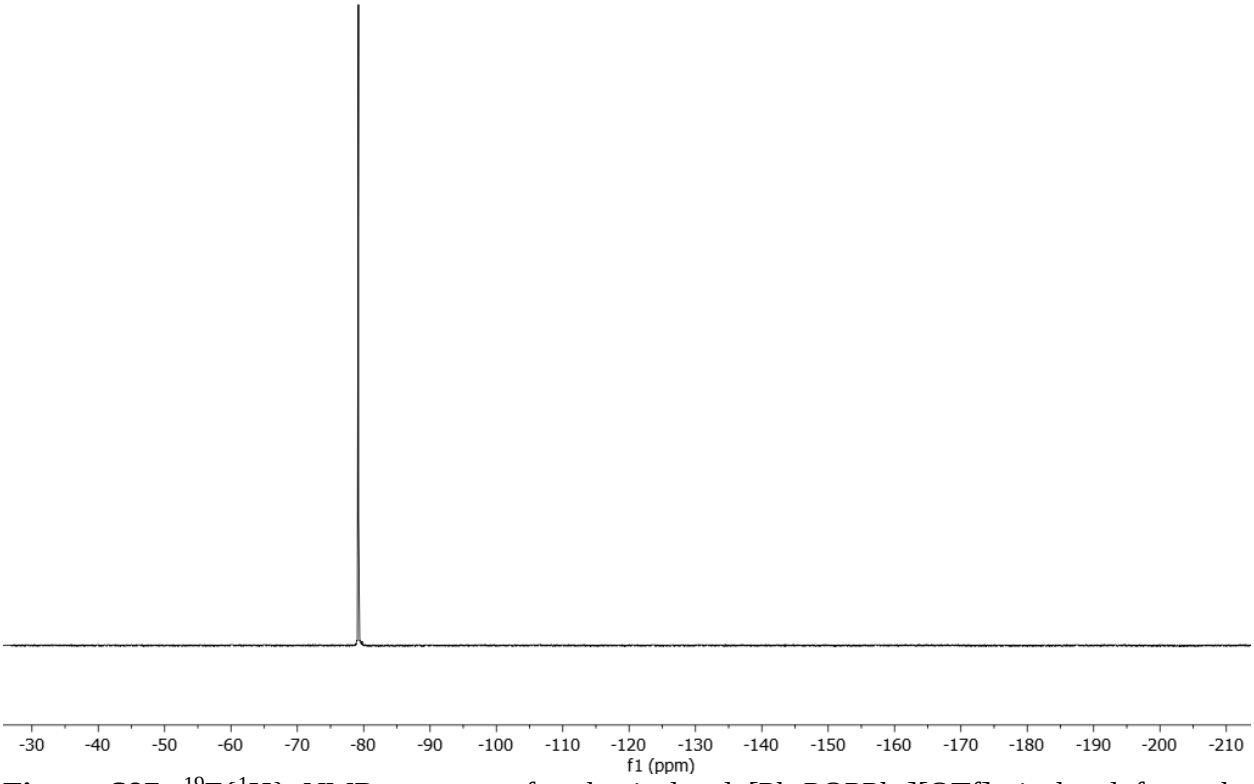

Figure S87. $^{19}F\{^{1}H\}$ NMR spectrum for the isolated $[Ph_3POPPh_3][OTf]_2$ isolated from the reaction between **1[OTf]$_2$** and 2 equivalents of Ph_3PO (CD_3CN, 377 MHz, 298K).

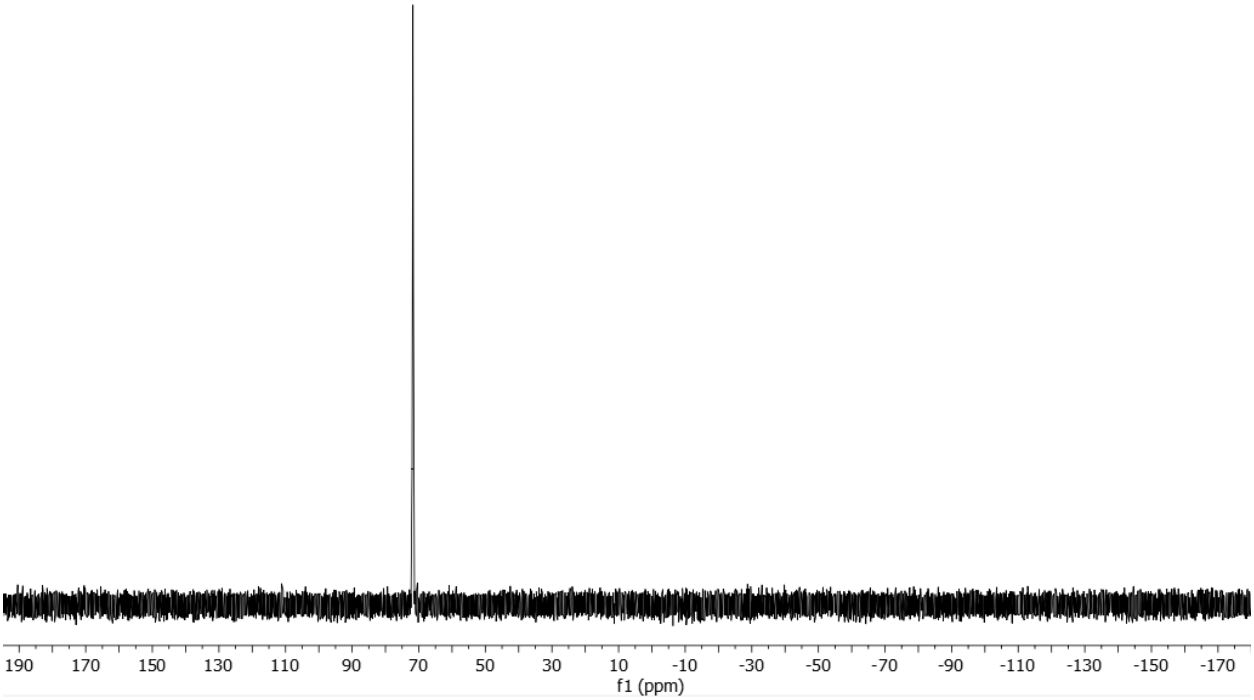

Figure S88. ^{31}P NMR spectrum for the isolated $[Ph_3POPPh_3][OTf]_2$ isolated from the reaction between **1[OTf]$_2$** and 2 equivalents of Ph_3PO (CD_3CN, 162 MHz, 298K).

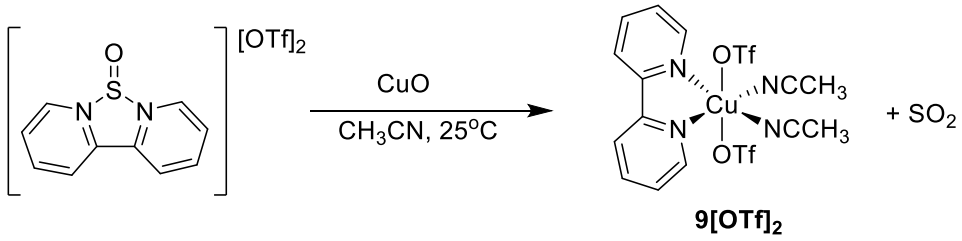

Reaction of 1[OTf]$_2$ with CuO:

To a stirring solution of **1[OTf]$_2$** (15 mg, 0.030 mmol) in acetonitrile (0.5 mL) was added copper(II) oxide (2.4 mg, 0.030 mmol) in acetonitrile (0.5 mL). After stirring for 1 hour, the solution turned bright blue and the solution was allowed to stir overnight at room temperature. The solution was dried *in vacuo*, washed with diethyl ether (3 x 1 mL), and dried further *in vacuo* to

afford a blue powder. **9[OTf]$_2$** was isolated as blue crystals from a layered solution of acetronitrile and diethyl ether (16.4 mg, 0.027 mmol, 91% yield).

^{1}H NMR (CH_3CN, 400 MHz, 298 K): δ (ppm) silent due to paramagnetism.

MS (DART+, CH3CN): m/z found 368.0 ([M -OTf -2 CH_3CN]+ $[(Bipy)CuOTf]^+$ ($C_{11}H_8Cu_1F_3N_2O_3S_1^+$) calc'd. 367.95), 157.1 ([M – Cu – 2OTf – 2CH_3CN]+ $[HBipy]^+$ ($C_{10}H_9N_2^+$) calc'd 157.08).

Elemental Analysis (calc'd./expt.): C (32.03/30.60), H (2.35/1.91), N (9.34/8.07).

5. Computational Methods

Computational Overview:

All calculations were computed using the Gaussian 09 program.[10] Geometry optimizations were performed with the PBE1PBE or B3LYP functional with the crystallographic coordinates used as starting geometries when available.[11-15] The cc-PVTZ or def2-TZVP basis sets were used for all calculations as described below.[16-17] The stationary nature of the converged geometry was confirmed by carrying out a frequency calculation and ensuring the absence of imaginary frequencies. Single-point energy calculations were carried out at either the PBE1PBE/cc-PVTZ or the B3LYP/def2-TZVP level of theory as described below. Where applicable, the Grimme-D3 dispersion correction and the acetonitrile self-consistent reaction field (SCRF) were applied to get more comparable Lewis acidity values for our polycationic systems.[18] Optimized structures were visualized using the Avogadro software.[19] Enthalpy values for the fluoride ion affinity (FIA) calculations were obtained as the thermally corrected values from the frequency calculations for structures that were optimized at the PBE1PBE/cc-PVTZ level of theory with the Grimme-D3 dispersion correction. Separate frequency calculations were undertaken from these optimized structures with an added acetonitrile SCRF to minimize the effects of cationic systems having overestimated Lewis acidities in the gas-phase.[20] FIA values were calculated using Hess's Law relative to the known FIA value of 208.8 kJ/mol for F_2CO.[21] NBO calculations were also performed at the PBE1PBE/cc-PVTZ level of theory with the Grimme-D3 dispersion correction with an acetonitrile SCRF.

Summary of Computational Results:

Table S1. Calculated fluoride ion affinities (FIA) for the listed Lewis acids. [a] PBE1PBE/cc-PVTZ level of theory with the Grimme-D3 dispersion correction. [b] PBE1PBE/cc-PVTZ level of theory with the Grimme-D3 dispersion correction and acetonitrile SCRF.

Lewis Acid	**FIA (kJ/mol)[a]**	**FIA (kJ/mol)[b]**	**S-O Distance (Å)**
$[BipySO]^{2+}$ (**1^{2+}**)	1068	325	1.432
$[t$BuBipySO$]^{2+}$ (**2^{2+}**)	996	315	1.435
$[TerpySO]^{2+}$ (**3^{2+}**)	942	265	1.442
$[4\text{-}PhTerpySO]^{2+}$ (**5^{2+}**)	899	256	1.444
$[4\text{-}ClTerpySO]^{2+}$ (**4^{2+}**)	943	271	1.442
$[(DMAP)_2SO]^{2+}$ (**6^{2+}**)	901	255	1.446
$[C_6(CH_3)_6SO]^{2+}$	1144	409	1.436
PF_5	377	354	N/A
BF_3	337	335	N/A
$(C_6F_5)_3PF^+$	761	361	N/A
Ph_3Si^+	855	482	N/A
$4\text{-}PhPhCH_2^+$	747	353	N/A
$PhCF_2^+$	844	413	N/A
SO^{2+}	2003	897	1.377
SOF^+	1030	508	1.404

Table S2. Summary of results from the Natural Bond Orbital (NBO) calculations at the PBE1PBE/cc-PVTZ level of theory with the Grimme-D3 dispersion correction and an acetonitrile SCF. WBI = Wiberg Bond Index.

Lewis Acid	**S-O WBI**	**N-S WBI**	**NBO Charge S (e)**	**NBO Charge O (e)**	**NBO Charge Terminal N (e)**	**NBO Charge Central N (e)**
$[BipySO]^{2+}$ ($\mathbf{1}^{2+}$)	1.5951	0.6583	1.627	-0.726	-0.455	N/A
$[t\text{BuBipySO}]^{2+}$ ($\mathbf{2}^{2+}$)	1.5641	0.678	1.620	-0.750	-0.470	N/A
$[TerpySO]^{2+}$ ($\mathbf{3}^{2+}$)	1.473	0.596 (Central) 0.423 (Terminal)	1.615	-0.808	-0.436	-0.446
$[4\text{-ClTerpySO}]^{2+}$ ($\mathbf{4}^{2+}$)	1.4709	0.605 (Central) 0.420 (Terminal)	1.617	-0.810	-0.436	-0.463
$[4\text{-PhTerpySO}]^{2+}$ ($\mathbf{5}^{2+}$)	1.452	0.634 (Central)	1.614	-0.825	-0.436	-0.480

		0.417 (Terminal)				
$[(DMAP)_2SO]^{2+}$ (**6**$^{2+}$)	1.4492	0.727	1.628	-0.836	-0.533	N/A
$[C_6(CH_3)_6SO]^{2+}$	1.5852	0.444 (S-C WBI)	1.367	-0.660	-0.02 (C)	N/A
SO^{2+}	2.5332	N/A	2.191	-0.191	N/A	N/A

Lewis Acid	**Lone Pair S character**	**Bonding Pair S-O (S) character**	**Bonding Pair S-O (O) character**	**Bonding Pair S-N (S) character**	**Bonding Pair S-N (N) character**
$[BipySO]^{2+}$ (**1**$^{2+}$)	65.3% s, 34.7% p	19.6% s, 79.3% p	23.2% s, 75.7% p	8.1% s, 90.1% p	21.1% s, 78.8% p
$[t$BuBipySO$]^{2+}$ (**2**$^{2+}$)	63.8% s, 36.1% p	19.9% s, 79.0% p	23.3% s, 75.6% p	8.8% s, 89.4 % p	21.6 % s, 78.3% p
$[TerpySO]^{2+}$ (**3**$^{2+}$)	68.9% s, 31.1% p	21.8% s, 77.2% p	24.1% s, 74.8% p	9.8% s, 88.6 % p	21.7% s, 78.3% p
$[4\text{-}ClTerpySO]^{2+}$ (**4**$^{2+}$)	68.7% s, 31.3% p	21.7% s, 77.3% p	24.1% s, 74.8% p	10.1% s, 88.4% p	22.2% s, 77.7% p
$[4\text{-}PhTerpySO]^{2+}$	67.8% s, 32.2 % p	21.7% s, 77.3% p	24.1% s, 74.8% p	10.9% s, 87.5% p	22.8% s, 77.2% p

(**5**$^{2+}$)					
[(DMAP)$_2$SO]$^{2+}$ (**6**$^{2+}$)	59.9% s, 40.1% p	20.7% s, 78.1% p	23.2% s, 75.8% p	10.2% s, 88.2% p	23.0% s, 76.9% p
[$C_6(CH_3)_6$SO]$^{2+}$	77.8% s, 22.2% p	15.9% s, 82.8% p	26.6% s, 72.4% p	N/A	N/A
SO^{2+}	86.5% s, 13.4% p	15.2% s, 83.3% p	23.5% s, 74.9% p	N/A	N/A

Computational Details of [2,2'-BipyridineSO]$^{2+}$ (1^{2+}):

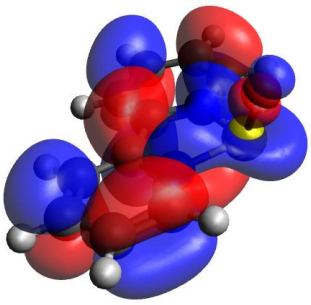

LUMO: -11.419 eV

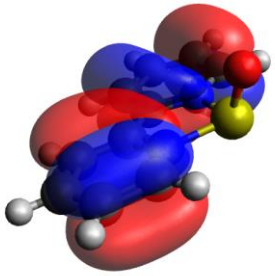

HOMO: -16.113 eV

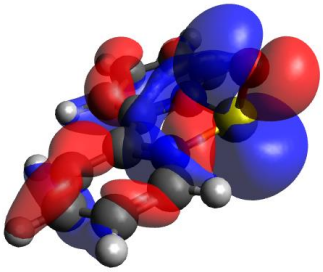

HOMO-1: -17.290 eV

LUMO (left), HOMO (middle), and HOMO -1 (right) (PBE1PBE/cc-PVTZ with Grimme's D3 empirical dispersion) for **1**$^{2+}$ in the gas-phase at a contour surface value of +/- 0.10 a.u.

Enthalpy Value for **1**$^{2+}$: -967.373168 Hartree

Enthalpy Value for [**1**-F]$^{+}$: -1067.561015 Hartree

FIA value: 1068 kJ/mol

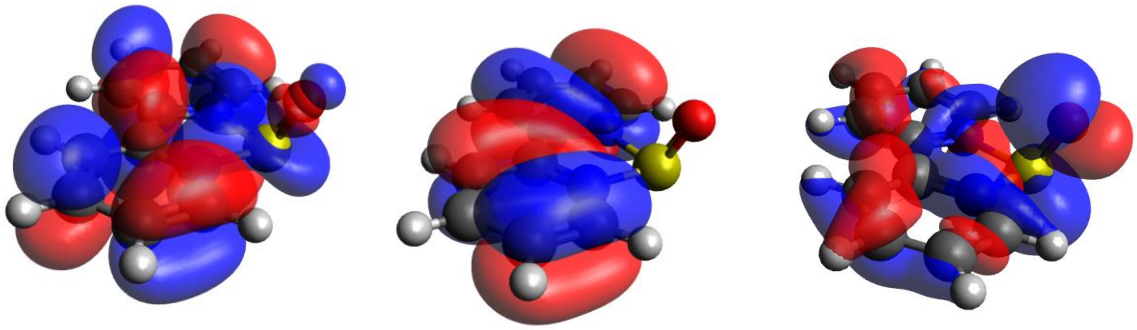

LUMO: -4.464 eV HOMO: -9.154 eV HOMO-1: -10.396 eV

LUMO (left) and HOMO (right) (PBE1PBE/cc-PVTZwith Grimme's D3 empirical dispersion and acetonitrile solvent correction) for $\mathbf{1}^{2+}$ at a contour surface value of +/- 0.10 a.u.

Enthalpy Value for $\mathbf{1}^{2+}$: -967.634842 Hartree

Enthalpy Value for [**1**-F]$^{+}$: -1067.631493 Hartree

FIA value: 325 kJ/mol

Table S3. Coordinates of $\mathbf{1}^{2+}$ (in Angstroms) after geometry optimization at PBE1PBE/cc-PVTZ with Grimme's D3 empirical dispersion.

S	-0.000034	1.777606	-0.31415
O	-0.000178	2.510042	0.916172
N	-1.219546	0.429585	-0.15736
N	1.219561	0.42965	-0.15718

C	-0.727366	-0.82332	-0.01971
C	0.72743	-0.82328	-0.0197
C	-1.599115	-1.88125	0.105755
H	-1.225655	-2.89133	0.213091
C	-3.437568	-0.31912	-0.03732
H	-4.496993	-0.09645	-0.04132
C	1.599205	-1.88123	0.105541
H	1.225748	-2.89133	0.212677
C	2.530884	0.712426	-0.16885
H	2.822814	1.751745	-0.27538
C	-2.53087	0.71232	-0.16908
H	-2.822846	1.7516	-0.27586
C	3.437601	-0.31901	-0.03725
H	4.497021	-0.09632	-0.04118
C	2.968318	-1.62064	0.096301
H	3.669871	-2.44083	0.196587
C	-2.968243	-1.6207	0.096506
H	-3.669756	-2.44091	0.196956

Table S4. Coordinates of [**1**-F]$^{+}$ (in Angstroms) after geometry optimization at PBE1PBE/cc-PVTZ with Grimme's D3 empirical dispersion.

O	-0.71862	2.307652	1.113415
N	-1.16652	-0.09676	-0.05249
N	1.360276	0.621904	0.134579
C	-0.23988	-1.08001	-0.04125
C	1.172363	-0.68014	-0.06284
C	-0.66289	-2.39713	0.051988
H	0.069828	-3.19089	0.067149
C	-2.93099	-1.65216	0.189595
H	-3.9919	-1.83119	0.295018
C	2.234234	-1.55625	-0.23912
H	2.075714	-2.60965	-0.42344
C	2.585393	1.120259	0.183719
H	2.670999	2.188182	0.35056
C	-2.47188	-0.35933	0.072222
H	-3.14102	0.489196	0.068065
C	3.705071	0.313658	0.037229
H	4.695575	0.744837	0.092938
C	3.520493	-1.04097	-0.1859
H	4.371913	-1.69617	-0.31932
C	-2.01046	-2.68799	0.16318

H	-2.33793	-3.71684	0.244196
S	-0.64543	1.787089	-0.21591
F	-2.12248	2.112461	-0.82393

Computational Details of [(4,4'-ditertbutyl)-2,2'-BipyridineSO]$^{2+}$ ($\mathbf{2}^{2+}$):

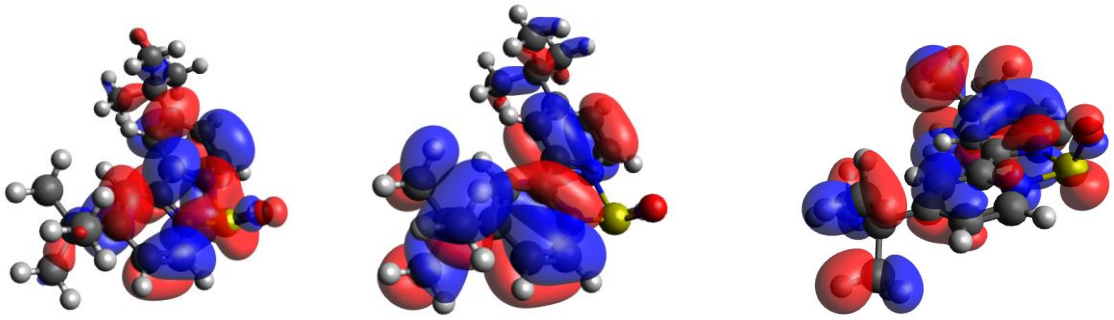

LUMO: -10.414 eV HOMO: -15.146 eV HOMO-8: -15.999 eV

LUMO (left) and HOMO (right) (PBE1PBE/cc-PVTZ with Grimme's D3 empirical dispersion) for $\mathbf{2}^{2+}$ in the gas-phase at a contour surface value of +/- 0.10 a.u.

Enthalpy Value for $\mathbf{2}^{2+}$: - 1281.425763 Hartree

Enthalpy Value for [**2**-F]$^{+}$: -1381.586065 Hartree

FIA value: 996 kJ/mol

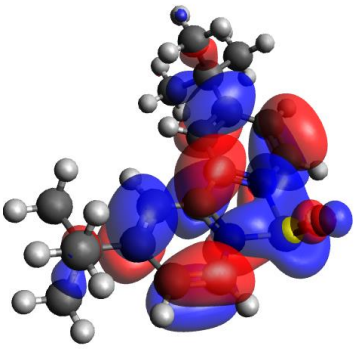

LUMO: -4.273 eV

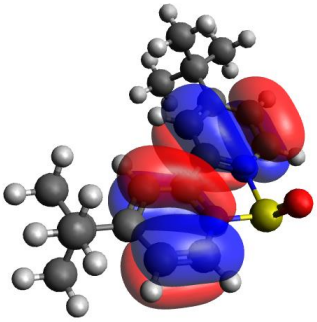

HOMO: -9.026 eV

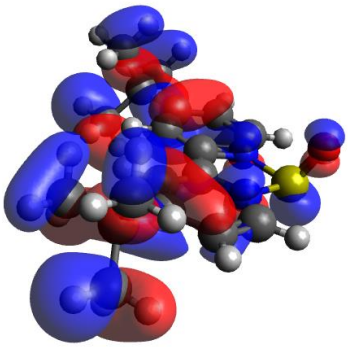

HOMO-8: -10.411 eV

LUMO (left) and HOMO (right) (PBE1PBE/cc-PVTZ with Grimme's D3 empirical dispersion and an acetonitrile solvent correction) for $\mathbf{2}^{2+}$ at a contour surface value of +/- 0.10 a.u.

Enthalpy Value for $\mathbf{2}^{2+}$: -1281.657275 Hartree

Enthalpy Value for $[\mathbf{2}\text{-F}]^{+}$: -1381.649919 Hartree

FIA value: 315 kJ/mol

Table S5. Coordinates of $\mathbf{2}^{2+}$ (in Angstroms) after geometry optimization at PBE1PBE/cc-PVTZ with Grimme's D3 empirical dispersion.

N	-1.21825	1.647309	-0.19194
N	1.19755	1.632465	-0.17653

C	-3.0109	-0.43893	-0.04204
C	2.964094	-0.47584	-0.03149
C	-0.74439	0.379007	-0.10988
C	3.958393	-1.6041	0.042541
C	-1.62039	-0.66949	-0.04019
H	-1.23463	-1.67773	0.022107
C	0.711114	0.372678	-0.1046
C	-2.5318	1.923143	-0.20047
H	-2.82466	2.965562	-0.25923
C	-3.96724	-1.59861	0.049155
C	3.406971	0.857541	-0.09631
H	4.462672	1.09035	-0.08917
C	2.518468	1.895956	-0.17143
H	2.821458	2.935646	-0.22017
C	1.575954	-0.69057	-0.037
H	1.178175	-1.69394	0.014497
C	-3.43778	0.893623	-0.12481
H	-4.48988	1.139948	-0.129
C	-3.70686	-2.53275	-1.14735
H	-3.88329	-2.02624	-2.09764
H	-2.69417	-2.94023	-1.151
H	-4.3949	-3.37644	-1.08353
C	4.806814	-1.40835	1.313839

H	5.363286	-0.47026	1.305384
H	4.193196	-1.44173	2.215685
H	5.534393	-2.21874	1.37122
C	3.283211	-2.97037	0.091912
H	2.657392	-3.09105	0.979782
H	2.686804	-3.16934	-0.80215
H	4.049482	-3.74368	0.138824
C	4.863519	-1.52843	-1.20161
H	4.290916	-1.64891	-2.12285
H	5.422101	-0.5933	-1.25743
H	5.590888	-2.33923	-1.14906
C	-3.68239	-2.34763	1.36479
H	-2.66758	-2.74717	1.409982
H	-3.84523	-1.70809	2.23377
H	-4.36739	-3.19324	1.436278
C	-5.42431	-1.14908	0.030889
H	-5.66817	-0.50417	0.878141
H	-5.68748	-0.63662	-0.89722
H	-6.06719	-2.0259	0.104023
O	-0.00549	3.634634	1.026035
S	-0.00077	2.977015	-0.24975

Table S6. Coordinates of [**2**-F]$^+$ (in Angstroms) after geometry optimization at PBE1PBE/cc-PVTZ with Grimme's D3 empirical dispersion.

N	-1.39725	1.416735	-0.1145
N	1.186914	1.677045	0.179691
C	-2.7108	-1.02673	0.012989
C	3.057407	-0.3784	0.004916
C	-0.66683	0.27751	-0.06523
C	4.105172	-1.4736	-0.08539
C	-1.31886	-0.93721	-0.01589
H	-0.72212	-1.83643	0.028769
C	0.792848	0.42393	-0.00754
C	-2.73196	1.371954	-0.06923
H	-3.25042	2.319289	-0.09721
C	-3.38853	-2.38005	0.070979
C	3.43729	0.949539	0.212936
H	4.4795	1.219179	0.31756
C	2.481326	1.943842	0.285323
H	2.753404	2.981908	0.440313
C	1.692443	-0.62774	-0.10809
H	1.338589	-1.63281	-0.28051
C	-3.41058	0.178019	-0.00032
H	-4.48918	0.207765	0.038049
C	-2.97677	-3.18383	-1.17097

H	-3.29061	-2.68381	-2.08915
H	-1.8984	-3.3444	-1.22016
H	-3.45437	-4.16428	-1.14017
C	4.898445	-1.50166	1.227923
H	5.410289	-0.55729	1.41803
H	4.248506	-1.7137	2.079119
H	5.657623	-2.28397	1.178387
C	3.483747	-2.84808	-0.31384
H	2.819785	-3.13813	0.504256
H	2.929206	-2.89643	-1.25418
H	4.274857	-3.59665	-0.36718
C	5.048963	-1.15749	-1.25342
H	4.507944	-1.12201	-2.20108
H	5.562658	-0.20449	-1.11918
H	5.811375	-1.93475	-1.32807
C	-2.92126	-3.10879	1.33939
H	-1.84248	-3.27323	1.349121
H	-3.19067	-2.5522	2.23885
H	-3.40292	-4.08639	1.389969
C	-4.90856	-2.25762	0.101863
H	-5.25733	-1.71485	0.983053
H	-5.29769	-1.76517	-0.79192
H	-5.34916	-3.25419	0.140526

O	-0.56898	3.659714	1.138212
S	-0.54641	3.160336	-0.20347
F	-1.92919	3.771764	-0.8358

Computational Details of [TerpyridineSO]$^{2+}$ (3)$^{2+}$:

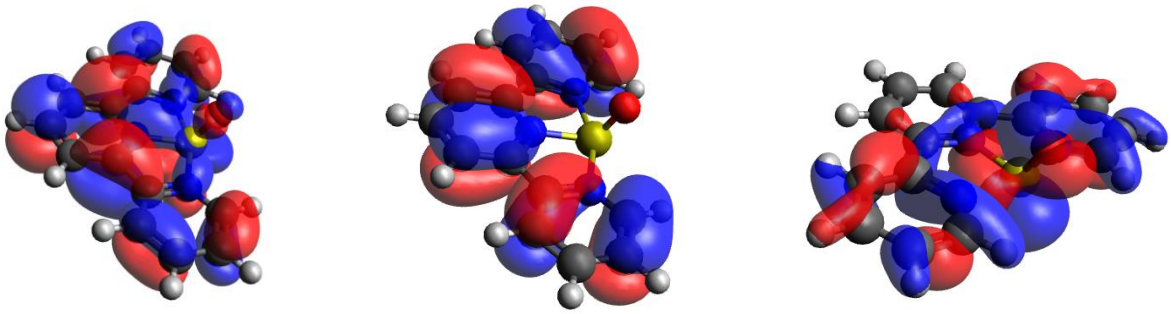

LUMO: -10.251 eV HOMO: -14.541 eV HOMO-1: -15.164 eV

LUMO (left) and HOMO (right) (PBE1PBE/cc-PVTZ with Grimme's D3 empirical dispersion) for **3**$^{2+}$ in the gas-phase at a contour surface value of +/- 0.10 a.u.

Enthalpy Value for **3**$^{2+}$: - 1214.25357 Hartree

Enthalpy Value for [**3**-F]$^{+}$: -1314.393 Hartree

FIA value: 942 kJ/mol

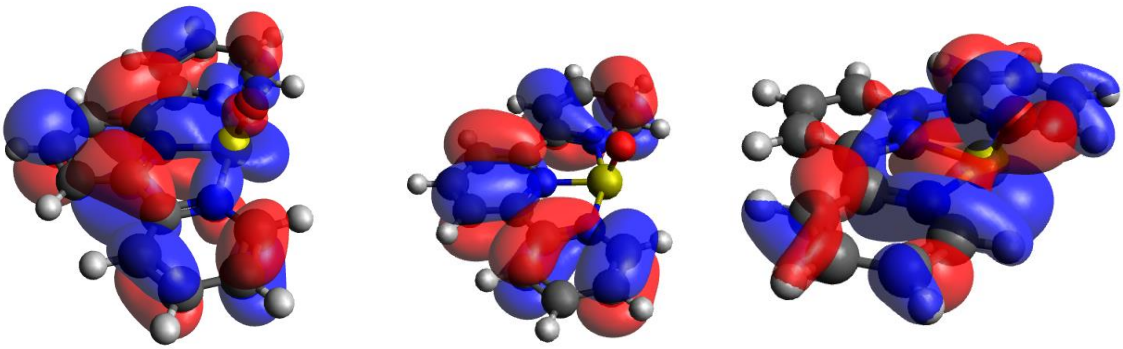

LUMO: -2.620 eV HOMO: -8.441 eV HOMO-1: -9.090 eV

LUMO (left) and HOMO (right) (PBE1PBE/cc-PVTZ with Grimme's D3 empirical dispersion and an acetonitrile solvent correction) for $\mathbf{3}^{2+}$ at a contour surface value of +/- 0.10 a.u.

Enthalpy Value for $\mathbf{3}^{2+}$: - 1214.483864 Hartree

Enthalpy Value for $[\mathbf{3}\text{-F}]^{+}$: -1314.457618 Hartree

FIA value: 265 kJ/mol

Table S7. Coordinates of $\mathbf{3}^{2+}$ (in Angstroms) after geometry optimization at PBE1PBE/cc-PVTZ with Grimme's D3 empirical dispersion.

S	0.000777	-1.2362	-0.10886
O	0.000511	-1.82732	1.20627
N	0.0001	0.638336	-0.02038
N	-1.99435	-0.87918	-0.12767

N	1.994086	-0.87855	-0.12748
C	-1.18485	1.286141	-0.00027
C	1.184779	1.28661	-0.00022
C	2.346198	0.407428	-0.05945
C	1.202186	2.667087	0.062581
H	2.144726	3.196232	0.082035
C	-4.2444	-1.55507	-0.16645
H	-4.9709	-2.35611	-0.20221
C	-1.20252	2.666662	0.062433
H	-2.14518	3.195604	0.081698
C	-0.00031	3.357367	0.100319
C	-2.3462	0.406826	-0.05949
C	-4.63642	-0.22643	-0.10337
H	-5.68826	0.031385	-0.09349
C	-2.89106	-1.85583	-0.17667
H	-2.51982	-2.87343	-0.21287
C	-3.67749	0.778526	-0.04737
H	-3.97034	1.818269	0.005634
C	2.890413	-1.85563	-0.17645
H	2.518787	-2.87311	-0.21226
C	3.677579	0.778653	-0.04759
H	3.970749	1.818316	0.005273
C	4.636167	-0.22666	-0.10361

H	5.68808	0.030862	-0.09395
C	4.243795	-1.55523	-0.16644
H	4.970075	-2.35646	-0.20229
H	-0.00049	4.439264	0.154921

Table S8. Coordinates of [**3**-F]$^{+}$ (in Angstroms) after geometry optimization at PBE1PBE/cc-PVTZ with Grimme's D3 empirical dispersion.

O	0.086233	-1.83223	1.183478
N	-0.12521	0.759757	-0.00399
N	-2.25946	-0.85864	-0.26983
N	2.138526	-0.62535	-0.0673
C	-1.33005	1.327265	-0.05412
C	0.981932	1.491068	-0.06839
C	2.23265	0.715707	-0.00229
C	0.944327	2.873278	-0.18817
H	1.846227	3.46369	-0.25947
C	-4.57317	-1.34321	0.037918
H	-5.36274	-2.08276	0.044594
C	-1.44333	2.713243	-0.17053
H	-2.41572	3.180426	-0.23418
C	-0.29854	3.483467	-0.23708
C	-2.50199	0.42717	-0.00567

C	-4.82644	-0.01383	0.323328
H	-5.82745	0.319123	0.566832
C	-3.2672	-1.71683	-0.24983
H	-3.02423	-2.75131	-0.46828
C	-3.77642	0.889833	0.301487
H	-3.95239	1.929508	0.541625
C	3.212636	-1.40836	0.029079
H	3.038268	-2.47408	-0.02479
C	3.483265	1.297517	0.148055
H	3.571993	2.372142	0.211628
C	4.610212	0.500424	0.240314
H	5.585701	0.953884	0.362968
C	4.475717	-0.87687	0.185795
H	5.327268	-1.53834	0.263636
H	-0.37165	4.55865	-0.34005
S	0.331177	-1.5217	-0.18962
F	1.086388	-2.8906	-0.71667

Computational Details of [4-PhTerpyridineSO]$^{2+}$ (5)$^{2+}$:

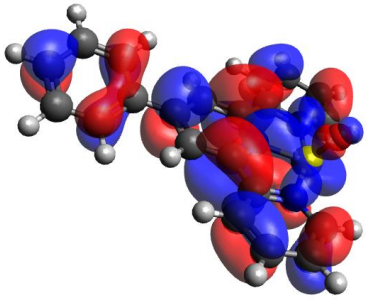

LUMO: -9.670 eV

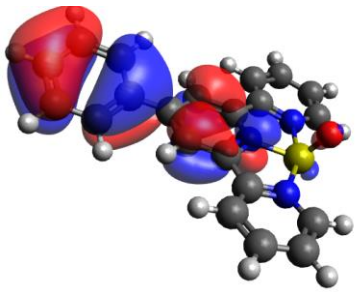

HOMO: -13.003 eV

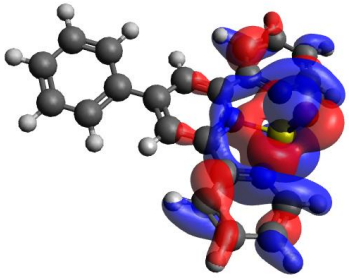

HOMO-3: -14.599 eV

LUMO (left) and HOMO (right) (PBE1PBE/cc-PVTZ with Grimme's D3 empirical dispersion) for **5**$^{2+}$ in the gas-phase at a contour surface value of +/- 0.10 a.u.

Enthalpy Value for **5**$^{2+}$: -1445.051171 Hartree

Enthalpy Value for [**5**-F]$^{+}$: -1545.174441 Hartree

FIA value: 899 kJ/mol

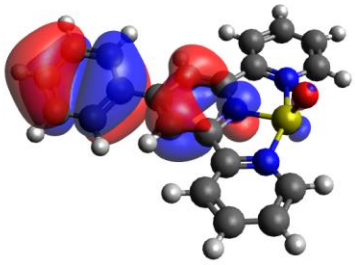

LUMO: -4.116 eV

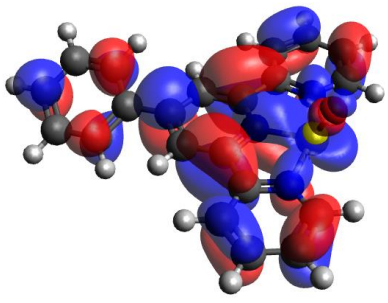

HOMO: -7.931 eV

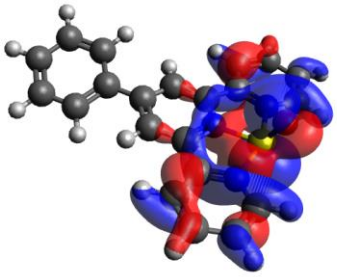

HOMO-3: -8.984 eV

LUMO (left) and HOMO (right) (PBE1PBE/cc-PVTZ with Grimme's D3 empirical dispersion and an acetonitrile solvent correction) for $\mathbf{5}^{2+}$ at a contour surface value of +/- 0.10 a.u.

Enthalpy Value for $\mathbf{5}^{2+}$: -1445.26621 Hartree

Enthalpy Value for [**5**-F]$^{+}$: -1545.236387 Hartree

FIA value: 256 kJ/mol

Table S9. Coordinates of $\mathbf{5}^{2+}$ (in Angstroms) after geometry optimization at PBE1PBE/cc-PVTZ with Grimme's D3 empirical dispersion.

S	-2.59268	0.002824	-0.07667
O	-3.1386	-0.02667	1.25992
N	-0.7543	0.001969	-0.05513
N	-2.24439	2.001198	-0.07193
N	-2.24577	-1.99355	-0.15848
C	-0.0828	1.182429	-0.04557
C	-0.08415	-1.17926	-0.06674
C	-0.95965	-2.34476	-0.127
C	1.285001	-1.19662	-0.0467

H	1.79419	-2.14828	-0.08682
C	-2.92421	4.248767	-0.03574
H	-3.72532	4.975664	-0.02498
C	3.473871	-0.00162	0.009372
C	1.286581	1.198123	-0.03374
H	1.7956	2.149899	0.005845
C	2.027778	0.000264	-0.02212
C	-0.95764	2.3501	-0.04531
C	-1.59295	4.639668	-0.01448
H	-1.3356	5.691268	0.009449
C	-3.22357	2.897204	-0.06396
H	-4.24052	2.522848	-0.06848
C	4.201876	1.09343	-0.48446
H	3.691954	1.935097	-0.93686
C	-0.58717	3.682089	-0.01808
H	0.453704	3.974	0.00341
C	-3.22544	-2.8882	-0.1992
H	-4.24207	-2.513	-0.20329
C	5.580684	1.083141	-0.4615
H	6.134307	1.920225	-0.86659
C	4.173977	-1.09902	0.537228
H	3.639876	-1.93821	0.96576
C	-0.59043	-3.67721	-0.14795

H	0.449937	-3.97085	-0.12554
C	5.552365	-1.09349	0.579852
H	6.083215	-1.93215	1.011311
C	6.258345	-0.00635	0.075628
H	7.341032	-0.00801	0.101553
C	-1.59663	-4.63304	-0.19744
H	-1.34017	-5.685	-0.21341
C	-2.92725	-4.24012	-0.22109
H	-3.72883	-4.96595	-0.25125

Table S10. Coordinates of [**5**-F]$^+$ (in Angstroms) after geometry optimization at PBE1PBE/cc-PVTZ with Grimme's D3 empirical dispersion.

O	3.182904	0.323116	1.137226
N	0.574549	0.108384	0.052397
N	2.267461	-1.92036	-0.03747
N	1.824231	2.45178	-0.33508
C	0.007271	-1.09339	0.052457
C	-0.17968	1.208276	0.018934
C	0.529406	2.506141	-0.01644
C	-1.56632	1.108456	-0.01164
H	-2.17038	2.001172	-0.08831

C	2.883015	-4.18794	0.219991
H	3.668774	-4.92869	0.270397
C	-3.65084	-0.26335	-0.04622
C	-1.36537	-1.26474	0.023761
H	-1.8095	-2.24937	0.036617
C	-2.18814	-0.13741	-0.00722
C	0.961295	-2.21472	0.095168
C	1.5461	-4.52798	0.346111
H	1.252731	-5.55881	0.499626
C	3.208373	-2.86184	0.026679
H	4.23082	-2.52793	-0.08309
C	-4.25509	-1.29691	-0.76364
H	-3.64585	-1.99435	-1.32689
C	0.583607	-3.53655	0.285266
H	-0.46086	-3.78498	0.403298
C	2.519181	3.577207	-0.392
H	3.568342	3.483541	-0.65171
C	-5.63379	-1.41042	-0.80361
H	-6.09181	-2.20618	-1.37749
C	-4.45762	0.649362	0.63472
H	-4.0044	1.438881	1.222672
C	-0.10787	3.708475	0.26921
H	-1.15083	3.73531	0.553551

C	-5.8358	0.52654	0.60348
H	-6.45101	1.231223	1.148689
C	-6.42676	-0.50134	-0.11766
H	-7.50528	-0.59363	-0.14543
C	0.624348	4.882908	0.208602
H	0.152757	5.831511	0.432252
C	1.963526	4.822398	-0.13259
H	2.572948	5.71442	-0.19009
S	2.865068	0.004516	-0.21974
F	4.324713	-0.543	-0.77836

Computational Details of $[(DMAP)_2SO]^{2+}$ ($\mathbf{6}^{2+}$):

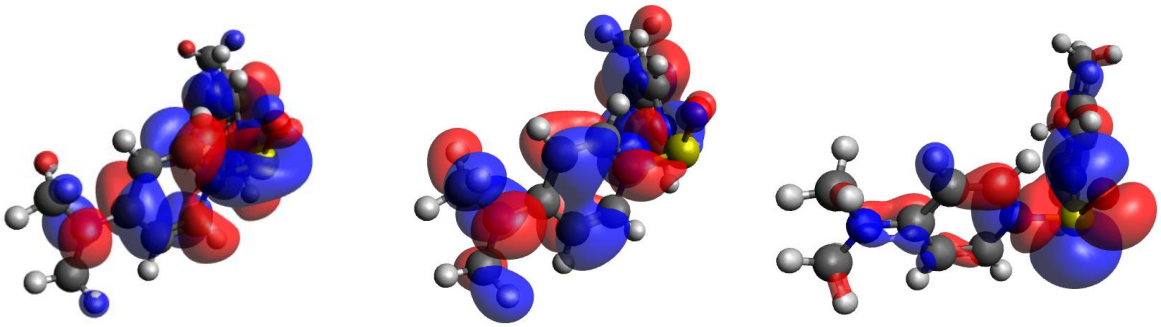

LUMO: -8.377 eV HOMO: -13.221 eV HOMO-4: -15.436 eV

LUMO (left) and HOMO (right) (PBE1PBE/cc-PVTZ with Grimme's D3 empirical dispersion) for $\mathbf{6}^{2+}$ in the gas-phase at a contour surface value of +/- 0.10 a.u.

Enthalpy Value for **6**$^{2+}$: -1236.220119 Hartree

Enthalpy Value for [**6**-F]$^{+}$: -1336.344207 Hartree

FIA value: 901 kJ/mol

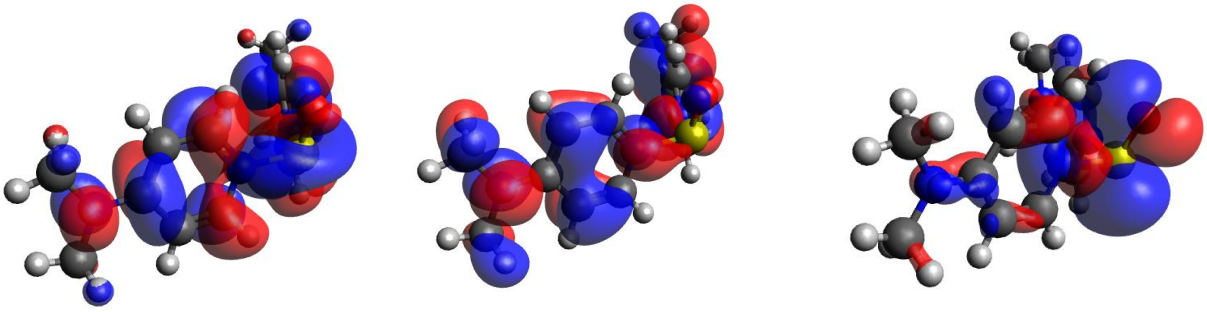

LUMO: -2.620 eV HOMO: -7.569 eV HOMO-4: -9.744 eV

LUMO (left) and HOMO (right) (PBE1PBE/cc-PVTZ with Grimme's D3 empirical dispersion with an acetonitrile solvent correction) for **6**$^{2+}$ at a contour surface value of +/- 0.10 a.u.

Enthalpy Value for **6**$^{2+}$: -1236.436162 Hartree

Enthalpy Value for [**6**-F]$^{+}$: -1336.406059 Hartree

FIA value: 255 kJ/mol

Table S11. Coordinates of $\mathbf{6}^{2+}$ (in Angstroms) after geometry optimization at PBE1PBE/cc-PVTZ with Grimme's D3 empirical dispersion.

S	0.000006	2.141988	-0.52755
O	0.00001	2.971933	0.657165
C	-1.91273	0.411808	-1.35534
C	-1.91415	0.892302	0.95826
C	-3.00869	-0.36995	-1.23045
H	-1.44704	0.596944	-2.31591
C	-3.01045	0.122726	1.146298
H	-1.45336	1.46036	1.756527
C	-3.62274	-0.55919	0.047958
H	-3.42235	0.064382	2.142254
C	1.912728	0.411801	-1.35535
C	1.914158	0.892295	0.958256
C	3.008689	-0.36997	-1.23046
H	1.447042	0.59694	-2.31592
C	3.010462	0.122715	1.14629
H	1.453377	1.460356	1.756523
C	3.622742	-0.5592	0.04795
H	3.422365	0.064367	2.142246
N	-1.35521	1.026901	-0.27555
N	1.355216	1.026896	-0.27555

H	3.414008	-0.824	-2.12174
H	-3.41401	-0.82399	-2.12173
N	4.702842	-1.30122	0.200632
N	-4.70286	-1.30121	0.200633
C	5.333935	-1.94633	-0.94747
H	5.654223	-1.205	-1.68197
H	6.210569	-2.48872	-0.60901
H	4.652175	-2.65774	-1.41731
C	5.315258	-1.46708	1.516092
H	6.13975	-2.16773	1.434861
H	5.706052	-0.51697	1.886372
H	4.595691	-1.87054	2.230127
C	-5.33395	-1.9463	-0.94748
H	-6.21058	-2.4887	-0.60903
H	-5.65424	-1.20496	-1.68196
H	-4.65219	-2.6577	-1.41734
C	-5.31528	-1.4671	1.516088
H	-5.70608	-0.51701	1.886389
H	-6.13977	-2.16776	1.434833
H	-4.59571	-1.87059	2.230115

Table S12. Coordinates of [**6**-F]$^+$ (in Angstroms) after geometry optimization at PBE1PBE/cc-PVTZ with Grimme's D3 empirical dispersion.

O	0.151969	2.913996	1.147303
C	-1.56206	0.071069	-1.0931
C	-2.14164	0.955526	0.92534
C	-2.693	-0.70445	-1.14714
H	-0.849	0.039924	-1.91244
C	-3.30293	0.224679	0.974559
H	-1.8886	1.644202	1.724754
C	-3.62606	-0.64875	-0.08699
H	-3.95664	0.344739	1.82542
C	2.296226	0.768879	-1.15835
C	1.580777	0.427937	1.039644
C	3.136764	-0.29907	-1.09366
H	2.219719	1.389077	-2.0421
C	2.402573	-0.64757	1.180065
H	0.941851	0.791074	1.83445
C	3.230214	-1.06081	0.102253
H	2.409195	-1.16467	2.126756
N	-1.26751	0.889329	-0.08126
N	1.534639	1.121263	-0.10816
H	3.733821	-0.53302	-1.96114

H	-2.85369	-1.33623	-2.00788
N	4.055603	-2.10273	0.207615
N	-4.75698	-1.37945	-0.09263
C	4.897547	-2.49032	-0.91097
H	5.585051	-1.68663	-1.18576
H	5.487317	-3.3567	-0.62748
H	4.297132	-2.75972	-1.78316
C	4.141922	-2.84905	1.451095
H	4.867683	-3.64823	1.335294
H	4.469046	-2.20911	2.274191
H	3.180182	-3.29831	1.710137
C	-5.06483	-2.23618	-1.21691
H	-6.00795	-2.74282	-1.03187
H	-5.16455	-1.66428	-2.14445
H	-4.29569	-3.00062	-1.36027
C	-5.69819	-1.27034	1.001366
H	-6.09182	-0.25375	1.09452
H	-6.53459	-1.9398	0.820511
H	-5.23948	-1.55414	1.952681
S	0.408705	2.563147	-0.22646
F	1.710206	3.496496	-0.60881

Computational Details of $[C_6(CH_3)_6SO]^{2+}$

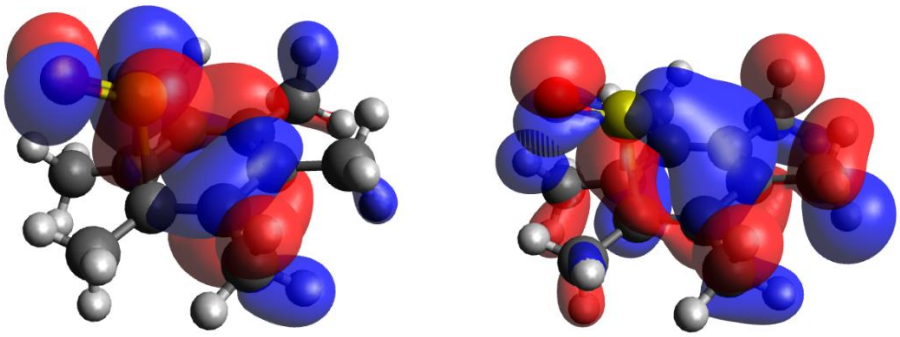

LUMO: -12.446 eV HOMO: -16.561 eV

LUMO (left) and HOMO (right) (PBE1PBE/cc-PVTZ with Grimme's D3 empirical dispersion) for **$[C_6(CH_3)_6SO]^{2+}$**in the gas-phase at a contour surface value of +/- 0.10 a.u.

Enthalpy Value for **$[C_6(CH_3)_6SO]^{2+}$**: -939.970385 Hartree

Enthalpy Value for [F-**$C_6(CH_3)_6SO$**]$^{+}$: -1040.187328 Hartree

FIA value: 1144 kJ/mol

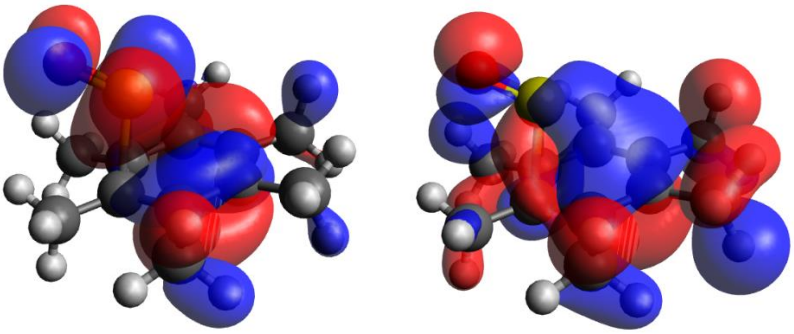

LUMO: -9.724 eV HOMO: -5.587 eV

LUMO (left) and HOMO (right) (PBE1PBE/cc-PVTZ with Grimme's D3 empirical dispersion and an acetonitrile solvent correction) for **$[C_6(CH_3)_6SO]^{2+}$** at a contour surface value of +/- 0.10 a.u.

Enthalpy Value for **$[C_6(CH_3)_6SO]^{2+}$**: -940.224694 Hartree

Enthalpy Value for $[F\text{-}C_6(CH_3)_6SO]^{+}$: -1040.253222 Hartree

FIA value: 409 kJ/mol

Table S13. Coordinates of **$[C_6(CH_3)_6SO]^{2+}$** (in Angstroms) after geometry optimization at PBE1PBE/cc-PVTZ with Grimme's D3 empirical dispersion.

O	-2.27189	-0.005111	1.79123
C	-0.93273	0.568713	-0.701588
C	-0.764221	-0.872465	-0.599703
C	0.546434	-1.414735	-0.336505
C	1.632924	-0.541513	-0.05129
C	1.476275	0.850378	-0.157317
C	0.182377	1.421937	-0.383381
S	-0.914277	-0.003211	1.322097
C	-1.927729	-1.761097	-0.887946
H	-2.874701	-1.291254	-0.627218

H	-1.952953	-1.9728	-1.962928
H	-1.864122	-2.709049	-0.359143
C	-2.23986	1.118877	-1.159862
H	-2.600722	0.542634	-2.012497
H	-3.007704	1.050973	-0.378757
H	-2.157668	2.159769	-1.458575
C	0.768783	-2.875319	-0.378835
H	0.838499	-3.293584	0.634208
H	-0.009514	-3.410587	-0.913389
H	1.730168	-3.09041	-0.851908
C	2.951575	-1.115511	0.330706
H	2.853832	-2.081438	0.821005
H	3.569756	-1.266526	-0.563664
H	3.503706	-0.451652	0.993193
C	2.649684	1.748533	-0.017434
H	2.807773	2.017358	1.035692
H	3.562071	1.264565	-0.361247
H	2.523515	2.676402	-0.57162
C	-0.006393	2.88912	-0.313651
H	0.676246	3.355554	0.394071
H	0.20873	3.321397	-1.301674
H	-1.026077	3.169408	-0.058101

Table S14. Coordinates of [F-$\mathbf{C_6(CH_3)_6SO}$]$^+$ (in Angstroms) after geometry optimization at PBE1PBE/cc-PVTZ with Grimme's D3 empirical dispersion.

O	-2.146298	-1.185633	1.391111
C	-0.028677	-1.246882	-0.742346
C	1.249877	-1.239814	-0.204334
C	1.886172	-0.0003	0.052469
C	1.244524	1.240612	-0.176164
C	-0.030349	1.258287	-0.72191
C	-0.752412	0.010408	-0.853216
S	-1.189798	-0.121528	1.254523
F	-2.057985	1.226239	1.316368
C	1.977434	-2.516308	0.099193
H	1.296878	-3.353641	0.22388
H	2.682163	-2.773867	-0.696523
H	2.547821	-2.429636	1.023057
C	-0.737036	-2.490773	-1.137358
H	-0.075222	-3.34936	-1.183001
H	-1.541633	-2.718365	-0.426928
H	-1.208086	-2.370346	-2.114074
C	3.295677	-0.003232	0.537657

H	3.320993	-0.020376	1.633804
H	3.841079	-0.878051	0.191888
H	3.83565	0.885223	0.219399
C	1.962736	2.514549	0.159599
H	2.537703	2.407172	1.078358
H	2.661458	2.803071	-0.630912
H	1.27294	3.340208	0.311381
C	-0.700927	2.518765	-1.144519
H	-1.47696	2.819014	-0.433478
H	0.002542	3.340558	-1.236387
H	-1.189897	2.386173	-2.110338
C	-2.104421	0.005469	-1.508094
H	-2.665344	0.910071	-1.286971
H	-1.987241	-0.063272	-2.592819
H	-2.701412	-0.845897	-1.184756

Computational Details of [4-ClTerpyridineSO]$^{2+}$ (4)$^{2+}$:

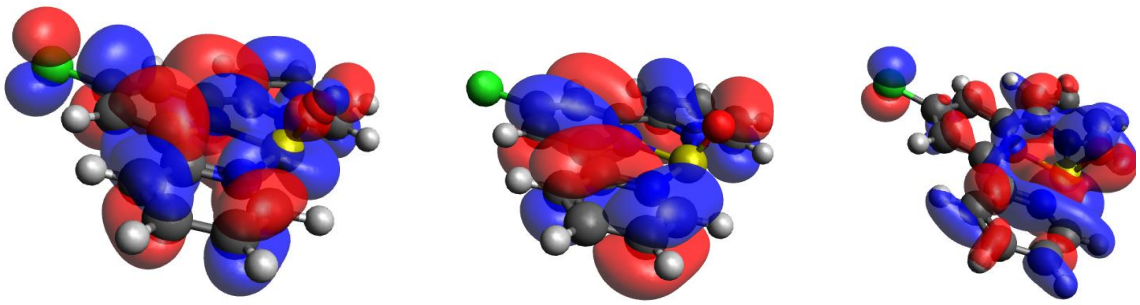

LUMO: -10.207 eV HOMO: -14.575 eV HOMO-1: -15.128 eV

LUMO (left) and HOMO (right) (PBE1PBE/cc-PVTZ with Grimme's D3 empirical dispersion) for **4**$^{2+}$ in the gas-phase at a contour surface value of +/- 0.10 a.u.

Enthalpy Value for **4**$^{2+}$: -1673.731998 Hartree

Enthalpy Value for [**4**-F]$^{+}$: -1773.872304 Hartree

FIA value: 943 kJ/mol

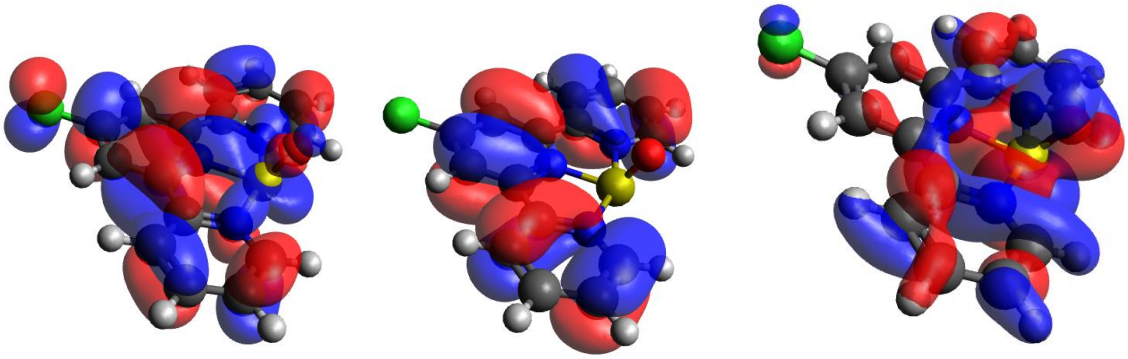

LUMO: -4.170 eV HOMO: -8.550 eV HOMO: -9.115 eV

LUMO (left) and HOMO (right) (PBE1PBE/cc-PVTZ with Grimme's D3 empirical dispersion and an acetonitrile solvent correction) for $\mathbf{4}^{2+}$ at a contour surface value of +/- 0.10 a.u.

Enthalpy Value for $\mathbf{4}^{2+}$: -1673.960895 Hartree

Enthalpy Value for [**4**-F]$^{+}$: -1773.936976 Hartree

FIA value: 271 kJ/mol

Table S15. Coordinates of $\mathbf{4}^{2+}$ (in Angstroms) after geometry optimization at PBE1PBE/cc-PVTZ with Grimme's D3 empirical dispersion.

O	0.001279	-2.30285	1.232317
N	0.00012	0.125479	-0.04269
N	-1.99678	-1.38222	-0.12332
N	1.997095	-1.38089	-0.12368
C	-1.18375	0.781756	-0.0338

C	1.183464	0.782623	-0.0337
C	2.348503	-0.09409	-0.07648
C	1.20698	2.157671	0.003134
H	2.145395	2.693852	0.012561
C	-4.24707	-2.05764	-0.14706
H	-4.97408	-2.85873	-0.16833
C	-1.20801	2.156818	0.003023
H	-2.1467	2.692498	0.012393
C	-0.00077	2.856653	0.028879
C	-2.34839	-0.09551	-0.0765
C	-4.63853	-0.72793	-0.10583
H	-5.69024	-0.46957	-0.09857
C	-2.89391	-2.35913	-0.15421
H	-2.52292	-3.37726	-0.17368
C	-3.6792	0.277409	-0.06843
H	-3.97188	1.317969	-0.03229
C	2.894161	-2.35791	-0.15468
H	2.523158	-3.37604	-0.17428
C	3.679275	0.278793	-0.06816
H	3.971913	1.319355	-0.03168
C	4.638608	-0.72657	-0.1057
H	5.690303	-0.46815	-0.09823
C	4.247272	-2.05632	-0.14732

H	4.974337	-2.85734	-0.16883
Cl	-0.00133	4.540422	0.083745
S	0.001145	-1.73858	-0.09453

Table S16. Coordinates of [**4**-F]$^+$ (in Angstroms) after geometry optimization at PBE1PBE/cc-PVTZ with Grimme's D3 empirical dispersion.

O	-0.38302	-2.34066	-1.13759
N	0.114849	0.25311	-0.04344
N	2.067538	-1.56802	0.277505
N	-2.28683	-0.8678	0.072133
C	1.373405	0.692955	-0.01419
C	-0.90316	1.104626	-0.00276
C	-2.23392	0.472172	-0.04049
C	-0.72262	2.476671	0.068442
H	-1.54664	3.172093	0.120719
C	4.315752	-2.30534	-0.0145
H	5.022629	-3.12409	0.005425
C	1.642687	2.057864	0.053932
H	2.655727	2.428945	0.101797
C	0.583006	2.946739	0.093591
C	2.44486	-0.32606	-0.03319

C	4.707307	-1.02175	-0.3489
H	5.736686	-0.80576	-0.60554
C	2.978829	-2.52816	0.287854
H	2.629084	-3.52259	0.543911
C	3.758962	-0.0116	-0.35902
H	4.04311	0.993986	-0.63785
C	-3.44113	-1.52974	0.004861
H	-3.38531	-2.60567	0.096305
C	-3.4122	1.18379	-0.21104
H	-3.38225	2.258699	-0.31362
C	-4.62108	0.513247	-0.2735
H	-5.54115	1.066975	-0.41145
C	-4.63876	-0.86748	-0.16955
H	-5.55848	-1.43327	-0.22273
Cl	0.877473	4.628341	0.192644
S	-0.58715	-1.95824	0.223573
F	-1.48807	-3.21364	0.797666

Computational Details of $[SO]^{2+}$:

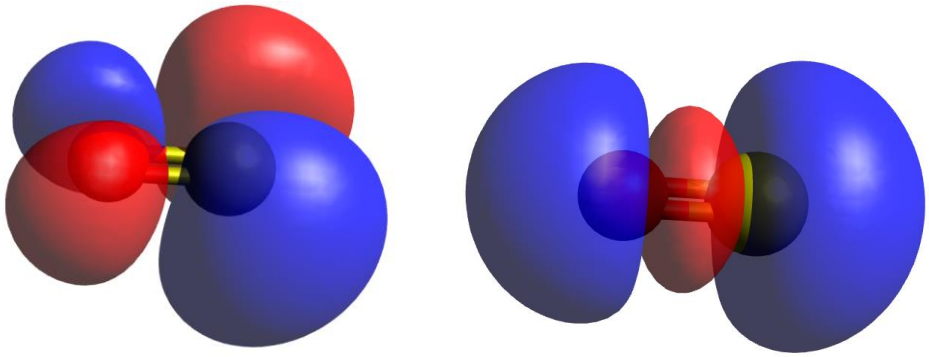

LUMO: -23.089 eV HOMO: -31.198 eV

LUMO (left) and HOMO (right) (PBE1PBE/cc-PVTZ with Grimme's D3 empirical dispersion) for $\mathbf{SO}^{2+}$ in the gas-phase at a contour surface value of +/- 0.10 a.u.

Enthalpy Value for $\mathbf{SO}^{2+}$: -472.07105 Hartree

Enthalpy Value for $[F\text{-}SO]^{+}$: -572.615171 Hartree

FIA value: 2003 kJ/mol

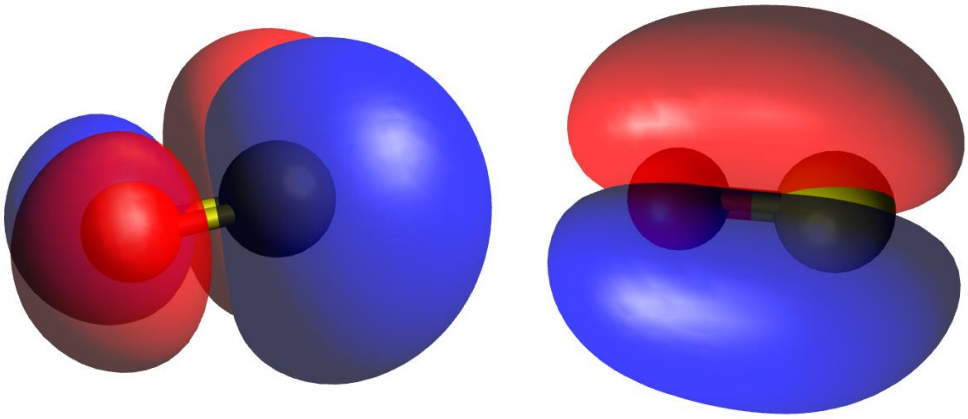

LUMO: -11.238 eV HOMO: -20.484 eV

LUMO (left) and HOMO (right) (PBE1PBE/cc-PVTZ with Grimme's D3 empirical dispersion and an acetonitrile solvent correction) for $\mathbf{SO}^{2+}$ at a contour surface value of +/- 0.10 a.u.

Enthalpy Value for $\mathbf{SO}^{2+}$: -472.511964 Hartree

Enthalpy Value for $[F\text{-}SO]^{+}$: -572.726156 Hartree

FIA value: 897 kJ/mol

Table S17. Coordinates of $\mathbf{SO}^{2+}$ (in Angstroms) after geometry optimization at PBE1PBE/cc-PVTZ with Grimme's D3 empirical dispersion.

S	0	0	0.458897
O	0	0	-0.9178

Table S18. Coordinates of $[\mathbf{F\text{-}SO}]^{+}$ (in Angstroms) after geometry optimization at PBE1PBE/cc-PVTZ with Grimme's D3 empirical dispersion.

S	0	0.431403	0
F	-1.11941	-0.59891	0
O	1.259333	-0.18903	0

Computational Details of $[SOF]^+$:

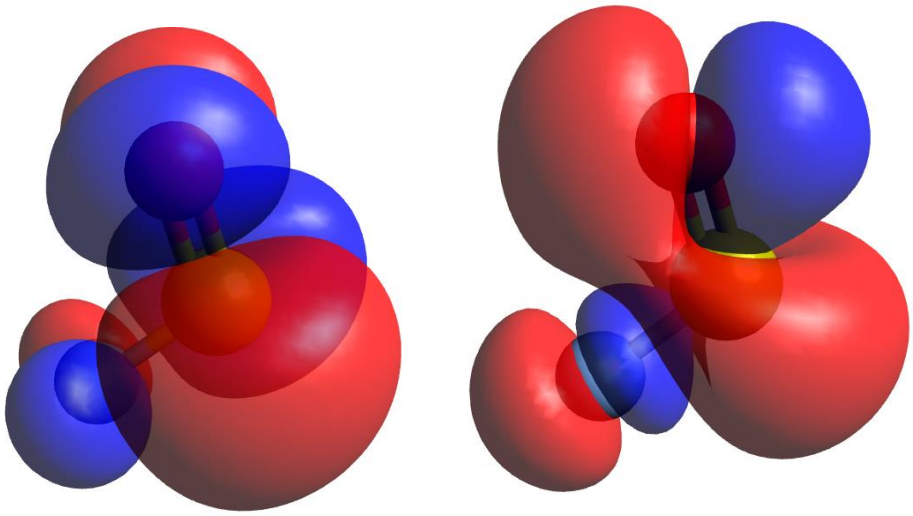

LUMO: -12.673 eV HOMO: -19.155 eV

LUMO (left) and HOMO (right) (PBE1PBE/cc-PVTZ with Grimme's D3 empirical dispersion) for **SOF^+** in the gas-phase at a contour surface value of +/- 0.10 a.u.

Enthalpy Value for **SOF^+**: -572.615171 Hartree

Enthalpy Value for F_2SO: -672.788411 Hartree

FIA value: 1030 kJ/mol

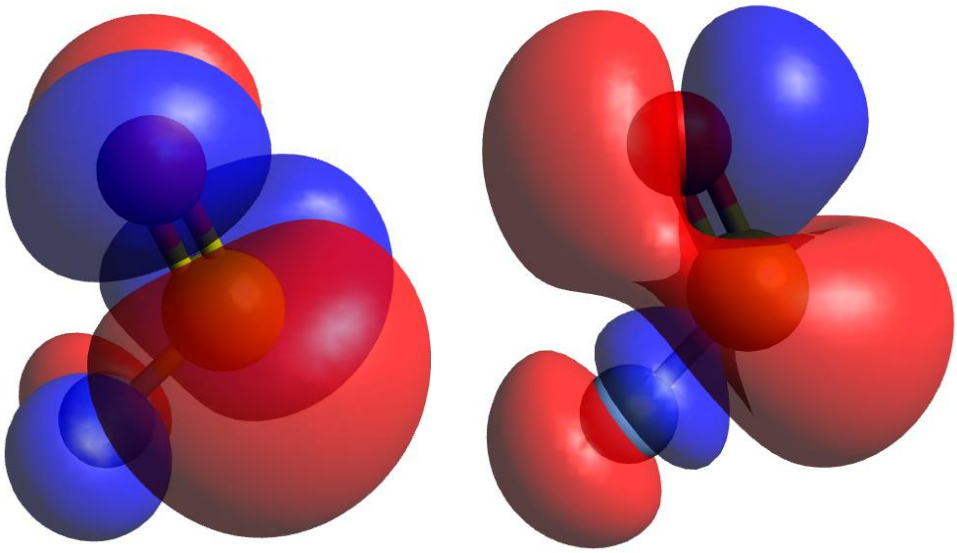

LUMO: -6.926 eV HOMO: -13.519 eV

LUMO (left) and HOMO (right) (PBE1PBE/cc-PVTZ with Grimme's D3 empirical dispersion and an acetonitrile solvent correction) for **SOF**$^+$ at a contour surface value of +/- 0.10 a.u.

Enthalpy Value for **SOF**$^+$: -572.726156 Hartree

Enthalpy Value for F_2SO: -672.792292 Hartree

FIA value: 508 kJ/mol

Table S19. Coordinates of **SOF**$^+$ (in Angstroms) after geometry optimization at PBE1PBE/cc-PVTZ with Grimme's D3 empirical dispersion.

S	0	0.431403	0

F	-1.11941	-0.59891	0
O	1.259333	-0.18903	0

Table S20. Coordinates of **F_2SO** (in Angstroms) after geometry optimization at PBE1PBE/cc-PVTZ with Grimme's D3 empirical dispersion.

S	-0.16153	0	0.406292
F	0.753746	1.160354	-0.20572
F	0.753747	-1.16035	-0.20572
O	-1.37288	0	-0.34973

Computational Details of [PF_5]:

PBE1PBE/cc-PVTZ with Grimme's D3 empirical dispersion for **PF_5** in the gas-phase:

Enthalpy Value for **PF_5**: -840.313619 Hartree

Enthalpy Value for **PF_6^-**: -940.238088 Hartree

FIA value: 377 kJ/mol

PBE1PBE/cc-PVTZ with Grimme's D3 empirical dispersion and an acetonitrile solvent correction:

Enthalpy Value for **PF_5**: -840.316138 Hartree

Enthalpy Value for **PF_6^-**: -940.32351 Hartree

FIA value: 354 kJ/mol

Table S21. Coordinates of **PF_5** (in Angstroms) after geometry optimization at PBE1PBE/cc-PVTZ with Grimme's D3 empirical dispersion.

P	0	0	0
F	0	0	1.585448
F	0	1.549691	0
F	-1.34207	-0.77485	0
F	0	0	-1.58545
F	1.342072	-0.77485	0

Table S22. Coordinates of **PF_6^-** (in Angstroms) after geometry optimization at PBE1PBE/cc-PVTZ with Grimme's D3 empirical dispersion.

P	0	0	0
F	0	0	1.624382
F	0	1.624382	0
F	1.624382	0	0
F	0	0	-1.62438
F	0	-1.62438	0
F	-1.62438	0	0

Computational Details of [BF_3]:

PBE1PBE/cc-PVTZ with Grimme's D3 empirical dispersion for **BF_3** in the gas-phase:

Enthalpy Value for **BF_3**: -324.354561 Hartree

Enthalpy Value for **BF_4^-**: -424.264092 Hartree

FIA value: 337 kJ/mol

PBE1PBE/cc-PVTZ with Grimme's D3 empirical dispersion and an acetonitrile solvent correction:

Enthalpy Value for **BF_3**: -324.356865 Hartree

Enthalpy Value for **BF_4^-**: -424.357305 Hartree

FIA value: 335 kJ/mol

Table S23. Coordinates of **BF_3** (in Angstroms) after geometry optimization at PBE1PBE/cc-PVTZ with Grimme's D3 empirical dispersion.

B	0	0	0
F	0	1.310398	0
F	1.134838	-0.6552	0
F	-1.13484	-0.6552	0

Table S24. Coordinates of **BF_4^-** (in Angstroms) after geometry optimization at PBE1PBE/cc-PVTZ with Grimme's D3 empirical dispersion.

B	0	0	0
F	0.81041	0.81041	0.81041
F	-0.81041	-0.81041	0.81041
F	-0.81041	0.81041	-0.81041
F	0.81041	-0.81041	-0.81041

Computational Details of $[(C_6F_5)_3PF]^+$:

PBE1PBE/cc-PVTZ with Grimme's D3 empirical dispersion for **$[(C_6F_5)_3PF]^+$** in the gas-phase:

Enthalpy Value for **$[(C_6F_5)_3PF]^+$:** -2622.653644 Hartree

Enthalpy Value for $(C_6F_5)_3PF_2$: -2722.724519 Hartree

FIA value: 761 kJ/mol

PBE1PBE/cc-PVTZ with Grimme's D3 empirical dispersion and an acetonitrile solvent correction:

Enthalpy Value for **$[(C_6F_5)_3PF]^+$:** -2622.721675 Hartree

Enthalpy Value for $(C_6F_5)_3PF_2$: -2722.731728 Hartree

FIA value: 361 kJ/mol

Table S25. Coordinates of **$[(C_6F_5)_3PF]^+$** (in Angstroms) after geometry optimization at PBE1PBE/cc-PVTZ with Grimme's D3 empirical dispersion.

P	-0.00123	-0.00157	0.703336
F	-0.10589	-2.73872	1.640935
F	-0.00346	-0.00418	2.257034
F	2.386268	0.014118	-1.25941
F	1.557592	-4.78941	1.100084
F	3.605415	-4.42295	-0.61529
F	2.41534	1.279729	1.65495
F	-1.19925	2.056317	-1.26651
F	4.010824	-2.03335	-1.78764
F	-0.23234	4.483108	-1.79876
F	2.035513	5.327936	-0.61852
F	3.366217	3.741579	1.108838
C	1.109996	-1.29843	0.241085

C	-1.68013	-0.31197	0.239738
C	2.255289	3.323344	0.551355
C	2.807622	-3.42817	-0.3421
C	0.567885	1.609301	0.243823
C	0.915252	-2.55664	0.821933
C	1.7524	2.070485	0.829191
C	-2.07566	-1.306	-0.65931
C	-0.09329	2.445708	-0.65977
C	-3.4118	-1.5102	-0.94785
C	-2.67037	0.486592	0.822856
C	2.169272	-1.14024	-0.65674
C	-4.37493	-0.71149	-0.34103
C	1.752022	-3.61664	0.546406
C	3.016194	-2.1933	-0.94643
C	1.569851	4.141307	-0.34329
C	0.398293	3.704008	-0.9515
C	-4.00736	0.294965	0.548365
F	-2.31533	1.459861	1.643401
F	-4.92362	1.050815	1.104157
F	-5.63607	-0.90227	-0.6129
F	-3.77307	-2.4498	-1.78997
F	-1.18645	-2.07191	-1.26379

Table S26. Coordinates of $(C_6F_5)_3PF_2$ (in Angstroms) after geometry optimization at PBE1PBE/cc-PVTZ with Grimme's D3 empirical dispersion.

C	1.806298	-0.2305	0.002413
C	2.393355	-1.28561	-0.68212
C	3.76408	-1.47506	-0.68234
C	4.575719	-0.58129	-0.00211
C	-1.09983	-1.44637	-0.0013
C	-0.76303	-2.60518	0.684467
C	-1.59072	-3.71418	0.68214
C	-2.79472	-3.66428	-0.0021
C	-3.15857	-2.51523	-0.68595
C	-2.30608	-1.42517	-0.68765
F	1.647394	-2.17041	-1.32736
F	4.30102	-2.50114	-1.32036
F	5.883818	-0.7468	-0.00434
F	0.001986	-0.00242	1.655155
F	0.388725	-2.69554	1.33332
F	-1.23923	-4.81711	1.320972
F	-3.59537	-4.71186	-0.00256
F	-4.31504	-2.46548	-1.32497
F	-2.69611	-0.33724	-1.33585
P	0.002808	-0.00088	0.001725

C	2.63977	0.644252	0.685261
C	4.014552	0.486127	0.680658
C	-0.70107	1.675178	0.003086
F	0.00558	0.001539	-1.65195
F	2.139762	1.686289	1.333228
F	4.792488	1.345871	1.316201
C	-0.08278	2.712421	-0.68123
C	-1.87556	1.957703	0.686652
C	-0.60651	3.993256	-0.68109
F	1.056869	2.511276	-1.3266
C	-2.42841	3.226266	0.682386
F	-2.52609	1.002832	1.335254
C	-1.78686	4.247051	-0.00077
F	0.011712	4.972638	-1.31889
F	-3.56197	3.467744	1.318739
F	-2.29997	5.461666	-0.00313

Computational Details of $[Ph_3Si]^+$:

PBE1PBE/cc-PVTZ with Grimme's D3 empirical dispersion for **$[Ph_3Si]^+$** in the gas-phase:

Enthalpy Value for **$[Ph_3Si]^+$**: -983.217907 Hartree

Enthalpy Value for **Ph_3SiF**: -1083.324715 Hartree

FIA value: 855 kJ/mol

PBE1PBE/cc-PVTZ with Grimme's D3 empirical dispersion and an acetonitrile solvent correction:

Enthalpy Value for **$[Ph_3Si]^+$:** -983.277706 Hartree

Enthalpy Value for **Ph_3SiF**: -1083.333853 Hartree

FIA value: 482 kJ/mol

Table S27. Coordinates of **$[Ph_3Si]^+$** (in Angstroms) after geometry optimization at PBE1PBE/cc-PVTZ with Grimme's D3 empirical dispersion.

Si	-0.00059	0.001114	0.005238
C	0.354795	-1.77946	0.003672
C	1.555135	-2.26564	0.548953
C	-0.56744	-2.686	-0.54617
C	1.818064	-3.62243	0.54935
H	2.273181	-1.58202	0.986849
C	-0.28902	-4.03972	-0.55523
H	-1.4933	-2.32821	-0.98148
C	0.899197	-4.50561	-0.00513
H	2.73799	-3.99571	0.981033
H	-0.99544	-4.73506	-0.99045
H	1.111467	-5.56785	-0.0087
C	1.364634	1.198211	0.002822
C	2.612257	0.849511	-0.54168
C	1.185644	2.48273	0.543899

C	3.646758	1.765935	-0.54997
H	2.765526	-0.13296	-0.97295
C	2.230458	3.387401	0.544827
H	0.233902	2.765782	0.978404
C	3.456112	3.029868	-0.00436
H	4.603264	1.499047	-0.98101
H	2.09359	4.372256	0.972947
H	4.270997	3.743564	-0.00707
C	-1.72036	0.583021	0.003661
C	-2.04535	1.835104	-0.54501
C	-2.74095	-0.21414	0.549018
C	-3.35713	2.270282	-0.55305
H	-1.27328	2.458586	-0.98069
C	-4.04777	0.235877	0.550216
H	-2.50729	-1.17774	0.986715
C	-4.35418	1.47333	-0.00334
H	-3.60667	3.229953	-0.98743
H	-4.83042	-0.37492	0.98186
H	-5.38043	1.820073	-0.00629

Table S28. Coordinates of Ph_3SiF (in Angstroms) after geometry optimization at PBE1PBE/cc-PVTZ with Grimme's D3 empirical dispersion.

Si	-0.00023	-0.00265	0.757016

C	0.437578	1.724133	0.200226
C	1.561349	1.977971	-0.58736
C	-0.37746	2.801882	0.559695
C	1.865606	3.267536	-1.0008
H	2.207668	1.157804	-0.88109
C	-0.07506	4.09104	0.152004
H	-1.26155	2.632015	1.165786
C	1.048262	4.32457	-0.63036
H	2.742237	3.447016	-1.61215
H	-0.71556	4.915653	0.442173
H	1.284865	5.332179	-0.95176
C	1.272165	-1.24396	0.189999
C	2.52088	-1.3211	0.812808
C	1.015176	-2.09164	-0.88856
C	3.481946	-2.21684	0.370315
H	2.743157	-0.67852	1.658369
C	1.976106	-2.98664	-1.33661
H	0.048614	-2.05712	-1.38037
C	3.210458	-3.04907	-0.70732
H	4.444027	-2.26811	0.866553
H	1.759827	-3.63912	-2.1744
H	3.96148	-3.74942	-1.05372
C	-1.71645	-0.47326	0.196886
C	-2.43902	-1.4515	0.884691
C	-2.2895	0.098932	-0.94003
C	-3.69483	-1.8452	0.449893
H	-2.01754	-1.90589	1.775044
C	-3.54418	-0.29673	-1.38143
H	-1.75212	0.869057	-1.48361
C	-4.24731	-1.26938	-0.68622
H	-4.24501	-2.60183	0.996931
H	-3.97549	0.157919	-2.26558
H	-5.22881	-1.57724	-1.02742
F	-0.00298	-0.02686	2.375552

Computational Details of 4-Ph-Ph-CH_2^+:

PBE1PBE/cc-PVTZ with Grimme's D3 empirical dispersion for **4-Ph-Ph-CH_2^+** in the gas-phase:

Enthalpy Value for **4-Ph-Ph-CH_2^+**: -501.086536 Hartree

Enthalpy Value for **4-Ph-Ph-CH_2F**: -601.151909 Hartree

FIA value: 747 kJ/mol

PBE1PBE/cc-PVTZ with Grimme's D3 empirical dispersion and an acetonitrile solvent correction:

Enthalpy Value for **4-Ph-Ph-CH_2^+**: -501.152064 Hartree

Enthalpy Value for **4-Ph-Ph-CH_2F**: -601.1594 Hartree

FIA value: 353 kJ/mol

Table S29. Coordinates of **4-Ph-Ph-CH_2^+** (in Angstroms) after geometry optimization at PBE1PBE/cc-PVTZ with Grimme's D3 empirical dispersion.

C	0.318317	-1E-06	0
C	1.046675	-1.19855	0.242284
C	2.40267	-1.2036	0.251673
C	3.142146	0.000001	0.000003
C	2.402669	1.203602	-0.25167
C	1.046675	1.198553	-0.24228
C	-1.12353	-1E-06	0.000001
C	-1.84427	-1.1838	-0.25131
C	-3.22182	-1.17735	-0.26517
C	-3.91408	0.000001	-1E-06
C	-3.22182	1.177356	0.265171
C	-1.84427	1.183796	0.251311
H	0.51065	-2.11038	0.464249

H	2.947551	-2.11695	0.459754
H	2.947549	2.116951	-0.45975
H	0.510648	2.110379	-0.46424
H	-1.32208	-2.10183	-0.48573
H	-3.76381	-2.08805	-0.48469
H	-4.99718	0.000002	-2E-06
H	-3.76381	2.088048	0.484692
H	-1.32208	2.10183	0.485732
C	4.498617	0.000001	0.000001
H	5.062337	-0.90488	0.19711
H	5.06233	0.904882	-0.19714

Table S30. Coordinates of 4-Ph-Ph-CH_2F (in Angstroms) after geometry optimization at PBE1PBE/cc-PVTZ with Grimme's D3 empirical dispersion.

C	0.148074	0.056831	-0.09068
C	-0.55277	1.186571	0.330827
C	-1.93446	1.23239	0.258557
C	-2.65692	0.155484	-0.24065
C	-1.96209	-0.97263	-0.66489
C	-0.58237	-1.02336	-0.58983
C	1.620126	0.004923	-0.01442
C	2.392578	1.129613	-0.30654

C	3.775158	1.079989	-0.23516
C	4.413887	-0.09568	0.131597
C	3.657758	-1.22108	0.425678
C	2.275346	-1.17114	0.352457
H	-0.00876	2.027641	0.743899
H	-2.46184	2.114928	0.603966
H	-2.51116	-1.81831	-1.06429
H	-0.05715	-1.90022	-0.94931
H	1.903239	2.045067	-0.61781
H	4.35701	1.962068	-0.47498
H	5.494989	-0.13454	0.188085
H	4.146598	-2.14161	0.721846
H	1.691886	-2.04779	0.608283
C	-4.14956	0.1869	-0.28713
H	-4.52695	-0.31053	-1.18497
H	-4.52269	1.214071	-0.26526
F	-4.68597	-0.47819	0.807955

Computational Details of $[PhCF_2]^+$:

PBE1PBE/cc-PVTZ with Grimme's D3 empirical dispersion for **$PhCF_2^+$** in the gas-phase:

Enthalpy Value for **$PhCF_2^+$**: -468.689208 Hartree

Enthalpy Value for **$PhCF_3$**: -568.791603 Hartree

FIA value: 844 kJ/mol

PBE1PBE/cc-PVTZ with Grimme's D3 empirical dispersion and an acetonitrile solvent correction:

Enthalpy Value for **$PhCF_2^+$**: -468.766081 Hartree

Enthalpy Value for **$PhCF_3$**: -568.79618 Hartree

FIA value: 413 kJ/mol

Table S31. Coordinates of **$PhCF_2^+$** (in Angstroms) after geometry optimization at PBE1PBE/cc-PVTZ with Grimme's D3 empirical dispersion.

C	-1.8644	-1.22147	-7.5E-05
C	-0.4935	-1.23543	-0.00022
C	0.201304	0	-2.9E-05
C	-0.4935	1.235425	0.000198
C	-1.8644	1.221467	0.000088
H	-2.41913	-2.15032	-0.00189
H	0.055941	-2.16835	-0.00134
H	0.055941	2.168346	0.001306
H	-2.41913	2.150323	0.001912
C	1.586639	0	-6.1E-05
C	-2.54311	0	0.000015
H	-3.62712	0	0.00003
F	2.28774	1.056275	-0.00093
F	2.28774	-1.05628	0.000984

Table S32. Coordinates of **$PhCF_3$** (in Angstroms) after geometry optimization at PBE1PBE/cc-PVTZ with Grimme's D3 empirical dispersion.

C	-2.12622	1.201951	0.001562
C	-0.74068	1.204705	-0.01911
C	-0.05205	0.000022	-0.03077
C	-0.74065	-1.20468	-0.01912
C	-2.12619	-1.20196	0.001557
C	-2.81909	-1.4E-05	0.012393
H	-2.6659	2.140884	0.006187
H	-0.19256	2.137933	-0.03421
H	-0.19251	-2.1379	-0.03422
H	-2.66585	-2.14091	0.006177
H	-3.90231	-2.8E-05	0.026333
C	1.448001	0.000012	-0.00317
F	1.961562	-1.07897	-0.60757
F	1.916894	-0.00033	1.255676
F	1.961594	1.079278	-0.60703

6. X-Ray Crystallography Data

Crystal Structure of 1[OTf]$_2$ (Hydrogen atoms eliminated for clarity)

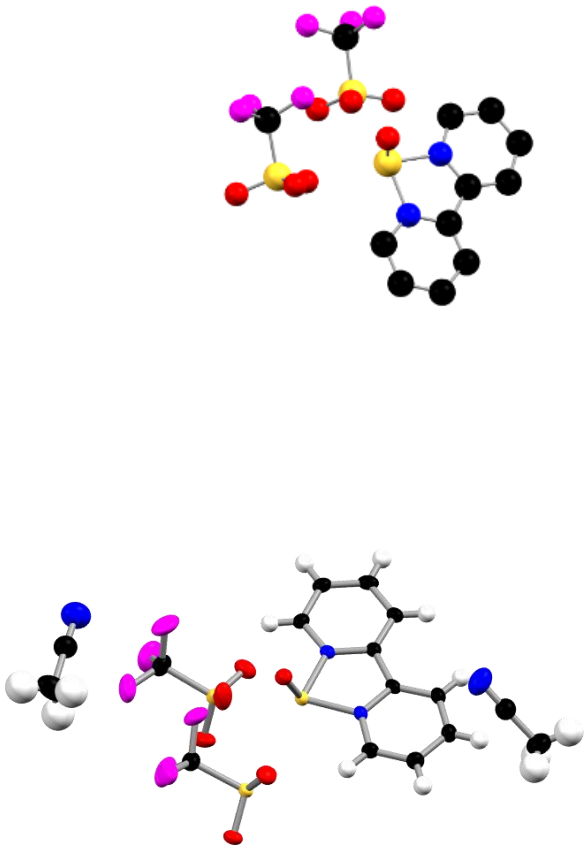

Crystal Structure of 3[OTf]$_2$ (Hydrogen atoms eliminated for clarity)

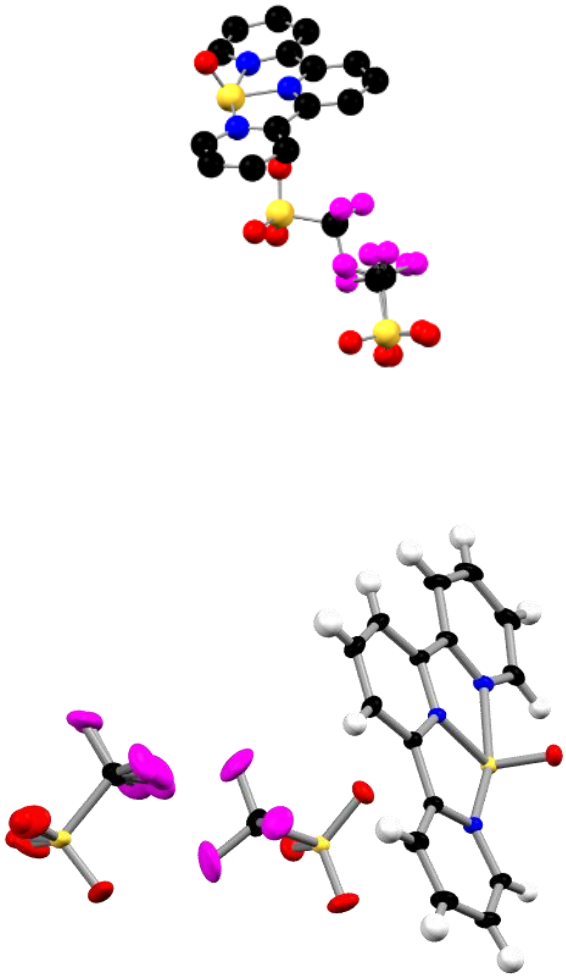

Poorly Resolved Crystal Structure of 4[OTf]$_2$ (Hydrogen atoms and 2 CH_3CN molecules eliminated for clarity)

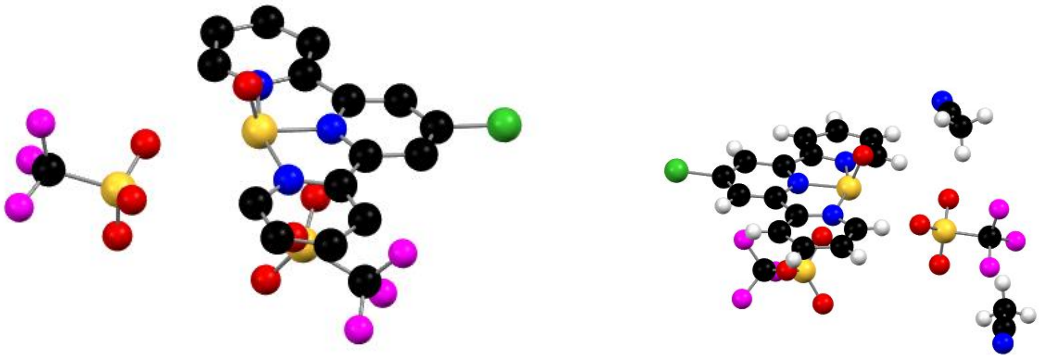

Crystal Structure of 5[OTf]$_2$ (Hydrogen atoms eliminated for clarity)

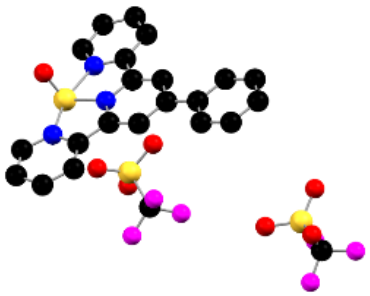

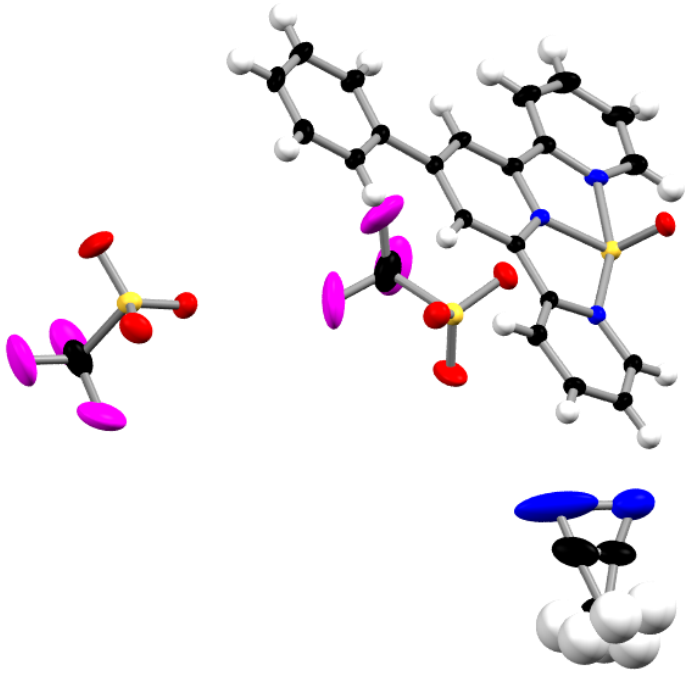

Crystal Structure of 6[OTf]$_2$ (Hydrogen atoms eliminated for clarity)

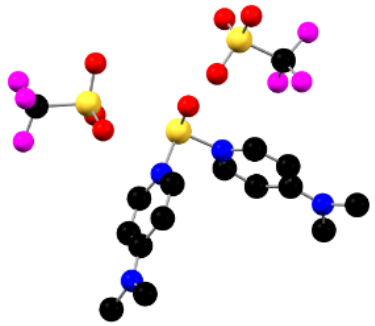

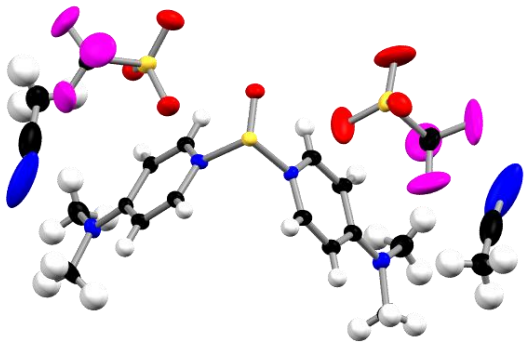

Poorly Resolved Crystal Structure of 7[OTf]$_2$ (Hydrogen atoms eliminated for clarity)

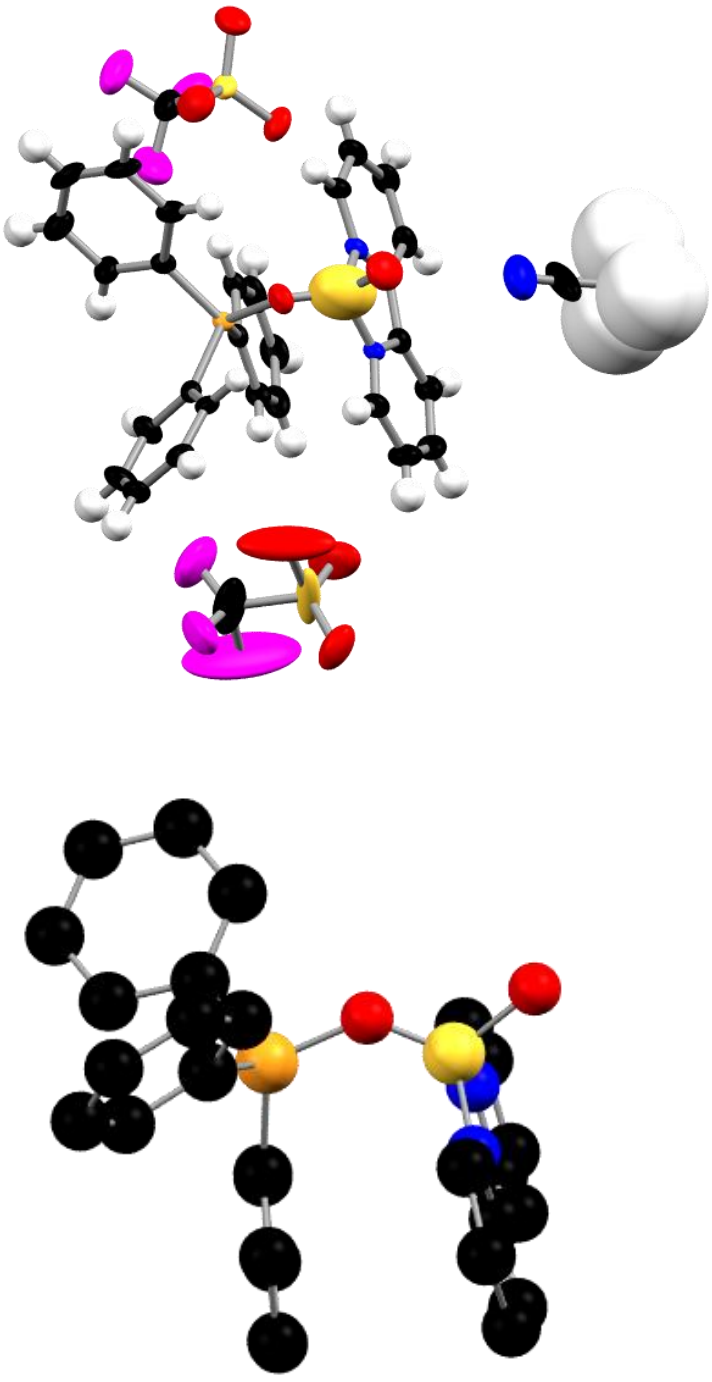

Crystal Structure of 8[OTf]$_2$ (Hydrogen atoms eliminated for clarity)

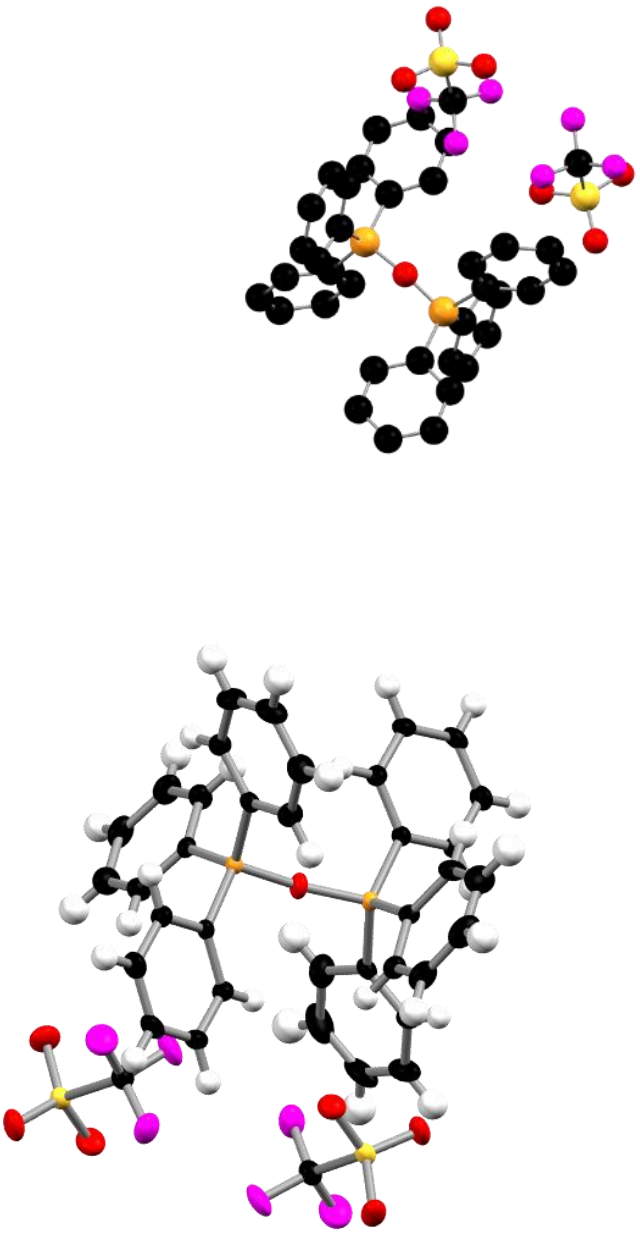

Crystal Structure of 9[OTf]$_2$ (Hydrogen atoms eliminated for clarity)

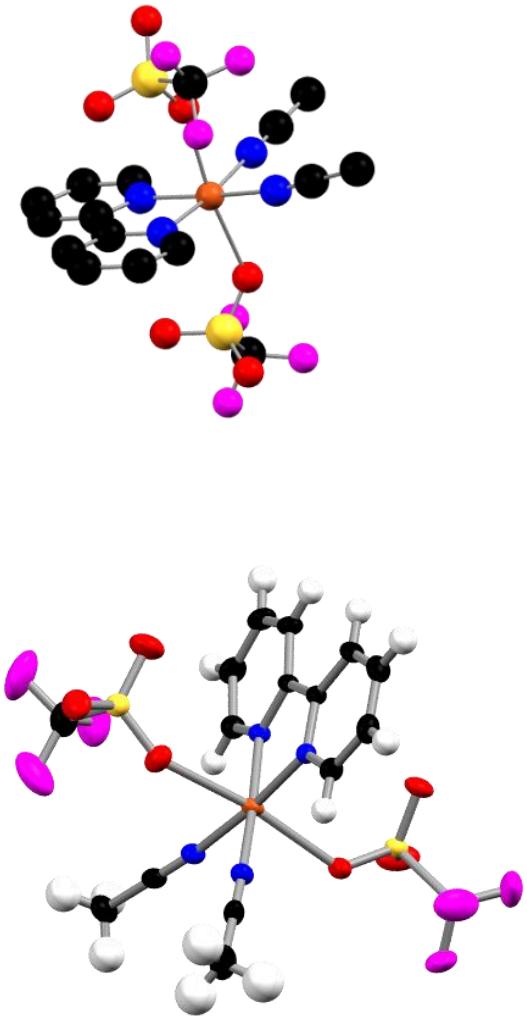

Crystal Structure of $[H_2Bipy][OTf]_2$ (Bipy occupancy = 0.5)

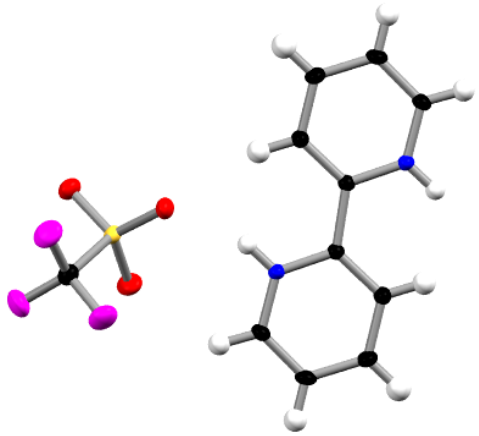

Packing of [H_2Bipy][OTf]$_2$ (8 triflate anions, 2 full H_2Bipy cations, 4 H_2Bipy cations of occupancy = 0.5).

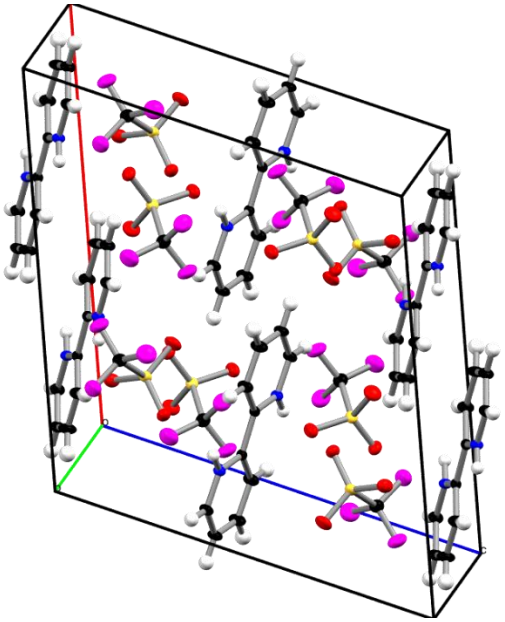

Crystal Structure of [H_2ClTerpy][OTf]$_2$ (Hydrogen atoms eliminated for clarity)

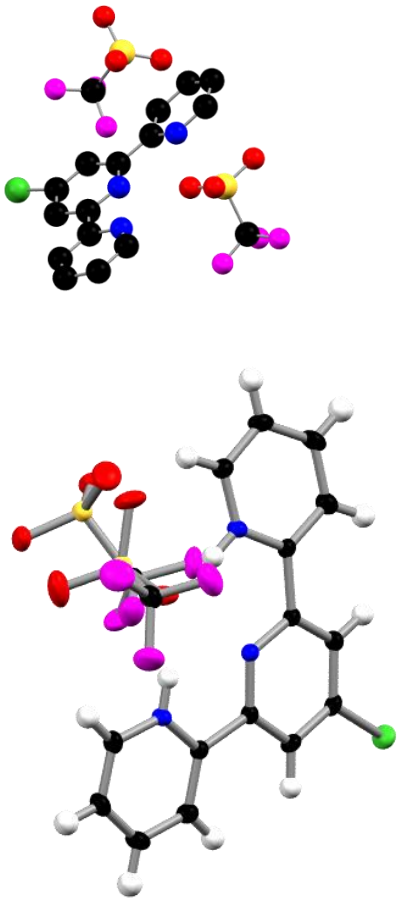

Crystal Structure of [HDMAP][OTf] (Hydrogen atoms eliminated for clarity)

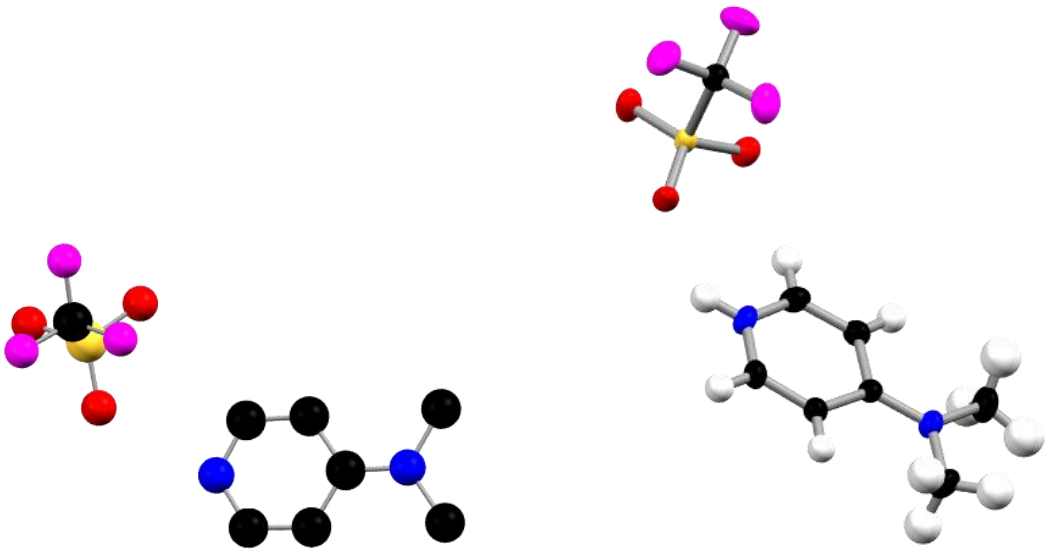

Crystal Structure of Ph_3SiOPh_3 (Hydrogen atoms omitted for clarity)

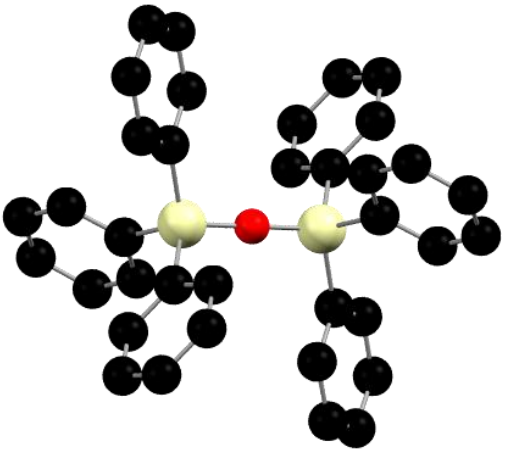

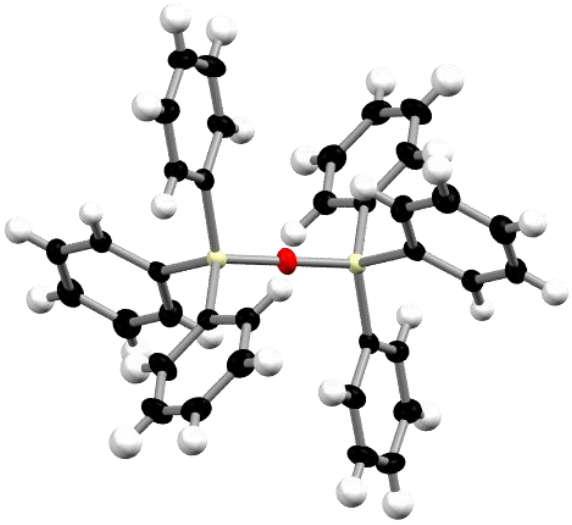

Table of Crystallographic Data

	1	3	5
empirical formula	C16 H14 F6 N4 O7 S3	C16.96 H11 F6.02 N3 O7.09 S2.99	C25 H18 F6 N4 O7 S3
formula weight	584.49	580.36	696.61
crystal system	orthorhombic	monoclinic	triclinic
space group	P b c a	C 1 2/c 1	P -1
a (Å)	16.5696(19)	29.7305(11)	8.5676(9)
b (Å)	12.2385(13)	8.0563(3)	12.7491(10)
c (Å)	22.989(2)	22.7955(9)	13.1888(13)
α (°)	90	90	89.126(5)
β (°)	90	128.183(2)	78.034(5)
γ (°)	90	90	87.794(5)
V (Å^3)	4661.9(8)	4291.7(3)	1408.2(2)
Z	8	8	2
D_{calc} (g·cm^{-3})	1.666	1.796	1.643
μ (mm^{-1})	0.412	0.446	0.356
reflections measured	64454	89987	24139
unique reflections, R_{int}	5781, 0.1305	14445, 0.0322	6741, 1408.2(2)

No. of parameters	327	437	427
R_1, wR_2	0.0612, 0.1567	0.0381, 0.1119	0.0540, 0.1285
GOF on F^2	1.126	1.033	1.014

	6[OTf]$_2$	**8[OTf]$_2$**	**9[OTf]$_2$**
empirical formula	C20 H26 F6 N6 O7 S3	C19 H15 F3 O3.50 P S	C16 H14 Cu F6 N4 O6 S2
formula weight	672.65	419.34	599.97
crystal system	triclinic	triclinic	monoclinic
space group	P -1	P -1	P 1 21/n 1
a (Å)	9.7593(10)	8.6157(9)	7.9129(3)
b (Å)	12.1850(14)	11.1675(11)	7.9129(3)
c (Å)	13.8693(15)	19.509(2)	11.8839(5)
α (°)	108.767(5)	94.582(4)	90
β (°)	107.547(4)	93.015(4)	93.087(3)
γ (°)	94.641(3)	98.970(4)	90
V (Å^3)	1459.8(3)	1844.2(3)	2295.01(16)
Z	2	4	4
D_{calc} (g·cm^{-3})	1.530	1.510	1.736
μ (mm^{-1})	0.342	0.312	1.223

reflections measured	33043	32039	34875
unique reflections, R_{int}	7238, 0.0667	32039, 0.0572	7038, 0.0776
No. of parameters	385	496	318
R_1, wR_2	0.0704, 0.2453	0.0469, 0.1178	0.0423, 0.0974
GOF on F^2	1.078	0.1178	1.008

	$[H_2ClTerpy][OTf]_2$	**$Ph_3SiOSiPh_3$**	**$[H_2Bipy][OTf]_2$**
empirical formula	C17 H12 Cl F6 N3 O6 S2	C36 H30 O Si2	C24 H20 F12 N4 O12 S4
formula weight	567.87	534.78	912.68
crystal system	triclinic	triclinic	monoclinic
space group	P -1	P -1	C 1 2/c 1
a (Å)	7.7029(17)	8.6037(19)	14.1458(9)
b (Å)	10.457(3)	9.488(2)	9.5520(9)
c (Å)	15.096(5)	10.993(3)	13.0726(10)
α (°)	108.987(8)	95.936(7)	90
β (°)	92.250(7)	111.775(5)	111.259(7)
γ (°)	110.503(7)	113.342(5)	90

V ($Å^3$)	1060.7(6)	731.4(3)	1646.2(2)
Z	2	1	2
D_{calc} ($g \cdot cm^{-3}$)	1.778	1.214	1.841
μ (mm^{-1})	0.473	0.148	0.426
reflections measured	7879	11935	25462
unique reflections, R_{int}	5706, 0.0664	4089, 0.0964	2876, 0.0732
No. of parameters	324	178	127
R_1, wR_2	0.0489, 0.1186	0.0641, 0.1711	0.0369, 0.0895
GOF on F^2	1.004	1.000	1.058

	[HDMAP][OTf]	**8[OTf]$_2$**
empirical formula	C16 H22 F6 N4 O6 S2	C32 H26 F6 N3 O8 P S3
formula weight	544.49	821.71
crystal system	monoclinic	monoclinic
space group	P 1 21/c 1	P 1 21/n 1
a (Å)	8.4711(14)	9.1128(9)
b (Å)	9.3527(12)	19.7390(18)

c (Å)	14.835(2)	20.468(2)
α (°)	90	90
β (°)	106.410(4)	94.868(3)
γ (°)	90	90
V (Å^3)	1127.4(3)	3668.5(6)
Z	2	4
D_{calc} (g·cm^{-3})	1.604	1.488
μ (mm^{-1})	0.327	0.329
reflections measured	12379	54166
unique reflections, R_{int}	2893, 0.0752	8400, 0.1498
No. of parameters	156	4821
R_1, wR_2	0.0480, 0.1378	0.1374, 0.4301
GOF on F^2	1.037	1.491

7. References

1. Constable, E. C.; Lewis, J.; Liptrot, M. C.; Raithby, P. R. The coordination chemistry of 4′-phenyl-2,2′:6′, 2″-terpyridine; the synthesis, crystal and molecular structures of 4′-phenyl-2,2′:6′,2″-terpyridine and bis(4′-phenyl-2,2′:6′,2″-terpyridine)nickel(II) chloride decahydrate. *Inorg. Chim. Acta* **1990**, *178*, 47-54.
2. APEX3, Bruker AXS Inc., Madison, WI, USA, **2016**.
3. SAINT, Bruker AXS Inc., Madison, WI, USA, **1998**.
4. SADABS. Program for Empirical Absorption Correction., University of Gottingen, Germany, **1996**.
5. Reddy, G. S.; Schmutzler, R. 31P and 19F Nuclear Magnetic Resonance Studies of Phosphorus-Fluorine Compounds. *Z. Naturforsch. B* **1970**, *25*, 1199-1214.
6. Bernstein, J.; Roth, J. S.; Miller, W. T. The Preparation and Properties of Some Substituted Benzyl Fluorides. *J. Am. Chem. Soc.* **1948**, *70*, 2310-2314.
7. Champagne, P. A.; Benhassine, Y.; Desroches, J.; Paquin, J.-F. Friedel–Crafts Reaction of Benzyl Fluorides: Selective Activation of C-F Bonds as Enabled by Hydrogen Bonding. *Angew. Chem. Int. Ed.* **2014**, *53*, 13835-13839.
8. Hendrickson, J. B.; Schwartzman, S. M. Triphenyl phosphine ditriflate: A general oxygen activator. *Tetrahedron Lett.* **1975**, *16*, 277-280.
9. Hendrickson, J. B.; Mistry, S. N.; Moussa, Z.; Al-Masri, H. T., in *Encyclopedia of Reagents for Organic Synthesis*, **2014**, pp. 1-9.
10. Gaussian 09 Rev. E.01, Gaussian, Inc., Wallingford, CT, USA, **2009**.
11. Adamo, C.; Barone, V. Toward reliable density functional methods without adjustable parameters: The PBE0 model. *J. Chem. Phys.* **1999**, *110*, 6158-6170.
12. Becke, A. D. Density-functional thermochemistry. III. The role of exact exchange. *J. Chem. Phys.* **1993**, *98*, 5648-5652.
13. Lee, C.; Yang, W.; Parr, R. G. Development of the Colle-Salvetti correlation-energy formula into a functional of the electron density. *Phys. Rev. B* **1988**, *37*, 785-789.
14. Vosko, S. H.; Wilk, L.; Nusair, M. Accurate spin-dependent electron liquid correlation energies for local spin density calculations: a critical analysis. *Can. J. Phys.* **1980**, *58*, 1200-1211.
15. Stephens, P. J.; Devlin, F. J.; Chabalowski, C. F.; Frisch, M. J. Ab Initio Calculation of Vibrational Absorption and Circular Dichroism Spectra Using Density Functional Force Fields. *J. Phys. Chem.* **1994**, *98*, 11623-11627.

16. Kendall, R. A.; Jr., T. H. D.; Harrison, R. J. Electron affinities of the first-row atoms revisited. Systematic basis sets and wave functions. *J. Chem. Phys.* **1992**, *96*, 6796-6806.
17. Weigend, F.; Ahlrichs, R. Balanced basis sets of split valence, triple zeta valence and quadruple zeta valence quality for H to Rn: Design and assessment of accuracy. *Phys. Chem. Chem. Phys.* **2005**, *7*, 3297-3305.
18. Grimme, S.; Antony, J.; Ehrlich, S.; Krieg, H. A consistent and accurate ab initio parametrization of density functional dispersion correction (DFT-D) for the 94 elements H-Pu. *J. Chem. Phys.* **2010**, *132*, 154104.
19. Hanwell, M. D.; Curtis, D. E.; Lonie, D. C.; Vandermeersch, T.; Zurek, E.; Hutchison, G. R. Avogadro: an advanced semantic chemical editor, visualization, and analysis platform. *J. Cheminform.* **2012**, *4*, 17.
20. Slattery, J. M.; Hussein, S. How Lewis acidic is your cation? Putting phosphenium ions on the fluoride ion affinity scale. *Dalton Trans.* **2012**, *41*, 1808-1815.
21. Christe, K. O.; Dixon, D. A.; McLemore, D.; Wilson, W. W.; Sheehy, J. A.; Boatz, J. A. On a quantitative scale for Lewis acidity and recent progress in polynitrogen chemistry. *J. Fluor. Chem.* **2000**, *101*, 151-153.